

NASA Contractor Report 181668

**Subsystem Design Analyses of a Rotating
Advanced-Technology Space Station
for the Year 2025**

**M.J. Queijo, A.J. Butterfield, W.F. Cuddihy, C.B. King,
R.W. Stone, J.R. Wrobel, and P.A. Garn**

**The Bionetics Corporation
Hampton, VA 23666**

(NASA-CR-181668) SYSTEM DESIGN ANALYSES OF
A ROTATING ADVANCED-TECHNOLOGY SPACE STATION
FOR THE YEAR 2025 Interim Report, Nov. 1987
- May 1988 (Bionetics Corp.) 250 pCSCL 22B

N89-13482

Unclas
G3/18 0179692

**Contract NAS1-18267
December 1988**

NASA

National Aeronautics and
Space Administration

Langley Research Center
Hampton, Virginia 23665-5225

TABLE OF CONTENTS

ABSTRACT.....	xi
ABBREVIATIONS AND ACRONYMS.....	xii
1.0 INTRODUCTION.....	1-1
References.....	1-5
2.0 ROTATING ADVANCED-TECHNOLOGY SPACE STATION CONFIGURATION.....	2-1
3.0 PURPOSE OF THIS STUDY.....	3-1
3.1 Electrical Power System Alternates.....	3-1
3.2 Attitude Stabilization and Control.....	3-2
3.3 Electrothermal Thrusters.....	3-3
3.4 Structures, Material, and Launch Vehicles.....	3-3
3.5 Lunar and Planetary Mission Support.....	3-4
3.6 Advanced Technology Identification.....	3-4
4.0 ONBOARD POWER GENERATION: A COMPARISON OF ALTERNATE HEAT SOURCES AND ADVANCED PHOTOVOLTAICS.....	4-1
4.1 Comparison Approach.....	4-1
4.2 General Results from Comparison.....	4-2
4.2.1 Advanced Photovoltaics, Lowest Mass, Least Complex.....	4-2
4.2.2 Radioisotope Decay heat Sources.....	4-6
4.2.3 Solar Dynamic (Baseline Configuration).....	4-6
4.2.4 Nuclear Fission Reactor.....	4-7
4.2.5 Fusion Power.....	4-7
4.3 Comparison of Systems.....	4-8
4.3.1 Comparison of System Masses and Mass Effects.....	4-9
4.3.2 Comparison of Control Requirements.....	4-15
4.3.3 Particular System and Operating Concerns.....	4-18
4.4 Overall Assessments.....	4-21
References.....	4-24
5.0 ATTITUDE AND ORBIT CONTROL.....	5-1
5.1 Environmental (Disturbance) Forces and Torques.....	5-1
5.2 Attitude Control.....	5-1
5.2.1 Reaction Jets.....	5-5
5.2.2 Control-Moment Gyros.....	5-12

5.2.3	Dual Counterrotating Annular Momentum Control Devices (DCAMCD).....	5-13
5.2.4	Use of the ATSS Counterrotator for Attitude Control.....	5-21
5.3	Discussion and Comparison of Attitude Control Mechanism.....	5-22
5.3.1	Reaction Jets.....	5-22
5.3.2	Control-Moment Gyros.....	5-22
5.3.3	Dual Counterrotating Annular Momentum Control Devices....	5-24
5.3.4	Use of the ATSS Counterrotators.....	5-24
5.3.5	General Remarks.....	5-24
5.4	Orbit Altitude Control.....	5-26
	References.....	5-27
6.0	EXAMINATION OF POTENTIAL APPLICATIONS OF ELECTROTHERMAL PROPULSION FOR ATTITUDES AND ORBIT CONTROL.....	6-1
6.1	Electrothermal Thruster.....	6-1
6.2	Application to the Gravity-Gradient Disturbance.....	6-3
6.3	Application to the Atmospheric Drag.....	6-5
6.4	Application to the Solar Radiation Disturbance.....	6-8
6.5	Arc Jet Electrothermal Thruster Option.....	6-8
6.6	Summary.....	6-10
	References.....	6-11
7.0	SPACE STATION STRUCTURES AND LAUNCH VEHICLE TECHNOLOGIES.....	7-1
7.1	Scope of Analyses and Discussions.....	7-1
7.2	Launch Vehicles.....	7-2
7.2.1	National Space Transportation System and Expendable Launch Vehicles.....	7-2
7.2.2	Past and Future United States Launch Vehicles.....	7-4
7.2.3	Launch Services Available from Foreign Nations.....	7-6
7.3	Expandable Structural Configurations.....	7-8
7.3.1	Structural Configurations for a NSTS Launch.....	7-8
7.3.2	Structural Configurations for a Saturn V Launch.....	7-16
7.3.3	Structural Configuration for a Jarvis Launch.....	7-20
7.3.4	Structural Configurations for an Advanced HLLV Launch....	7-23
7.4	Modular Structure Concepts using NSTS External Tanks.....	7-23
7.4.1	Torus from Tanks.....	7-23
7.4.2	Elemental Rotating Space Station from Tanks.....	7-26

7.5	Structural Weight Trades of Aluminum Alloy Versus Aerospace Advanced Structural Composites.....	7-27
7.6	Payload Mass Savings Effect on Number of Launches Required.....	7-36
7.7	Conclusions and Recommendations.....	7-37
	References.....	7-40
8.0	ATSS APPLICATION FOR LUNAR BASE BUILD-UP AND MARS MISSION SUPPORT.....	8-1
8.1	Planetary Missions.....	8-1
8.2	Lunar Base Build-up.....	8-5
8.3	Interface Between the ATSS and Lunar and Planetary Missions.....	8-9
	References.....	8-11
9.0	IDENTIFICATION AND ASSESSMENT OF TECHNOLOGY DEVELOPMENTS REQUIRED FOR THE ADVANCED-TECHNOLOGY SPACE STATION.....	9-1
9.1	Identification and Ranking of Pacing Technologies.....	9-1
9.1.1	Improved Resistojet Thruster Systems.....	9-5
9.1.2	Attitude Control Technology Assessment.....	9-6
9.2	Technology Trends.....	9-7
	References.....	9-11
APPENDIX:	ATSS ON-BOARD POWER GENERATION SYSTEM DESCRIPTIONS.....	A-1
A.1	RADIOISOTOPE DECAY HEAT SOURCE (Pu ²³⁸).....	A-2
A.1.1	Radioisotope Decay System Considerations.....	A-2
A.1.2	System Features for a Radioisotope Decay Power Source....	A-6
A.1.2.1	Core Concept, Power Level Definition.....	A-6
A.1.2.2	Heat Transfer Considerations.....	A-8
A.1.2.3	Accommodations for Fueling and Start Up.....	A-11
A.1.3	Shielding Requirements.....	A-13
A.1.4	Summary of System Masses.....	A-17
A.1.4.1	Core Elements.....	A-17
A.1.4.2	Shields.....	A-19
A.1.4.3	Converters.....	A-19
A.1.4.4	Radiators.....	A-21
A.1.5	Control Considerations.....	A-23

A.1.6	Particular Considerations.....	A-28
A.1.6.1	Helium Released as Alpha Particles.....	A-28
A.1.6.2	Thermal Control During Fabrication and Transport.....	A-28
A.2	FUSION POWER.....	A-29
A.2.1	Fusion as a Potential Heat Source.....	A-29
A.2.1.1	Magnetically Confined, Plasma Ignited Fusion.....	A-30
A.2.1.2	Inertially Confined Laser Ignited Systems.....	A-33
A.2.1.3	Muon Catalyzed Fusion.....	A-34
A.2.2	Fusion System Considerations for the ATSS Application....	A-36
A.2.3	ATSS Fusion System Features.....	A-39
A.2.3.1	Reactor Vessel, Energy Containment.....	A-39
A.2.3.2	Fuel Encapsulation and Feed.....	A-44
A.2.3.3	Laser Igniters.....	A-48
A.2.3.4	Liquid Metal Heat Transfer.....	A-50
A.2.3.5	Scavenge and Recovery, Vacuum Control, and Separation of Gasses.....	A-52
A.2.4	Mass Assessments for the Fusion System.....	A-53
A.2.4.1	Reactor and Containment Section.....	A-53
A.2.4.2	Fuel Feed Encapsulation.....	A-55
A.2.4.3	Laser Units.....	A-55
A.2.4.4	Scavenge and Separation.....	A-56
A.2.4.5	Heat Transfer Section.....	A-56
A.2.4.6	Convertors and Radiators.....	A-57
A.2.5	Fusion System Control Requirements.....	A-57
A.2.6	Particular Considerations for a Fusion Power System.....	A-63
A.3	ADVANCED PHOTOVOLTAIC ENERGY SOURCES.....	A-65
A.3.1	Photovoltaic System Considerations.....	A-65
A.3.2	Solar Array Areas and Solar Panel Requirements.....	A-67
A.3.3	Energy Storage Considerations.....	A-70
A.3.4	Photovoltaic System Definition and Location.....	A-76
A.3.5	Summary of Mass Estimates.....	A-77
A.3.5.1	Panel Mass Estimates.....	A-82
A.3.5.2	Panel Support Structure Estimates.....	A-82
A.3.5.3	Radiator Estimates.....	A-83
A.3.6	Effects of Concentration.....	A-83
A.3.7	Photovoltaic System Controls.....	A-88
A.3.8	Particular Considerations.....	A-94
	References.....	A-96

LIST OF TABLES

TABLE 4.1-1	ATSS ELECTRICAL POWER GENERATION ALTERNATES FOR COMPARISON, SUMMARY OF FEATURES AND CONSIDERATIONS.....	4-3
TABLE 4.1-2	SYSTEM DEFINITION AND EVALUATION CRITERIA.....	4-5
TABLE 4.3-1	COMPARISONS RANKING OF POWER SYSTEM MASS ASSESSMENTS FOR 2550 kW CONTINUOUS IN LOW EARTH ORBIT.....	4-10
TABLE 4.3-2	COMPARISON OF MASS CONTRIBUTIONS FOR THE ATSS POWER SYSTEM ALTERNATES.....	4-12
TABLE 5.2-1	TORQUE AND ANGULAR MOMENTUM REQUIREMENTS (from Reference 5-2).....	5-7
TABLE 7.1-1	STRUCTURES CONCEPTS EVALUATED FOR SELECTED LAUNCH VEHICLES.....	7-3
TABLE 7.2-1	SOME CURRENT USA LAUNCH VEHICLES COMPARED WITH THE SATURN VEHICLES.....	7-5
TABLE 7.2-2	EXPENDABLE LAUNCH VEHICLES OF THE WORLD (adapted from Reference 7-9).....	7-7
TABLE 7.3-1	HOW TO PUT A 15.24 m (50 ft) DIAMETER TUBE IN SOMETHING SMALLER (DAISY PETAL FOLD CONCEPT)	7-15
TABLE 7.5-1	COMPOSITE COMPONENT DEVELOPMENT (Reference 7-18).....	7-29
TABLE 7.5-2	EXAMPLES OF MATRIX RESINS.....	7-31
TABLE 7.5-3	COMPARISON OF MECHANICAL PROPERTIES OF SOME STRUCTURAL MATERIALS (Reference 7-18).....	7-31
TABLE 7.5-4	COMPARATIVE PROPERTIES OF A STRUCTURAL SHAPE (Reference 7-19).....	7-35
TABLE 7.7-1	POTENTIAL LAUNCH SYSTEMS COMPARED FOR DELIVERY OF TORUS SEGMENTS TO LEO (TELESCOPIC vs. MODULAR).....	7-38
TABLE 8.1-1	SUMMARY OF REFERENCE MANNED MARS MISSION REQUIREMENTS (Reference 8-1).....	8-2
TABLE 8.1-2	PLANETARY MISSIONS PERFORMANCE SUMMARY (Reference 8-2).....	8-3
TABLE 8.1-3	PLANETARY MISSION IMPACTS ON THE SPACE STATION (Reference 8-2).....	8-4
TABLE 8.3-1	SURVEY OF LUNAR AND PLANETARY MISSION REQUIREMENTS ON ATSS.....	8-10

TABLE 9.1-1	RANKING CRITERIA FOR TECHNICAL NEED OR CRITICALITY RELATIVE TO THE ADVANCED-TECHNOLOGY SPACE STATION.....	9-2
TABLE 9.1-2	SUMMARY OF THE TECHNOLOGICAL REQUIREMENTS FOR THE ADVANCED-TECHNOLOGY SPACE STATION.....	9-3
TABLE 9.2-1	POTENTIAL FUNCTIONS TO BE SUPPORTED BY THE ADVANCED-TECHNOLOGY SPACE STATION.....	9-8
TABLE A-1	SUMMARY OF ENERGY CONVERSION PARAMETERS FOR 2550 kW.....	A-4
TABLE A-2	SUMMARY OF THERMODYNAMIC PERFORMANCE AND PHYSICAL PARAMETERS FOR A Pu238 RADIOISOTOPE DECAY HEAT SOURCE.....	A-14
TABLE A-3	SUMMARY OF RADIATION SHIELDING PARAMETERS FOR A Pu238 RADIOACTIVE DECAY POWER SOURCE.....	A-16
TABLE A-4	SUMMARY OF MASS ESTIMATES FOR A Pu238 RADIOACTIVE HEAT SOURCE.....	A-18
TABLE A-5	SUMMARY OF Pu238 HEAT SOURCE CONTROL REQUIREMENTS.....	A-24
TABLE A-6	SUMMARY OF CONTROL REQUIREMENTS FOR A 450 kW 400 Hz CONVERTER (CLOSED CYCLE GAS TURBINE DRIVEN, LIQUID METAL HEAT TRANSFER ENERGY INPUT).....	A-26
TABLE A-7	OPERATING PARAMETERS FOR AN ATSS FUSION HEAT SOURCE SCALED FROM A PROPOSED INERTIALLY CONFINED LASER-IGNITED POWER STATION CONCEPT.....	A-37
TABLE A-8	PERTINENT FEATURES FOR THE ATSS INERTIALLY CONFINED LASER-IGNITED FUSION HEAT SOURCE.....	A-39
TABLE A-9	SUMMARY MASS ESTIMATES FOR INERTIALLY CONFINED LASER-IGNITED FUSION HEAT SOURCE.....	A-54
TABLE A-10	FUSION POWER SYSTEM CONTROL REQUIREMENTS.....	A-58
TABLE A-11	ATSS LOCATIONS AND AREAS AVAILABLE FOR PHOTOVOLTAIC PANEL INSTALLATIONS.....	A-69
TABLE A-12	ATSS ELECTROCHEMICAL ENERGY STORAGE OPTIONS SUMMARY.....	A-71
TABLE A-13	ATSS FLYWHEEL ENERGY STORAGE, OPTIONS.....	A-73
TABLE A-14	SUMMARY OF MASS ESTIMATES FOR ATSS PHOTOVOLTAIC SYSTEM OPTIONS.....	A-81
TABLE A-15	EFFECTS OF SOLAR CONCENTRATION.....	A-87

TABLE A-16 SUMMARY OF SYSTEM MASSES FOR SOLAR
CONCENTRATION SYSTEM..... A-89

TABLE A-17 SUMMARY OF PHOTOVOLTAIC POWER SYSTEM CONTROL
REQUIREMENTS..... A-90

LIST OF FIGURES

Figure 1.0-1	Baseline Configuration Dual-Keel Space Station, Principal Features.....	1-2
Figure 1.0-2	Advanced-Technology Space Station Concept, Principal Features of Reference Configuration.....	1-3
Figure 2.0-1	ATSS Subassembly Masses.....	2-2
Figure 2.0-2	ATSS Dimensions.....	2-3
Figure 5.0-1	Orientation of the ATSS in Orbit.....	5-2
Figure 5.1-1	Aerodynamic Force on the ATSS as a Function of Orbit Angle.....	5-3
Figure 5.1-2	Aerodynamic Torque on the ATSS as a Function of Orbit Angle.....	5-3
Figure 5.1-3	Solar Radiation Force on the ATSS as a Function of Orbit Angle.....	5-4
Figure 5.1-4	Gravity Gradient Torque on the ATSS as a Function of Orbit Angle.....	5-4
Figure 5.2-1	Aerodynamic Momentum on the ATSS as a Function of Orbit Angle.....	5-6
Figure 5.2-2	Gravity Gradient Momentum on the ATSS as a Function of Orbit Angle.....	5-6
Figure 5.2-3	Typical Space Station/NASA Configuration--Power Tower (from Reference 5-3).....	5-7
Figure 5.2-4	Assumed Thrust Jet Locations.....	5-10
Figure 5.2-5	Geometry of Dual Counterrotating Annular Momentum Control Device Wheels.....	5-14
Figure 5.2-6	Flywheel Shape Factors for Various Geometries.....	5-16
Figure 5.2-7	Flywheel Materials.....	5-17
Figure 5.2-8	Values of k/r_0 , K_S , and K_S' for Various Flywheel Cross Sections.....	5-18
Figure 5.2-9	Effect of Materials and Geometry on Mass Required to Generate Angular Momentum.....	5-20
Figure 5.3-1	Advanced IPACS Unit Design Concept (from Reference 5-3).....	5-23
Figure 6.1-1	Operational Regimes for Electrical Thrusters.....	6-2

Figure 6.1-2	Resistojet Specific Impulse Trends.....	6-2
Figure 6.1-3	Thrust-to-Power Ratio vs. Specific Impulse.....	6-2
Figure 7.2-1	Soviet Space Launcher Fleet (adapted from Reference 7-10).....	7-9
Figure 7.2-2	International Expendable Launch Vehicles (adapted from Reference 7-11).....	7-10
Figure 7.3-1	ATSS Torus Assembly of Cylindrical Segments (Reference 7-2).....	7-11
Figure 7.3-2	Expandable Habitat Module, Harden-In-Space.....	7-12
Figure 7.3-3	Hinge Foldable Cylinder for a Shuttle Launch.....	7-14
Figure 7.3-4	Shuttle Launched Telescopic Cylinders to Form a Torus.....	7-17
Figure 7.3-5	Hinge Foldable Cylinder for a Saturn Launch.....	7-18
Figure 7.3-6	Saturn Launched Telescopic Cylinders to Form a Torus.....	7-19
Figure 7.3-7	Hinge Foldable Cylinder for a Jarvis Launch.....	7-21
Figure 7.3-8	Jarvis Launched Telescopic Cylinders to Form a Torus.....	7-22
Figure 7.4-1	NSTS External Tank Structure (adapted from References 7-14 and 7-15).....	7-24
Figure 7.4-2	Elemental Rotating Space Station.....	7-28
Figure 7.5-1	Relative Strength of Aircraft Materials (adapted from Reference 7-18).....	7-33
Figure 8.2-1	Lunar Base Launch Requirements.....	8-6
Figure 8.2-2	Material at Lunar Base at Years End.....	8-7
Figure 8.2-3	Estimated Manning Levels of Lunar Base (Reference 8-2).....	8-8
Figure A-1	Concept for a Pu ²³⁸ Radioisotope Decay Heat Source.....	A-7
Figure A-2	Concept for a Pu ²³⁸ Radioisotope Decay Heat Source.....	A-9
Figure A-3	Pu ²³⁸ -BeO Core Component Details.....	A-10
Figure A-4	Concept for a Liquid Metal Electromagnetic Pump (from Reference A-7).....	A-12

Figure A-5	Shield Element Model.....	A-15
Figure A-6	Converter Section Concept.....	A-20
Figure A-7	Radiator Panel Concept (102 for Each Converter).....	A-22
Figure A-8	Principal Features for a Magnetically Confined Toroid, "Tokamak", Fusion Heat Source (from Reference A-8).....	A-32
Figure A-9	Concept for the ATSS Fusion Power System, Plan View.....	A-41
Figure A-10	Concept for the ATSS Fusion Power System, Side View.....	A-42
Figure A-11	Cross Section Through the Fusion Reactor Vessel.....	A-43
Figure A-12	Concept for Liquid Lithium Flow within the Reactor....	A-45
Figure A-13	Concept for Establishing a Flowing Liquid Lithium Wall within the Reactor Vessel.....	A-46
Figure A-14	Candidate Configurations for Encapsulated Fusion Fuel Pellets.....	A-47
Figure A-15	Concept for a Rotating Wheel Fuel Pellet Injector.....	A-49
Figure A-16	Features of a Liquid Lithium to NaK Heat Exchanger.....	A-51
Figure A-17	ATSS Prime Areas for Locating Photovoltaic Panels.....	A-68
Figure A-18	Concept for an Energy Storage Unit Using a Glass Fiber Composite Flywheel.....	A-74
Figure A-19	Photovoltaic Panel Locations on the Platform.....	A-78
Figure A-20	Concept for Mounting Photovoltaic Panels on the Torus.....	A-79
Figure A-21	Torus Mounted Panel Concept and Features.....	A-80
Figure A-22	Concept for a Concentrating Solar Photovoltaic Power Module.....	A-84
Figure A-23	Geometric Considerations for Linear Parabolic Reflecting Concentrators.....	A-86

ABSTRACT

This is the fourth in a series of reports which document studies of an advanced-technology space station configured to implement subsystem technologies projected for availability in the time period 2000 to 2025. The principal objectives of these studies have been to examine the practical synergies in operational performance available through subsystem technology selection and to identify the associated advanced technology development needs. In this study further analyses are performed on power system alternates, momentum management and stabilization, electrothermal propulsion, composite materials and structures, launch vehicle alternatives, and lunar and planetary missions. Concluding remarks are made regarding the advanced-technology space station concept, its intersubsystem synergies, and its system operational and subsystem advanced technology development needs.

ABBREVIATIONS AND ACRONYMS

AC	Alternating Current (amperes)
ACC	Aft Cargo Carrier
ALSEP	Apollo Lunar Science Experiment Pallet
ATSS	Advanced-Technology Space Station
CMG	Control-Moment Gyro
C/O	Checkout, Electrical Acceptance Test
C_3	Velocity Factor for Trajectory Energy Requirement, m/sec^2 (ft/sec^2)
CTRSS	Current Technology Rotating Space Station
D	Inner Diameter of a Radiation Shield, m (ft)
DC	Direct Current (amperes)
DCAMCD	Dual Counterrotating Annular Momentum Control Devices
E	Modulus of Elasticity for a Material, GPa (lb/in^2) and Kinetic Energy, Joules ($ft-lb$)
ECLSS	Environmental Control and Life Support Systems
ELV	Expendable Launch Vehicle
EIR	Eastern Test Range
EVA	Extravehicular Activity
F	Factor to Account for Supporting Structure
F_{TU}	Ultimate Tensile Strength, Pa (lb/in^2)
G	Gravitational Constant, $\frac{N-m^2}{kg^2}$ ($\frac{ft^2}{lb}$)
g	Earth Gravitational Acceleration, $9.8 m/sec^2$ ($32.2 ft/sec^2$)
GN&C	Guidance, Navigation, and Control
GEO	Geosynchronous Equatorial Orbit
H	Angular Momentum about an axis, N-m sec ($lb-ft-sec$)
HEO	High Earth Orbit
HL	Half Life for a Radioactive Isotope Decay (time)

HLLV	Heavy Lift Launch Vehicle
I	Moment of Inertia, $\text{kg}\cdot\text{m}^2$ (lb-ft ²)
IDEAS ²	Integrated Design Engineering Analysis Software - Interactive Design and Evaluation of Advanced Spacecraft
IOC	Initial Operating Capability
IPACS	Internal Powered Attitude Control System
Isp	Specific Thrust, $\frac{\text{N}\cdot\text{sec}}{\text{kg}}$ (sec)
IVA	Intravehicular Activity
k	Radius of Gyration for a Rotating Shape, m (ft)
K _S	Dimensionless Shape Factor for Flywheels
K _S '	Dimensionless Shape Factor for Flywheels Relative to the Outer Radius
ksi	Thousands of Pounds per Square Inch
L	Torque, N-m (lb-ft)
ℓ	Moment Arm, m (ft)
LAMB	Large Angle Magnetic Bearing
LEO	Low Earth Orbit
m	Mass Element, kg (lb)
M	Total Mass, kg (lb)
M _e	Mass of the Earth, kg (lb)
MPD	Magnetoplasmadynamic Propulsion Systems
N	Number
NaK	Sodium Potassium Mix, Liquid at Ordinary Temperatures
NSTS	National Space Transportation System
OMV	Orbital Maneuvering Vehicle
OTV	Orbital Transfer Vehicle
r	Radius, cm (in)
r ₀	Maximum Allowable Wheel Radius, m (ft)

R_0	Radius from the Center of the Earth to Orbit, km (mi)
rf	Radio Frequency Electromagnetic Waves
SNAP	Space Nuclear Auxiliary Power Unit
SSO	Sun Synchronous Orbit
T	Thrust, N (lb) or, Thickness of a Radiation Shield (Appendix), m (ft)
T	Total, (subscript)
TaCHO	Tantalum Aldehyde
TDRSS	Tracking and Data Relay Satellite System
ULV	Unmanned Launch Vehicle
UV	Ultraviolet
VOL	Volume, m^3 (ft^3)
W	Total Mass of Fuel, kg (lb)
w	Mass of Fuel used for each Jet, kg (lb)
α	Angle Between the Axis of the ATSS Central Tube and Local Nadir to Earth, deg
β^-	Radioactively Emitted Electron
θ	Orbit Angle Measured from Solar Zenith, deg
λ	Relaxation Length, cm (in). Attenuates Radiation by a Factor of "e" (2.718)
μ	Relative to a Counterrotator (subscript)
ν	Tilt Angle for Counterrotators, deg
ρ	Density, kg/m^3 (lb/ft^3)
σ	Working Stress, Pa (lb/in^2)
τ	Time Duration of Thrust, sec
ω	Angular Velocity, rad/sec

Superscripts

-	Average
.	Derivative with Respect to Time

1.0 INTRODUCTION

One of the goals of the United States Space Program is the establishment of permanent manned space stations, and current plans are to have an initial operating capability (IOC) as Space Station Freedom in low Earth orbit by 1995. The design is still evolving; however, a proposed dual-keel configuration is shown in Figure 1.0-1. References 1-1 and 1-2 provide some of the details for the dual-keel configuration. As the design progresses, changes may eliminate the dual-keel and reduce the structure. However, Space Station Freedom will operate nadir pointing and rotate about its transverse axis at the rate of one revolution per orbit. Space Station Freedom will provide a microgravity environment and be a stable platform for observation of the Earth. It will support a broad range of space-related operations or scientific investigations.

Studies of space stations are under way for the more distant future. These will utilize advanced technology and perform functions in support of future space missions. One series of studies is concerned with examining various aspects of a space station for the time period around the year 2025. Three reports have been published in this series of studies (References 1-3 through 1-5). The first study (Reference 1-3) led to the conceptual configuration shown in Figure 1.0-2, which is basically a rotating space station with an inertially oriented central section. The second study (Reference 1-4) used that configuration as a starting point to examine the configuration and its functions in some detail, and to identify pacing technology areas. The third study (Reference 1-5) performed trade studies in the station power system, analyzed the dynamics of the rotating station, studied locomotion and

ORIGINAL PAGE IS
OF POOR QUALITY

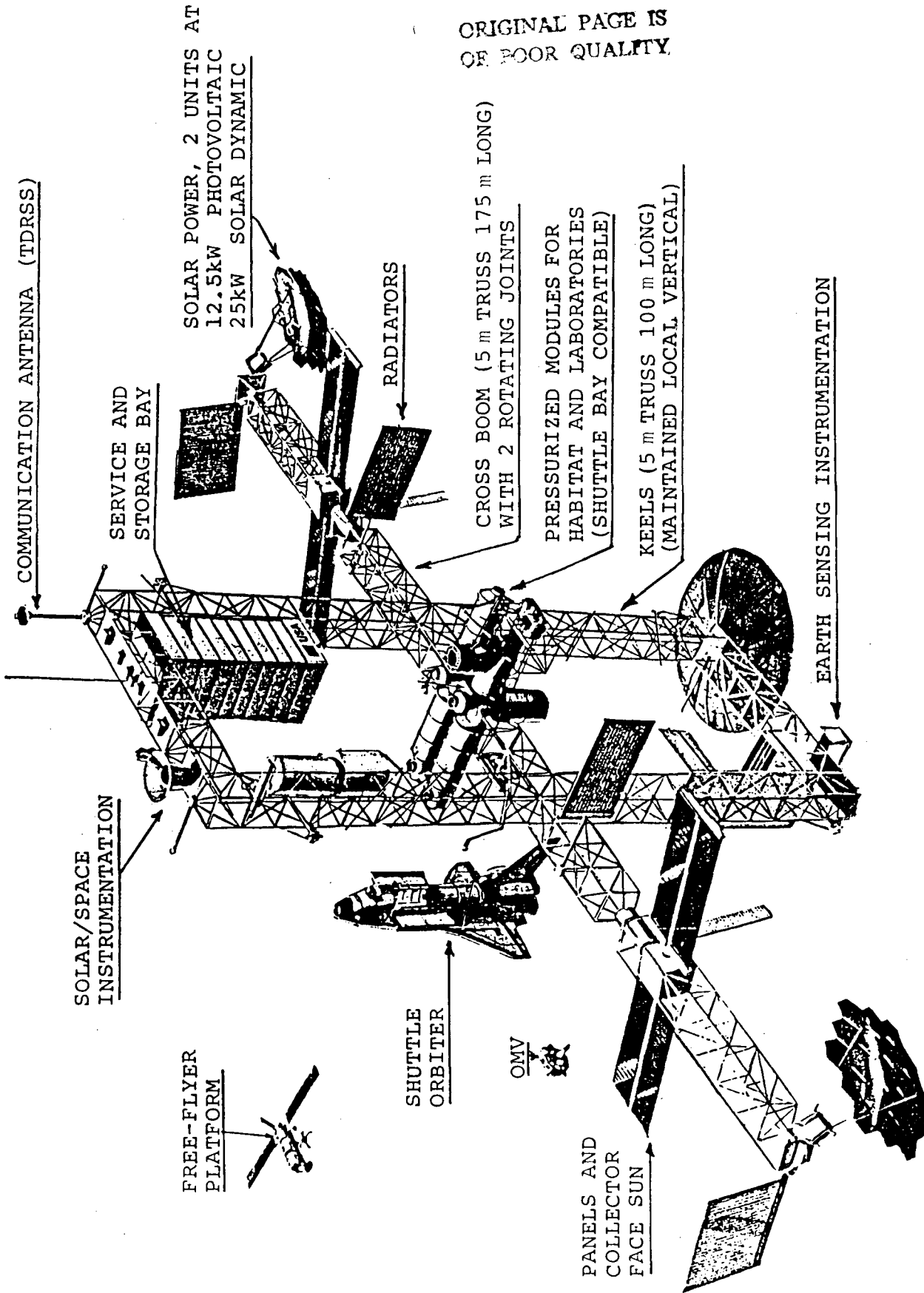
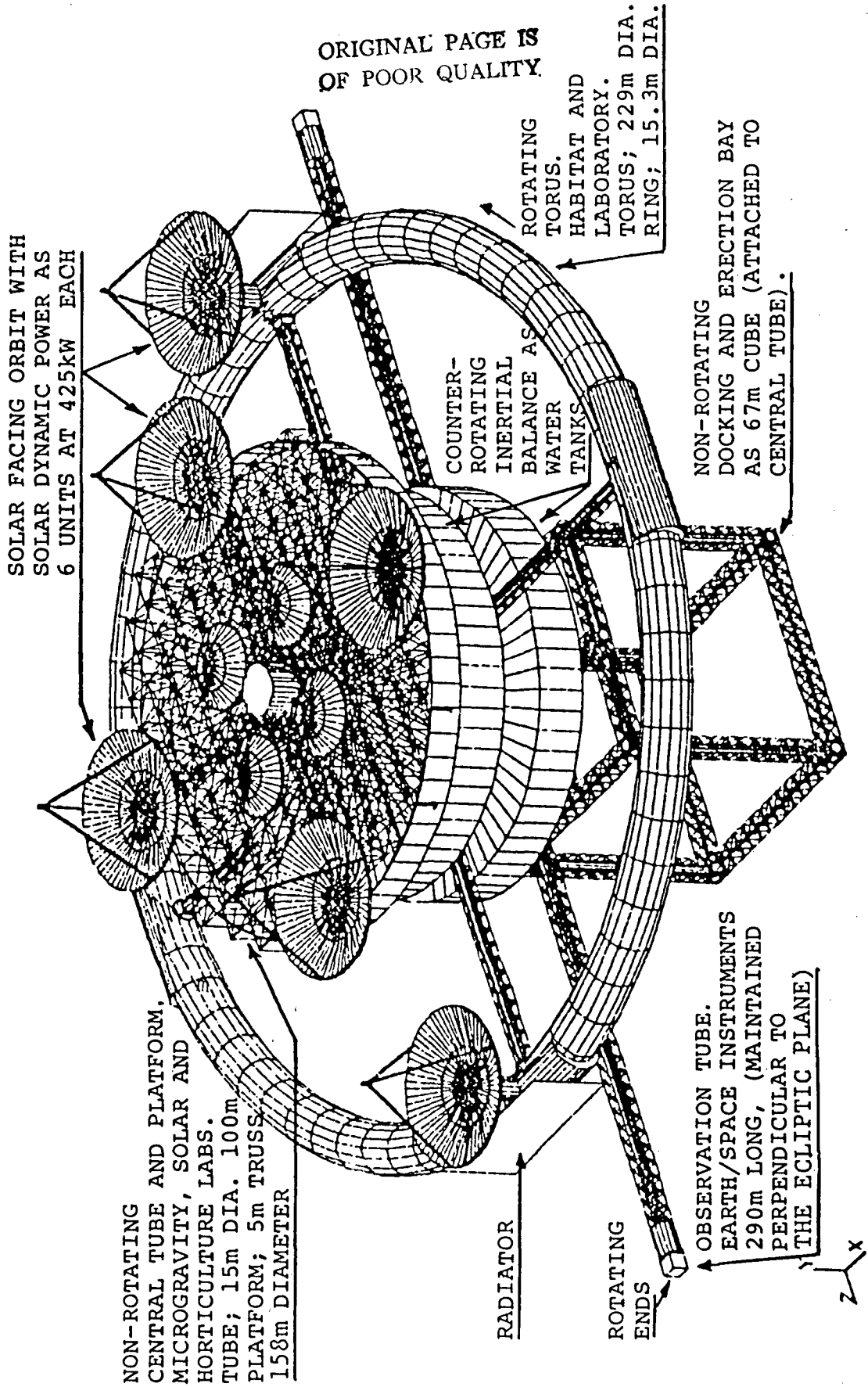


Figure 1.0-1 Baseline Configuration Dual-Keel Space Station, Principal Features



ORIGINAL PAGE IS
OF POOR QUALITY.

SOLAR FACING ORBIT WITH
SOLAR DYNAMIC POWER AS
6 UNITS AT 425kW EACH

NON-ROTATING
CENTRAL TUBE AND PLATFORM,
MICROGRAVITY, SOLAR AND
HORTICULTURE LABS.
TUBE; 15m DIA. 100m
PLATFORM; 5m TRUSS.
158m DIAMETER

RADIATOR

ROTATING
ENDS

OBSERVATION TUBE.
EARTH/SPACE INSTRUMENTS
290m LONG, (MAINTAINED
PERPENDICULAR TO
THE ECLIPTIC PLANE)

COUNTER-
ROTATING
INERTIAL
BALANCE AS
WATER
TANKS

ROTATING
TORUS.
HABITAT AND
LABORATORY.
TORUS; 229m DIA.
RING; 15.3m DIA.

NON-ROTATING
DOCKING AND ERECTION BAY
AS 67m CUBE (ATTACHED TO
CENTRAL TUBE).

Figure 1.0-2 Advanced-Technology Space Station Concept, Principal Features of Reference Configuration

material transfer under artificial gravity forces, and examined design considerations for support of a manned Mars mission. Reported herein are the results of the fourth and final study in the series on an advanced-technology space station (ATSS).

The rotating ATSS (summarized in Section 2) provides an artificial gravity field, which reduces medical and physiological problems associated with weightless long-duration space flight. This approach introduces unique challenges in attitude stabilization and accommodation of large rotating elements. Furthermore, the ATSS is designed to host a large crew and perform numerous experiments, which means it is very large and has a heavy electrical power demand. In addition, the ATSS is designed to support missions beyond low Earth orbit which bring new operational challenges. Some aspect of each of these major challenges-attitude control, size, mass, power, and operations - is analyzed in this study. Specific topics include: Power System Alternates (Section 4); momentum management and stabilization (Sections 5 and 6); structures, materials, and launch vehicles (Section 7); and lunar and planetary missions (Section 8). Concluding remarks regarding R&D requirements-the driving theme in all four studies - are made on the subjects of advanced subsystem technology needs, station design to enhance intersubsystem technology needs, station design to enhance intersubsystem synergies, and space station operations for mission support (Section 9).

References

- 1-1 Space Station Reference Configuration Description. NASA Report JSC 1989, August 1984
- 1-2 Architectural Control Document. Preliminary Report, NASA JSC Space Station Office, June 1986
- 1-3 Queijo, M. J. et al.: An Advanced-Technology Space Station for the Year 2025. Study and Concepts, NASA CR-178208, March 1987
- 1-4 Queijo, M. J. et al.: Analysis of a Rotating Advanced-Technology Space Station for the Year 2025, NASA CR-178345, January 1988
- 1-5 Queijo, M. J. et al.: Some Operational Aspects of a Rotating Advanced-Technology Space Station for the Year 2025, NASA CR 181617, June 1988.

2.0 ROTATING ADVANCED-TECHNOLOGY SPACE STATION CONFIGURATION

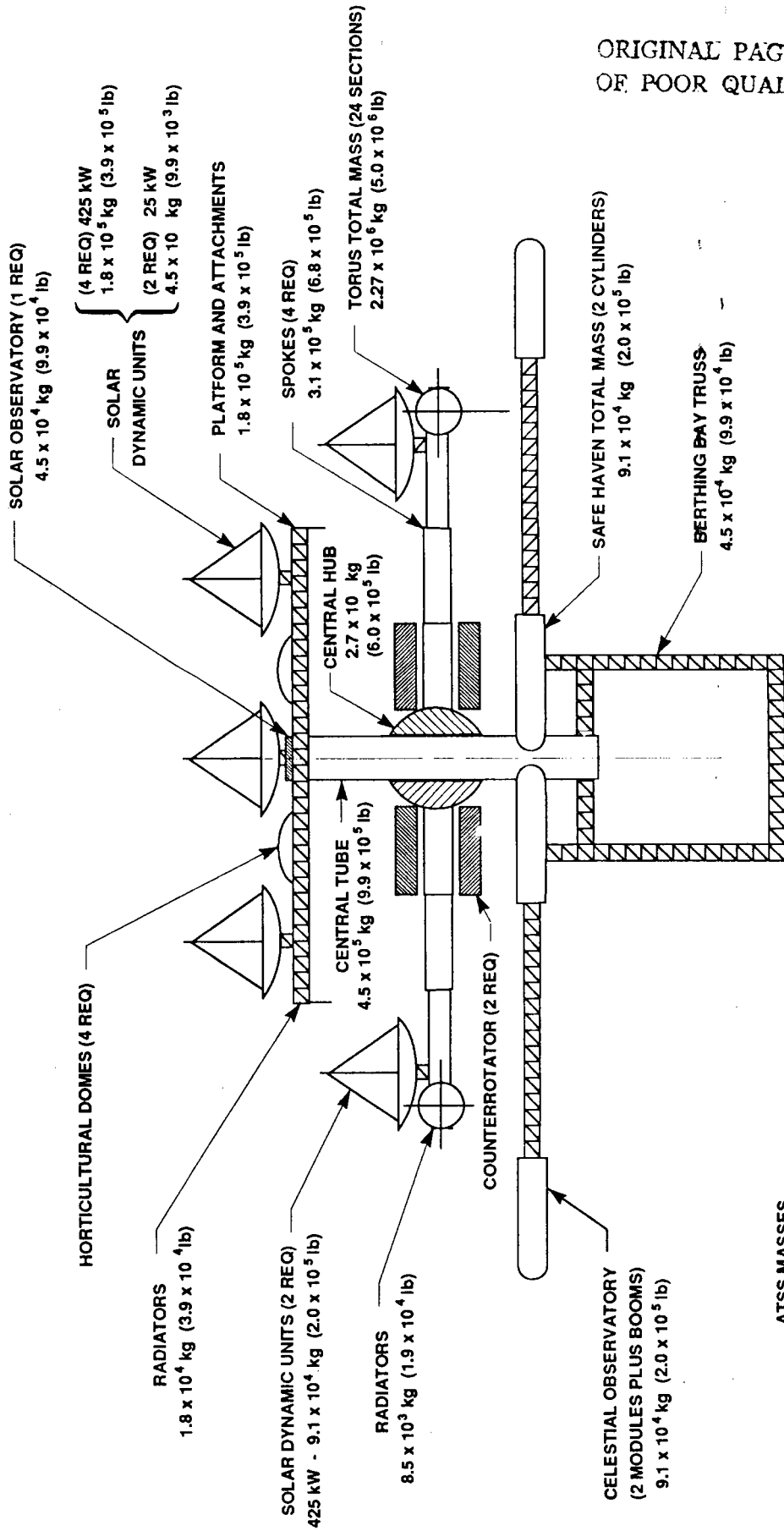
The configuration used as a starting point for the present study is described in some detail in Reference 1-4, and the major features are repeated here for convenience and reference. Relevant weights and dimensions of elements of the ATSS are given in Figure 2.0-1 and 2.0-2, respectively.

A major feature of the ATSS is the large rotating torus which provides artificial gravity (centrifugal force) for the crew in their primary habitat and work area, and also provides for gas (O_2 and H_2) storage. An artificial gravity of one Earth g , 9.8 m/sec^2 (32.2 ft/sec^2), can be obtained at 2.8 revolutions per minute. Two solar dynamic units on the torus provide electrical power for use in the torus.

The other components of the ATSS are attached to a central tube which does not rotate with the torus. These units include Earth, solar, and celestial observatories; a platform with horticultural domes and four solar dynamic units; plus a section for berthing, loading, and unloading spacecraft. The entire ATSS is Sun-pointing; therefore, it must precess at the rate of one revolution per year.

The baseline configuration had two alternatives, one with and one without storage tanks that counterrotate with respect to the torus. Reasons for considering and selecting the use of counterrotating tanks are discussed in Section 5 of Reference 1-4. The tanks store fluid (water) and reduce the net angular momentum of the ATSS. This ATSS configuration is the baseline used for the analyses of this study.

ORIGINAL PAGE IS
OF POOR QUALITY.



ATSS MASSES

TORUS AND NONROTATING 4.2×10^6 kg (9.3×10^6 lb)

ATSS WITH COUNTERROTATORS 8.5×10^6 kg (1.9×10^7 lb)

Figure 2.0-1 ATSS Subassembly Masses

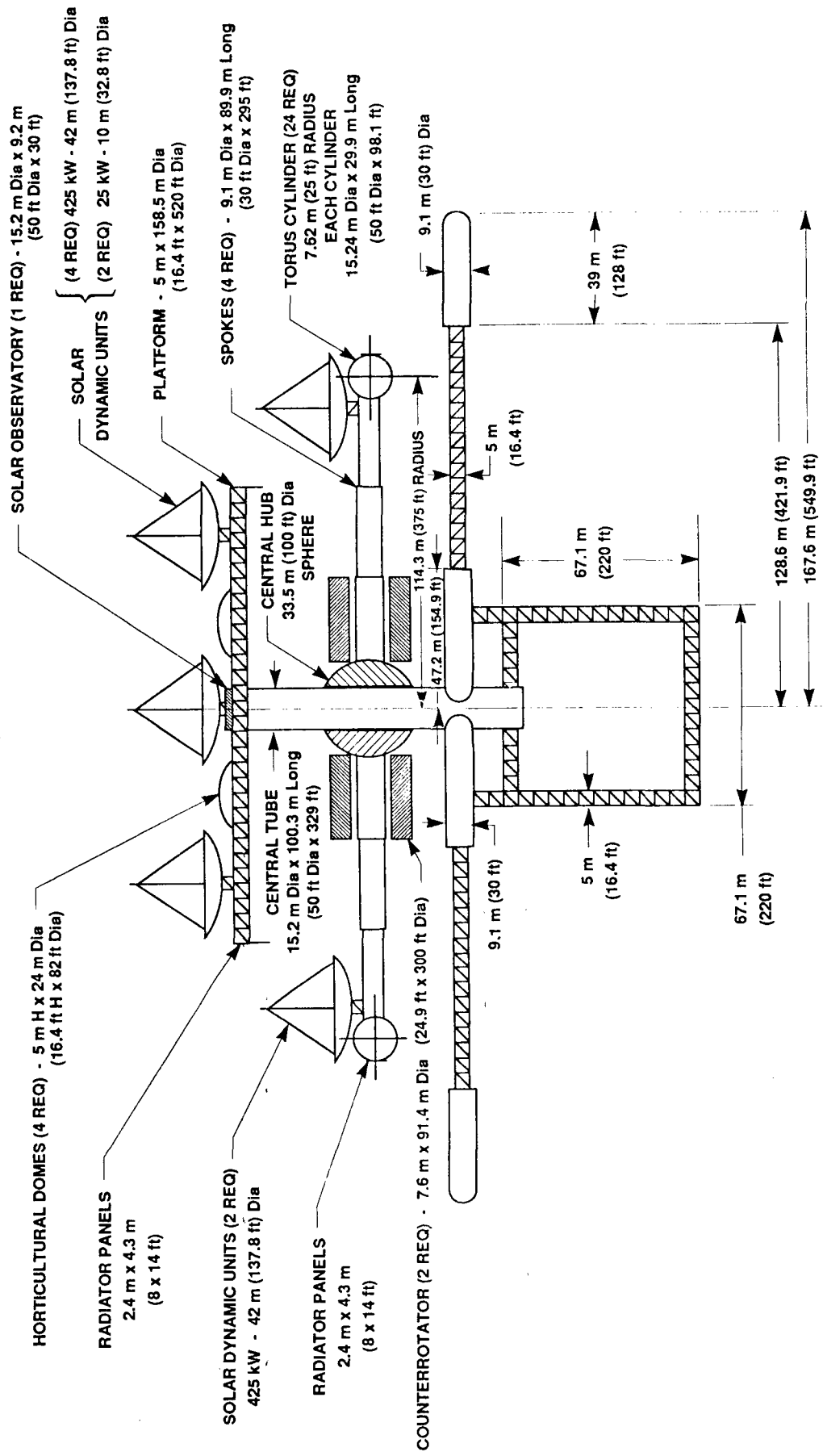


Figure 2.0-2 ATSS Dimensions

3.0 PURPOSE OF THIS STUDY

This study is a continuation of the work reported in References 1-3, 1-4, 1-5. The general tasks are:

1. Compare system alternates for power generation.
2. Examine momentum management and stabilization of a large space station with substantial rotating constituents.
3. Evaluate electrothermal propulsion options to fulfill the requirements for attitude stabilization and control.
4. Survey opportunities and advantages of incorporating composite materials and space expandable structures into the space station design.
5. Enumerate the roles and functions of an advanced space station in support of a lunar base mission and a manned Mars mission.
6. Identify advanced technology development needs to achieve the projected subsystem capabilities in the 2025 time frame.

Some specific issues associated with each of the task topics are described in the following paragraphs.

3.1 Electrical Power System Alternates

The baseline configuration consists of six identical solar concentrating thermodynamic power units that provide a combined power output capacity of 2.5 MW. Their operation requires solar pointing for the ATSS and accommodating the interruption of solar input during each orbit. A nuclear fission power system which operates continuously and does not need solar pointing was examined and described in Reference 1-5. In this study three additional alternate systems are examined for comparative purposes. Two of the systems, radioisotope decay and nuclear

fusion, operate continuously and do not need solar pointing. The third is an advanced solar photovoltaic system and does require pointing. Subsystem masses and ATSS performance capabilities for these alternate power systems are examined and compared to provide information on recommended technology requirements.

The major area of technology advance required for the solar photovoltaic system is in solar cell output efficiency. For the radioisotope thermodynamic power generation system, the merits of such a configuration in performance and simplicity of control are compared to the nuclear fission power system concept. A nuclear fusion power system is also discussed and compared. Each power alternate introduces specific constraints on operations and some potential advantages to the ATSS performance. The overall system effects of these power subsystem characteristics are defined. The trade studies and results illustrate areas for potential technology improvements.

3.2 Attitude Stabilization and Control

The presence of a large rotating torus introduces rotational momentum considerations into control evaluations. The combination of large non-symmetric masses and solar pointing creates large, cyclic, gravity gradient torques, and these offer the opportunity to examine novel control approaches. Attitude stabilization, pointing, and precession of the ATSS while experiencing environmental forces were studied to evaluate the capacity of reaction control systems and to examine options such as the use of control-moment gyros to assist in stabilization. The thrust levels required to achieve stability and control as well as the total control propellant requirements are defined.

The potential application of angular momentum control devices and an integrated power and control system are addressed.

3.3 Electrothermal Thrusters

The baseline ATSS configuration uses chemical combustion rocket thrusters for station keeping. These thrusters utilize hydrogen and oxygen generated from electrolysis of water as the propellant. The application of electrothermal thrusters are studied as an alternate because they also offer a potential synergy in using propellants which are byproducts of the life support subsystem. The electrothermal thrusters offer competitive specific impulse in the advanced technology versions but consume considerable electrical power and are limited in their upper level of thrust.

3.4 Structures, Material, and Launch Vehicles

The ATSS is comprised of numerous structural components of large mass and volume. The baseline design configuration incorporates modular aluminum pressure components assembled on orbit and requires a heavy lift launch vehicle (HLLV) for delivery to orbit. The potential is evaluated for alternate launch vehicles which can take advantage of the reduced unit volume afforded by several expandable structural concepts. Additional usage of composite structural materials is also examined to assess the benefit of a reduced number of launches to deliver the components of a rotating space station like the ATSS to LEO.

3.5 Lunar and Planetary Mission Support

The ATSS has the size and operational capability to function as a staging site for outbound missions from Earth. The lunar base support and planetary explorations are candidate future missions which were examined in a preliminary way to identify and describe the operational support functions that could be performed by the ATSS. Some typical prospects include: crew staging, vehicle assembly, propellant manufacturing and transfer, and post-mission experiment support.

3.6 Advanced Technology Identification

The advanced-technology space station (ATSS), as its name implies, is based on the assumption that new and emerging technologies will have advanced to the point of being viable for use in the ATSS, circa 2025.

Toward this end, ATSS system operational and subsystem technology needs, and associated synergistic benefits identified in this study, are described in context with those identified in the earlier studies in this series.

4.0 ONBOARD POWER GENERATION: A COMPARISON OF ALTERNATE HEAT SOURCES AND ADVANCED PHOTOVOLTAICS

The baseline for electrical power generation onboard the ATSS has been established as 2550 kW continuous provided by six identical solar dynamic units which deliver 425 kW each (Reference 4-1). A continuing study compared the solar dynamic units with a power generation system based upon a nuclear fission heat source. That study also defined the individual electrical power generators as closed cycle gas turbines driving 400 Hz, 440 V alternators operating with overall efficiency of 0.4 in converting thermal to electrical energy (Reference 4-2). The initial results from that comparison indicated a need to expand the comparison evaluation to include heat sources from radioisotope decay and fusion. In addition, the comparison evaluation needed to include a system based upon advanced photovoltaics which used correspondingly advanced techniques for energy storage as batteries, fuel cells, and flywheels. This section describes the additional comparisons.

4.1 Comparison Approach

These three additional power generating systems extend the previous comparisons of mass, control requirements, and configuration related considerations. The same general approach has been used. The initial step defines a configuration for the power generation system. The estimates of masses, the definition of control requirements, and the discussions of configuration related considerations are all based upon the system definition. For the radioisotope decay, fusion and advanced photovoltaic systems, the Appendix contains the individual system descriptions, estimates of mass, definitions of control requirements, and particular considerations. The comparisons utilize the results from each

of the system definitions and include the two previously compared. Table 4.1-1 summarizes the five electrical power generation systems and identifies the principal features included in the comparisons. The system definitions, mass estimates, and identification of control requirements were all intended to identify technology requirements and take advantage of any synergies with other systems or functions of the ATSS. The system definitions all utilized the same set of general guidelines or criteria. Table 4.1-2 lists these criteria, and they provide the basis for the comparison evaluations which follow.

4.2 General Results from Comparison

The comparison evaluations for the five alternates are contained in Section 4.3 below. The evaluations did reveal some significant differences, and the general results are summarized below in the order of increasing system mass and increasing system complexity.

4.2.1 Advanced Photovoltaics, Lowest Mass, Least Complex

The advanced photovoltaic system with energy storage as advanced fuel cells, appeared as the lowest-mass, least-complex system which can produce 2550 kW continuous electrical power. The configuration defined for the ATSS requires a significant improvement in the conversion efficiency of photovoltaics. The ATSS with an onboard generation of O₂ and H₂ for other uses makes fuel cells the most attractive energy storage option. The advanced system would provide electrical power at about 40 kg/kW. The use of solar concentrators for the photovoltaic system resulted in a factor of three mass penalty from the support structure and thermal considerations.

TABLE 4.1-1 ATSS ELECTRICAL POWER GENERATION ALTERNATES FOR COMPARISON, SUMMARY OF FEATURES AND CONSIDERATIONS

SYSTEM AND LOCATION OF DESCRIPTION	SYSTEM FEATURES AND DESCRIPTION	CONTROL REQUIREMENTS	PARTICULAR CONSIDERATIONS
Solar Dynamic Reference 4-1	Six identical units, four on the platform two on the torus. Full paraboloid of resolution concentrator with collector-converter assembly at focus. Each unit stores energy in phase change material during illumination, recovers energy during dark transit. Delivered electrical output is 425 kW as 400 Hz 440 V three phase AC powered by a closed cycle gas turbine operating at 0.4 thermal to electrical conversion efficiency.	<ul style="list-style-type: none"> o Solar pointing o Sunset-sunrise transitions o Energy storage o Thermal environment for the collector-converter assembly 	<ul style="list-style-type: none"> o Optical alignment during on-orbit assembly o Start up-shutdown transient o Solar pointing on a rotating torus
Fission Reactor Reference 4-1	Two cores of enriched U ²³⁵ moderated by BeO with liquid sodium coolant. Each core drives three converters by liquid Na to NaK heat exchangers. Both cores and all six heat exchangers are within a common radiation shield. Options: Radiation shields as lead, steel, concrete, and water	<ul style="list-style-type: none"> o Reactor heat extraction o Converter heat transfer materials at end of life o Radiation environment monitor o Provisions for emergency shutdown 	<ul style="list-style-type: none"> o Recovery of radioactive materials at end of life
Pu ²³⁸ Radioisotope Decay Appendix, A-1	Two cores of PuO ₂ -BeO mix each driving three converters. Core NaK coolant has direct heat exchange with the gas turbines. Both cores within a common radiation shield. Options: Radiation shields as lead or steel.	<ul style="list-style-type: none"> o Core heat transfer o Core start-up and shutdown transients 	<ul style="list-style-type: none"> o Thermal control of fuel elements during launch, supply flight, on-board preparation and end of life return

TABLE 4.1-1 ATSS ELECTRICAL POWER GENERATION ALTERNATES FOR COMPARISON, SUMMARY OF FEATURES AND CONSIDERATIONS (concluded)

SYSTEM AND LOCATION OF DESCRIPTION	SYSTEM FEATURES AND DESCRIPTION	CONTROL REQUIREMENT	PARTICULAR CONSIDERATIONS
Fusion: Inertially confined laser ignited Appendix A.2	Single reactor cavity with flowing liquid lithium walls. Fuel pellet injection and ignition by dual feeds and dual lasers. Reactor lithium flow is scavenged to recover tritium formed during fusion. Eight converters powered by liquid Li to NaK heat exchangers.	<ul style="list-style-type: none"> o Reactor liquid metal flow balance o Fuel encapsulation and feed o Laser timing and pulse generation o Reactor internal environment control o Extraction and separation of gases and products of fusion o Liquid metal heat transfer 	<ul style="list-style-type: none"> o Installation and start-up power requirements
Advanced Photovoltaic Appendix A.3	Advanced photovoltaic cell arrays deliver 0.2 solar input as electrical power at 280 V DC. Solar panels on both torus and platform. Energy stored during illumination is recovered during dark transit. Optional methods for energy storage: advanced batteries, O ₂ -H ₂ fuel cells, and advanced flywheels.	<ul style="list-style-type: none"> o Energy storage input o Energy recovery operation o Sunset-sunrise transitions 	<ul style="list-style-type: none"> o Thermal control during installation and start-up o Space debris impact damage

TABLE 4.1-2 SYSTEM DEFINITION AND EVALUATION CRITERIA

1. **Power Generation:** Each system provides a continuous source of electrical power that delivers 2550 kW to the operating systems within the ATSS. The individual systems may need to generate additional increments of power to overcome losses or other purposes, and these conditions are identified.
2. **Power Generation Equipment and Efficiency:** The rotating generator equipment utilizes a gas turbine driven alternator operating at 12000 rpm to produce three-phase alternating current at 400 Hz and 440 V. The turbine-alternator operates with a thermal-to-electrical energy conversion (throughput) efficiency of 0.4 and produces 450 kW total within each unit. All units are the same within each of the systems.
3. **Thermal Parameters Definitions:** Previous studies have defined the principal thermal parameters such as the solar energy input levels and the radiator temperatures and their corresponding thermal fluxes. These values together with power generation requirements establish the major "fixed" parameters for each system such as solar concentrator areas and radiator areas, fission fuel consumption, radioisotope decay, etc.
4. **Configurations Defined to Identify Technology:** The individual components and elements have been defined to identify technology needs. For components or elements which are presently in development such as the converters and photovoltaics, the definitions are development goals and indicate the degree of improvement required. For structure or material related items, the components are defined for present conventional materials (aluminum, 79Ni-13Cr-7Fe alloys, ZrO₂) to indicate the potential margins for improvement.
5. **Synergies:** The principal synergies are utilization of waste heat and multiple uses of water. The entire 2550 kW will be dissipated in some manner throughout the ATSS, and this dissipation will have opportunities to provide heat in one location utilizing the reject from another. For the specific case of the radiators which provide the heat sinks for the gas turbines, these have been configured as water-filled flat panels fabricated from aluminum. This radiator configuration is intended to show margin for improvement.

4.2.2 Radioisotope Decay Heat Sources

The Pu²³⁸ system provides an attractive source for a mission that requires a constant uninterrupted electrical power supply. The mass requirements for radiation shielding and the converter radiators dominate the configuration. Advanced radiators coupled with an optimized fueled core and shield design can bring the specific mass for this system to less than 100 kg/kW. Transport of the Pu²³⁸ fuel to the ATSS has to accommodate a large continuous heat release from the radioisotope, and requires a dedicated carrier spacecraft.

4.2.3 Solar Dynamic (Baseline Configuration)

The baseline system has six identical units which provide continuous power. Solar dynamic units can begin delivering usable power as soon as the first unit is in place, and the ATSS would not be limited to just six units. Within the configurations for a solar dynamic unit, the structure in the concentrators and the radiators are the prime areas where new technology can reduce mass such that a specific mass of 100 kg/kW appears achievable. The solar dynamic configuration does show control complexities which involve the continuous balancing of the collector coolant liquid metal loop and the converter liquid metal loop while performing the cyclic operations associated with orbital sunset, sunrise, and solar pointing. The need to focus solar energy into a small aperture requires an extensive optical alignment process as part of the assembly on orbit. These operations would have to be performed as some form of EVA, and thereby, complicates the assembly and start-up sequence for each unit.

4.2.4 Nuclear Fission Reactor

The nuclear reactor system appears essentially equal to the baseline solar dynamic system in terms of on-orbit mass. Nuclear fission reactors have the advantage of delivering almost any level of power from a core up to the limit of heat transfer capabilities. The advantage gained from heat generation is offset by the requirements for radiation shielding, such that a man-rated shield becomes the dominating mass for any fission reactor system. The results of the evaluations indicate that careful core design plus improvements in the radiator mass could bring the specific mass of such a fission reactor system to about 100 kg/kW. The controls for a reactor system operate near steady-state conditions and involve a continuous flow balance in the liquid metal loops which power the converters. Recovery of irradiated materials after final shutdown is a recognized complexity; however, these complications have been addressed for ground and shipboard applications.

4.2.5 Fusion Power

Fusion has the unique capability for extracting one portion of its fuel from onboard water and generating the other portion of its fuel from within its heat transfer medium. Fusion systems can produce almost any power level; however, they have a large internal power demand which adds to the mass and complexities of the system. Fusion power systems require large heat rejection radiators and a large quantity of high-temperature insulation materials. Any improvements in these technology areas would reduce the total mass of the system. A specific mass approaching 100 kg/kW appears potentially achievable. The control system for a fusion reactor addresses a significant complexity in the requirements to balance

five interdependently operating subsystems, such as fuel preparation, fuel injection, laser ignition, heat extraction, power generation, and operating atmosphere control.

A fusion system needs to have a major power source in place and operating in order to initiate the fusion power system. Therefore, a fusion system has to be a replacement or extension to an onboard operating electrical power system.

In summary, the comparison shows that a system based upon advanced photovoltaics will be a viable alternate for low Earth orbit operation particularly when operating with an efficient energy storage system that has a minimal need for radiators. The dynamic systems where the energy input is from a heat source, do not show any feature that precludes any of the alternates from operating aboard the ATSS. The selection of a heat source for power generation should be determined by the requirements of the mission rather than any feature of the power generating system.

4.3 Comparison of Systems

The comparisons of the five systems and their options is based upon the results contained in the system descriptions. Table 4.1-1 identifies the location of the descriptions either in a previous study (Reference 4-1) or within the Appendix. The comparisons begin with assessments of mass and mass related effects. The comparison of control requirements results in a ranking in relative complexity, and the comparison of particular considerations results in a ranking of relative difficulty or concern.

4.3.1 Comparison of System Masses and Mass Effects

The estimates of total mass for the five alternate systems (including options) range over a factor of twenty. Table 4.3-1 lists the five alternates and options within the alternates in the order of increasing mass. This comparison shows that an advanced photovoltaic system can provide 2550 kW continuous with less than 100,000 kg (220000 lb). The energy storage method and the efficiencies of storage and retrieval contribute to the 20 percent total mass variation among the three storage options. This comparison does not identify any preferred method for energy storage. For the ATSS where O_2 and H_2 are generated and stored onboard in quantity, fuel cells give an operating advantage as a short term extra power capability. This advantage offsets the mass penalty.

The estimate of total mass for a radioisotope decay heat source makes this alternate attractive for a power system that uses rotating machinery. Flight units in the 10-kW range are now under active development for space application (Reference 4-3). The present facilities for generating Pu^{238} cannot support a system of ATSS size; however, a change in energy policy that reprocesses spent reactor fuel could result in sufficient Pu^{238} as a byproduct (Reference 4-4). The radioactive decay heat source has the advantage of continuity (no interruption by orbital position). At the same time, however, it also has the disadvantage of continuity; the heat generation rate cannot be changed.

The concepts for fusion, solar dynamic, and nuclear fission show an essential equality with regard to total mass required. In the options for nuclear fission, neither the concrete nor the water radiation shield

TABLE 4.3-1 COMPARISONS RANKING OF POWER SYSTEM MASS ASSESSMENTS
FOR 2550 kW CONTINUOUS IN LOW EARTH ORBIT

SYSTEM	FEATURES	SHIELD OPTIONS	TOTAL MASS kg	TOTAL MASS (lb)	SPECIFIC MASS kg/kW
Solar Photovoltaic	Photovoltaics with 0.2 solar energy throughput. Deliver 1275 kW-hr from storage; storage options are: a. Li-Na-liquid sulphur advanced batteries b. Graphite fiber composite flywheels c. O ₂ -H ₂ fuel cells	None	86251	(190183)	33.8
Radioisotope Decay	Pu ²³⁸ in two cores driving six converters, central location	Lead Steel	330537 342352	(728834) (754886)	129.6 134.25
Fusion, Inertially Confined, Laser Ignited	Single reactor with dual feeds and lasers driving eight converters, central location	Steel and ZrO ₂	412900	(910450)	161.9
Solar Dynamic (Baseline)	Identical units, fusion phase change energy storage- Four units on the platform; Two units on the torus	None	414858	(914761)	162.7
Nuclear Fission	Two cores of enriched U ²³⁵ driving six converters central location	Lead Steel Concrete Water	398015 438636 767225 1899970	(877623) (967192) (1691731) (4189433)	156.1 172.0 300.9 745.1

options are considered practical for a system which originated from the Earth.

A comparison of mass contributions from the major portions of each system provides some insight for the technical and physical considerations that apply to a power system for the ATSS; Table 4.3-2 lists the masses for each of the five alternates and summarizes the contributions from six major system elements.

This comparison highlights the mass advantage offered by the advanced photovoltaic system in which 70 percent or more of the total mass is directly involved with the energy conversion. At a solar energy throughput efficiency of 0.2, photovoltaics show a factor of 3 mass advantage over the closest alternate. The ATSS can produce 2550 kW continuous power with a solar throughput efficiency as low as 0.067 if the entire area available for panel installation were covered. The configuration would require some auxiliary cooling for cells mounted on the torus or over the counterrotators. If auxiliary cooling equals 20 percent of the solar input, the radiator requirement will exceed those for the gas turbines. Such a photovoltaic system would show no mass advantage. These thermal considerations show that mass estimates for the ATSS photovoltaic systems are not linear with conversion efficiency. In effect, any need for auxiliary thermal control such as radiators will decrease the mass advantage offered by advanced photovoltaics.

The radioisotope decay heat source coupled with gas turbine driven converters provide a mass effective means to generate electrical power. For this system, radiator and shielding requirements comprise more than 80 percent of the total mass. Mass reductions can make the system more competitive, and the estimates show the areas open to significant

TABLE 4.3-2 COMPARISON OF MASS CONTRIBUTIONS FOR THE ATSS POWER SYSTEM ALTERNATES

ALTERNATES	SOLAR PHOTOVOLTAIC	RADIOISOTOPE DECAY	FUSION	SOLAR DYNAMIC	NUCLEAR FISSION
Mass Total, kg	86251 to 105934	330537 to 342352	412900	414858	398015 to 1899970
Thermal Energy Elements, kg	33340 (10%) · Pu ²³⁸ Fuel Mix · Cladding · Heat Transfer Elements	73870 (18%) · Reactor · Fuel Feed · Lasers and Optics · Separators · Heat Exchangers	56628 (14%) · Collector Assy · Phase Change Matl. · Heat Transfer Elements	13622 (3%) · Core · Control Rods · Heat Transfer · Reflector	
Electrical Conversion, kg	61677 to 73480 (70% to 74%) · Photovoltaic Panels · Batteries · Flywheels, or Fuel Cells	16662 (5%) · Converters · Heat Exchangers · Controls	22216 (5%) · Converters · Heat Exchangers · Controls	16662, kg (4%) · Converters · Heat Exchangers · Controls	16662 (5%) · Converters · Heat Exchangers · Controls
High Temperature Thermal Insulation (ZrO ₂), kg		15698 (5%) · Core Blankets · Converter Heat Exchangers	69598 (17%) · Reactor Blanket · Heat Exchanger Blanket · Converter Heat Exchangers	32982 (8%) · Collector Blanket · Converter Heat Exchangers	11126 (2%) · Core Blankets · Converter Heat Exchangers
Structure, kg	16175 to 18025 (16% to 17%) · Panel Mounts		Included in Reactor	135804 (33%) · Concentrators · Tripods · Collector Converter Housing · Mounting Pedestals · Aperture Doors	
Radiators, kg	4008 to 14429 (4% to 13%) · Energy Storage Heat Sink	163536 (49%) · Precoolers	245304 (60%) · Precoolers · Laser	167628 (41%) · Precoolers · Secondary Radiator	163536 (42%) · Precoolers
Radiation Shields, kg	None	101305 (31%) · Lead 113120 (33%) · Steel	Included in Reactor and Reactor Blanket	None	193163 (48%) · Lead 233693 (53%) · Steel 562333 (73%) · Concrete 1695028 (89%) · Water

improvement. A reduction in the radiator mass by a factor of two appears attainable. A less dense insulator offers an additional increment of mass reduction. The thermal and electrical elements offer some mass reduction potential especially from materials for cladding and heat exchangers. Although the mass of PuO_2 is fixed by power generation and life requirements, the fuel mix can be adjusted; less BeO is a possibility. A smaller core operating at higher power densities and higher internal temperatures appears reasonable even though the entire core is running "full red" which limits the margin for reduction. A reduction in core size that permits a 25 percent reduction in shield mass along with the other reductions could bring the Pu^{238} system mass down to about 200,000 kg (441,000 lb) and the specific mass below 100 kg/kW.

Fusion power systems will involve massive containment elements in any of the configurations that use the deuterium-tritium fusion reaction and generate the tritium by a neutron interaction with lithium. The methods used to control or initiate fusion such as magnetic confinement, laser ignition, and generation of negatively charged subatomic particles all have heavy demands for internal electrical power. The present goal in fusion system development is to generate just enough power to make the system "break even". Fusion systems for the ATSS have a large internal power usage requirement that increases the radiator area by about 50 percent relative to any of the other alternates. The mass for fusion power system benefits from any improvements in radiators and high temperature insulation. A 50 percent mass reduction in each results in a system specific mass value of about 100 kg/kW.

The solar dynamic option selected as the baseline for comparison shows a larger than anticipated estimate for total mass principally

because of structure and radiator requirements. Significantly, the energy collection and conversion portions of the system are very nearly equal to those for the photovoltaics. Mass reduction in the collector and in the converter equipment involve high temperature materials and high temperature phase-change energy storage materials. Improvements can be anticipated. Improved radiators and high temperature insulators appear as fertile areas for mass reduction. Within solar dynamic systems, structure for the concentrator becomes a major consideration. A material for the concentrators that results in half the mass of an equivalent aluminum plate structure will make a significant reduction. This coupled with improved radiators and insulators can reduce the specific mass for the solar dynamic alternate to a value below 100 kg/kW.

Power generation from a fission reactor heat source is limited only by the capability to remove heat from the core. In the nuclear fission alternate, the mass requirement for the core elements plus the converters show the lowest total for energy conversion among all the alternates and are less than half the mass required for a photovoltaic system. Here the radiator and the man-rated shield account for 90 percent (or more) of the total mass of the system. Cores can be made to operate at higher power densities than used for the system defined for this comparison; such operation reduces the volume of the core. A reduction the volume of the shield follows but not in a linear manner because shield thickness is a function of the core activity which generates the power. An optimized core could result in a 25-percent reduction in shield mass. This would then be coupled with mass improvements in the radiators and insulators

and can reduce the specific mass to **about** 103 kg/kW for a lead-shielded system and to about 115 kg/kW for a **steel**-shielded system.

In conclusion, the comparison of mass estimates and the assessments of developmental results indicate that an advanced photovoltaic system will remain a viable alternate for an ATSS operating in LEO. This alternate becomes most attractive if it operates with a conversion throughput efficiency of 20 percent and does not require auxiliary radiators for thermal control. The other four alternates show a degree of equality such that mass criteria alone does not identify a preferred system. This extended comparison underscores the previous observation that other mission requirements must determine the appropriate method for generating electrical power aboard the ATSS.

4.3.2 Comparison of Control Requirements

The control requirements for the five systems can be qualitatively ranked for complexities. The ranking assessments in terms of increasing complexities is summarized as follows:

Photovoltaics

The control requirements reflect the dynamics of orbital operation where power sharing and power switching are the critical functions. The system has limited flexibility in generating capacity; the power must be utilized. The battery storage option has a requirement that only consists of a monitor and control of cell voltage build-up as charge accumulates. The flywheel option has a somewhat greater requirement; rotating speed must be monitored and rotating inertia balance maintained throughout a multi-unit storage system. Fuel cells and electrolytic cells have the greatest requirement for a control system. These elements

are used in a cyclic operation ~~between~~ two independent units, with the attendant requirements for handling the gaseous fuels.

In summary, the control for a photovoltaic will have the least number of input parameters and the least complex control algorithm for any of the five systems.

Radioisotope Decay Heat Pu²³⁸

The control of the radioisotope decay system has to maintain a constant energy throughput by keeping six turbine-generator units in synchronous balance. The individual control inputs and elements controlled tend to be straightforward and near steady state. They include flows, temperatures, voltages, and currents. The control for the radioisotope decay is the least complex for a system that uses rotating machinery. The principal inputs to the control algorithm are temperatures within the cores. Temperatures are maintained within narrow limits by control of the current and voltages in liquid metal pumps. These pumps maintain the heat transfer, and here a single liquid metal loop transfers the heat from the cores to the gas turbines. In comparison with a photovoltaic system, this control system would have two to three times as many inputs and have about the same factor of increase in the complexity of the control algorithm.

Nuclear Fission

The control for a nuclear fission system operates in the same general manner as the control for the radioisotope decay system. Both systems involve an essentially steady state heat transfer and keeping six turbine generator units in synchronous balance. The additional features introduced by nuclear fission are control of the neutron flux within the cores and operation with a liquid metal to liquid metal heat exchanger in

each of the turbine-generator loops. The net effect doubles the number of inputs to the control algorithm and doubles the number of liquid metal pumps needed to accomplish the heat transfer. Within the control algorithm, the determination of the neutron flux establishes the output power delivered, and the neutron flux is controlled by the adjustment in position of control rods. A nuclear fission control system shows about two times the complexity of a radioisotope decay control system.

Solar Dynamic

The control for the solar dynamic systems are six repetitions of the controls for an individual unit with all six synchronized. The individual unit controls must operate a double liquid metal loop that accomplishes energy storage and retrieval by a fusion phase change. The individual unit controls will have the same types of temperature inputs and liquid metal pump operation as for the radioisotope decay system, however, this algorithm will have to include the complexities of cyclic energy input. The control must accommodate the sunset-sunrise events, and maintain solar pointing and tracking within the specified angular limits. The inputs and items controlled in the solar dynamic are estimated to be the same as for nuclear fission. The control algorithm trades the neutron considerations for cyclic effects and adds the element for solar pointing. As a total system, the total solar dynamic control appears incrementally more complex than the controls for a nuclear fission system.

Nuclear Fusion

The nuclear fusion control system must maintain five independent subsystem processes which involve precise timing while keeping eight turbine-generators in synchronous balance. Estimates for ground based

power stations indicate an order of magnitude more control inputs than a conventional steam powered station (Reference 4-5), and the estimate appears to follow for space applications. The control for a laser ignited fusion system must operate with the unique feature of energy released in bursts. The reactor vessel and its control sensors must accept 426-kJ bursts (approximately equal to 0.12 kg (0.25 lb) of TNT) at 20 times each second. The combination of requirements and operating environment contribute to the result that the control for a fusion system has about ten times the complexity of that for a radioisotope decay.

In summary, these systems do show a range in complexity for their control systems, and even the least complex case for a photovoltaic power system must address a demanding control situation. On the other hand, all the systems can be controlled, and the control algorithms can be generated for an ATSS application. As in the case for mass considerations, the control requirements do not identify a preference, mission requirements must provide the criteria for selecting the power generating system.

4.3.3 Particular System and Operating Concerns

Each of the five alternates shows some degree of special concern at times in the operating sequences. All of the power systems share the concerns that accompany a continuous type of operation. The special concerns can be ordered in a manner that reflects increasing impact on the ATSS or special constraints placed upon the ATSS. The order is as follows.

Photovoltaic

The concerns for photovoltaics are thermal degradation, which could result from exposure to a solar input without an electrical connection, and impact damage from space debris. To avoid an unwanted temperature excursion from exposure during installation, the solar panel field needs to be installed in modules in which a section of photovoltaics and an element of energy storage are emplaced at the same time. Power can then be absorbed when a panel is exposed to the solar input. Some provisions for masking may be required to prevent an unwanted exposure during installation or repairs. The ATSS will require spares as a precaution for breakage or damage from space debris impact. These concerns appear modest and can be accommodated within the initial assembly sequence or the plan for contingency repairs.

Solar Dynamic

The solar dynamic units require an extended start-up sequence. The large area concentrators require assembly and an optical alignment of the individual reflector elements as part of the on-orbit sequence. The location for the collector and converters at the focus of the concentrator complicates the start-up sequence. An operational shutdown without damage to the system is significantly complex. Both cases require careful planning and extensive EVA to accomplish.

Radioisotope Decay

The concern for radioisotope decay systems stems from its continuous heat release. The fuel mix must always have heat removal. The critical time occurs during transport from the ground to the ATSS. A reasonable inventory such as half power equivalent for a 450-kW converter will evaporate more than 1000 kg of water per hour at atmospheric pressure.

The same fuel upon return after ten years in the core will still have a heat release at 92 percent of the original level. A radioisotope decay power system will require a special purpose transporter which can operate between the ground and the orbit of the ATSS.

Nuclear Fission

The concern relates to the handling and recovery of the core components after final shutdown. The materials subjected to neutron radiation will show an induced radioactivity that can range from nil in shield elements to lethal-intense from fuel elements and control rods. Dismantling and removal of these components will require specialized remote handling equipment and shielded casks for transport. Provision for recovery have to be included in the initial design for each element of the system that has any exposure to neutrons or encounters the products of fission.

Fusion

The energy requirements for starting the system are almost equal to the initial system output. The energy input requirements for the lasers alone are equal to the output of one converter. The start-up of the liquid metal systems and establishment of the vacuum for operating pressure represent heavy, short-term demands on electrical power. The fusion option, therefore, must be installed as a replacement or supplement to an in-place and operating electrical power capability.

In summary, the photovoltaic and the solar dynamic systems appear to have the least requirement for any auxiliary equipment to support the installation, start up, operation, or retrieval of the system. The radioisotope decay and nuclear fission systems both will need special purpose support items of significant complexity. Fusion has such an

input power demand that the system cannot be considered as an initial configuration for the ATSS.

4.4 Overall Assessments

The comparisons of masses, control requirements, and configuration-particular effects lead to an overall assessment and ranking of the five alternates. The ranking and pertinent comments are:

Photovoltaics

An advanced photovoltaic system is a candidate power system for operation in LEO. The ATSS application has defined the needed improvements in cell conversion efficiency, cell life capability, and techniques for energy storage. The present activities to develop photovoltaics for other nearer term missions address most of the requirements for ATSS. In such a context, the ATSS comparison study underscores the need to continue developments of photovoltaic system related components as solar cells, battery cells, flywheels, and O₂-H₂ fuel cells.

Radioisotope Decay

A radioisotope decay power system offers the advantage of a continuous heat source and would relieve the ATSS from some of the present solar pointing requirements. The comparison based upon Pu²³⁸ selected an isotope of choice without regard to source or availability. A change in national energy policy to reprocess spent reactor fuel could make the isotope available in the quantities needed. On the other hand, other isotopes either singly or in a mix, could be used. The ATSS could be configured to accept the increased complexity in handling and the extra shielding required for man-rating. The present developments to operate

rotating converters from a Pu^{238} heat source are considered an initial step toward an ATSS sized installation.

Solar Dynamic - Nuclear Fission

These two systems are presently achievable through technical developments which can be identified. The operating principles for the systems are well defined. The technology advances needed to implement the systems can build upon the present base of knowledge, neither of these systems require a change in national energy policy or a major technical breakthrough as part of their implementation plan.

These two systems are considered essentially equal. The complexity associated with solar pointing and solar cyclic operation offsets the considerations for a man-rated radiation shield and the eventual handling of radioactive waste. Within the five alternates, the fission reactor is the only system which can vary its power output in response to demand and thereby offers the advantage of flexibility while at the same time relieving the ATSS from the solar pointing requirements. Both types of systems have development activities underway that are steps toward an ATSS sized application. However, the need for large area concentrators with the structural integrity to withstand operation in a rotating acceleration field appears as an ATSS-unique requirement for a precision-surfaced space structure.

Fusion Power

A fusion heat source offers an almost unlimited power generation capability with a minimum of fuel transport to orbit. For the ATSS, the deuterium can be obtained from the electrolysis of wastewater from crew support. The conversion of lithium into tritium and helium consumes less than a kilogram of lithium per year.

REFERENCES

- 4-1 Queijo, M. J. et al: An Advanced-Technology Space Station for the Year 2025, Study and Concepts. NASA CR 178208 March 1987.
- 4-2 Queijo, M. J. et al: Some Operational Aspects of a Rotating Advanced-Technology Space Station for the Year 2025. NASA CR 181617, June 1988.
- 4-3 Nuclear Power Demonstration Units, Aviation Week, Vol. 127, No. 25, December 21, 1987, pp. 28.
- 4-4 Zinn W. W. et al: Nuclear Power USA, McGraw Hill Book Co., 1961.
- 4-5 Gross, R. A.: Fusion Energy, John Wiley and Sons, 1984.

The achievement of fusion power is a long term goal. Achievement of a break-even power operation is the recognized first critical step. A laser ignited, inertially confined system appears dependent upon technology advances in both lasers and fuel encapsulation. Other national priorities presently define the development goals in these areas. For the ATSS, a fusion power system appears as a candidate for an upgrading of ATSS capability. Fusion power becomes most attractive for missions which involve space manufacturing and the generation of O_2-H_2 for propulsion fuel. An ATSS which supports a lunar base could have such a need.

5.0 ATTITUDE AND ORBIT CONTROL

The ATSS operates in a specified circular orbit and maintains Sun orientation (Figure 5.0-1). Various forces and torques tend to disturb the station from the desired orientation and orbit. The attitude control system must null these disturbances. This section examines these disturbances and discusses various means of nulling. Qualitative trends in nulling the disturbances are derived.

5.1 Environmental (Disturbance) Forces and Torques

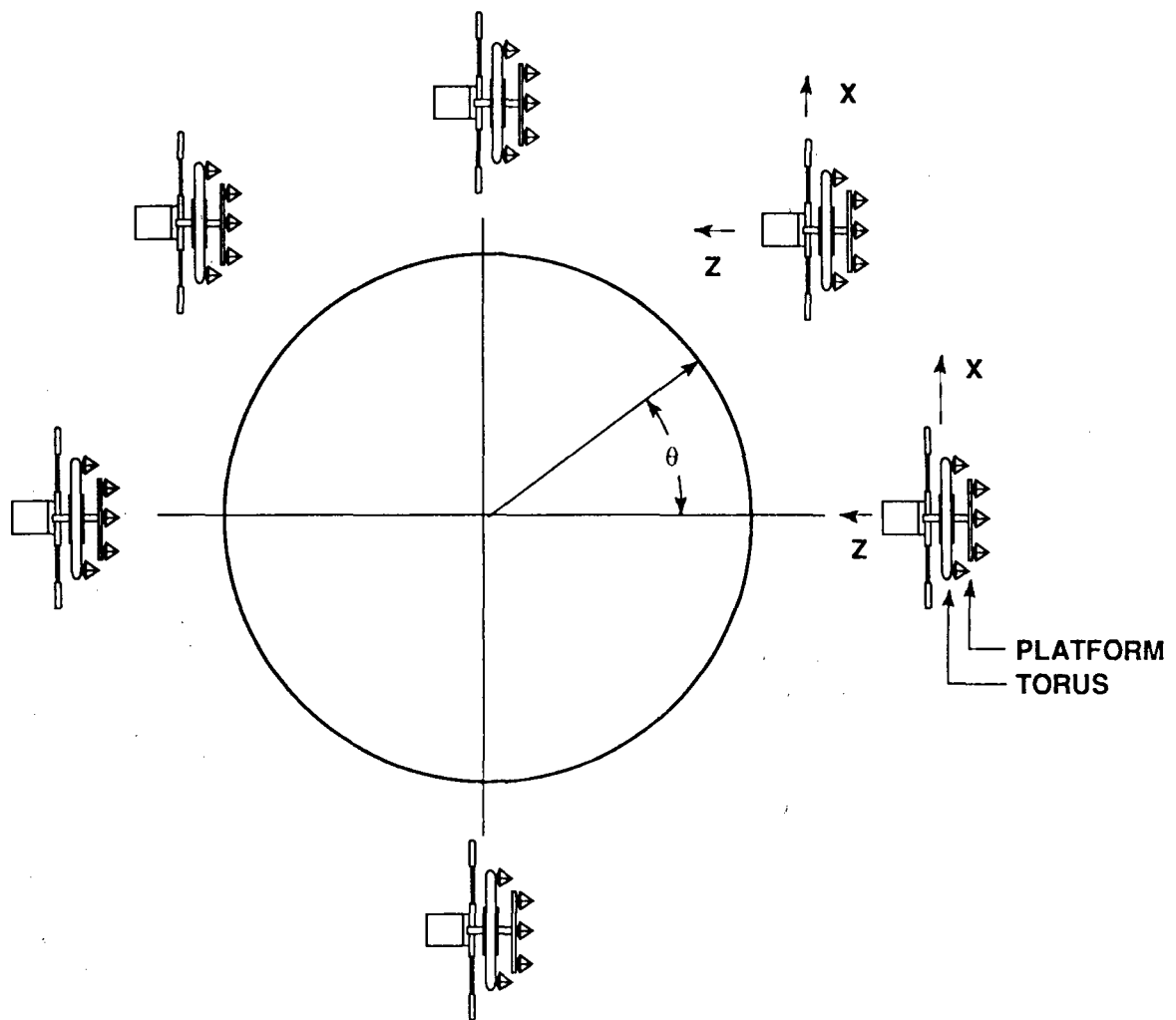
The environmental forces and torques are those associated with aerodynamic drag forces and torques, solar radiation pressure forces, and gravity (gradient) torques. These are given as functions of orbit angle in the following figures (from Reference 5-1).

Aerodynamic forces	Figure 5.1-1
Aerodynamic torques	Figure 5.1-2
Solar radiation forces	Figure 5.1-3
Gravity gradient torques	Figure 5.1-4

There are no torques associated with radiation pressure because of the orientation and symmetry of the ATSS. Note that the gravity gradient torque is much greater than that caused by aerodynamic pressure.

5.2 Attitude Control

Several classes of devices for attitude control are considered. These are reaction jets, control-moment gyros, dual counterrotating annular moment control devices (DCAMCD) and the possible use of the ATSS counterrotators. Note that both ATSS counterrotators turn counter to the torus.



Notes for a Solar Facing Orbit

1. θ is the orbit angle measured from solar zenith.
2. y axis is positive away from the plane of view.
3. The origin for the axis system is 0.856 m (2.8 ft) toward to platform from the plane of rotation for the torus.

Figure 5.0-1 Orientation of the ATSS in Orbit

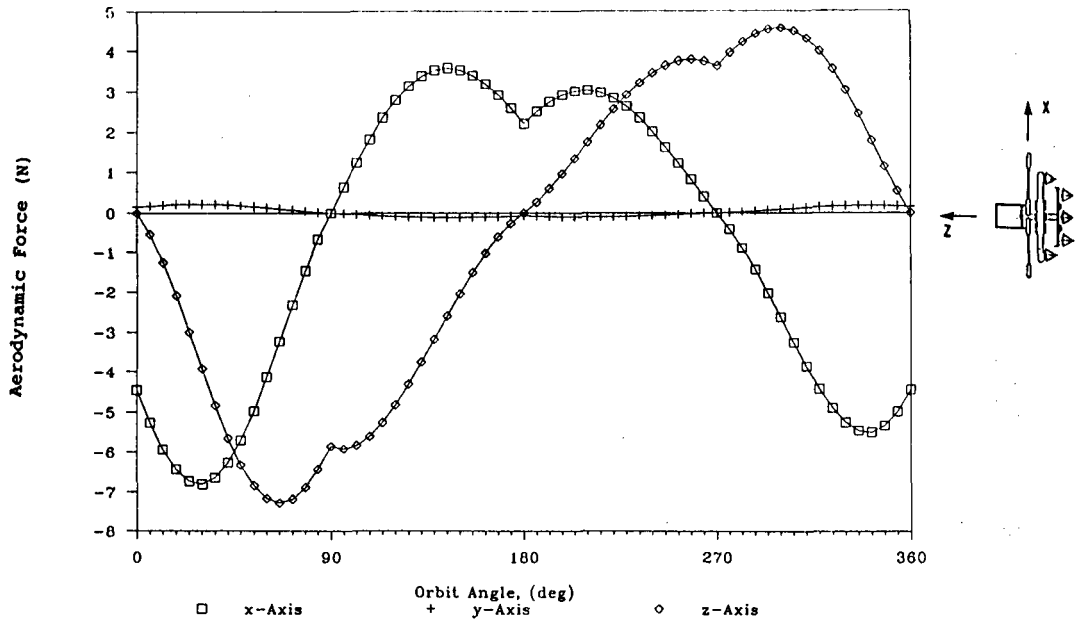


Figure 5.1-1 Aerodynamic Force on the ATSS as a Function of Orbit Angle

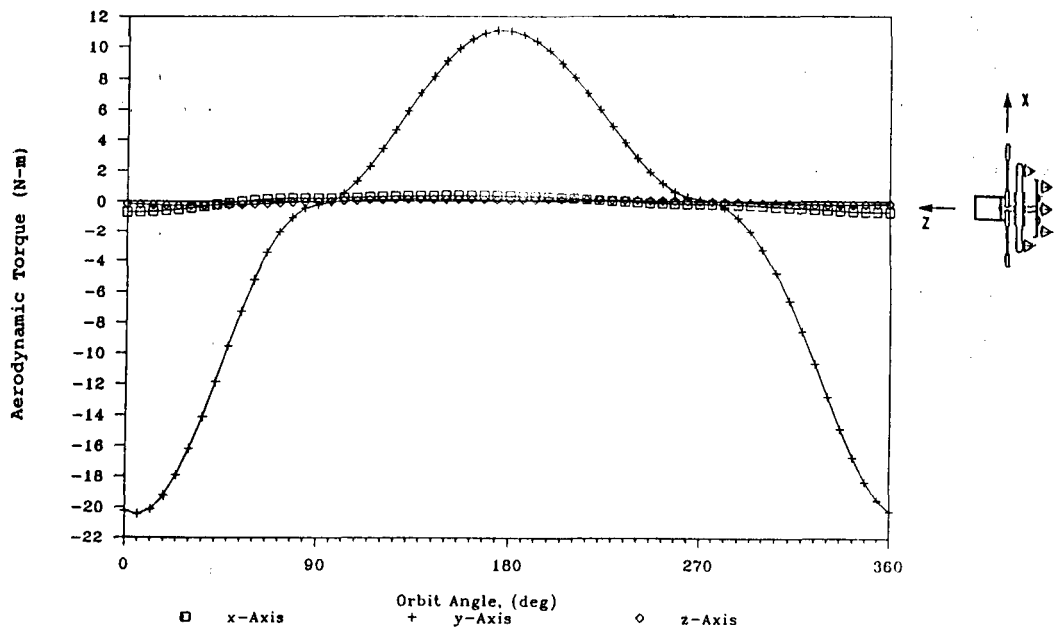


Figure 5.1-2 Aerodynamic Torque on the ATSS as a Function of Orbit Angle

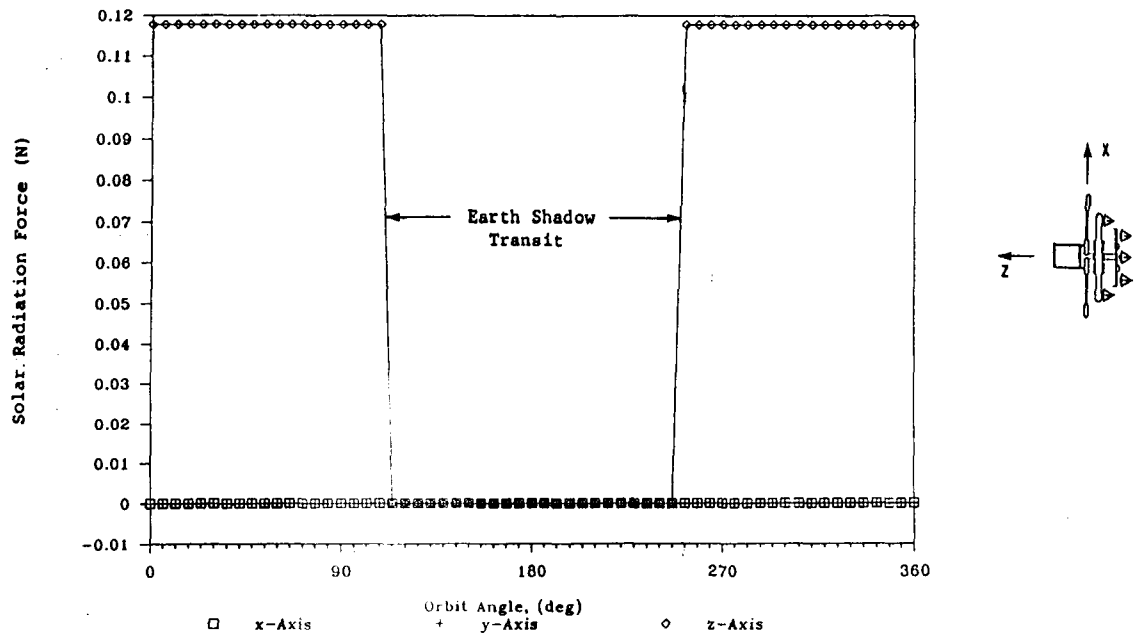


Figure 5.1-3 Solar Radiation Force on the ATSS as a Function of Orbit Angle

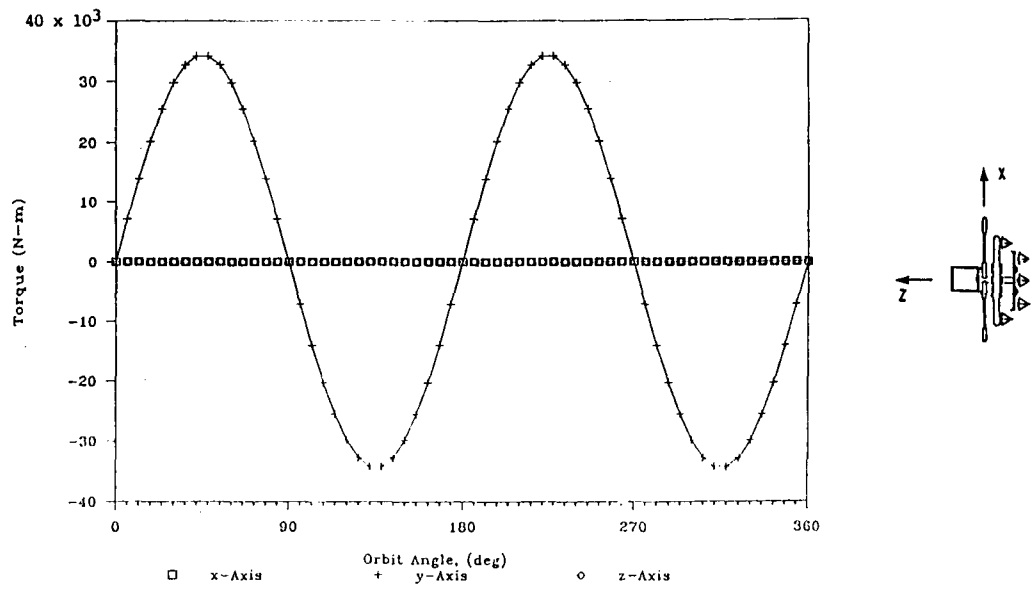


Figure 5.1-4 Gravity Gradient Torque on the ATSS as a Function of Orbit Angle

Each of the attitude control devices considered must be able to produce a torque at least as great as (but opposing) the environmental torque. In addition, each must be able to negate the maximum angular momentum ($\int \text{torque dt}$) imposed on the ATSS by the environmental torques. The momentum associated with aerodynamic torque and the momentum associated with gravity gradient torque vary continuously throughout an orbit. Figures 5.2-1 and 5.2-2, respectively, show these variations as a function of orbit angle. The figures show that the maximum torque and angular momentum are approximately 34,000 N-m (25000 lb-ft) and 31.0×10^6 N-m-sec (22.86×10^6 lb-ft-sec), respectively, and they are caused by the gravity gradient. Aerodynamic effects are very small and will be ignored in this preliminary study.

It should be noted that these values are several orders of magnitude greater than those of current or proposed spacecraft, as shown in Table 5.2-1 (from Reference 5-2) and for an early NASA space station as the power-tower configuration (Figure 5.2-3, from Reference 5-3).

5.2.1 Reaction Jets

It is assumed that the reaction jets thrust continuously at the level required to counteract the environmental torque. The jets are in four clusters of six and are aligned with the ATSS axes. It is further assumed that all jets operate at the same level and that in producing torque about any axis all jets capable of producing a torque about that axis will be operating. For example, to produce a torque about the y-axis, thrusters aligned with the x- and z-axes will be used. A total of eight jets can be used simultaneously to produce torques about each body axis.

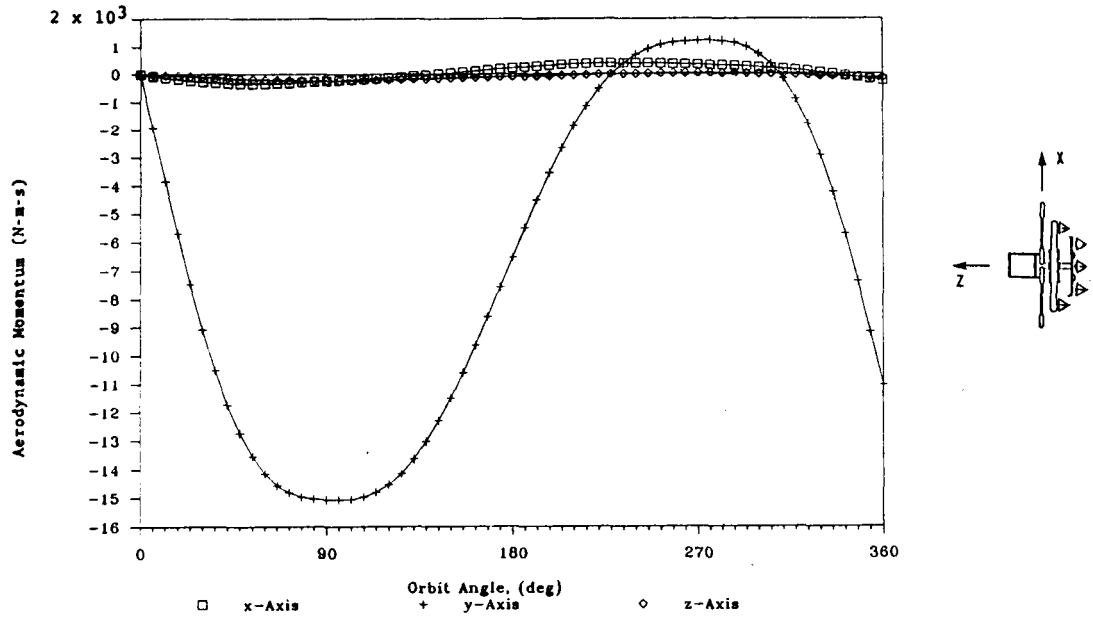


Figure 5.2-1 Aerodynamic Momentum on the ATSS as a Function of Orbit Angle

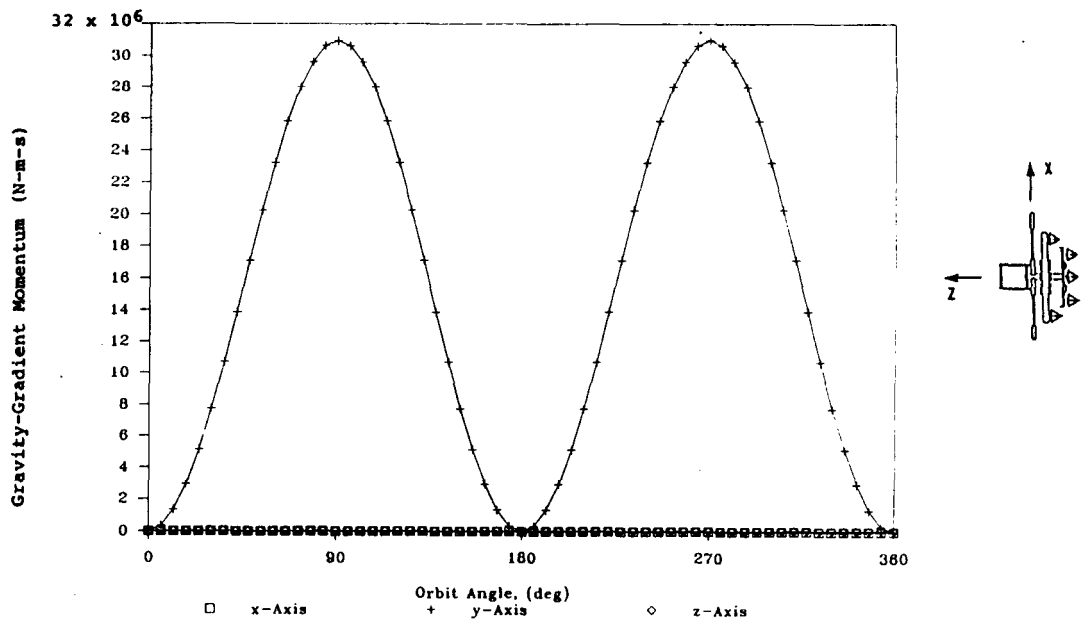
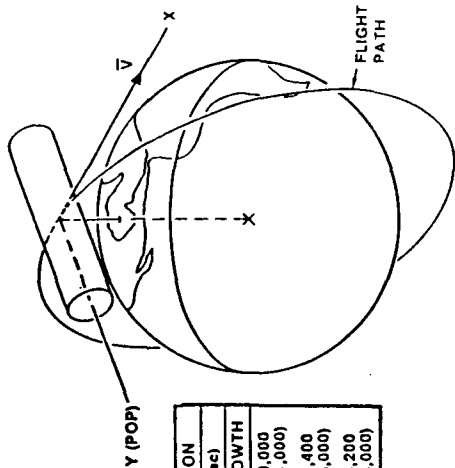


Figure 5.2-2 Gravity Gradient Momentum on the ATSS as a Function of Orbit Angle

TABLE 5.2-1 TORQUE AND ANGULAR MOMENTUM REQUIREMENTS (from Reference 5-2)

Mission	Control torque		Momentum storage	
	N-m	ft-lb	N-m-sec	ft-lb-sec
RAM	9.5 (per torquer)	7 (per torquer)	2034 (planar)	1500 (planar)
TDRS	0.021 (per axis)	3 in.-oz (per axis)	16.9 (bias)	12.5 (bias)
EOS	0.049 (per axis)	7 in.-oz (per axis)	24.4 (bias)	18 (bias)
MJS	0.014 (per axis)	2 in.-oz (per axis)	0.068	0.05
MSS	678 (per axis)	500 (per axis)	2758 (planar)	2034 (planar)
30-day Shuttle	163 (per torquer)	120 (per torquer)	7118 (planar)	5250 (planar)

RAM Advanced Solar Observatory
 TDRS Tracking and Data Relay Station
 EOS Earth Orbiting Satellite
 MJS Mars, Jupiter, Saturn Mission
 MSS Modular Space Station (Rockwell)



MOMENTUM COMPONENT	CONFIGURATION	
	INITIAL	GROWTH
ΔH_y	34,500 (25,500)	69,000 (51,000)
$\Delta H_x - \Delta H_z$	12,200 (9,000)	24,400 (18,000)
VECTOR SUM	38,800 (27,000)	73,200 (54,000)

• ALTITUDE: 476 KM (257 NMI)

• INCLINATION: 28.5 DEGREES

• FLIGHT ORIENTATION:

- TOWER AXIS LOCAL VERTICAL, SOLAR ARRAY BOOM AXIS PERPENDICULAR TO ORBIT PLANE

• POWER DELIVERED AT BUS (VALUES ASSUMED FOR STUDY)

- INITIAL OPERATING CAPABILITY (IOC): 75 KW

- GROWTH CAPABILITY: 150 KW

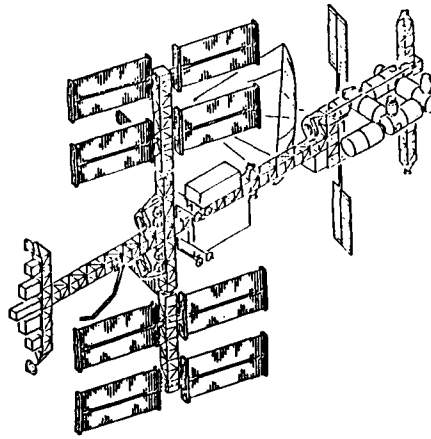


Figure 5.2-3 Typical Space Station/NASA Configuration--Power Tower (from Reference 5-3)

The torque about any axis is given by

$$L = \sum_{j=1}^N T_j \ell_j$$

L = Torque
 N = Number of jets thrusting
 T = Thrust from each jet
 ℓ = Moment arm

If all jets are thrusting at the same level,

$\bar{\ell}$ = The average moment arm

$$L = T \sum_{j=1}^N \ell_j = N T \bar{\ell} \quad (5-1)$$

The fuel used to produce the required torque over a given time period can be readily calculated based on the following:

$$T = \dot{w} \text{ Isp} \quad (5-2)$$

\dot{w} = weight of fuel used per second, per jet
 Isp = specific impulse of fuel

Substituting equation (5-2) into (5-1) results in

$$L = N \dot{w} \text{ Isp } \bar{\ell}$$

and, on integrating and solving for w,

$$w = \frac{\int_0^{\tau} L \, dt}{N \text{ Isp } \bar{\ell}}$$

τ = Time duration of thrust

The total fuel used by the N operating jets is

$$N w = \frac{\int_0^{\tau} L \, dt}{\text{Isp } \bar{\ell}} \quad (5-3)$$

The assumed jet locations on the ATSS are indicated in Figure 5.2-4 and have the coordinates

Cluster	x,m	y,m	z,m
1	35	-30	45
2	35	30	45
3	-35	-30	45
4	-35	30	45

From these values it is seen that

$$\begin{aligned}\bar{\ell}_x &= 37.5 \text{ m} \\ \bar{\ell}_y &= 40.0 \text{ m} \\ \bar{\ell}_z &= 32.5 \text{ m}\end{aligned}$$

Since the torque is, by far, the greatest around the y-axis, torques about the x and z axes will be ignored for this preliminary analysis. Since the maximum torque to be generated is 34,000 N-m (Figure 5.1-4), there are eight jets that can produce torque about the y-axis, and the average moment arm about the y-axis is 40 m, the maximum thrust required per jet is, from equation (5-1), about 106 N (23.8 lb).

The fuel used to generate the gravity-gradient torque variation shown in Figure 5.1-4 can be determined as follows:

The torque variation as a function of orbit angle (θ) can be approximated by

$$L = L_{\max} \sin 2\theta \quad (5-4)$$

Since $\dot{\theta}$ is constant for a circular orbit $\theta = \dot{\theta}t$ Equation (5-4) becomes

$$L = L_{\max} \sin 2\dot{\theta}t \quad (5-5)$$

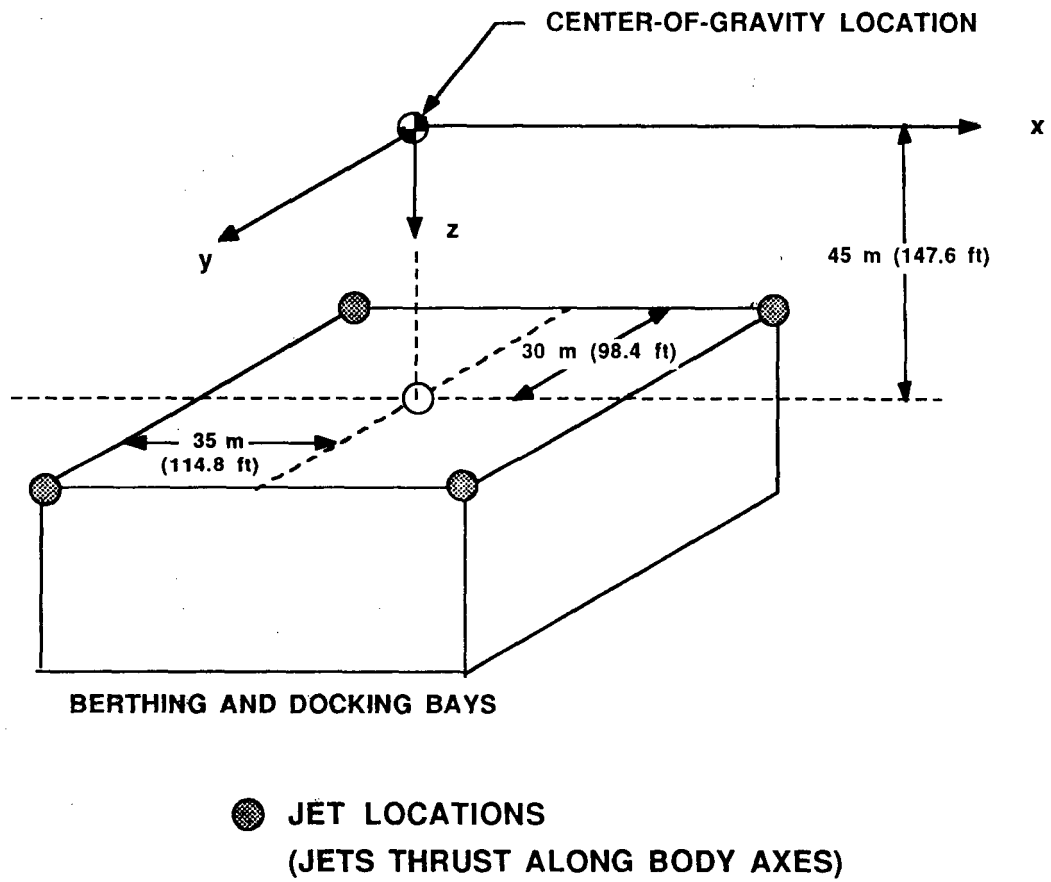


Figure 5.2-4 Assumed Thrust Jet Locations

Substituting equation (5-5) into equation (5-3) results in

$$Nw = W = \frac{L_{\max} \int_0^{\tau} \sin 2\dot{\theta} t \, dt}{I_{sp} \bar{\ell}} \quad (5-6)$$

which can be integrated to yield

$$W = \frac{L_{\max}}{I_{sp} \bar{\ell}} \left[\frac{1}{20} \cos 2\theta t \right]_0^{\tau}$$

The fuel used for one quarter orbit ($\dot{\theta} t = 90^\circ$) is

$$W_{\frac{1}{4} \text{ orbit}} = \frac{L_{\max}}{I_{sp} \bar{\ell} \dot{\theta}}$$

or, for a complete orbit

$$W_{\text{orbit}} = 4 \frac{L_{\max}}{I_{sp} \bar{\ell} \dot{\theta}} \quad (5-7)$$

The important parameters in determining the mass of fuel used are readily apparent and permit calculating the mass required for an O₂-H₂ system.

For the ATSS the nominal circular-orbit attitude is 500 km (311 miles), and the corresponding angular velocity is 0.0011 radians per second. Using the following values

$$\begin{aligned} L_{\max} &= 34,000 \text{ N-m} \\ I_{sp} &= 4310 \text{ N-sec/kg for O}_2\text{-H}_2 \\ \bar{\ell}_y &= 40.0 \text{ m} \end{aligned}$$

in equation (5-7) results in

$$W_{\text{orbit}} = 717 \text{ kg (1580 lb) per orbit}$$

or a fuel use of 982,000 kg (2.17 x 10⁶ lb) in 90 days.

This is obviously too large, which makes the use of chemical reaction jets impractical for angular momentum control.

5.2.2 Control-Moment Gyros

If a control momentum gyro (or group of gyros) is to be used for attitude control, the angular momentum capacity of the gyro is closely related to the maximum angular momentum imposed on the ATSS by environmental forces (Figure 5.2-2). Since the imposed momentum is cyclic, but always in one direction, it is advantageous to displace the gyro wheel so that its total displacement permits absorption of the total angular momentum. In this case, the maximum angular momentum required of the gyro would be about 15.5×10^6 N-m-s (11.46×10^6 lb-ft-sec).

The maximum gravitational torque of 34×10^3 N-m (25×10^3 lb-ft) and the associated angular momentum, 15.5×10^6 N-m-s (11.46×10^6 lb-ft-sec), set the requirements for a control momentum gyro system. These values are several orders of magnitude greater than those available with current CMGs. For example, one of the commercially available higher capacity CMG's units has a double gimbal with an output torque of 272 N-m (200 lb-ft) and angular momentum of 6100 N-m-s (4500 lb-ft-sec), and a total mass of 295 kg (650 lb) (Reference 5-4). Therefore, approximately 126 of these gyros would be required to produce the torque required for the ATSS and add about 37,000 kg (82,000 lb). Absorbing the angular momentum generated over the quarter orbit period would require about 2550 of these gyros and add about 748,000 kg (1.67×10^6 lb).

5.2.3 Dual Counterrotating Annular Momentum Control Devices (DCAMCD)

The geometry involved in dual counterrotating wheels is shown in Figure 5.2-5. The transverse angular momentum which is available from two wheels is given by

$$H_T = 2H_\mu \sin \nu \quad (5-8)$$

H_T = Total angular momentum required
 H_ν = Angular momentum of each wheel
 ν = Tilt angle of the wheel

If a required value of H_T is specified, then the required angular momentum per wheel is

$$H_\mu = \frac{H_T}{2 \sin \nu}$$

or for small angles,

$$H_\mu = \frac{H_T}{2\nu} \quad (5-9)$$

The size, shape, weight, and rotational speed all enter into the value of H_μ . Some of these factors are discussed in the following section. It is of interest to minimize the weight needed to produce the desired value of H_μ , while remaining within whatever constraints are applicable (that is, size limitations, allowable stress levels, etc.).

A convenient place to start these considerations is the study of Reference 5-5, which relates the energy in a flywheel to its mass by the equation

$$\frac{E}{m} = K_S \frac{\sigma}{\rho} \quad (5-10)$$

E = Kinetic energy of the flywheel
 m = Mass of flywheel
 σ = Material design stress level
 ρ = Material mass density
 K_S = is a dimensionless shape factor

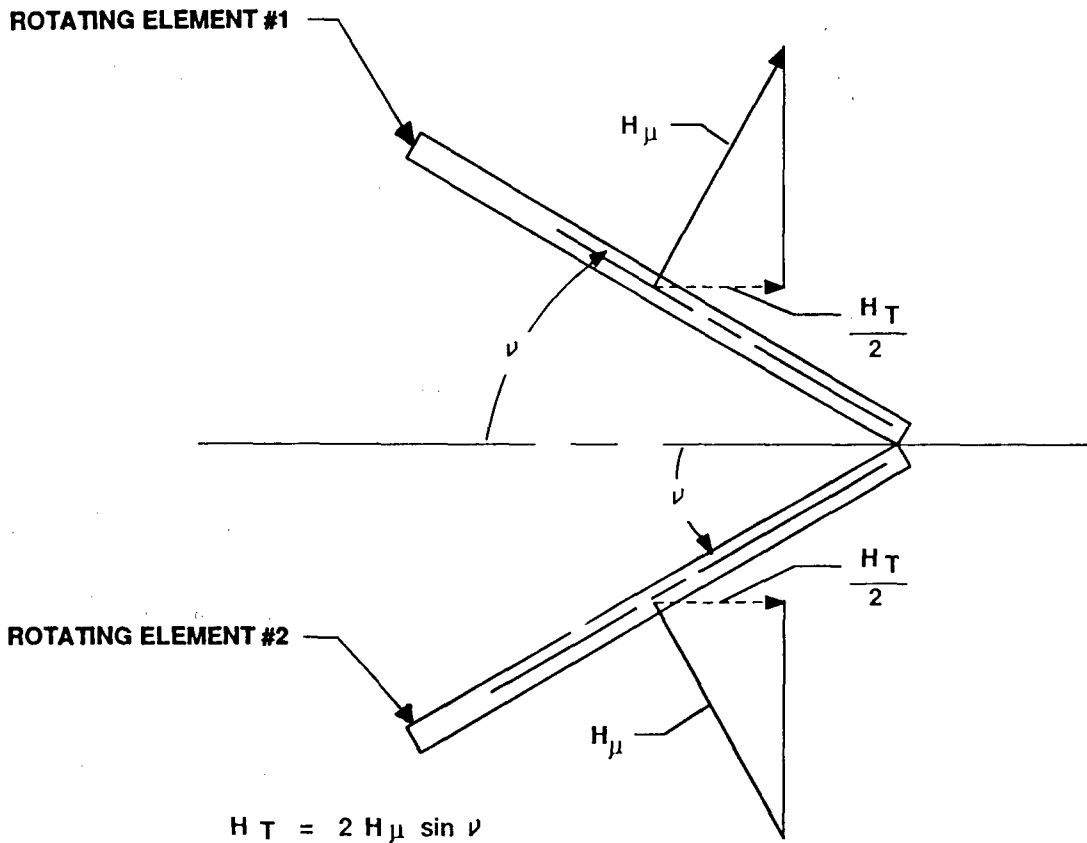


Figure 5.2-5 Geometry of Dual Counterrotating Annular Momentum Control Device Wheels

In developing equation (5-10), all constraints other than these due to stress considerations were removed. Figure 5.2-6, from Reference 5-5, lists values of K_S for various wheel cross sections, and Figure 5.2-7 from the same reference lists some mechanical properties of various materials. Following the procedure of Reference 5-6, one may use the following relations:

$$E = \frac{1}{2} I \omega^2$$

$$H = I \omega = mk^2 \omega$$

$I = \text{Moment of inertia}$
 $\omega = \text{Angular velocity}$
 $k = \text{Radius of gyration}$

with equation (5-10) to show that

$$\frac{H}{m} = k \left[2 K_S \frac{\sigma}{\rho} \right]^{1/2} \quad (5-11)$$

Also, if r_0 is the maximum allowable radius of the wheel, equation (5-11) can be written as,

$$\frac{H}{m} = r_0 \left[2 K'_S \frac{\sigma}{\rho} \right]^{1/2}$$

from which

$$m = \frac{H}{r_0 \left[2 K'_S \frac{\sigma}{\rho} \right]^{1/2}} \quad (5-12)$$

where

$$K'_S = \left(\frac{k}{r_0} \right)^2 K_S \quad (5-13)$$

For a flywheel of given radius (r_0) and material, the mass for the required value of H can be minimized by selecting a flywheel shape having a maximum K'_S . Figure 5.2-8 lists ranges of k/r_0 , K_S , and K'_S for several flywheel shapes, and shows that the thin rim flywheel has the

Flywheel Geometry	Cross Section or Pictorial View	Shape Factor (K _s)
Constant - Stress Disc (OD → ∞)		1,000
Modified Constant - Stress Disc (Typical)		0.931
Truncated Conical Disc (Typical)		0.806
Flat Unpierced Disc		0.606
Thin Rim (ID/OD → 1.0)		0.500
Shaped Bar (OD → ∞)		0.500
Rim with Web (Typical)		0.400
Single Filament Bar		0.333
Flat Pierced Disc		0.305

Suitable for Homogeneous Materials Only
 Suitable for Homogeneous or Filamentary Materials

$E =$ Energy
 $\sigma =$ Design Stress
 $\rho =$ Mass Density

$$E = K_s \frac{\sigma}{\rho} m$$

Figure 5.2-6 Flywheel Shape Factors for Various Geometries

MATERIAL	MASS DENSITY, ρ		RECOMMENDED WORKING STRESS, σ		σ/ρ ($\times 10^6$)	
	$\frac{\text{lb}}{\text{ft}^3}$	(kg/m^3)	$\frac{\text{lb}}{\text{ft}^2}$ ($\times 10^6$)	$\frac{\text{N}}{\text{m}^2}$ ($\times 10^6$)	$\frac{\text{ft}^2}{\text{sec}^2}$	$\left(\frac{\text{m}^2}{\text{sec}^2}\right)$
18 Ni-400 (Maraging Steel)	15.510	8000	37.44	1793	2.414	0.2240
18 Ni-300 (Maraging Steel)	15.510	8000	28.80	1379	1.857	0.1720
4030 Steel	15.190	7836	18.72	896	1.232	0.1140
Cast Iron	15.030	7753	2.88	138	0.192	0.0180
2024-T851 (Aluminum)	5.528	2852	3.74	179	0.677	0.0628
6 Al-4V (Titanium)	8.586	4429	11.81	565	1.376	0.1276
"E" Glass	4.025	2076	9.65	462	2.396	0.2230
S-1014 Glass	3.864	1993	12.53	606	3.243	0.3041

Figure 5.2-7 Flywheel Materials

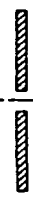
Cross - Section of Wheel	k/r_o	K_S	K_S'
	0.3	0.806	0.0725
	0.5	0.305	0.0760
	1.0	0.500	0.5000
	$0.5 < k/r_o < 1.0$	$0.305 < K_S < 0.500$	$0.0725 < K_S' < 0.5000$

Figure 5.2-8 Values of k/r_o , K_S , and K_S' for Various Flywheel Cross-Sections

largest K_S value (equal to 0.5). For the case of a thin rim flywheel, equation (5-12) becomes:

$$m = \frac{H_{\mu}}{r_o \left(\frac{\sigma}{\rho} \right)^{1/2}} \quad (5-14)$$

Equation (5-14) is the mass of one flywheel having angular momentum H_{μ} and operating at its design value of (σ/ρ) . If a flywheel pair is to produce a specified transverse angular momentum H_T , then equation (5-9) can be used with equation (5-14) to result in

$$m = \frac{H_T}{2 r_o v \left(\frac{\sigma}{\rho} \right)^{1/2}} \quad (5-15)$$

and is the mass of one of the flywheels. If a factor F to account for supporting structure, electronics, etc. is included in the calculation, then the total mass of the dual counterrotating wheel system (2 wheels) is:

$$M = \frac{F H_T}{r_o v \left(\frac{\sigma}{\rho} \right)^{1/2}} \quad (5-16)$$

Equation (5-16) shows the importance of selecting materials and geometry for dual counterrotating wheels. Figure 5.2-9 can be used to estimate the mass required for absorption of transverse momentum as a function of wheel geometry and material.

The required transverse angular momentum H_T is 31×10^6 N-m-s for an ATSS application (Figure 5.2-2). If the DCAMCD rotors are fabricated from S-1014 glass with a radius of 50 m, a structural factor $F = 1.1$, and a 5-degree allowable deflection angle, then the total mass for the two wheels is 14,263 kg (31,500 lb). The effect of changing the wheel radius or allowable deflection angles is readily visible from equation (5-16).

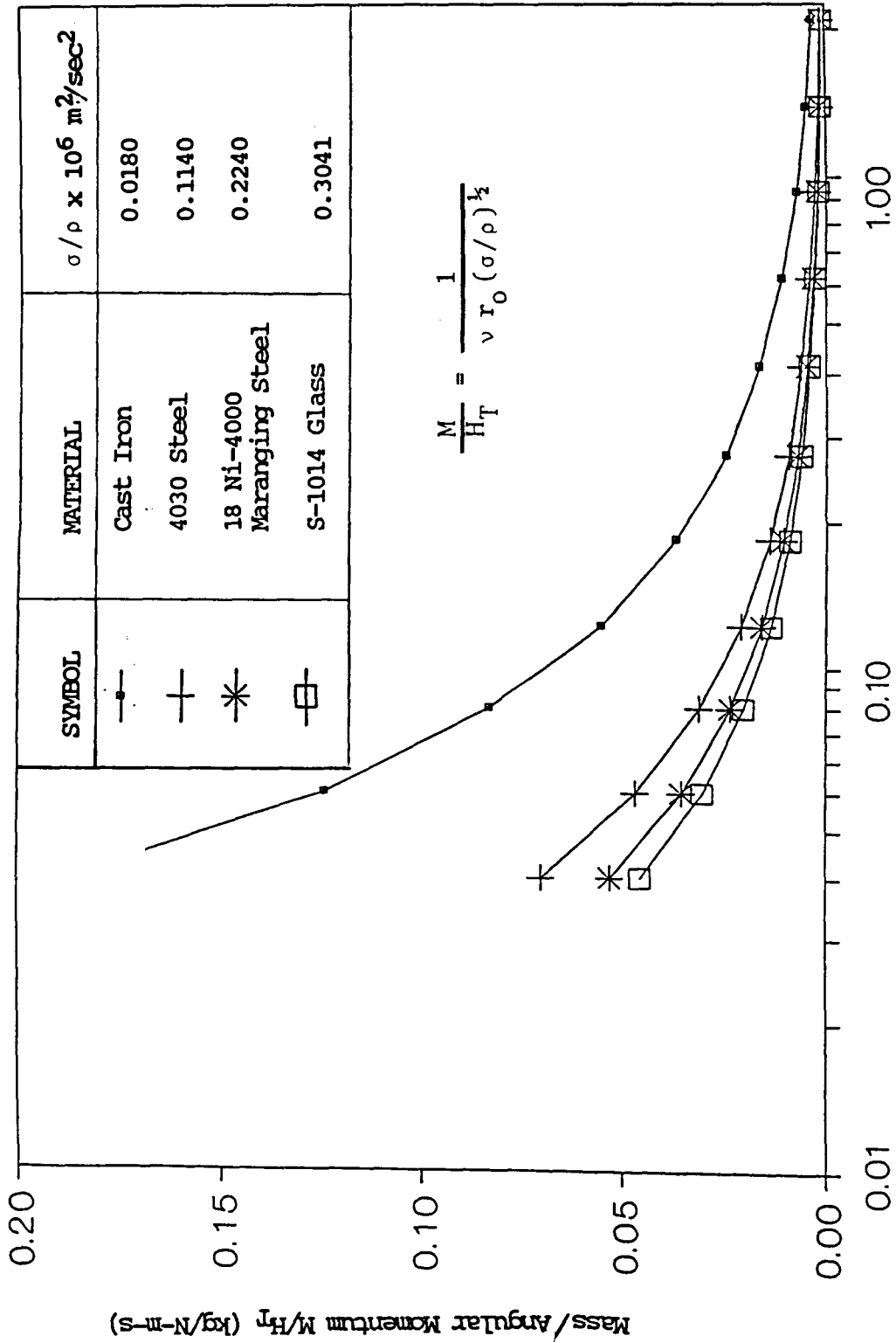


Figure 5.2-9 Effect of Materials and Geometry on Mass Required to Generate Angular Momentum

The use of large DCAMCDs begins to appear somewhat reasonable, particularly if they could also be used for energy storage. Note that there is a trade-off involved because changes in rotational speed of the DCAMCDs will translate into changes in (σ/ρ) . However, this can be adjusted to some extent by simultaneous variation in the tilt angle.

5.2.4 Use of the ATSS Counterrotator for Attitude Control

Since the ATSS has two large counterrotating wheels (both running counter to the torus), it is interesting to determine if they could be used to negate the gravity gradient torque. In such an application, the counterrotators would be tilted in unison to counteract the environmental torque. Assuming that only the torque about the y-axis (gravity-gradient torque) needs to be considered, then a tilt of the wheels around the x-axis can counteract the environmental torque. The tilt required can be determined through use of equation (5-8), that is,

$$\sin v = \frac{H_T}{2 H_\mu}$$

For such a case, H_T , the maximum environmental transverse angular momentum, remains at 31.0×10^6 , N-m-sec. The angular momentum for the two counterrotators has to equal that for the torus and, from Reference 5-7, for an equivalent Earth gravity $2H_\mu = 9.36 \times 10^9$ N-m-sec. The resulting tilt angle $v = 0.0033$ rad, approximately 0.2 deg. The same control could be applied by tilting just one of the counterrotators through a maximum of about 0.4 deg. These angles are small enough to cause no appreciable exchange in the angular momentum about the axis of symmetry. Techniques for possible mechanization of such a system have not been considered in depth.

5.3 Discussion and Comparison of Attitude Control Mechanism

The major disturbance to the described Sun-pointing orientation of the ATSS is caused by gravity-gradient torques. For the assumed orientation of the ATSS, the torque is primarily around the y-axis, and there is little disturbance about the x and z axes. This permits an elementary comparison of various attitude control devices. Before comparing devices, it is beneficial to make some general remarks relative to each of the systems.

5.3.1 Reaction Jets

Use of reaction jets does not appear viable because of the indicated large fuel (H_2-O_2) usage of 975,000 kg (2.15×10^6 lb) in 90 days. Increasing the moment arms of the jets, or using fuels of higher specific impulse would reduce fuel use (equation 5-7). However, these are limited by geometric and structural considerations and by available fuels. The use of chemical-fuel thrusters does not appear viable.

5.3.2 Control-Moment Gyros

The angular momentum requirements for the ATSS are several orders of magnitude greater than those currently available for control-moment gyros. The use of new, yet undeveloped CMG's or use of multiple CMGs does not appear attractive because of the inherent weight of current CMG designs. Proposed new spherical large-angle magnetic bearing (LAMB) CMGs (Reference 5-3) would provide for some weight reduction, but probably would be feasible only if also used for other purposes such as power storage. The design concept of Figure 5.3-1 (from Reference 5-4) uses magnetic bearings and has application to energy storage as well as

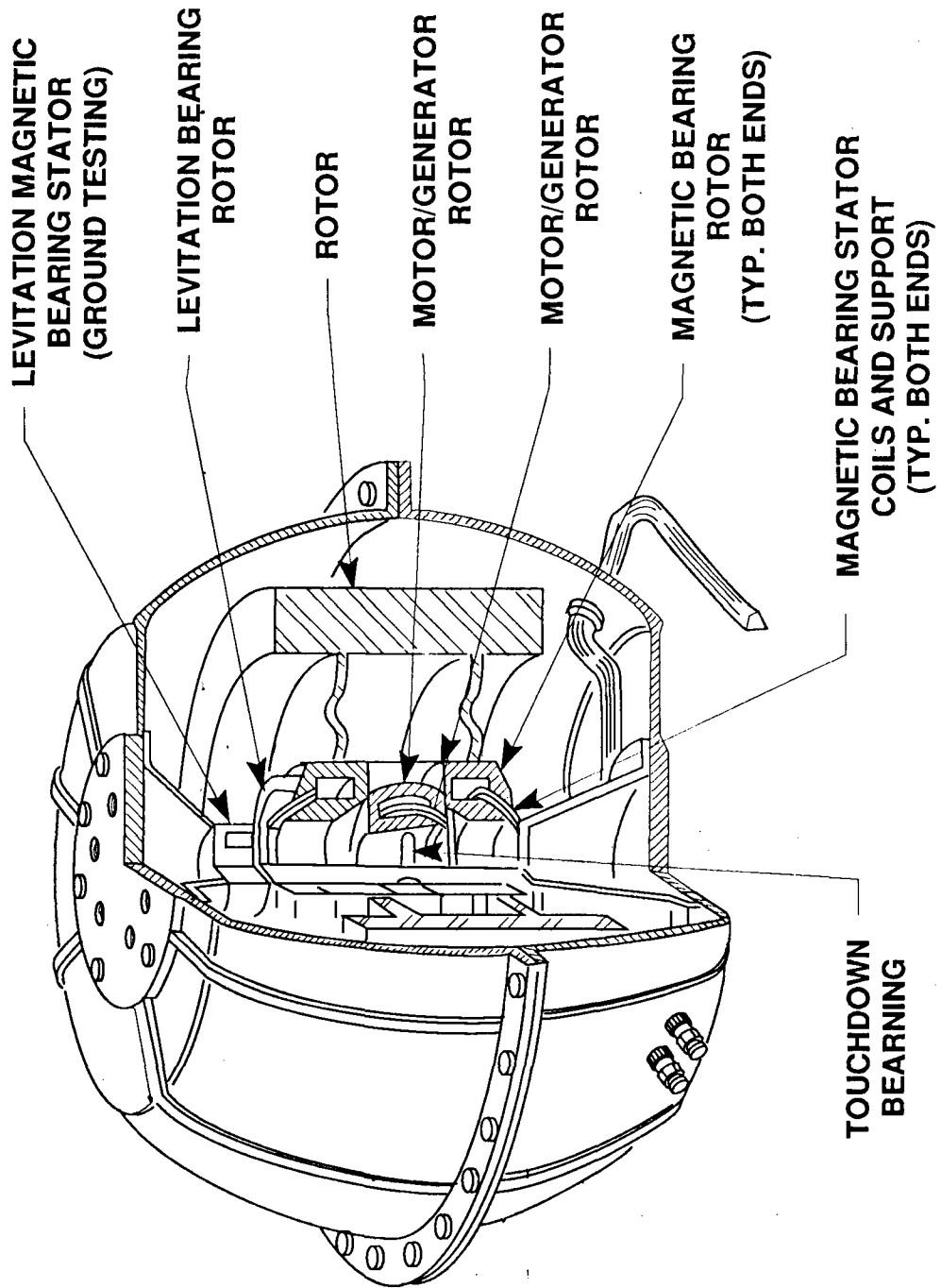


Figure 5.3-1 Advanced IPACS Unit Design Concept (from Reference 5-3)

angular momentum control. References 5-3, 5-5, and 5-8 contain much useful information relating to energy-storage flywheels and also on integrating these devices with angular momentum control aspects.

Recent developments in superconductive materials may greatly alter the prospective relative to control-moment gyros. This topic is discussed briefly in Section 9.

5.3.3 Dual Counterrotating Angular Momentum Control Devices

The mass required for a suitable DCAMCD system is greatly influenced by the allowable tilt of the wheels and the wheel radius. As shown in paragraph 5.2.3, using two wheels of 50-m radius and a 5 deg tilt of each wheel still required a total wheel weight of 14,263 kg (31,500 lb) if the wheels were operating close to design stress. A larger tilt angle and/or larger wheel radius would reduce the mass to an acceptable value.

5.3.4 Use of the ATSS Counterrotators

The counterrotators can be considered as inertia wheels to be tilted to counteract the gravity gradient. As shown in paragraph 5.2.4 only a small tilt angle is required for the ATSS. Implementing a mechanism to permit the tilt, which should vary over a small range about the zero value may be feasible.

5.3.5 General Remarks

The driving factor that sizes the angular momentum requirements for the ATSS is gravity-gradient torque and associated angular momentum. The

torque is given by approximately:

$$L = \frac{3 G m_e}{2 R_o^3} (I_z - I_x) \sin 2\alpha$$

G = Gravitational constant
 m_e = Mass of Earth
 R_o = Radius of the ATSS orbit
I = ATSS moment of inertia
about an axis
 α = Angle between the z axis
and local nadir

There are several factors to consider in reducing the torques, or in making acceptable the weight penalties associated with use of angular momentum control devices. These factors are:

1. Maintain a low value of α . This would require departing from a Sun-pointing orientation, which in the case of the ATSS, would greatly complicate the problem of collecting solar energy.
2. Reduce the difference $I_z - I_x$. For the ATSS, this could be accomplished by spreading the elements along the z-axis. For example, displacing each of the counterrotators about 53 m (174 ft) further from the plane of the torus would reduce $(I_z - I_x)$ to zero. However, this would require elongation of the central tube, complicate transfer of materials between station elements, increase mass, etc.
3. The use of inertial-wheel-type devices generally involve weight penalties; however, these penalties become viable if the device(s) serve multiple required tasks - for example, energy storage. Care must be taken, however, to account for any possible changes in available torque from the wheels, and resulting changes in dynamic behavior of the ATSS, associated with any change in overall angular momentum.
4. Tilting the counterrotators appears to be a method for meeting the angular momentum requirements.

5.4 Orbit Altitude Control

The aerodynamic drag acting on the ATSS will cause it to lose altitude. The drag is the resultant of the x and z forces shown in Figure 5.1-1 (from Reference 5-1). One of the outputs of the I-DEAS² programs (Reference 5-9) is the linear impulse applied by the drag in one orbit, and that value was 29,450 N-sec. The fuel needed to overcome a given linear impulse can be calculated by the use of equation (5-2). If H₂-O₂ fuel is assumed (Isp = 4310 N-sec/kg), then the fuel used in one orbit is 6.83 kg (15 lb).

REFERENCES

- 5-1 Queijo, M. J. et al.: Some Operational Aspects of a Rotating Advanced-Technology Space Station for the Year 2025, NASA CR-181617, June 1988.
- 5-2 Notti, J. E.; Cormach III, A.; and Schmill, W. C.: Integrated Power/Attitude Control System (IPACS) Study, NASA CR-2383.
- 5-3 Oglieve, R. E.; and Eisenhaure, D. B.: Integrated Power and Attitude Systems for Space Station, AIAA-85-0358, January 14-17, 1985.
- 5-4 Downer, James R. et al: Application of Magnetic Bearings to High-torque Satellite Attitude Control Wheels, In: IECEC '87; Proceedings of the Twenty-second Intersociety Energy Conversion Engineering Conference, Philadelphia, PA, August 1987.
- 5-5 Lawson, Louis J.: Design and Testing of High Energy Density Flywheels for Application to Flywheel/Heat Engine Hybrid Vehicle Driver 1971 Intersociety Energy Conversion Engineering Conference, Boston, Massachusetts, August 3-5, 1971.
- 5-6 Anderson, Willard W., and Groom, Nelson J.: The Annular Momentum Control Device (AMCD) and Potential Applications, NASA TND-7866, March 1975, February 7-9, 1984.
- 5-7 M. J. Queijo, et al: Analyses of a Rotating Advanced-Technology Space Station for the Year 2025, Study and Concepts, NASA CR 178345, January 1988.
- 5-8 An Assessment of Integrated Flywheel System Technology, NASA Conference Publication 2346.
- 5-9 "I-DEAS² Users Manual", Structural Dynamics Research Corporation, San Diego, CA, December 1985.

6.0 EXAMINATION OF POTENTIAL APPLICATIONS OF ELECTROTHERMAL PROPULSION FOR ATTITUDES AND ORBIT CONTROL

The large masses of chemical fuel (H_2-O_2) or of control-moment gyro devices required for ATSS attitude control led to the thought of examining electrothermal propulsion because of the high specific impulse available. It was realized that such devices would involve a trade-off between high specific impulse and electrical power usage. This section presents a brief assessment of the potential application of electrothermal propulsion for orbit and attitude control of the ATSS.

6.1 Electrothermal Thruster

Electrothermal thrusters include the resistojet and the arc jet. Both apply electrical energy to an inert propellant stream to generate a high discharge velocity gas jet. The technology represents an advance over cold gas and monopropellant chemical hydrazine thrusters. Numerous applications of resistojets have been implemented for unmanned spacecraft. The nominal ranges of thrust and electrical power for the electrothermal thrusters and some other electric propulsion options is presented in Figure 6.1-1 from Reference 6-1. These data show that practical applications limit the maximum thrust to about 10 N (2.2 lb) for electrothermal units. Specific impulses developed by these thrusters depends on the propellant selected as well as the design features of the device itself. A technology trend prediction from Reference 6-1 is presented in Figure 6.1-2 for three typical propellants in resistojets. The practical specific impulse limits as a function of the specific power ratio from Reference 6-2 are presented in Figure 6.1-3 for electrothermal thrusters. For comparison purposes, the baseline ATSS assumes a

PRECEDING PAGE BLANK NOT FILMED

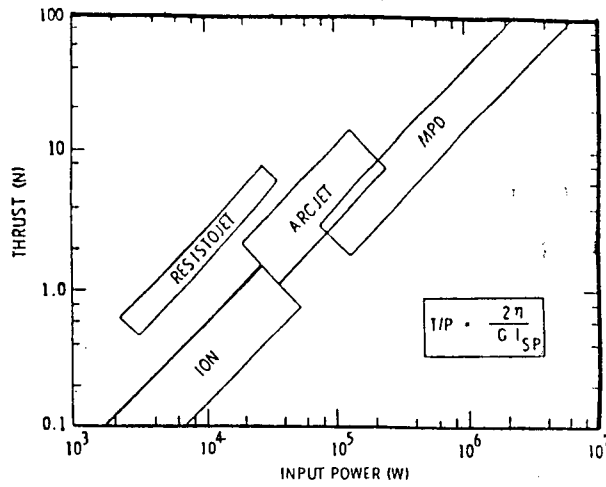


Figure 6.1-1 Operational Regimes for Electrical Thrusters

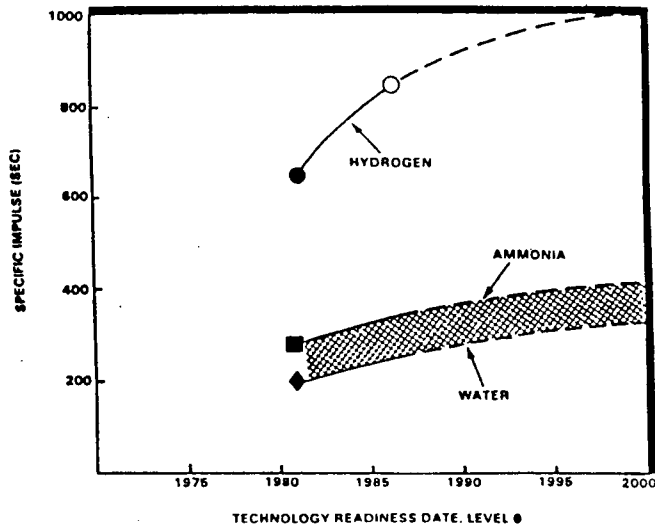


Figure 6.1-2 Resistojets Specific Impulse Trends

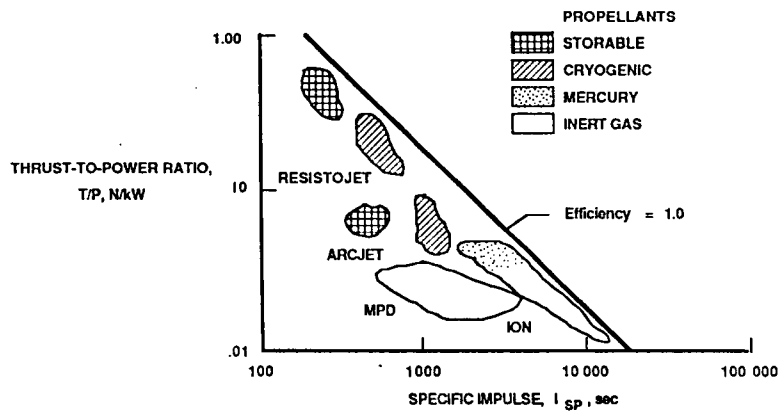


Figure 6.1-3 Thrust-to-Power Ratio vs. Specific Impulse

hydrogen-oxygen chemical thruster mechanization with a specific impulse of 4310 N-sec/kg (440 sec).

6.2 Application to the Gravity-Gradient Disturbance

The ATSS configuration coupled with the flight orientation requires a thruster moment capability of up to 34,000 N-m (25,000 ft-lb) to null gravity-gradient torque. Using a total of eight active jets with an average moment arm of 40 m (131 ft), the thrust at each application point is approximately as follows to develop the reactive moment:

$$\text{Thrust} = \frac{\text{Moment}}{(\text{Number of Jets}) (\text{Moment Arm})} = \frac{35000}{(8) (40)} = 106 \text{ N (24 lb)}$$

This thrust level may be the sum of several clustered jets in proper alignment at each of the grid points. The maximum combined thrust required to react the gravity-gradient effect is 850 N (187 lb).

The gravity-gradient disturbance torque varies with time as a sine function at one-half the orbital period. Therefore, matching the disturbance will require a time variable reaction moment. This may be achieved by proportional thrusting or by constant thrusting for discrete time intervals. The latter is simpler to implement. The fixed thrust per thruster required to perform such a stabilization could be less than the maximum demand, i.e., 106 N (24 lb). For purposes of preliminary design, a fixed thrust per thruster of 53 N (12 lb) is suggested for reaction to the gravity-gradient disturbance and maintaining an acceptable limit cycle of excursions. With no thrusting reaction to the gravity-gradient moment, the angular displacement amplitude monotonically increases, which is unacceptable for effective solar pointing. The fixed thrust to provide a limit cycle excursion of 1 deg, which is the nominal

requirement, has not been determined. This would require the definition of a control algorithm for the preliminary evaluation. The ultimate selection of a thrust level will be influenced by the mass of propellant consumed to maintain the attitude within limits. This would require a trade-off of three parameters; the thruster level, the limit cycle amplitude, and the propellant mass consumed. In the studies to date, only the extreme conditions for zero thrusting and for fixed attitude (perfect alignment) thrusting have been examined. The propellant consumption for gravity-gradient stabilization for the ideal fixed attitude case, and at a specific impulse of 4310 N-sec/kg (440 sec), is approximately 717 kg (1577 lb) per orbit. The control logic that is applied and the limit cycle excursions that are acceptable from the solar pointing attitude will determine the propulsive impulse required for reaction to the gravity-gradient disturbance. There is an opportunity for significant mass savings if gravity-gradient stabilization can be performed without application of chemical fueled thrusting. These options were discussed in Section 5.

Using typical thrust-to-power ratios from Reference 6-2, i.e., 0.13-0.31 N/kW (0.03 - 0.07 lb/kW) for resistojets, results in a peak power requirement of from 2741 - 6538 kW for the gravity-gradient application. Even using a time average thrust level total of 425 N (94 lb) continuously and allowing for attitude excursions which, over an orbit would average out, results in a power demand which consumes all, or the majority of, the ATSS electrical generating capacity.

Another factor to consider is that the current and planned technology for electrothermal thrusters is in the range of thrust up to approximately 10 N (2 lb), as shown in Figure 6.1-1 from Reference 6-1.

The gravity-gradient application for the ATSS requires development of thrusters which are 10 to 100 times this current planned thrust level, depending upon the number that may be considered practical to cluster at one point.

The influence of the two system parameters, i.e., total thrust and peak power are such that electrothermal thrusters within the practical range of overall efficiency cannot be applied to the ATSS gravity-gradient reaction requirement. The peak unit thrust of 106 N (23 lb) implies the use of a chemical rather than electrothermal thruster implementation. The electrothermal options may still be considered for drag make-up or other attitude control functions. However, the complete stabilization system would require the higher thrust chemical thrusters to maintain control under the gravity-gradient influence, unless a gyro approach is used. (See Section 5.)

6.3 Application to the Atmospheric Drag

The atmospheric drag force has a peak value of approximately 7 N (1.5 lb) over the nominal orbital path, as shown in Figure 5.1-1. Although the atmospheric drag is a continuously varying parameter throughout the orbit, it is practical to consider applying the reboost thrust at a fixed level over an interval to achieve the desired effect. The baseline ATSS orbit-keeping thrusters use approximately 6.8 kg (15 lb) of hydrogen and oxygen propellant per orbit to maintain altitude. Considering the low thrust level and modest propellant consumption, the orbit-keeping function is potentially suited for application of the electrothermal thruster option. Space Station Freedom uses a resistojet for this function.

The electrical power required to operate a resistojet at 5 N (1.1 lb) thrust level can range from 16 to 38 kW based upon the predictions of Reference 6-1. This power level is practical for the ATSS. The baseline propulsion system uses hydrogen and oxygen as the propellants, which are electrolyzed from water. The electrolysis process, at a 70 percent efficiency, develops propellant gas at the equivalent ratio of 0.202 N/kW (0.0452 lb/kW) for power consumption. For the nominal 5 N (1.1 lb) thruster, this is the equivalent of 22.7 kW in electrical power demand. Therefore, if water is used as the resistojet propellant, the power consumption would be comparable to that for the baseline chemical rocket system. One difference is that for the chemical rocket, the electrical energy use may be displaced in time and spread over time compared with the time of thrusting. In the resistojet the electrical energy is used in real time with the thrusting event. At the level of power being used, i.e., 20 kW compared with the total capacity of 2500 kW, this time related difference should not prove to be significant.

A significant effect is the potential difference in specific impulse of the chemical and the electrothermal thrusters. The chemical (hydrogen-oxygen) thruster is projected to develop a specific impulse of 4310 N-sec/kg (440 sec). A water propellant resistojet would be limited to specific impulse of approximately 2942 N-sec/kg (300 sec), as illustrated in Figure 6.1-2. Therefore, approximately 50 percent more water would be consumed by the electrothermal thruster to perform the same function with the same or lower power level. To improve the mass effectiveness would require going to higher power levels and selecting a propellant such as hydrogen.

Hydrogen, as the propellant generated from electrolysis of water onboard the ATSS, would increase the power demand for propulsion. Since water is comprised of only one-ninth hydrogen by mass, the electrical demand per unit mass of hydrogen generated is the equivalent of 0.045 N/kW (0.099 lb/kW) for a hydrogen jet with specific impulse of 8630 N-sec/kg (880 sec). In addition, the hydrogen must be heated in the resistojet, using an additional power allocation of about 0.2 N/kW. This brings the total power for the 5 N (1.1 lb) thruster level to the sum of:

$$\frac{5}{0.045} + \frac{5}{0.2} = 111 + 25 = 136 \text{ kW}$$

This hydrogen resistojet would consume six or more times the power of the water resistojet when the electrolysis energy is included. Also the mass of oxygen liberated would have to be allocated to the resistojet system mass as being a non-propulsion byproduct. Some of the excess oxygen could be allocated to atmospheric leakage from the ATSS environment, but the leakage is not anticipated to consume the daily surplus of oxygen equivalent to the hydrogen propellant. Therefore, onboard generated hydrogen for a resistojet results in a distinct disadvantage in total power consumption and also equivalent mass (propellant) consumption when compared with the baseline chemical thruster option or the water resistojet. If hydrogen or ammonia is resupplied from Earth, then the power to synthesize the propellant and the penalty of surplus oxygen are not allocated to the resistojet mechanization. However, hydrogen is a bulky, i.e., lower density commodity to resupply, and the baseline ATSS has elected not to resupply hydrogen.

The selection of a low (5 N, 1.1 lb) thrust resistojet option for drag make-up, or orbit-keeping will also depend upon the navigation system choices. Instead of essentially continuous orbit-keeping, it may

be determined that corrections would only be made after a number of orbits. The latter would favor high thrust options such as the chemical thruster approach.

6.4 Application to the Solar Radiation Disturbance

The solar radiation pressure force is about 0.1 N (0.02 lb) during the sunlit portion of the orbit. This small effect and action time does not require a separate mechanization.

6.5 Arc-Jet Electrothermal Thruster Option

The arc jet is another type of electrothermal thruster to be evaluated as a low thrust candidate. In the arc jet, the electrical energy is introduced into the propellant gas stream from an arc discharge spanning the gas flow. The propellant is dissociated and ionized into a plasma state and expanded through a nozzle to provide thrust. This approach differs from the resistojet in that the electrically generated heat does not first pass through a resistance material in contact with the gas. The operating temperatures can be much higher in the arc jet, and therefore the jet velocity and specific impulse are higher than for the resistojet. The arc jet has a typically low electrical conversion efficiency due to several intrinsic loss effects. Chemical recombination of the plasma is not achieved in the expansion, and there are large losses associated with unrecovered chemical energy. Other losses include thermal radiation and electrode-arc effects. The net electrical efficiency is in the range of 10 to 20 percent insofar as the usable energy that is recovered in the jet compared with the input. Another characteristic of the arc jet is that the electrodes erode under the

influence of the arc, which limits their operating life. Operation in a pulsed arc mode has been suggested as a method for prolonging electrode life.

Power consumption is the key consideration in evaluating the arc-jet application to the ATSS. The thrust versus power characteristic of arc jets is presented in Figure 6.1-1 from Reference 6-1. Arc jets appear to require three to four times the power of an equivalent resistojet. Reference 6-1 reported thrust to power ratios of from 0.036 to 0.18 N/kW (0.008 to 0.04 lb/kW) for arc jets as compared with 0.14 to 0.31 N/kW (0.03 to 0.07 lb/kW) for resistojets. The power consumption of an arc jet with 5-N (1.1-lb) of thrust would be in the range of 28 to 140 kW. The 5-N (1.1-lb) thrust level is approximately the magnitude of the aerodynamic drag force that must be overcome to maintain the selected orbit. The arc-jet application, if any, to the ATSS is best suited for the function of aerodynamic drag make-up using water as the propellant medium. The power demand to generate 5 N (1.1 lb) of thrust is approximately five percent of the generating capability of the power system and the prospective benefit over the use of options other than the arc jet is a reduction in propellant mass of 1 to 2 kg (2 to 4 lb) per orbit. The technology would have to be developed for long life operation with water as the propellant in the arc jet. Configuration of an arc-jet thruster is propellant-specific because the current-voltage characteristic of the power supply depends upon the electrical conductivity of the plasma generated between the electrodes. Contemporary arc-jet thrusters are being developed for use with ammonia and hydrogen propellant to take advantage of the potentially high

specific impulse with these propellants. As was noted, hydrogen generation on the ATSS is a heavy power consumer.

6.6 Summary

In summary, it appears that the resistojet with water as the propellant could be applied to the atmospheric drag make-up function of the ATSS. The thrust required is compatible with the planned capability for resistojets. The electrical power consumption is comparable to that for the hydrogen-oxygen chemical thruster when the electrolysis energy is included. The overall specific impulse for the water resistojets is about two-thirds that of the chemical thruster, and therefore more water is consumed. However, the effect is approximately 3.4 kg (7.5 lb) per orbit for the mass penalty. The use of hydrogen as the propellant in a resistojet thruster would reverse this mass penalty but would increase power consumption and require hydrogen resupply to be practical for the ATSS application. The thrust level that can be achieved at reasonable power levels is compatible with the drag make-up application requirements and would permit more or less continuous correction to be accomplished.

REFERENCES

- 6-1 Anon., "NASA Space Systems Technology Model, Data Base Technology Forecasts", Volume I, Part A, NASA TM 88176, June 1985.
- 6-2 Stone, J. R., "NASA Electrothermal Auxiliary Propulsion Technology", AIAA Paper 86-1703, June 1986.

7.0 SPACE STATION STRUCTURES AND LAUNCH VEHICLE TECHNOLOGIES

The ATSS concept described in References 7-1, 7-2, and 7-3 uses expandable structures which include modular, telescopic, and erectable trusses that are launched as subassemblies and assembled on low Earth orbit (LEO). The habitats contain a pressure that is the equivalent of one Earth atmosphere, and they rotate at less than 3 rpm to simulate the gravity of Earth in the torus. Heavy lift launch vehicles (HLLV) with capabilities for handling payloads having masses up to 2.7×10^5 kg (6×10^5 lb) (Reference 7-4) will be required to deliver the 24 torus subassemblies of the ATSS to LEO in approximately 12 launches. This section examines the potential for alternate launch vehicle capability to deliver torus subassemblies to orbit based on several expandable structures concepts. The payload envelope size and mass limitations dictate the number and size of the modules and subassemblies. The usage of composite structural materials is also examined to assess the benefit of launching reduced mass payloads.

The launch vehicles, structural concepts, selection of materials, number of launches to LEO, and the level of extravehicular activity (EVA) to assemble a rotating torus and other ATSS subassemblies are reviewed for the purpose of more clearly focusing on the real need for and potential benefits of advances in structures, materials, and launch vehicle technologies,

7.1 Scope of Analyses and Discussions

The structural design of a rotating space station must be altered from the ATSS configuration if it is to be delivered to LEO by launch vehicles with different mass and volume capabilities than the HLLV

assumed for the ATSS. Four expandable structural concepts have been examined for this purpose. The large rotating torus was configured using selected expandable structures concepts to fit four classes of launch vehicles. In addition, a smaller rotating space station was configured using launch vehicle elements as building blocks. These selections are shown in Table 7.1-1. The Saturn V is not a real option but is included for comparison purposes. The Jarvis HLLV is being proposed for use in the 1990's.

In the discussions of these example applications, the structural concepts are defined, estimates are made of the number of launches required to deliver the torus or station to LEO, the orbital assembly techniques are identified, and estimates of EVA and intravehicular activity (IVA) are made as appropriate. This section includes a discussion of mass savings using composite structural materials instead of aluminum and a summary of conclusions regarding advanced technologies of structures, materials, and launch vehicles.

7.2 Launch Vehicles

7.2.1 National Space Transportation System and Expendable Launch Vehicles

The National Space Transportation System (NSTS) consists of an Orbiter (Space Shuttle), an external tank, and two strap-on solid rocket motors. The Orbiter is flown back to Earth from LEO and is reused. The solid rocket motor boosters are recovered after each launch and reused. The external tank is expendable and is jettisoned just prior to the Shuttle Orbiter being inserted in LEO. The external tank reenters the Earth's atmosphere and is destroyed over the ocean (Reference 7-5). The Shuttle Orbiter is designed to transport a maximum of 2.9×10^4 kg ($6.5 \times$

TABLE 7.1-1 STRUCTURES CONCEPTS EVALUATED FOR SELECTED LAUNCH VEHICLES

LAUNCH VEHICLE CLASS	EXPANDABLE STRUCTURES CONCEPT			
	INFLATABLE (Flexible)	HINGE FOLDABLE (Semirigid)	TELESCOPIC (Semirigid)	MODULAR (Rigid)
NSTS	TORUS	TORUS	TORUS	TORUS AND ROTATING SPACE STATION
SATURN V		TORUS	TORUS	
JARVIS		TORUS	TORUS	
ADVANCED HLLV				TORUS

10^4 lb) mass to LEO but it is currently rated to transport 1.77×10^4 kg (4×10^4 lb) to a 407 km (220 nmi) circular orbit at an inclination of 28.45° . An increase in rocket motor thrust with a flight qualification test program is required to rate the Orbiter for its maximum payload lift capability. The cargo bay is 4.6 m (15 ft) in diameter by 18.3 m (60 ft) in length. Each payload and its support fixtures must fit within the flight envelope of the cargo bay, requiring close coordination with the NASA Johnson Space Center payload manifest specialists.

The Space Shuttle is this nation's primary launch vehicle that is capable of transporting a payload of large mass and size to LEO. The current Shuttle launch schedule shows two launches in 1988, nine launches during 1989, and eight during the year 1990. These are followed by an increase during each succeeding year to a total of 14 by the mid-1990's*

Expendable launch vehicles (ELV) such as Titan III and Titan IV complement the NSTS by launching payloads which do not justify or are not compatible with Shuttle launches. The Titan IV ELV has a payload size comparable to the Shuttle. The present payload mass launch capability to LEO is 1.77×10^4 kg (3.9×10^4 lb) (Reference 7-6). Several United States ELVs are also available that can transport a lesser mass and size payload to LEO and are listed in Table 7.2-1.

7.2.2 Past and Future United States Launch Vehicles

The Saturn V was a heavy lift launch vehicle abandoned in 1973 after the Apollo and Skylab programs. It could launch a 9×10^4 kg (2×10^5 lb) payload to a 500-km (270 nmi) circular orbit at an inclination of 50

*Telephone interview with Mr. Craig Carothers, NASA-JSC, March 2, 1988

TABLE 7.2-1 SOME CURRENT USA LAUNCH VEHICLES COMPARED WITH THE SATURN VEHICLES

LAUNCH VEHICLE	PAYLOAD MASS TO LEO FROM ETR 10 ³ kg (10 ³ lb)	PAYLOAD SIZE Diameter x Height m (ft)	INFORMATION SOURCE
SATURN 1B*	16.8 (37)	3.9 x 11.3 (13 x 37)	Reference 7-7
SATURN V*	94.3 (208)	6.7 x 35.9 (22 x 118)	Reference 7-7
SHUTTLE	18.1 (40)	4.6 x 18.3 (15 x 60)	Tel/Con Mr. Craig Carothers, NASA - JSC, 3/2/88
SCOUT	0.21 (0.475)	0.8 x 1.5 (2.5 x 5)	Tel/Con Mr. Larry Tant, NASA - LaRC, 4/7/88
DELTA II	3.9 (8.78)	2.7 x 3.0 (9 x 10)	Tel/Con Mr. Dick Sciafford, NASA - GSFC, 2/26/88
ATLAS CENTAUR I	5.4 (12)	3.7 x 4.6 (12 x 15)	Tel/Con Mr. Robert C. White, General Dynamics, 4/1/88
TITAN 3	14.3 (31.6)	3.7 x 14.3 (12 x 47)	Tel/Con Mr. L. L. Quiram, Martin Marietta, Denver, CO, 4/13/88
TITAN 4	17.7 (39)	4.6 x 20.4 (15 x 67)	Tel/Con Mr. L. L. Quiram, Martin Marietta, Denver, CO, 4/13/88

* ABANDONED 1973

deg. The Skylab workshop payload size envelope was 6.7 m (22 ft) in diameter by 36 m (118 ft) in height. The Saturn V launch vehicle is mentioned here for comparison with the payload mass launch capability of current and proposed HLLVs (Reference 7-7).

The Jarvis launch vehicle is a proposed HLLV concept capable of launching a 8.4×10^4 kg (1.85×10^5 lb) payload to LEO. The payload envelope would be 8.4 m (27.5 ft) in diameter by 25.6 m (84 ft) in length. The Jarvis is a shuttle-derived vehicle that would use shuttle main engines, external tank, and strap-on solid rocket motors as designed for current manufacturing methods (Reference 7-8).

A future HLLV has been studied at the NASA Marshall Space Flight Center for the year 1995 and beyond which could launch a payload of 2.7×10^5 kg (6×10^5 lb) to LEO (Reference 7-4). The payload size envelope would be 15.2 m (50 ft) in diameter by 61 m (200 ft) in length.

7.2.3 Launch Services Available from Foreign Nations

Russia, India, China, France, and Japan have developed launch capabilities which could be provided to the United States. Table 7.2-2 is a list of international expendable launch vehicles identified by the payload mass they can deliver to orbit (Reference 7-9). Russia's Proton (SL-13) and France's Ariane IV are capable of delivering payloads to LEO in the same mass category as the currently rated Shuttle Orbiter (References 7-10 and 7-11). The Proton launch vehicle has proven very reliable with over 100 successful launches. Russia's Energiya HLLV is capable of launching a 1×10^5 kg (2.2×10^5 lb) payload to LEO which compares with the payload launch capabilities of the Saturn V launch vehicle. The features of Soviet launch vehicles are summarized in Figure

TABLE 7.2-2 EXPENDABLE LAUNCH VEHICLES OF THE WORLD
(Adapted from References 7-9 and 7-10)

COUNTRY	NAME	LAUNCH MASS Tonne (10 ³ lb)	PAYLOAD MASS AND ORBIT kg (lb)			STATUS
CHINA	CZ-1C	88 (194)	400 (880)	SSO	OPERATIONAL	
	CZ-2	191 (420)	2,600 (5,720)	LEO	OPERATIONAL	
	CZ-2/4L	419 (921)	9,000 (19,800)	LEO	FIRST FLIGHT 1990	
	CZ-3	202 (444)	1,400 (3,080)	GTO	OPERATIONAL	
	CZ-3/4L	420 (924)	5,000 (11,000)	GTO	FIRST FLIGHT 1992	
EUROPE	ARIANE 4	471 (1,036)	4,200 (9,240)	GTO	FIRST FLIGHT 1987	
	ARIANE 5/H10	550 (1,210)	8,200 (18,040)	GTO	FIRST FLIGHT 1994	
	ARIANE 5/L4	550 (1,210)	15,000 (33,000)	LEO	FIRST FLIGHT 1995	
INDIA	ASLV	40 (88)	150 (330)	LEO	FIRST FLIGHT 1987	
	PSLV	276 (607)	1,000 (2,200)	SSO	FIRST FLIGHT 1989	
	GSLV	N/A	1,300 (2,860)	GTO	PROPOSAL	
JAPAN	M-3S	49 (108)	290 (638)	LEO	OPERATIONAL	
	M-3S2	61 (134)	770 (1,304)	LEO	OPERATIONAL	
	H-2	258 (568)	2,000 (4,400)	GEO	FIRST FLIGHT 1992	
USSR	VOSTOK	279 (614)	1,000 (2,200)	SSO	OPERATIONAL	
	SOYUZ	326 (717)	7,000 (15,400)	LEO	OPERATIONAL	
	SL-3	290 (638)	6,300 (13,860)	LEO	OPERATIONAL	
	SL-4	310 (682)	7,500 (16,500)	LEO	OPERATIONAL	
	SL-6	310 (682)	2,100 (4,620)	LEO	OPERATIONAL	
	SL-8	120 (264)	1,700 (3,740)	LEO	OPERATIONAL	
	SL-11	180 (396)	4,000 (8,800)	LEO	OPERATIONAL	
	SL-12	680 (1,496)	N/A	LEO	OPERATIONAL	
	SL-13 } PROTON	670 (1,474)	19,500 (42,900)	LEO	OPERATIONAL	
	SL-13 }	680 (1,496)	2,000 (4,400)	GEO	OPERATIONAL	
	SL-14	190 (418)	5,500 (12,100)	LEO	OPERATIONAL	
	SL-16	400 (880)	15,000 (33,000)	LEO	OPERATIONAL	
	HLLV	2,000 (4,400)	100,000 (220,000)	LEO	UNDER DEVELOPMENT	
HLLV W/SPACEPLANE	2,000 (4,400)	30,000 (66,000)	LEO	UNDER DEVELOPMENT		
USA	ATLAS H	130 (286)	1,361 (2,994)	LEO	OPERATIONAL	
	ATLAS G/CENTAUR	164 (361)	2,177 (4,789)	GTO	OPERATIONAL	
	ATLAS K/CENTAUR	215 (473)	2,948 (6,485)	GTO	PROPOSED	
	TITAN 2	200 (440)	1,905 (4,191)	LEO	OPERATIONAL	
	TITAN 3	760 (1,672)	14,470 (31,834)	LEO	OPERATIONAL	
	TITAN 4	1,000 (2,200)	17,690 (38,918)	LEO	FIRST FLIGHT 1988	
	DELTA 3920	193 (425)	1,284 (2,825)	GTO	OPERATIONAL	
	DELTA 6920	N/A	1,447 (3,183)	GTO	FIRST FLIGHT 1988	
	DELTA 7920	N/A	1,615 (3,553)	GTO	FIRST FLIGHT 1990	
	ENHANCED DELTA 2	N/A	1,819 (4,002)	GTO	PROPOSAL	
	SCOUT G-1	21 (46)	200 (440)	LEO	OPERATIONAL	
	UPGRADED SCOUT	N/A	550 (1,210)	LEO	PROPOSAL	
	CONESTOGA	N/A	1,360 (2,992)	LEO	UNDER DEVELOPMENT	
	AMROC	N/A	1,878 (4,132)	LEO	UNDER DEVELOPMENT	
	LIBERTY	281 (618)	9,070 (19,954)	LEO	PROPOSAL	
	JARVIS	N/A	38,500 (84,700)	LEO	PROPOSAL	

7.2-1 and show the SL-13 Proton in comparison with the heavy lift configurations under development. Figure 7.2-2 provides a summary of current and proposed international ELVs.

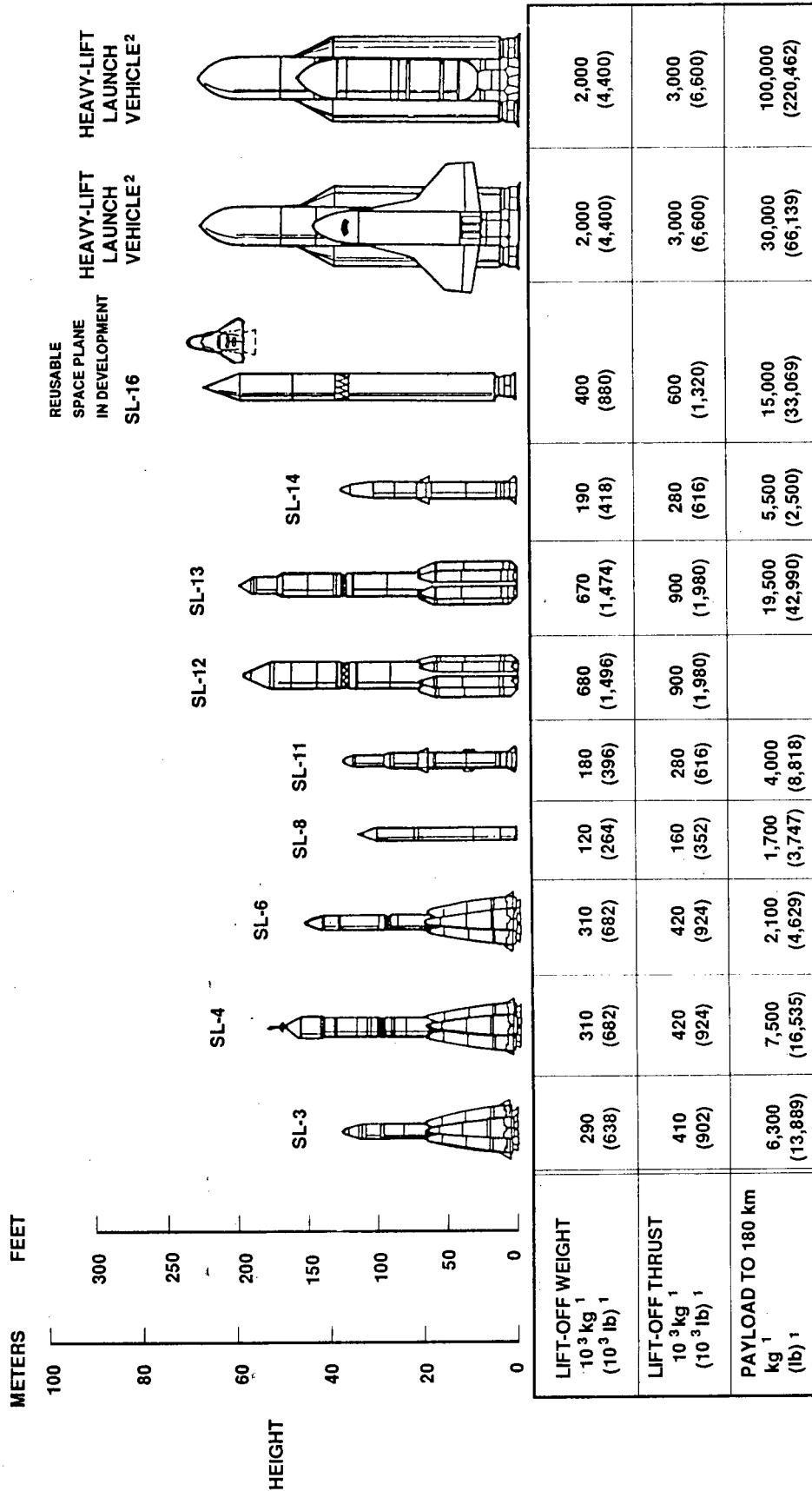
7.3 Expandable Structural Configurations

The configuration of the ATSS torus assembled from 24 completely outfitted modules is shown in Figure 7.3-1 for comparison purposes with the torus assembly concepts described in this section.

7.3.1 Structural Configurations for a NSTS Launch

These alternate configurations are designed of components, modules, telescopic assemblies, and erectable truss structure sized to permit transport to LEO via the NSTS. The ATSS habitat torus is assembled of equal length segments having a 7.6-m (25-ft) minor radius and a 114.3-m (375-ft) major radius. Three expandable structures concepts are defined which permit on-orbit assembly of a torus having a near comparable volume to the torus proposed for the ATSS. The concepts are inflatable, hinge foldable, and telescopic structures. A torus formed of cylindrical segments is sized and designed to fit within the payload envelope of the NSTS.

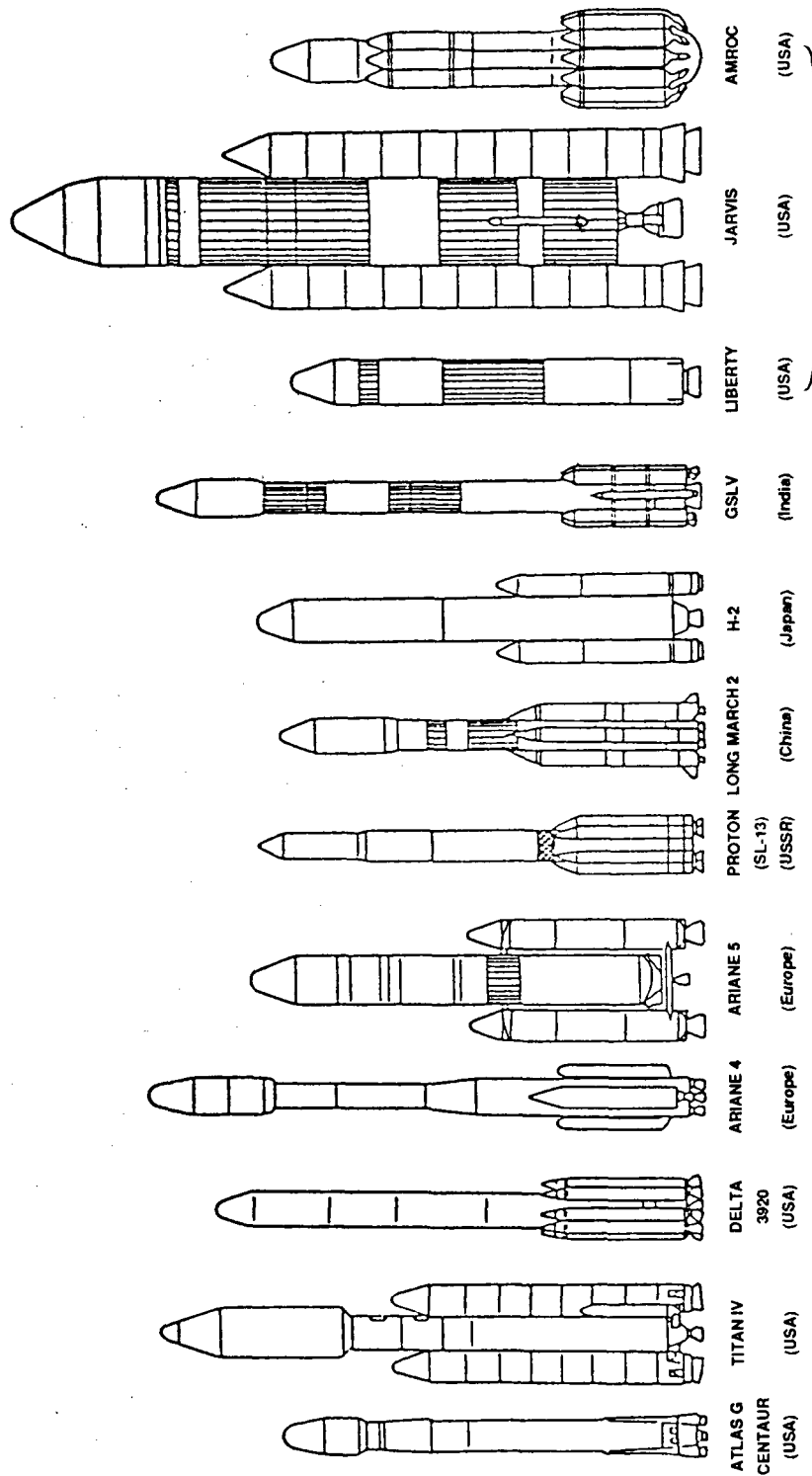
The first concept uses an inflatable torus segment 15.2 m (50 ft) in diameter by 18.3 m (60 ft) in length constructed as a stressed skin pressure vessel. The composite vessel wall is tape or filament wound of glass fiber reinforced plastic. The plastic matrix resin is partially polymerized ("B" staged) to permit the wound vessel segment to be foldable. A fold pattern as shown in Figure 7.3-2 permits a 12 ray folded segment to fit within a 4.6-m (15-ft) diameter payload envelope.



¹ APPROXIMATE

² IN FINAL STAGES OF DEVELOPMENT

Figure 7.2-1 Soviet Space Launcher Fleet (adapted from Reference 7-10)



Not to Scale

HEIGHT m (ft)	40 (131)	50 (164)	39 (128)	45 (148)	45-52 (148-171)	52 (171)	46 (151)	54 (177)	Unknown	38 (125)	63 (207)	25 (82)
TOTAL MASS 10^3 kg (10^3 lb)	163 (359)	868 (1,910)	194 (427)	470 (1,034)	500 (1,100)	695 (1,529)	419 (922)	240 (528)	275 (605)	282 (620)	Unknown	Unknown
PAYLOAD kg (lb)	2,364 (5,211)	4,545 (10,020)	1,272 (2,804)	4,270 (9,414)	8,000 (17,636)	2,200 (4,850)	2,000 (4,409)	2,004 (4,418)	1,800 (3,968)	3,000 (6,614)	7,954 (17,536)	1,878 (4,140)
ORBIT	GTO	GEO	GTO	GTO	GTO	GEO	GTO	GEO	GTO	GTO	GEO	LEO

Figure 7.2-2 International Expendable Launch Vehicles (adapted from Reference 7-11)

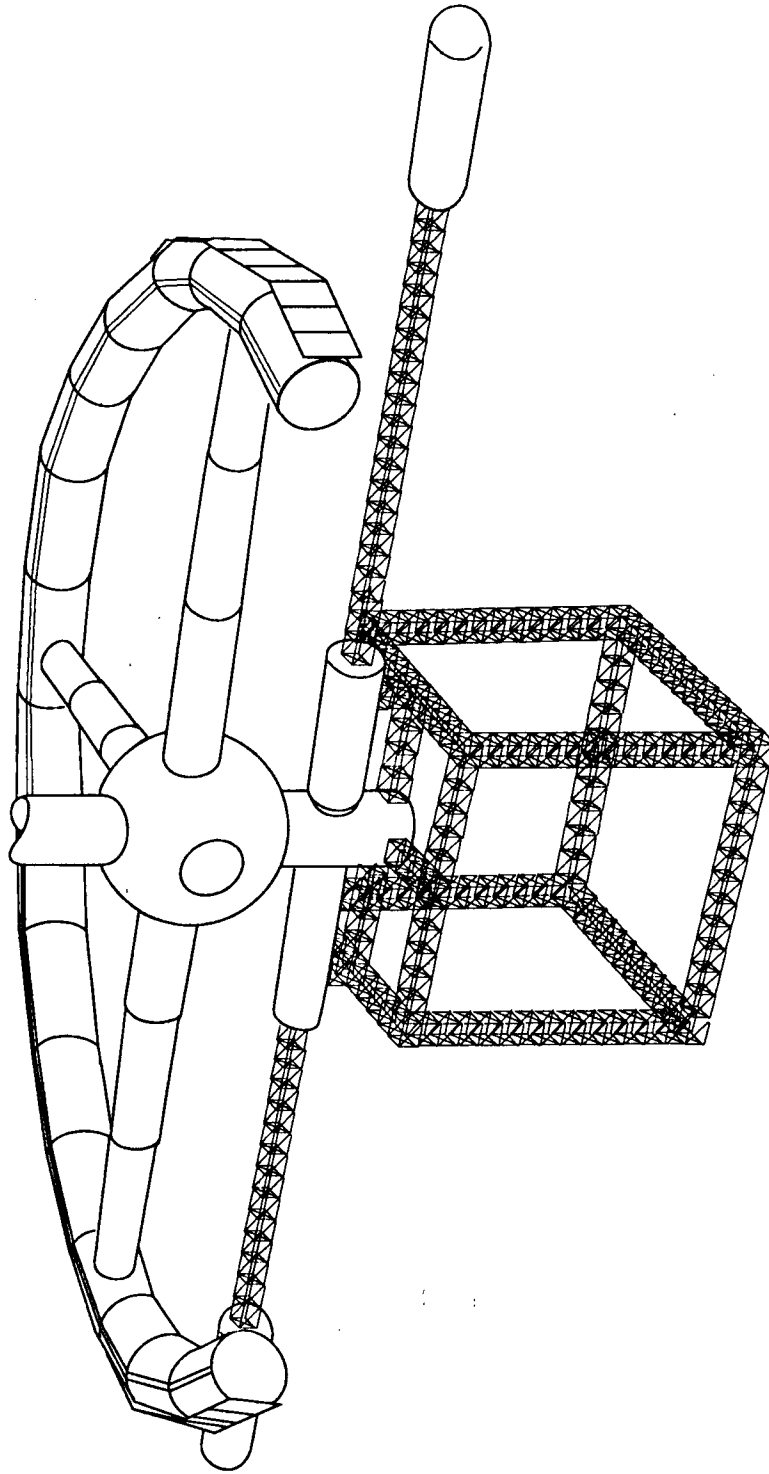


Figure 7.3-1 AISS Torus Assembly of Cylindrical Segments
(Reference 7-2)

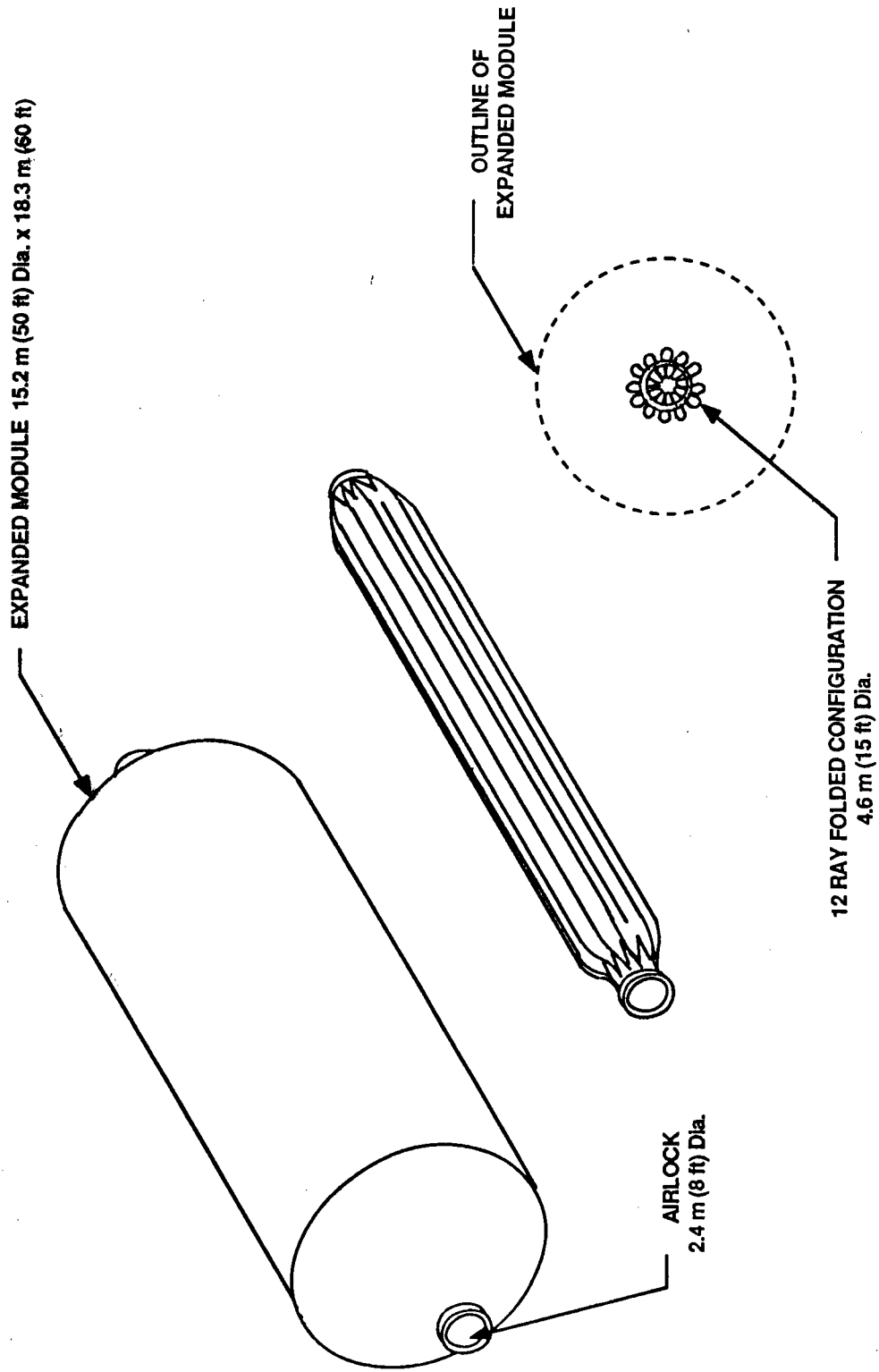


Figure 7.3-2 Expandable Habitat Module, Harden-In-Space

After delivery to LEO, the module is inflated and the matrix resin polymerized (hardened) to "C" stage using solar ultraviolet light or electron beam energy (References 7-12 and 7-13). A total of 40 such segments would be required to form a torus that has a major radius of 114.3 m (375 ft).

A second concept uses a semirigid hinge foldable structure. The cylinder is formed of rigid, narrow curved panels which permit folding the cylinder into a daisy-petal cross-sectional configuration. Thus, the 15.2-m (50-ft) diameter cylinder, when folded, fits within the 4.6-m (15-ft) diameter payload envelope of the Shuttle Orbiter (Figure 7.3-3). The daisy-petal fold pattern provides a high packaging density payload for transport aboard the Shuttle Orbiter. Upon delivery to orbit, the folded configuration is unfolded and locked into a cylindrical shape with elastomeric vacuum tight seals at the hinge joints. Closures required at the ends of the cylinder are made of a "B" staged matrix resin filament or tape wound composite structure which is unfolded on-orbit for attachment to the cylinder ends and hardening in place. The daisy-petal fold concept for expandable structure is reviewed in Table 7.3-1, whereby different fold patterns are evaluated to form a 15.2-m (50-ft) diameter cylinder on-orbit. The number of petals of the fold pattern will dictate the minimum radius for the folded cylinder to establish a specific payload size. Decreasing the number of daisy petal folding segments increases the minimum radius of the folding system. Forty of these erectable cylinders are required to permit assembly of the torus on-orbit.

A third concept of placing a torus in LEO via the Shuttle is accomplished by transporting three telescoped cylinders to orbit per each

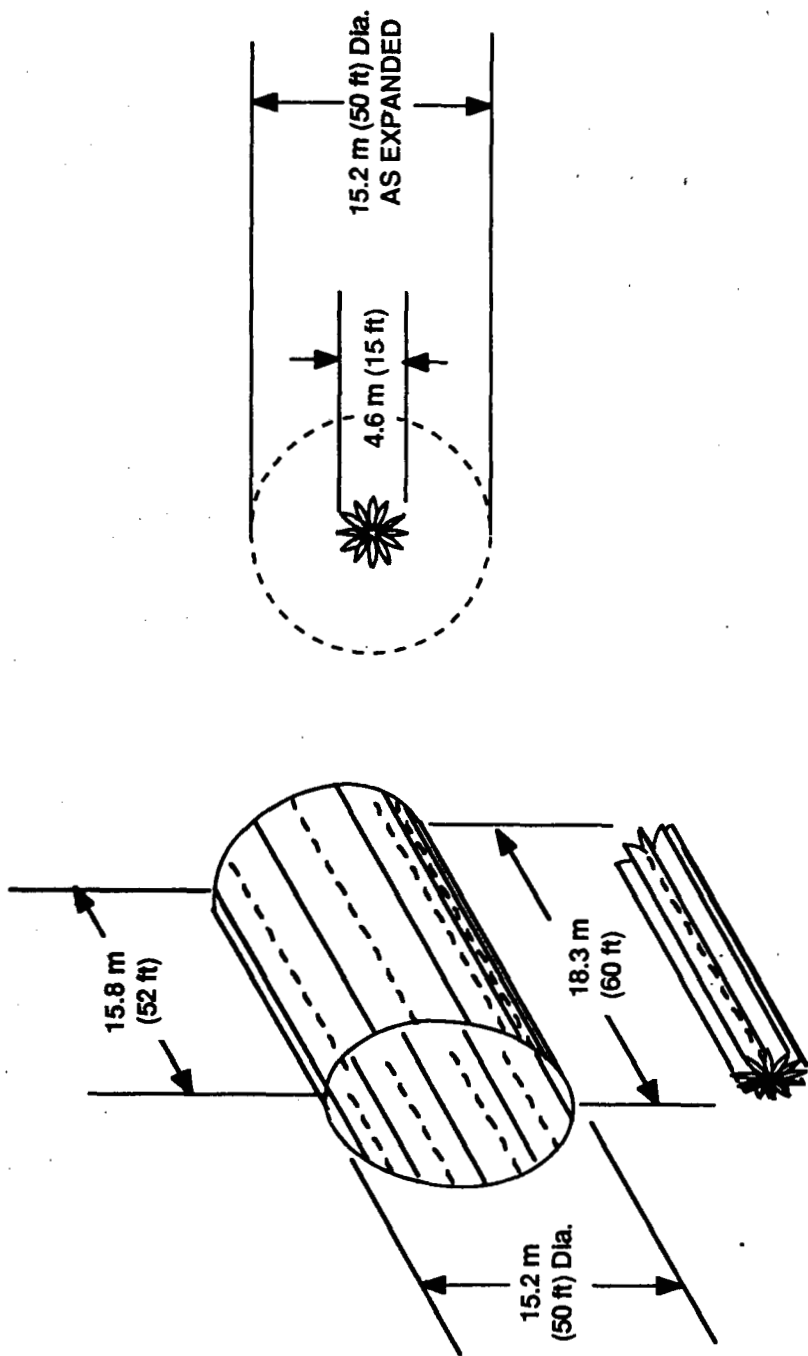


Figure 7.3-3 Hinge Foldable Cylinder for a Shuttle Launch

TABLE 7.3-1 HOW TO PUT A 15.24 m (50 ft) DIAMETER TUBE IN SOMETHING SMALLER
(DAISY PETAL FOLD CONCEPT)

NUMBER OF PETAL SEGMENTS	ANGLE OF SEGMENTS	NUMBER OF PETALS	MINIMUM RADIUS OF PETALED SYSTEM m (ft)	ARC LENGTH OF PETAL SEGMENTS m (ft)	MINIMUM ANGLE BETWEEN PETALS	MINIMUM PACKAGE ANGLE OF PETAL SYSTEM
24	15°	12	1.99 (6.53)	2.00 (6.54)	15°	172.5°
16	22.5°	8	2.97 (9.75)	3.00 (9.82)	22.5°	168.75°
12	30°	6	3.94 (12.94)	4.00 (13.09)	30°	165°
8	45°	4	5.83 (19.13)	5.98 (19.64)	45°	157.5°
6	60°	3	7.62 (25.00)	7.98 (26.18)	60°	150°

Shuttle launch. The inner cylinders are extracted and joined with other cylinders on-orbit. Nine cylinders assembled as shown in Figure 7.3-4 constitute one torus segment. The 18.3-m (60-ft) length requires on-orbit assembly of 40 segments to form the torus. A total of 120 Shuttle launches are required to deliver the telescoped cylinders to orbit, and extensive EVA and IVA are required to assemble the 360 individual cylinders into a complete torus.

7.3.2 Structural Configurations for a Saturn V Launch

The Saturn V vehicle could lift 9×10^4 kg (2×10^5 lb) to LEO with a payload size of 6.7 m (22 ft) in diameter by 30.5 m (100 ft) in length. Two concepts were considered to deliver the torus segments to LEO aboard a Saturn V vehicle. The first concept uses the daisy-petal fold configuration, and the second concept uses telescopic cylinders.

The first concept of the daisy-petal fold configuration uses 30.5-m (100-ft) length segments which fold to fit within the diameter of the payload envelope. Upon delivery to orbit, the torus segment is unfolded to form a 15.2-m (50-ft) diameter by 30.5-m (100-ft) length segment as shown in Figure 7.3-5. This concept provides a 24-segment torus assembly requiring 24 Saturn V launches. The torus formed by this concept would have to be equipped with end closures, flooring, air locks, and a complete life support subsystem to provide a habitat.

A second concept telescopes three cylinders, one within the other, to form a payload assembly 6.7 m (22 ft) in diameter by 30.5 m (100 ft) in length. The cylinders are disassembled and reassembled in an array as shown in Figure 7.3-6. Six cylinders are required per segment, requiring 48 launches for assembly of a complete torus. The innermost cylinder is

ORIGINAL PAGE IS
OF POOR QUALITY.

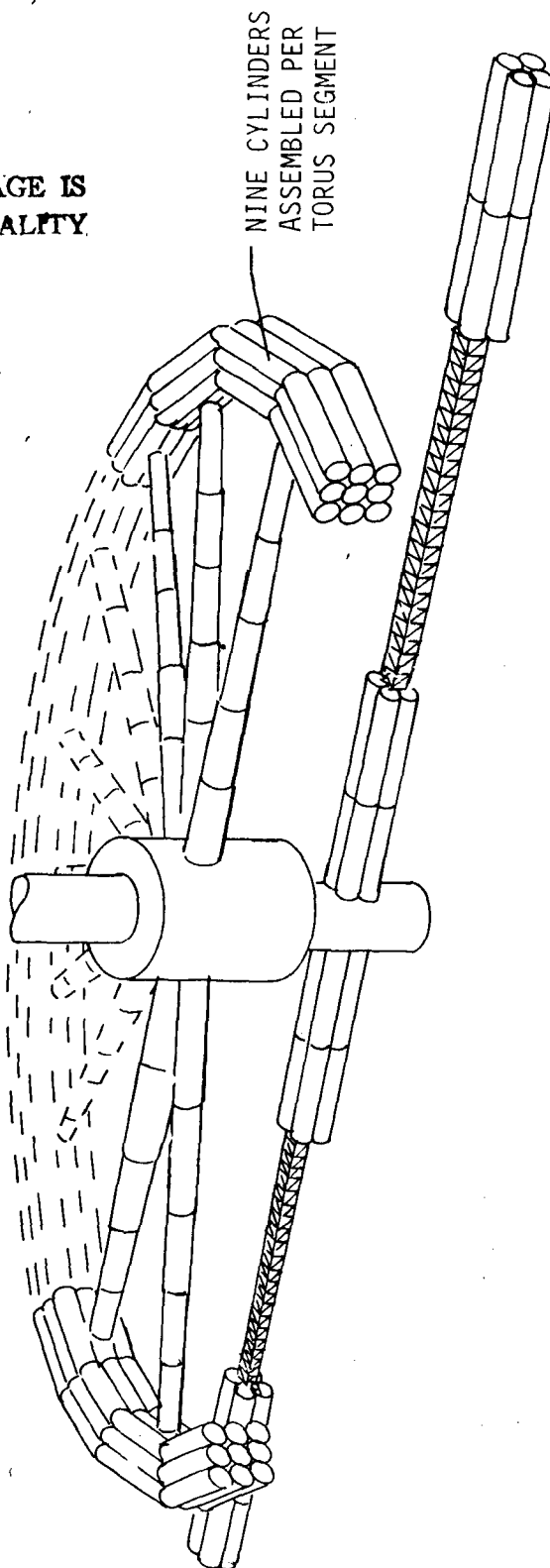


Figure 7.3-4 Shuttle Launched Telescopic Cylinders to Form a Torus

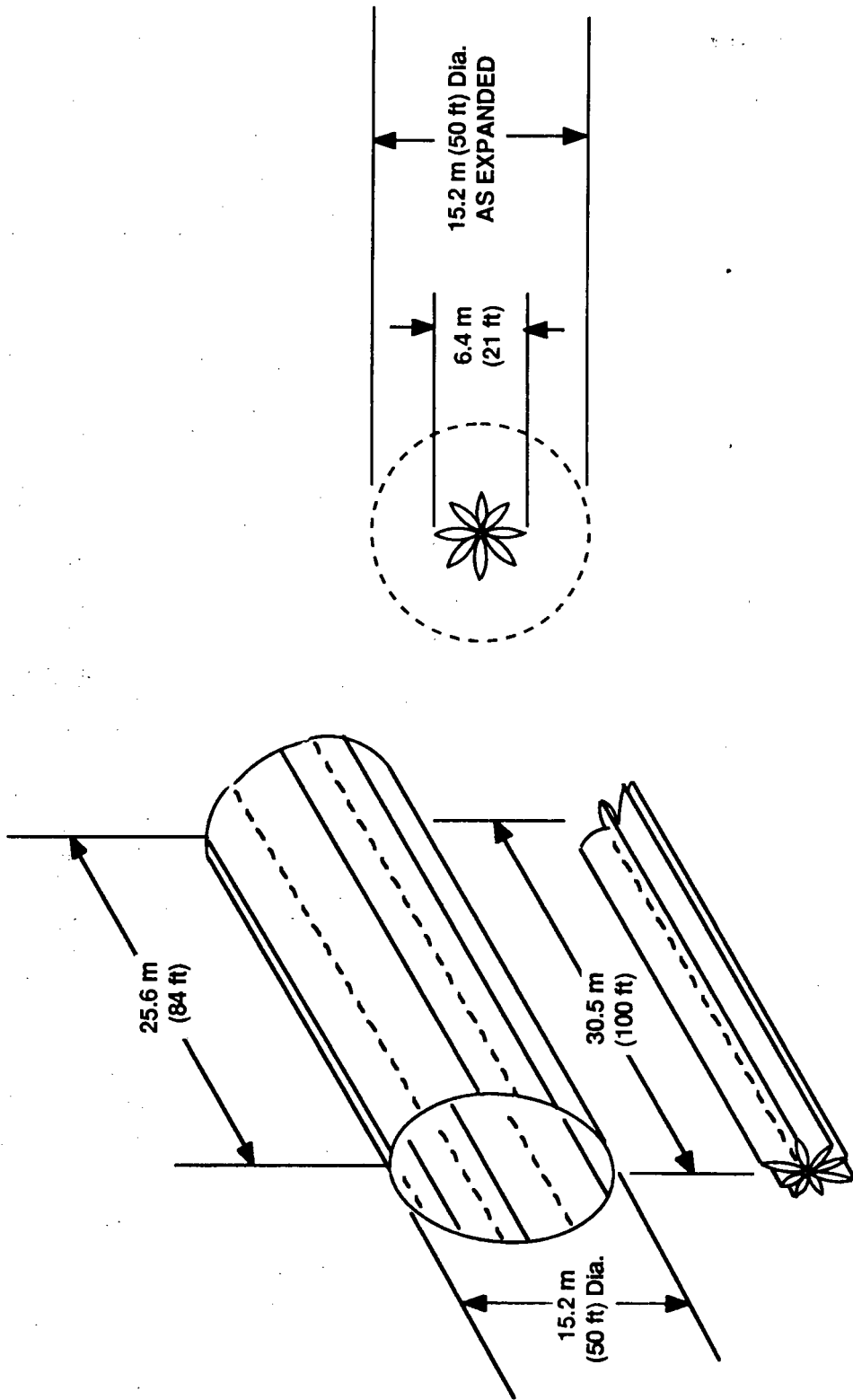


Figure 7.3-5 Hinge Foldable Cylinder for a Saturn Launch

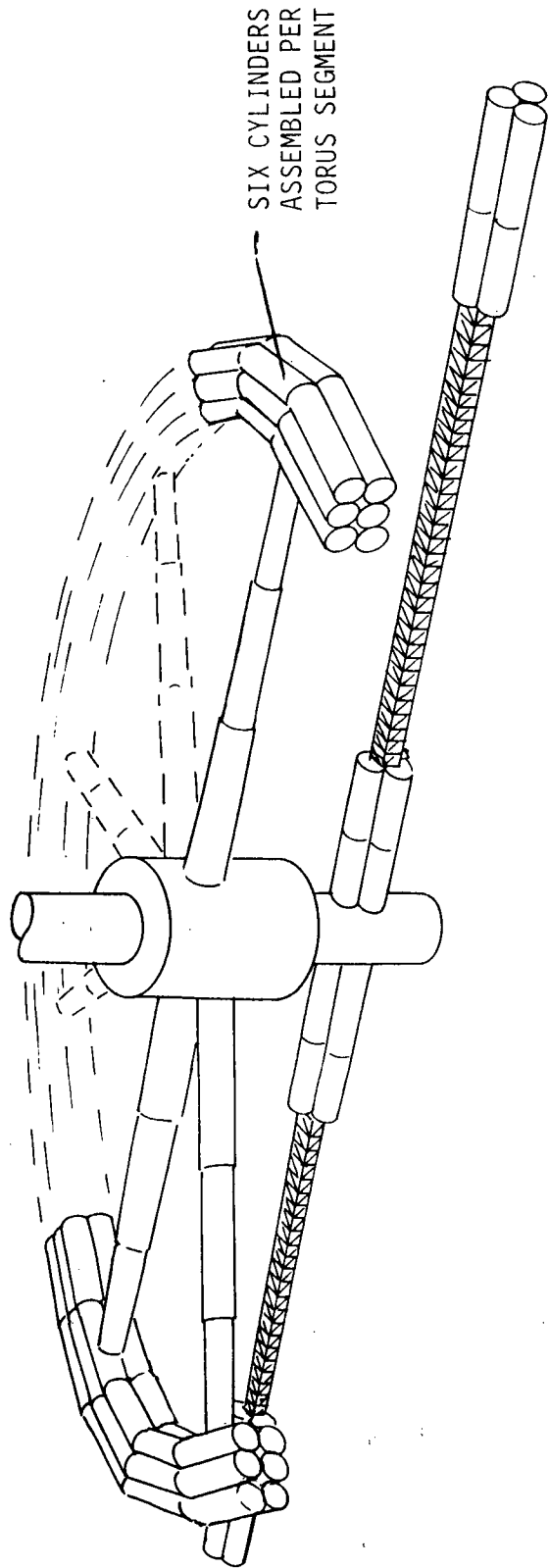


Figure 7.3-6 Saturn Launched Telescopic Cylinders to Form a Torus

completely outfitted with end closures, air locks, flooring, life support, and other subsystems for delivery to orbit. Two outer cylinders of each launch assembly are delivered to orbit as empty shells, each having one end closure. The empty shells are scarred to receive flooring and subsystem equipment after assembly on-orbit.

7.3.3 Structural Configuration for a Jarvis Launch

The Jarvis launch vehicle will have a payload lift capability of 8.4×10^4 kg (1.85×10^5 lb) to LEO and a payload size of 8.4 m (27.5 ft) in diameter by 25.6 m (84 ft) in length. The Jarvis vehicle could deliver torus segments to orbit using the two concepts reviewed for the Saturn V vehicle. The first concept, shown in Figure 7.3-7, constructs a cylinder 15.2 m (50 ft) in diameter by 25.6 m (84 ft) in length using a daisy-petal fold configuration. Twenty-eight HLLV launches would be required to deliver the segments for assembly of a torus. Upon assembly, the torus would require the addition of end closures, air locks, flooring, partitioning, life support equipment, and other subsystems required to form a habitat.

The second concept assembles a torus on-orbit by joining 28 segments, each comprised of three contiguous cylinders. The Jarvis vehicle delivers three telescoped cylinders to orbit per launch, requiring 28 Jarvis launches to deliver the complete torus. The torus assembly concept is shown in Figure 7.3-8 and would require extensive EVA and IVA for assembly of the 84 cylinders.

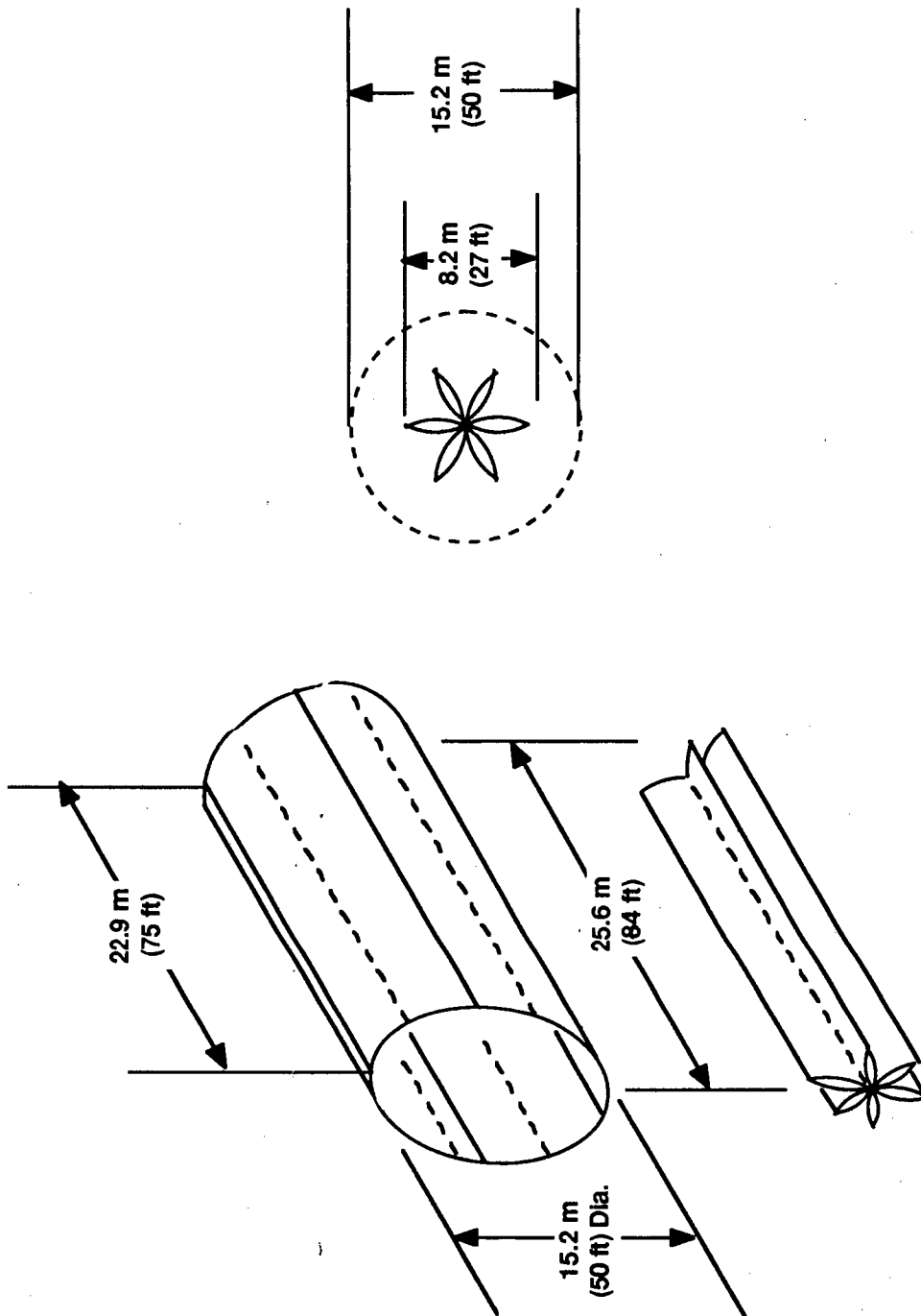


Figure 7.3-7 Hinge Foldable Cylinder for a Jarvis Launch

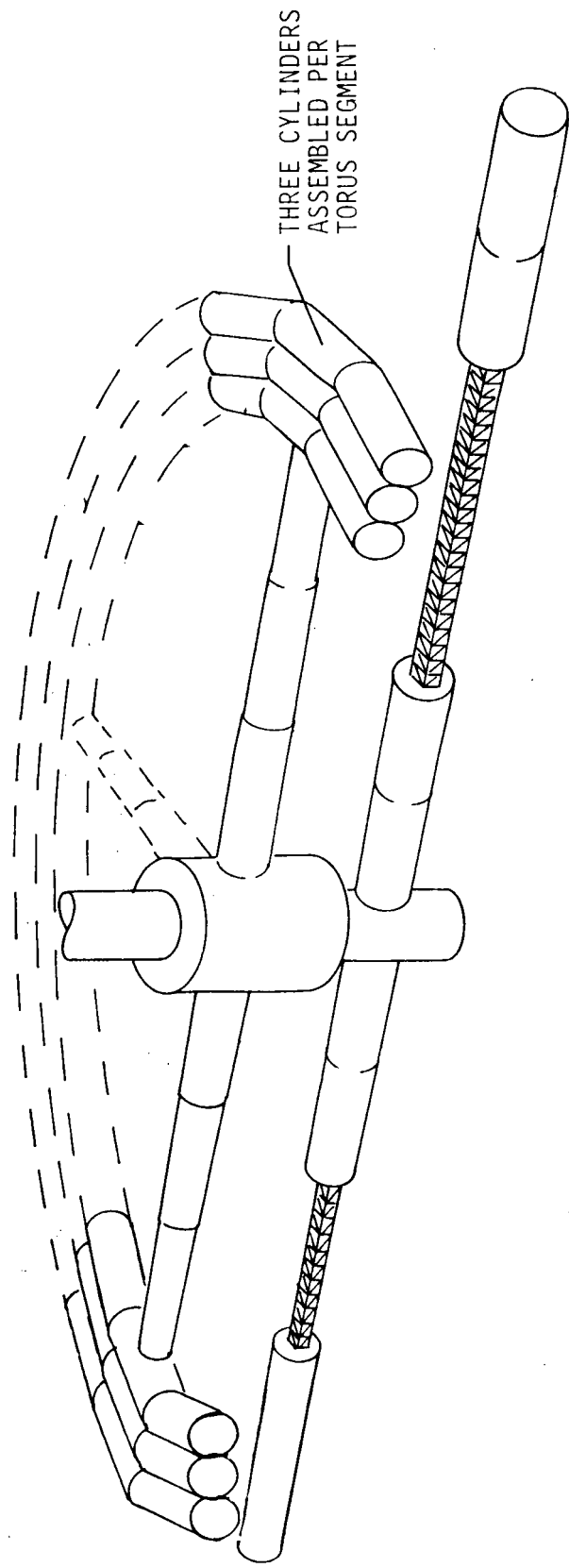


Figure 7.3-8 Jarvis Launched Telescopic Cylinders to Form a Torus

7.3.4 Structural Configurations for an Advanced HLLV Launch

One HLLV proposed for 1995 could lift 2.72×10^5 kg (6×10^5 lb) to LEO with a payload size envelope of 15.2 m (50 ft) in diameter by 61 m (200 ft) in length (Reference 7-4). This capacity accommodates the ATSS concept; twelve launches are required to deliver 24 completely outfitted segments, each 30.5 m (100 ft) in length, for on-orbit assembly of a complete torus as shown in Figure 7.3-1.

7.4 Modular Structure Concepts Using NSTS External Tanks

7.4.1 Torus from Tanks

The external tank of the Shuttle Orbiter is comprised of two cryogenic vessels joined by an intertank structure (Figure 7.4-1). The cylindrical hydrogen tank is 8.4 m (27.5 ft) in diameter by 29.3 m (96 ft) in length. The smaller oxygen tank, of tear-drop design, has a major diameter of 8.4 m (27.5 ft). Normally, the external tank is jettisoned just prior to orbital insertion of the Shuttle Orbiter and is destroyed during atmospheric re-entry.

In this modular concept, the hydrogen tanks are modified to provide air locks, and scarring of internal and external structural reinforcements permits on-orbit assembly of the tanks (one per launch) into a torus. The orbiter's external tank carries sufficient contingency fuel for placement of the external tank into orbit with the Shuttle Orbiter; however, the extra boost velocity for the tank reduces the payload capability for the orbiter. To make the tanks usable in orbit, the cargo bay payload lift capability of the Shuttle Orbiter is further reduced to allow the necessary mass increases due to structural modifications of the external tank. For example, 1.36×10^4 kg (3×10^4

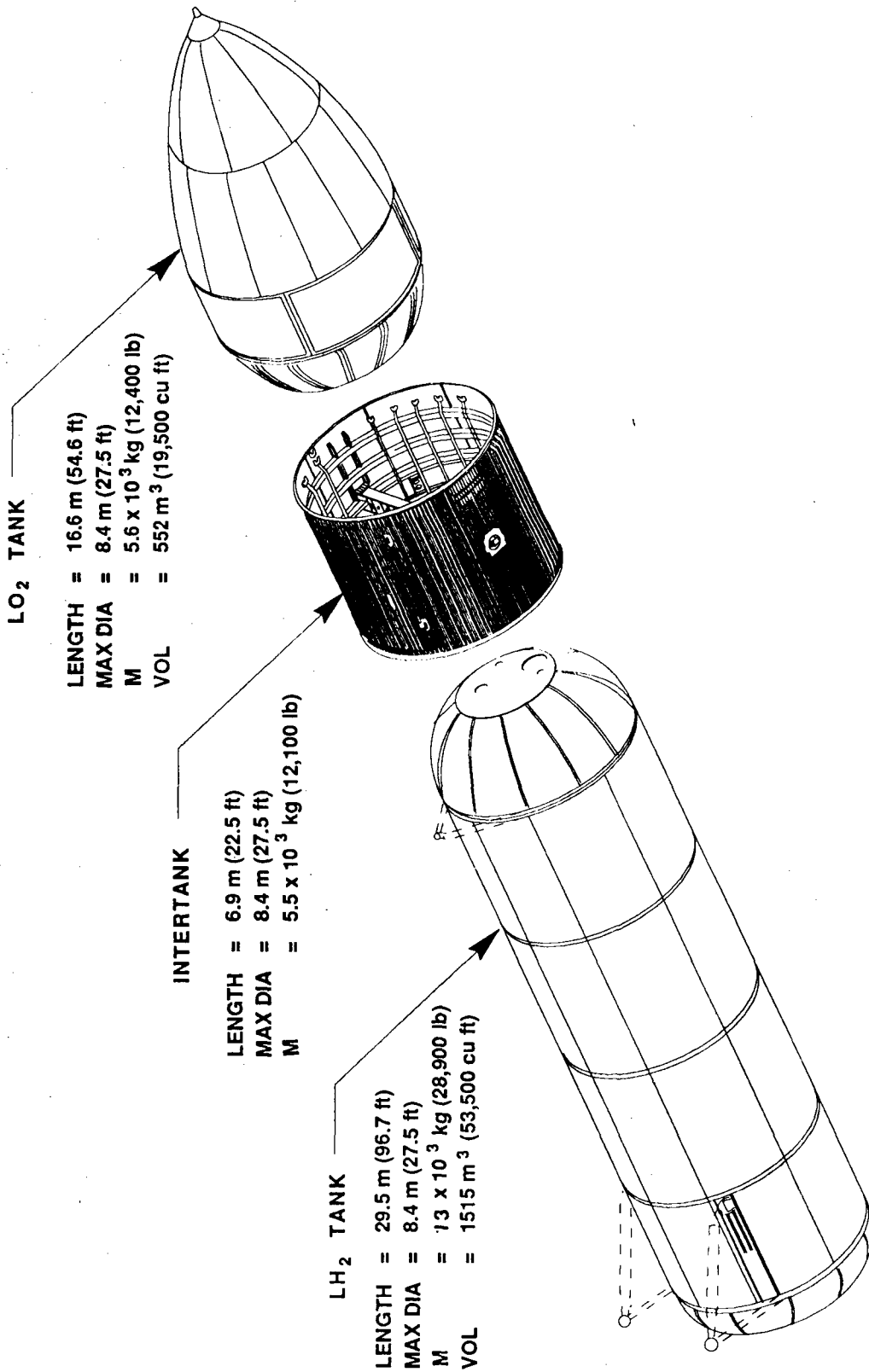


Figure 7.4-1 NSIS External Tank Structure (adapted from References 7-14 and 7-15)

lb) of structural modifications, air locks, and thermal insulation added to the external tank reduces the cargo bay transport capability from 2.9×10^4 kg (6.5×10^4 lb) to 1.59×10^4 kg (3.5×10^4 lb). The cargo bay payload consists of various equipment modules and experiments that are installed in the hydrogen tank on-orbit to outfit a functional laboratory. The liquid oxygen tank is repositioned and attached to the hydrogen tank to provide a cryogenic storage vessel for liquid oxygen for life support. Even though the hydrogen tank diameter and resulting volume are not as great as those for the ATSS, the tank does provide (with current technology) a pressure-tight man-rated vessel that is proof tested at 248 kPa (36 psi) internal differential pressure. Assembling the torus from 24 hydrogen tanks requires 24 Shuttle launches. Follow-on flights of the Shuttle can deliver tanks which become the modules of the Earth observatories and the solar observatory. The central tube is fabricated from a hydrogen tank with a rotating hub attached. Telescopic spokes are delivered to LEO in the cargo bay of the Shuttle, but their size is limited by the cargo bay diameter to less than 4.6 m (15 ft).

The hydrogen tank of the Shuttle external tank assembly may require an increase in tank wall thickness to contain one Earth atmospheric pressure with an adequate safety factor. An evaluation was made of the effects of reducing the internal atmospheric pressure of the torus on the performance of the astronauts. It was concluded that a minimum atmospheric pressure of 70.3 kPa (10.2 psia) comprised of 27-percent oxygen and 73-percent nitrogen is required to assure an adequate partial pressure of oxygen in the lungs. These percentages and pressure relationships were chosen to minimize the materials flammability hazards

in the cabin and yet, assure the astronauts would live and work in an Earth normal atmosphere equivalent to approximately a 4,000 ft altitude. Normal, healthy people could readily adapt and perform well in this pressure range (Reference 7-16). Significant materials flammability hazards are introduced if the oxygen atmospheric percentage exceeds 30 percent and restricts the selection of materials that are compatible with an oxygen rich atmosphere (Reference 7-17).

The Shuttle Orbiter's external tank is clad with a spray-on foam insulation formulated of polyurethane resin. This foam material outgases in vacuum and is not acceptable for use in the vicinity of sensitive optical instrumentation (Reference 7-14). Therefore, a low outgassing cryogenic insulation clad with a suitable micrometeoritic protective shield would be applied to the tank exterior.

Studies were reported in Reference 7-3 of an aft cargo carrier (ACC), 8.4 m (27.5 ft) in diameter by 6.1 m (21 ft) in length as an add-on module at the aft end of the hydrogen tank. The ACC can transport cargo having a diameter almost twice that of the Shuttle's cargo bay (Reference 7-14).

7.4.2 Elemental Rotating Space Station from Tanks

One of the top priority technology requirements identified in Reference 7-3 was the need to determine the physiological effects of artificial gravity on astronauts. This information is vital and will dictate the habitat design of the ATSS as related to space station rotation rate, habitat design, astronaut adaptability to long term space travel, and many other factors.

An orbiting elemental rotating space station could be placed in LEO with today's technology to permit study of the effects of artificial gravity on humans. The rotation rate of the elemental rotating station could be controlled to vary the artificial gravity from near zero to the equivalent of one Earth gravity. The station could consist of two NSTS external tanks, serving as habitats. Each tank could be placed at diametrically opposite ends of telescopic spokes which rotate about a central hub. The spokes would be designed to fit within the Shuttle cargo bay and extend to approximately 107 m (350 ft) from a central hub. The hub would have two air lock docking nodes to provide the ability for rendezvous and transfer of crew. The elemental rotating space station is shown in Figure 7.4-2 to indicate the method of external tank attachment to the ends of the spokes. The life support, thermal, and power subsystems used for the Skylab workshop are employed to upgrade the hydrogen tanks as habitats. A propulsion subsystem controls and maintains the rotation rate of the station and maintains orbital altitude.

7.5 Structural Weight Trades of Aluminum Alloy Versus Aerospace Advanced Structural Composites

The limited lift capability of currently available launch vehicles encourages the saving of structural weight of the payloads wherever practical. In an effort to reduce aircraft weight, military and civilian aircraft structure have been fabricated of structural composites, and the percentage of weight saved versus using conventional aluminum alloy construction is shown in Table 7.5-1. The weight savings range from 15 to 47 percent depending on the design, matrix material, and structural reinforcement selected (Reference 7-18).

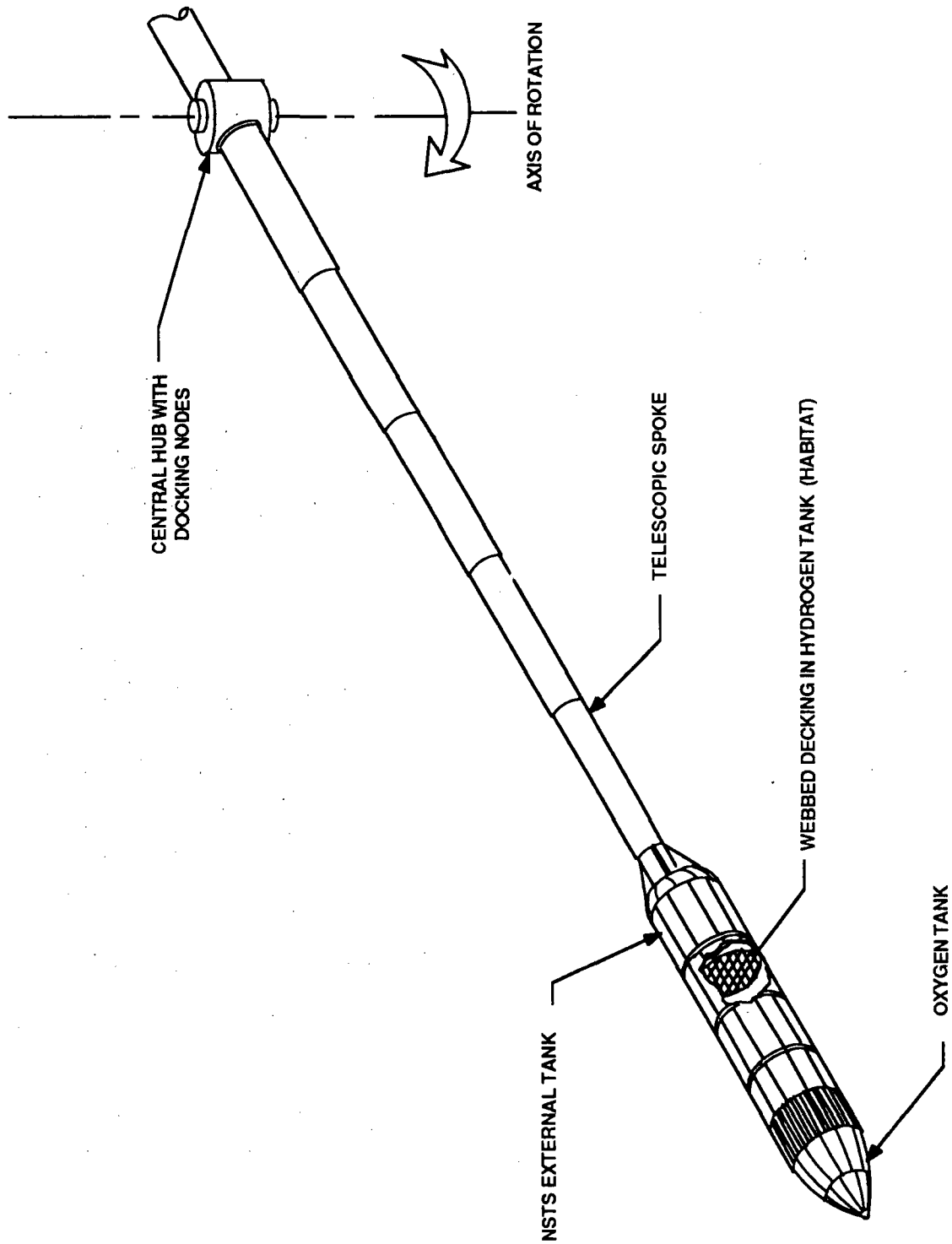


Figure 7.4-2 Elemental Rotating Space Station

TABLE 7.5-1 COMPOSITE COMPONENT DEVELOPMENT (Reference 7-18)

COMPONENT	MATERIAL	WEIGHT SAVINGS, %	CONTRACTOR
F-4 rudder	Boron/epoxy	35	McDonnell Aircraft Co.
F-15 stabilator	Boron/epoxy	22	McDonnell Aircraft Co.
F-111 stabilator	Boron/epoxy	25	General Dynamics Convair Aerospace, Fort Worth Operation
F-5 landing gear door	Boron/epoxy	29	Northrop Corp, Norair Division
F-14 stabilator	Boron/epoxy	20	Grumman Aircraft Engineering Corp.
A-4 flap	Boron/epoxy	32	Douglas Aircraft Co.
A-4 flap	Graphite/epoxy	47	Douglas Aircraft Co.
A-4 stabilator	Graphite/epoxy	32	Douglas Aircraft Co.
VC-10 aileron strut	Graphite/epoxy	43	Royal Aircraft Establishment
C-5A leading edge slat	Boron/epoxy	15	Lockheed-Georgia Corp.
T-39A wing box section	Boron/epoxy	37	North American Rockwell-LAD
Advanced composite wing structure	Boron/epoxy	20	Grumman
F-5 leading edge section	Graphite/epoxy	21	Northrop Corp, Norair Division
F-111 fuselage	Boron/epoxy	18	General Dynamics Convair Aerospace, Fort Worth Operation
Tubular struts	Boron/aluminum	30	North American Rockwell Space Division

Aerospace advanced structural composites are comprised of continuous filament reinforcements in a woven, or non-woven, form embedded in a synthetic resin matrix. The matrix resin is a means of binding layers or plies of filaments, or woven yarns together to achieve a load transference capability from filament to filament and from ply-layer to ply-layer. The strength directional properties of the laminate can be controlled by tailoring the reinforcement plies predominant strength in specific orientations. The more widely used reinforcement filaments are glass, carbon, graphite, aramid, and boron. The matrix resins are classed as thermosetting and thermoplastic. The thermosetting matrix resins are chemically hardened and do not soften with heating but will char and decompose at high temperature. In contrast, the thermoplastic matrix resins soften when heated and harden upon cooling without chemical change. Some thermoplastics become quite fluid at elevated temperature, and provide an efficient thermal lamination process for preimpregnated reinforcements not readily achieved with the thermosetting matrix resin systems. Some examples of thermosetting and thermoplastic resins are listed in Table 7.5-2.

The largest data base of advanced structural composites has been generated using thermosetting epoxy matrix resins. Some examples of the strength and stiffness of various reinforcement filaments and the combination of filaments embedded in an epoxy resin matrix are compared with steel, aluminum, titanium and beryllium in Table 7.5-3.

Structural composites offer a significant reduction of individual piece part count due to the limited use of mechanical fastening methods required to assemble the structure. For example, a curved composite shell with trapezoidal hat-shaped stiffeners could be laminated in one

ORIGINAL PAGE IS
OF POOR QUALITY

TABLE 7.5-2 EXAMPLES OF MATRIX RESINS

MATRIX RESIN CLASSES	
THERMOSETTING	THERMOPLASTIC
EPOXY	POLYCARBONATE
PHENOLIC	PHENOXY
POLYIMIDE	ACRYLIC
SILICONE	POLYETHER SULFONE
ACRYLIC	POLYIMIDE
	POLYARYLENE ETHER

TABLE 7.5-3 COMPARISON OF MECHANICAL PROPERTIES OF SOME STRUCTURAL MATERIALS
(Reference 7-18)

MATERIAL	YOUNG'S	ULTIMATE TENSILE	DENSITY,	SPECIFIC MODULUS,	SPECIFIC STRENGTH,
	MODULUS, $E, \text{psi} \times 10^6 \text{ (GPa)}$	STRENGTH, $\sigma, \text{psi} \times 10^3 \text{ (MPa)}$	$\rho, \text{lb/in.}^3 \text{ (kg} \times 10^3 \text{ /m}^3 \text{)}$	$E/p, \text{in.} \times 10^6 \text{ (m} \times 10^7 \text{)}$	$\sigma/p, \text{in.} \times 10^6 \text{ (m} \times 10^6 \text{)}$
E-glass fiber*	10.5 (72.3)	460 (3170)	0.092 (2.55)	1.1 (2.8)	5.00 (1.24)
S-glass fiber*	12.0 (82.7)	600 (4130)	0.090 (2.50)	1.3 (3.3)	6.66 (1.65)
E-glass in epoxy	7.5 (51.7)	200 (1380)	0.070 (1.94)	1.1 (2.8)	2.86 (0.71)
S-glass in epoxy	7.5 (51.7)	300 (2070)	0.070 (1.94)	1.1 (2.8)	4.29 (1.07)
Aramid fiber*	20.0 (137.8)	500 (3445)	0.060 (1.69)	3.3 (8.1)	8.33 (2.04)
Aramid in epoxy	12.0 (82.7)	280 (1930)	0.055 (1.40)	5.9 (3.6)	5.09 (1.38)
HM graphite fiber*	55 (379)	300 (2070)	0.069 (1.90)	7.8 (19.8)	4.3 (1.09)
HT graphite fiber*	35 (241)	350 (2410)	0.064 (1.77)	5.6 (14.2)	5.5 (1.36)
AS or T-300 fiber*	30 (207)	400 (2760)	0.067 (1.85)	6.0 (11.2)	6.0 (1.49)
HM graphite in epoxy	30 (207)	135 (930)	0.058 (1.61)	5.2 (13.2)	2.3 (0.58)
HT graphite in epoxy	22 (152)	205 (1410)	0.054 (1.50)	4.1 (10.4)	3.8 (0.94)
AS or T-300 in epoxy	17 (117)	230 (1580)	0.056 (1.55)	4.1 (10.0)	4.1 (1.01)
Boron filaments*	60 (143)	400 (2760)	0.095 (2.63)	6.3 (16.0)	4.2 (1.05)
Boron in epoxy	31 (214)	220 (1520)	0.075 (2.08)	4.1 (10.4)	2.9 (0.73)
Maraging steel	28 (193)	300 (2070)	0.289 (8.00)	0.97 (2.5)	1.0 (0.26)
Aluminum 7075	10 (68.9)	82 (565)	0.100 (2.77)	1.00 (2.5)	0.8 (0.20)
Titanium 6Al-4V	15 (103)	155 (1070)	0.155 (4.29)	0.97 (2.5)	1.0 (0.25)
Beryllium	35 (241)	90 (620)	0.066 (1.83)	5.3 (13.5)	1.4 (0.34)

*Fibers only; does not include resin.
NOTE: Fibers and composites are unidirectional.
Metals are isotropic.

piece using autoclave processing, thus eliminating the need for riveting or adhesive bonding of the stiffeners to the shell. Thin sheets of chemically milled or machined titanium metal have been laminated locally between plies of a structural composite to provide high load bearing attachment points for assembly with other structure. Titanium has been selected for these applications based on specific strength, bearing strength, corrosion resistance, and low coefficient of thermal expansion. Specific adhesion is accomplished between the titanium metal insert and the matrix resin of the structural composite to achieve a highly reliable structural assembly method. The titanium insert's shape and thickness profile are closely controlled to distribute shear stresses at a low level and minimize stress raisers between the matrix resin and metal interface.

The ultimate tensile strength of aircraft materials is compared in the bar chart of Figure 7.5-1 to indicate the strength of structural composites versus selected aircraft metals. Aluminum metal is the widely accepted aerospace structural material with a large applications data base. Aluminum has near uniform strength properties in all directions. By contrast, structural composites may be highly anisotropic due to the preferred orientation of reinforcement plies. The ability to control the preferred strength direction of a composite laminate by orienting the predominant strength direction of each ply can yield a composite having high strength in one direction. The composite would have lesser strength in the transverse planar direction and in the direction normal to the plane of the reinforcement plies. A structural composite having preferred reinforcement orientation can surpass the tensile strength of titanium and have masses only 60 percent of an equivalent aluminum item.

ORIGINAL PAGE IS
OF POOR QUALITY

MATERIAL AND DENSITY, kg/m³ (lb/in³)

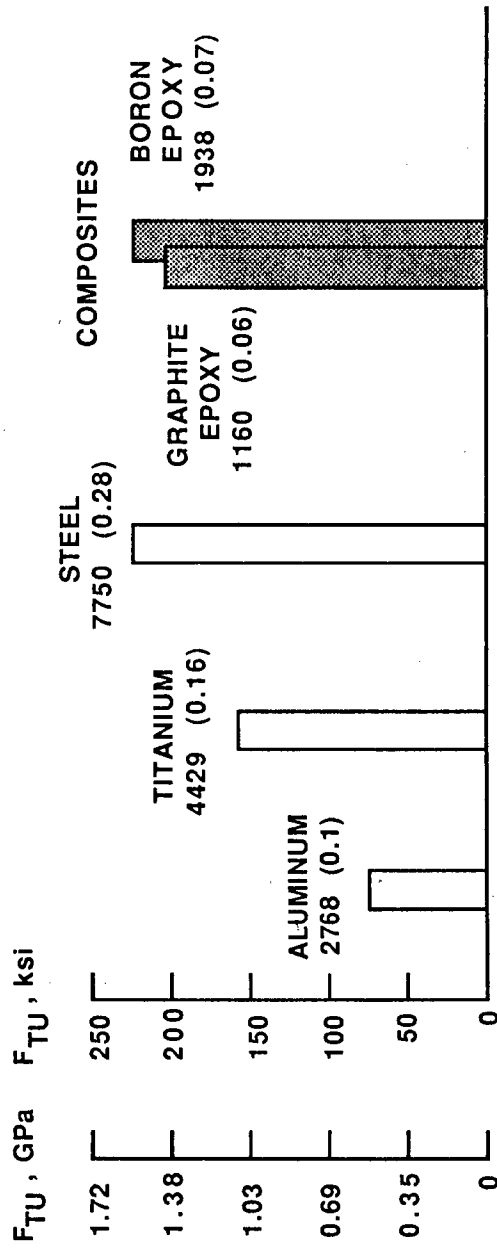


Figure 7.5-1 Relative Strength of Aircraft Materials (adapted from Reference 7-18)

The military and NASA have generated a substantial data base on applications of advanced structural composites for aerospace.

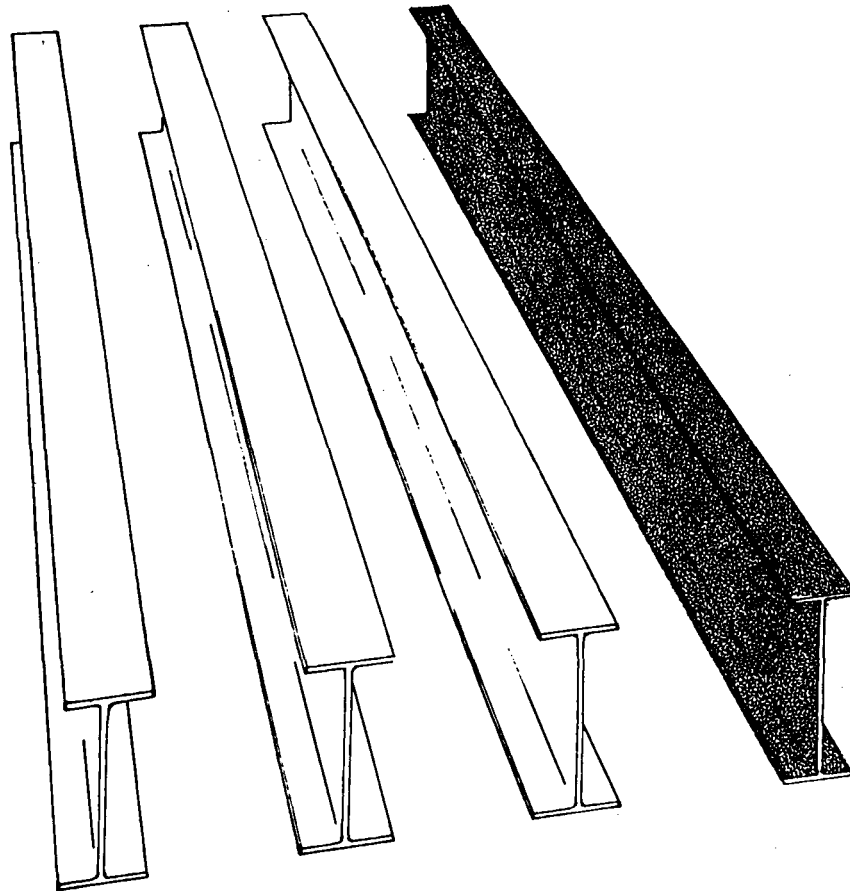
The mechanical properties of structural "I" beams made of steel, titanium, aluminum, and graphite epoxy composite are compared in Table 7.5-4. The moment of inertia of each of the beams is identical to permit correlation of beam stiffness "EI" and mass per unit length. The stiffness of the graphite epoxy composite compares favorably with that of the steel beam at approximately one-fifth the mass. Judicious placement of composite reinforcement plies in the construction of structural members can equalize the stress levels throughout the composite structure with a consequent savings in mass.

In summary, aerospace advanced structural composites can be fabricated into complex shapes with a significant piece part count reduction. The ability to laminate structure with metal inserts provides increased capability of attaching the structure at high load bearing locations. Smooth laminate surfaces may be achieved without surface distortion where structural reinforcements are attached by lamination or adhesive bonding. Laminate thickness control and predominant ply reinforcement orientation can provide custom tailored structure designed with minimum mass to perform its load carrying function. Mass savings of 15 to 47 percent have been achieved by substituting advanced structural composites for conventional aluminum aircraft construction. It is anticipated that ATSS structures fabricated of advanced structural composites would provide similar factor in mass savings.

Filament or tape wound structures provide a stressed skin pressure vessel from which habitats, safe havens, and gas pressure bottles can be

ORIGINAL PAGE IS
OF POOR QUALITY

TABLE 7.5-4 COMPARATIVE PROPERTIES OF A STRUCTURAL SHAPE
(Reference 7-19)



	Steel A36	Titanium 6 Al-4V	Aluminum 7075-T6	Graphite/Epoxy Composite
Moment of Inertia, I cm ⁴ (in ⁴)	520.7 (12.51)	520.7 (12.51)	520.7 (12.51)	520.7 (12.51)
Modulus of Elasticity, E GPa (10 ⁶ psi)	186 (27)	117 (17)	69 (10)	179 (26)
Stiffness, EI MN-m ² (10 ⁸ lb-in ²)	0.97 (3.38)	0.61 (2.13)	0.36 (1.25)	0.93 (3.25)
Ultimate Tensile Stress MPa (ksi)	552 (80)	1103 (160)	572 (83)	965 (140)
Mass per Unit Length kg/m (lb/ft)	7.7 (5.2)	4.3 (2.9)	2.8 (1.9)	1.5 (1.0)

made. Further matrix resin development is required to prevent resin crazing when used for cryogenic storage of liquified gasses.

7.6 Payload Mass Savings Effect on Number of Launches Required

The use of advanced structural composites can influence the number of launches required to assemble spacecraft components and subassemblies on-orbit. Each launch vehicle system is both payload size and mass limited, therefore, structural composites provide mass savings permitting the delivery of more internal structures and equipment per launch. For example, a structural composite might be substituted for a steel structure providing equivalent strength and stiffness for approximately one-fifth the mass. This savings in mass suggests a means for fabricating hand tools, support frames, machine tools, compressors, and related equipment with significant mass savings.

The assembly of the torus on-orbit requires multiple launches to deliver subassemblies of expandable structure to LEO. The expandable structures concepts identified in Table 7.1-1 as inflatable, hinge foldable, and telescopic could each be fabricated of advanced structural composites with significant savings in weight and consequent savings of launch vehicle fuel. The inflatable and hinge foldable concepts are payload volume restricted, therefore, no additional payload can be carried within their folded configurations. The innermost cylinder of the three telescoped cylinders could carry additional payload up to the payload mass capability of the launch vehicle, thus reducing the number of follow-on launches by one-third required to deliver subsystem modules for outfitting the cylinders.

The rigid modular NSTS external tank structure is fabricated of aluminum metal and could not be outfitted with subsystem modules until after delivery to LEO. Follow-on launches would be required to deliver the subsystem equipment for installation in the tanks.

7.7 Conclusions and Recommendations

The payload capacities for the five potential launch systems are summarized in Table 7.7-1 and shown in conjunction with their ability to deliver a torus configuration to LEO. This comparison summary together with the description of the alternates permit the following conclusions or observations regarding a torus assembly, an elemental rotating space station, expandable structures concepts, use of composites, and proposed launch vehicles.

- o A torus can be assembled on-orbit from cylinders.
- o The cylinders can be fabricated as inflatable, hinge-foldable, and telescopic of advanced structural composites.
- o Advanced structural composites can provide significant mass savings over conventional aluminum alloy fabricated structure.
- o The NSTS can deliver the cylinders to orbit.
- o The innermost of the telescoped cylinders could be delivered to orbit outfitted with subsystem equipment.
- o The hinge foldable and telescopic torus cylinders could be delivered to LEO in a lesser number of launches than required for the NSTS if the Saturn V or Jarvis launch vehicles were available.
- o The NSTS external tank could be delivered to orbit for assembly of a torus or used as habitat modules of an elemental rotating space station.
- o A HLLV proposed for the year 1995 can deliver fully assembled and outfitted cylindrical modules for on-orbit assembly of a torus.
- o An advanced HLLV can deliver the torus in a minimum number of launches and requires the least EVA and IVA for assembly on-orbit.

TABLE 7.7-1 POTENTIAL LAUNCH SYSTEMS COMPARED FOR DELIVERY OF TORUS SEGMENTS TO LEO (TELESCOPIC VS. MODULAR)

POTENTIAL SYSTEMS						
POTENTIAL PAYLOAD SIZE	HLLV (ATSS)	NSTS (SHUTTLE)	SATURN V	JARVIS (SHUTTLE DERIVED VEHICLE)	NSTS (EXTERNAL TANK)	
Diameter, m (ft)	15.24 (50)	4.57 (15)	6.55 (21.5)	8.38 (27.5)	8.38 (27.5)	
Length, m (ft)	60.96 (200)	18.29 (60)	30.48 (100)	25.60 (84)	29.50 (96.7)	
Weight, kg (lbs)	272,155 (600,000)	18,144 (40,000)	94,347 (208,000)	83915 (185,000)	24,221 (53,400)	
POSSIBLE TORI						
Max Segment Lengths m (ft)	30.48 (100)	18.29 (60)	30.48 (100)	25.60 (84)	29.50 (96.7)	
Number of Segments	24	40	24	28	24	
Number of Cylindrical Elements per Segment	1	9	6	3	1	
Relative Volume of Full Torus, % of ATSS	100	82.5	102	79.4	31	
Weight per Segment, kg (lbs)	94,584 (208,521)	56,750 (125,112)	94,584 (208,521)	81,072 (178,732)	24,221 (53,400)	
Launches per Segment	1/2	3	2	1	1	
Weight per Launch kg (lbs)	189,167 (417,042)	18,765 (41,371)	47,292 (104,260)	81,072 (178,732)	24,221 (53,400)	
EVA and IVA Forecast	Limited	Extensive	Intermediate	Intermediate	Intermediate	
TOTAL LAUNCHES	12	120	48	28	24	

Based on the above, it is recommended that an advanced technology development program should encompass space station expandable structures and launch vehicle technologies.

REFERENCES

- 7-1 M. J. Queijo, et al: An Advanced-Technology Space Station for the Year 2025, Study and Concepts, NASA CR 178208, March 1987.
- 7-2 M. J. Queijo, et al: Analyses of a Rotating Advanced-Technology Space Station for the Year 2025, Study and Concepts, NASA CR 178345, January 1988.
- 7-3 M. J. Queijo, et al: Some Operational Aspects of a Rotating Advanced-Technology Space Station for the Year 2025, NASA CR 181617, June 1988.
- 7-4 Toelle, Ronald: Heavy Lift Launch Vehicles for 1995 and Beyond, NASA Technical Memorandum-86520, September 1985.
- 7-5 Sunday, Terry L.: Shuttle 2, Planning the Next Generation of Spaceplanes, Space World, October 1985.
- 7-6 Smith, Bruce A: Defense Department Developing Range of Launch Vehicle Concepts, Aviation Week and Space Technology, March 9, 1987.
- 7-7 Belew, L. F., Editor: Skylab, Our First Space Station, NASA SP-400, 1977.
- 7-8 Kolcum, Edward H.: Boeing Offers to Underwrite New Jarvis Development Concept, Aviation Week and Space Technology, December 15, 1986.
- 7-9 Space Daily, November 4, 1987, page 1260.
- 7-10 Space Daily, December 10, 1987, pages 1438 and 1440.
- 7-11 Space Daily, October 22, 1987, page 1189.
- 7-12 Zopf, Richard F.: UV Cationic Epoxy Systems for Dielectric Applications, Radiation Curing, November 1982.
- 7-13 Campbell, Francis J. and Brenner, Walter: Curing High Performance Structural Adhesives by Electron-Beam Radiation, Naval Engineers Journal, June 1982.
- 7-14 Gimarc, J. Alex: Report on Space Shuttle External Tank Applications, Space Studies Institute, December 1, 1985.
- 7-15 Space Daily, February 16, 1988, page 3.
- 7-16 Space Resources and Space Settlements, NASA SP-428, 1979.

- 7-17 LeDoux, Paul W.: Spacecraft Material Flammability Testing and Configuration, Proceedings of Spacecraft Fire Safety Workshop, NASA-Lewis Research Center, August 20, 1986.
- 7-18 Lubin, George, Editor: Handbook of Composites, Van Nostrand Reinhold Company, Inc. Copyright 1982.
- 7-19 LeWark, Blaise A., Sr.: Introduction to Advanced Composites, Composites in Manufacturing 7 Conference and Exposition, Long Beach, California, December 7-10, 1987.

8.0 ATSS APPLICATION FOR LUNAR BASE BUILD-UP AND MARS MISSION SUPPORT

This section will provide a cursory examination of the requirements on the ATSS for lunar and Mars missions. The purpose is to indicate areas where these missions might impact the design or operations of the ATSS rather than to provide a detailed examination of the support that could be required as lunar and Mars mission are better defined.

One of the design objectives of the ATSS is to support space missions that could use the ATSS as a base for LEO operations. To this end, the ATSS has quarters allocated for transient personnel, a large assembly and berthing bay, and onboard manufacturing and fueling facilities.

8.1 Planetary Missions

In Reference 8-1, three different reference manned Mars missions were examined for their impact on the ATSS. These Mars missions are summarized in Table 8.1-1. The impacts on the ATSS were determined to be nominal, since as indicated above, one of the design objectives of the ATSS is to support planetary missions. The major new requirements are operations related and deal with items such as spacecraft assembly, OTV activities, and onboard fuel production (which requires large energy use if H_2 and O_2 are produced on-board rather than being delivered from Earth).

Five planetary missions were examined in Reference 8-2 for their impact on a growth version of the Space Station Freedom. The missions and the impacts as described are presented in Tables 8.1-2 and 8.1-3. The projected manhours required as shown in Table 8.1-3 for planetary missions support appear to be optimistic; the actual operational hours might be many times the estimates shown.

TABLE 8.1-1 SUMMARY OF REFERENCE MANNED MARS MISSION REQUIREMENTS (Reference 8-1)

MARS MISSION	DELIVERY TO LEO			VEHICLES	VEHICLE MASS (kg)	PROPULSION	FUEL-OXIDIZER OR Hg PROPELLANT MASS	AEROBRKING		ARTIFICIAL GRAVITY	
	MASS (kg)	HLV FLIGHTS						AT MARS	EARTH RETURN		
		8.1 x 10 ⁴ kg EACH	2.7 x 10 ⁵ kg EACH								
LANGLEY RESEARCH CENTER SPACE STATION OFFICE "SPLIT-OPTION MISSION"	1.1 x 10 ⁶	12	4	INTERPLANETARY VEHICLE	2.2 x 10 ⁵	H ₂ -O ₂	7.2 x 10 ⁵	yes	yes	3g	
				MARS CARGO VEHICLE	8.8 x 10 ⁵	H ₂ -O ₂		yes	...		
				MARS EXCURSION MODULE	7.2 x 10 ⁴	H ₂ -O ₂		yes	...		
MASS. INST. TECH. ADVANCED SPACE SYSTEMS DESIGN COURSE	1.5 x 10 ⁶	17	6	INTERPLANETARY VEHICLE	5.7 x 10 ⁵	Nuclear-Hg	4.2 x 10 ⁵	no	no	1g	
				CARGO LANDER	1.5 x 10 ⁵	MMH-N ₂ O ₄		yes	...		
				MANNED LANDING & RETURN VEH.	1.2 x 10 ⁵	MMH-N ₂ O ₄		yes	...		
				MOON EXCURSION VEHICLE	6.3 x 10 ³	MMH-N ₂ O ₄			
				OTV (LEO TO MEO & RETURN)	1.6 x 10 ⁴	H ₂ -O ₂		...	yes		
UNIV. OF TEXAS AT AUSTIN TEXAS A&M SUMMER INTERN TEAM	1.1 x 10 ⁶	12	4	INTERPLANETARY VEHICLE	3.7 x 10 ⁵	Nuclear-Hg	2.8 x 10 ⁴	no	no	1g	
				CARGO LANDERS (3 Vehicles)	2.2 x 10 ⁴ ea	CH ₄ -O ₂		included in PV Allocation	yes		...
				MARS ASCENDING VEH. (3 Vehicles)	4.0 x 10 ⁴ ea	CH ₄ -O ₂ & Strep-ton		8.0 x 10 ⁴ ea 4.5 x 10 ⁴ ea	yes		...
				TAXI (LEO TO MEO & RETURN)	1.8 x 10 ⁴	H ₂ -O ₂		6.7 x 10 ⁴	...		yes

TABLE 8.1-2 PLANETARY MISSIONS PERFORMANCE SUMMARY (Reference 8-2)

Parameter	C ₃	Type of OTV*	Payload out of LEO	LEO total departure mass	OTV propellant load	Propellant + payload (lift req.)
Mission	($\frac{\text{km}}{\text{sec}^2}$)		(metric tons)	(metric tons)	(metric tons)	(metric tons)
Mars Sample Return	9.0	1 stage reusable	8.89	44.03	27.76	36.65
Kopff Sample Return	80.7	2 stage 1st stage returns	8.38	92.49	71.51	79.89
Ceres Sample Return	9.9	2 stage 1st stage returns	43.57	131.59	75.47	119.04
Mercury Orbiter	18.7	1 stage reusable	5.63	41.62	28.90	34.53
Titan Probes/ Saturn Orbiter	50.5	1 stage expandable	6.34	53.54	41.81	48.15

*Isp = 4446 N-sec/kg (455.4 sec), all stages have a total propellant capacity of 42 metric tons.

TABLE 8.1-3
 PLANETARY MISSION IMPACTS ON THE SPACE STATION (Reference 8-2)

Requirements	Mars Sample Return	Kopff Sample Return	Ceres Sample Return	Mercury Orbiter	Titan Probes/ Saturn Orbiter
o Space station hardware required					
No. of OTVs expended (not returned)	0	1	1	0	1
No. of OTV refurbish kits	1	2	2	1	1
Gantry to stack two stages		yes	yes		
Checkout equipment for two stage stack		yes	yes		
Quarantine module	yes	yes	yes		
Additional power, kW	5	5	5		
Additional thermal control, no. of standard modules	1	1	1		
o Space station manhours required					
OTV refurbishment	52	103	103	52	52
Aerobrake removal		21	21		21
OTV/payload integration and C/O	11	21	21	11	11
Fuel, release, and launch	24	36	36	24	24
Rendezvous/retrieve OTV using OMV	12	12	12	12	
Shuttle rendezvous/payload removal	3	2	12	2	2
ULV fuel delivery	7	17	18	7	10
Sample retrieval using OMV	8	8	8		
Sample analysis and shipment	24	16	16		
Total mission manhours	<u>141</u>	<u>236</u>	<u>247</u>	<u>108</u>	<u>120</u>

8.2 Lunar Base Build-Up

Some of the details of the lunar base build-up of Reference 8-2 are given here. Although these projections were based on a growth version of the Space Station Freedom and planned for the years 2005 through 2015, they can be applied to the ATSS as well. The projected cargo and propellant delivery to LEO needed to support a proposed ten-year lunar base build-up is shown in Figure 8.2-1. Fuel needed for lunar sorties is delivered from Earth as LH_2 and LO_2 and constitutes a large fraction of total launch mass. An ATSS based mission would still need the same amount of fuel, but on-board production using water delivered from Earth supplemented by space station waste water would provide some saving as indicated in Section 9 of Reference 8-1. The resultant projected material required to be delivered to the lunar surface is shown in Figure 8.2-2. Most of this material is for a permanent base consisting of five habitability modules, five research units, three production plants for oxygen, ceramics, and metals, and various support equipment. The level of support activity at the ATSS impacts the on-board operations and manpower time lines. In addition to receiving payloads from Earth and sending materials to the Moon, OTV or other transport vehicle servicing and repair will require ATSS manpower and facilities.

The lunar base manpower build-up is shown in Figure 8.2-3. Implicit in this build-up is crew rotation, short stay-time specialists, visiting dignitaries, and medical emergency trips, all of which require a steady flow of traffic through the ATSS. The ATSS supports a crew of 60 which includes an allowance for about 14 transients. Since the lunar base total population is projected at 18, the lunar base traffic should not pose an undue problem for the ATSS.

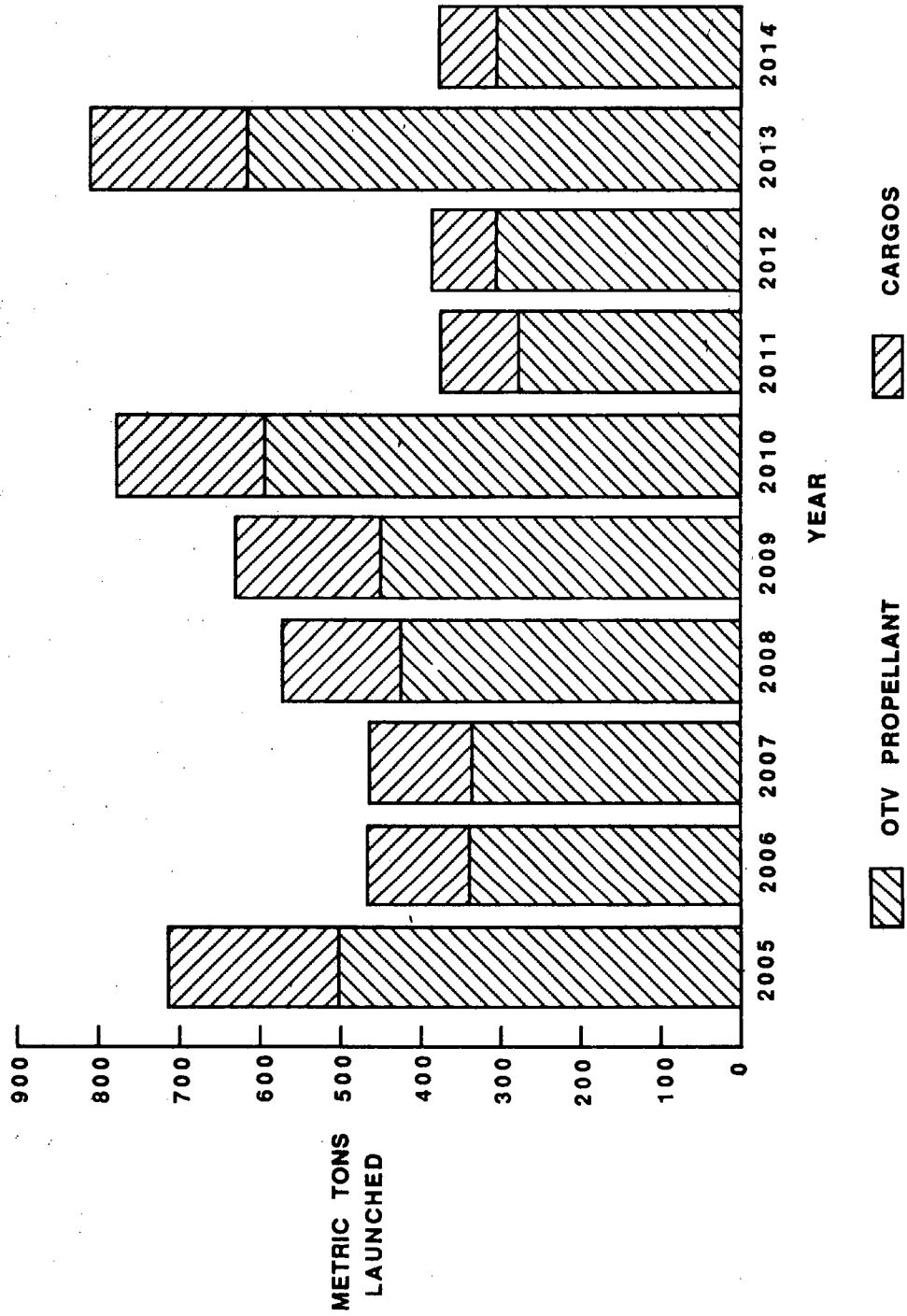


Figure 8.2-1 Lunar Base Launch Requirements

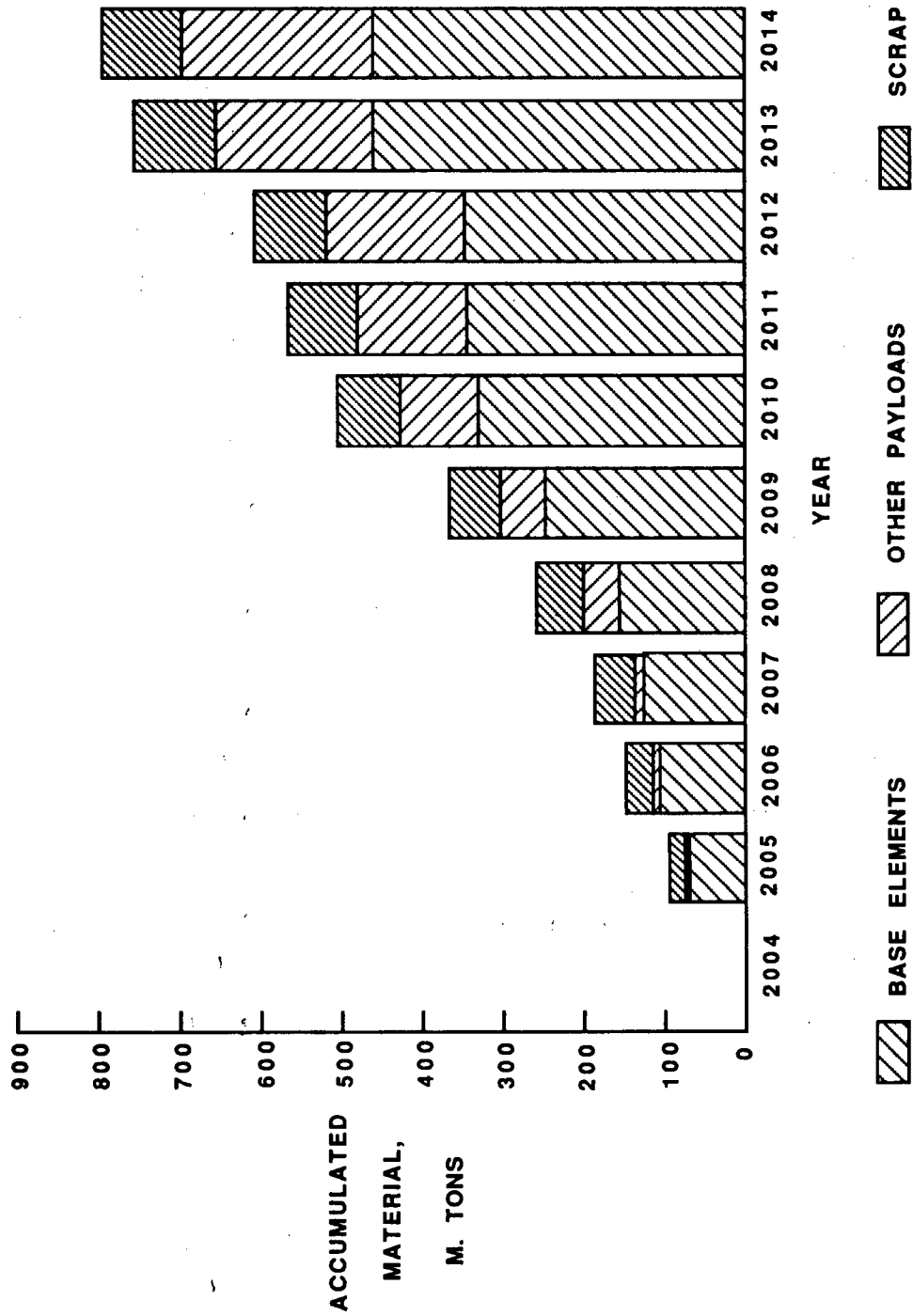


Figure 8.2-2 Material at Lunar Base at Years End

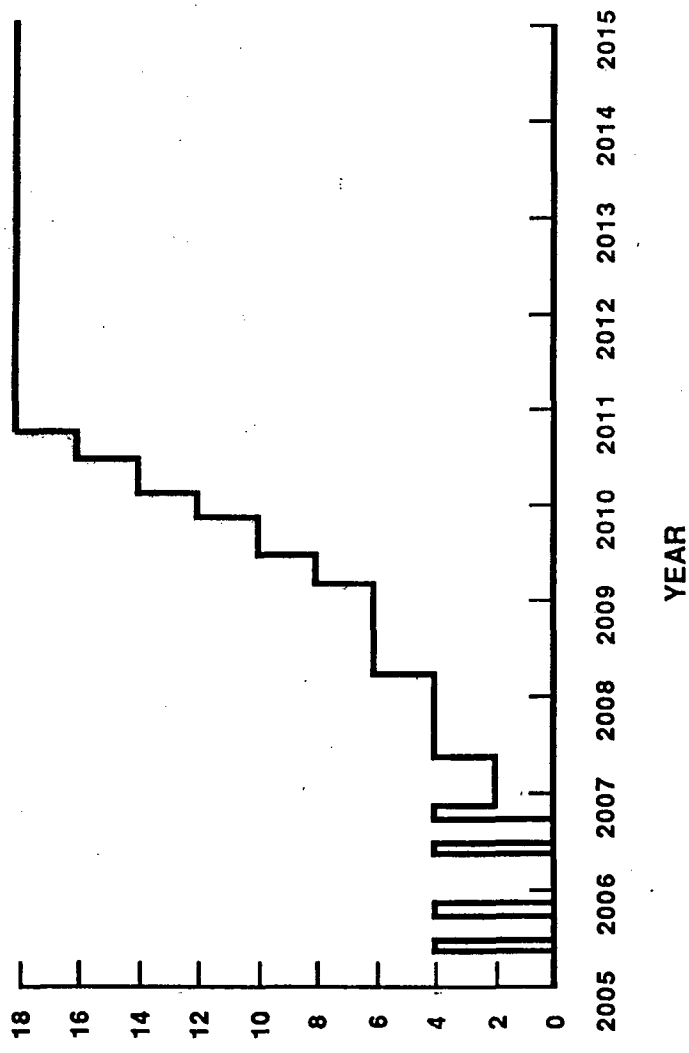


Figure 8.2-3 Estimated Manning Levels of Lunar Base (Reference 8-2)

8.3 Interface Between the ATSS and Lunar and Planetary Missions

The interfaces between the ATSS lunar and planetary missions are summarized in Table 8.3-1. This table covers a range of possible missions (Reference 8-3), and some of the items would not be applicable at the same time. For instance, nuclear engines for a planetary mission require OTV delivery of the crew to an originally unmanned planetary vehicle at HEO, whereas a chemically fueled engine would require vehicle fueling and crew departure from LEO.

TABLE 8.3-1 SURVEY OF LUNAR AND PLANETARY MISSION REQUIREMENTS ON ATSS

Mission Requirement	ATSS Impact
Delivery to ATSS of mission related hardware, crew, and supplies from Earth	<ul style="list-style-type: none"> o Frequency of HLLVs, shuttles, aerospace planes or other vehicles to dock and service
Delivery to ATSS of fuel needed for mission support	<ul style="list-style-type: none"> o Fuel handling o Fuel storage o Possible nuclear or fission fuel handling
Fuel production on-board ATSS for mission spacecraft	<ul style="list-style-type: none"> o Delivery of H₂O from Earth followed by H₂ and O₂ production on the ATSS o Delivery of regolith from the Moon followed by O₂ production on the ATSS o Cryogen facilities on ATSS to liquefy and store fuels
Assembly at ATSS of mission spacecraft	<ul style="list-style-type: none"> o Assembly in berthing and assembly bay o Assembly of spacecraft too large for berthing and assembly bay o Docking accessibility of other vehicles during mission spacecraft assembly o ATSS to mission spacecraft interconnections: air locks, power, fluid exchanges, thermal control systems, communications
ATSS controllability effects	<ul style="list-style-type: none"> o Variable center of mass, center of pressure, and system inertia during build-up of mission spacecraft
Operational support by ATSS	<ul style="list-style-type: none"> o Delivery of Mars crew to HEO after unmanned spacecraft traverse through Van Allen radiation belts o Quarantine facilities and sample processing on ATSS for Mars sample return o Lunar sorties of OTVs supporting a lunar base buildup (-14 sorties per year for 10 years) o Machine shop and other facilities that provide repair for parts and vehicles that otherwise would be returned to Earth or scrapped

REFERENCES

- 8-1 Queijo, M. J. et al.: Some Operational Aspects of a Rotating Advanced-Technology Space Station for the Year 2025, NASA CR-181617, June 1988.
- 8-2 Anon.: Impact of Lunar and Planetary Missions on the Space Station, NASA CR-171832, November 1984.
- 8-3 M. B. Duke and P. W. Keaton, Editors : Manned Mars Missions, Working Group Papers.
Volume 1, Sections 1 through 4, NASA TM-89320 and
Volume 2, Sections 5 through Appendix NASA TM-89321
May 1986.

9.0 IDENTIFICATION AND ASSESSMENT OF TECHNOLOGY DEVELOPMENTS REQUIRED FOR THE ADVANCED-TECHNOLOGY SPACE STATION

The ATSS, as its name implies, is based on the assumption that new and emerging technologies will have advanced to the point of being viable for use in the ATSS. The purpose of this section is to review these pacing technologies as covered in previous reports of this series, to add further technology items, and to briefly assess possible variations of the ATSS as now configured.

9.1 Identification and Ranking of Pacing Technologies

A review of the state-of-the-art technology and technology forecast for the NASA Space Systems Technology Model (Reference 9-1) helped identify technology trends to the year 2000. Literature reviews provided indications of developments and projected developments in many areas of technology. In References 9-2 through 9-4, state-of-the-art subsystems were reviewed, areas of studies identified, and pacing technologies assessed, respectively.

Ranking criteria were developed for indicating the technical need or criticality of technology areas felt necessary to make the ATSS feasible by 2025. This criteria translate to a number from one to ten for each technology area, with the higher numbers indicating the greater need. The ranking criteria as developed in Reference 9-4 are listed in Table 9.1-1. In Reference 9-4, pacing technology items were identified and ranked, and these are included in Table 9.1-2. Reference 9-4 also provides the discussion of subsystem and synergies, function performed, particular features, and development status for each of these items.

Two additional items, resistojet thruster systems and attitude control technology of Table 9.1-2, are covered below.

TABLE 9.1-1 RANKING CRITERIA FOR TECHNICAL NEED OR
 CRITICALITY RELATIVE TO THE ADVANCED-TECHNOLOGY
 SPACE STATION

<u>CRITICALITY ASSESSMENT</u>	<u>CRITICALITY RANKING*</u>
The technical advance will enhance the performance of the subsystem or element. Alternate means for accomplishment exist and could be incorporated with a modest compromise in weight, performance, operating complexity, etc.	1
The degree of technical advance will define the performance of the subsystem. Alternate means would limit the subsystem performance and compromise other subsystem operations.	2
	3
The technical advance is required for subsystem operation. Reduced performances would compromise other subsystems and impact the functioning capability of the ATSS.	4
	5
The technical advance has no alternative for accomplishing the subsystem performance and identified synergies.	6
	7
The ATSS cannot be configured without this technology capability.	8
	9
	10

*Higher numbers indicate greater need.

TABLE 9.1-2 SUMMARY OF THE TECHNOLOGICAL REQUIREMENTS FOR THE
ADVANCED-TECHNOLOGY SPACE STATION

<u>Technology Item</u>	<u>Technology Area</u>	<u>Criticality Ranking</u>
1. Artificial Gravity Technology	Human Factors GN&C	10
2. Telerobotic Assembly Machines and Orbital Maneuvering Vehicles	Struct/Mechanisms	10
3. Large Diameter Gas Seals for Rotating or Otherwise Moving Joints	Struct/Mechanisms	10
4. Large Diameter Rotating Joints and Servo Controlled Drives	Struct/Mechanisms	10
5. Heavy Lift Launch Vehicle	Transportation/ Operations/ Logistics	9
6. Articulated Air Lock Doors and Seals	Struct/Mechanisms	9
7. Predictions of Dynamics and Control of Large Space Vehicles with Flexible, Rotating, and Articulating Components	GN&C	8
8. Gas Separation by Semipermeable Membranes	ECLSS	7
9. Attitude Control and Reboost Thruster System Based on Using H ₂ -O ₂ Fuel	Propulsion	7

TABLE 9.1-2 SUMMARY OF THE TECHNOLOGICAL REQUIREMENTS FOR THE
ADVANCED-TECHNOLOGY SPACE STATION (concluded)

<u>Technology Item</u>	<u>Technology Area</u>	<u>Criticality Ranking</u>
10. Concentrating Solar Dynamic Power Generators	Electrical Power	7
11. Supercritical Wet Air Oxidation	ECISS	7
12. Expandable and Modular Structural Concepts	Struct/Mechanisms	6
13. High Pressure Space Suit	EVA	6
14. Lightweight Industrial Equipment	Operations	6
15. Improved Thermal Control Devices and Radiators	Thermal	6
16. Ambient Atmosphere Selection Less Than 1 Atm	Operations	5
17. Magnetic Torquing with Superconductivity	GN&C	4
18. Spent External Tankage as Structural Building Elements of Spacecraft	Struct/Mechanisms	4
19. Filament Reinforced Structural Composites	Struct/Mechanisms	4
20. Booster Fuel Tanks for Cryogen	Propulsion	4
21. Cargo Carrier for Shuttle-Type Vehicles	Transportation	4
22. Improved Structural Design, Analysis, and Assembly Methods	Struct/Mechanisms	4
23. Attitude Control Technology	GN&C	4
24. Resistojet Thruster Systems	Propulsion	3

9.1.1 Improved Resistojet Thruster Systems

The use of water as the propellant for orbit station keeping to counteract drag forces permits common resupply and competitive power consumption for the ATSS with no change in mass required for the propellant. The resistojets can use water reclaimed from crew functions, the synergy with life support functions extends to use of the extra water generated from the oxidation of carbonaceous waste products.

The resistojet propulsion system for the ATSS will need improvements for contemporary technology in four areas. The thrust level of individual thrusters should be in the 5-10 N (1-2 lb) thrust range to be compatible with the requirement for drag make-up. The target specific impulse for mass equality needs to be 4044 N sec/kg (400 sec) or higher. Specific power consumption, which is a measure of electrical conversion effectiveness, should equal or exceed 0.3 N/kW (0.067 lb/kW). In addition, lifetime should approach ten years of continuous service for the ATSS application.

Resistojet technology using water as the propellant is being developed for the Space Station Freedom station keeping application. The target lifetime is 10,000 hours, and the present specific impulse goal is approximately 2528 N sec/kg (250 sec). The Space Station Freedom application emphasizes a multi-propellant capability to take advantage of the constituents available from the environmental control system. The performance and life features of the Space Station Freedom application are influenced by this multi-propellant choice. The technology advances required for the ATSS application includes the development of higher temperature water compatible materials for the resistor component to achieve the higher level of specific impulse. The current temperature

limit is approximately 1400°C (2500°F). The development of greater thrust levels and power efficiency should improve with scale size. The thrust level must be increased to accommodate the magnitude of the ATSS drag compared with that for the Space Station Freedom.

Criticality Ranking: 3

9.1.2 Attitude Control Technology Assessment

As spacecraft increase in size, the environmental torques (due to gravity gradient, aerodynamic forces, and solar pressure forces), and the associated angular momenta acting on the spacecraft will also increase. Section 5 of this report showed that for the ATSS, the environmental torques (primarily that caused by the gravity gradient) and angular momentum were several orders of magnitude greater than those to which act upon existing spacecraft. It was also shown overcoming these environmental disturbances required a large, probably unacceptable, mass carried either as fuel or a number of current technology control-moment gyros.

The situation has been anticipated and was a driver in the development of dual counterrotating wheels, magnetically suspended angular momentum control devices, and large-angle magnetic bearing gyros. These devices provide some relief relative to the mass (and power) requirements of the more conventional CMGs.

The discovery of "high-temperature" superconducting materials appears to hold much promise for application to the development of reasonably low-weight, low-power torquers. Reference 9-5 discusses this area of development and contains preliminary estimates of the power and mass of several types of torquers designed for an application requiring a

torque of 34,000 N-m (25000 lb-ft); the angular momentum is 50,000 N-m-s (36,880 lb-ft-sec). A comparison of the devices is as follows:

<u>Torquers</u>	<u>Power, kW</u>	<u>Mass, kg</u>	<u>(lb)</u>
Superconducting Magnetic Bearings	7	530	(1170)
Gimbal Torquers	60	12700	(28000)
Conventional Magnetic Bearings	200	2500	(5510)
Large Angle Magnetic Bearings	11.5	5300	(11700)

These preliminary results are quite impressive relative to the potential of superconducting technology application to torquers. Developments in this area should be followed closely.

9.2 Technology Trends

The conceptual configuration of the ATSS was based on three major premises:

- 1) Technology trends would be reviewed, and new technology deemed available around the year 2025 would be used where feasible.
- 2) The ATSS would support the 17 functions identified in Reference 9-2 and repeated herein as Table 9.2-1.
- 3) Artificial gravity would be a necessity and would be provided by a rotating habitat.

An observation often made about technology projections is that we tend to be too optimistic in the short run and too pessimistic in the long term. Perhaps it is because it is easier to see the need for a sometimes costly improvement on a current concept (without always considering the schedule and cost implications) than to accurately assess how a new technology gain in another field may be applied to the same

TABLE 9.2-1 POTENTIAL FUNCTIONS TO BE SUPPORTED
BY THE ADVANCED-TECHNOLOGY SPACE STATION

1. A permanent observatory to look down upon the Earth and out into the universe.
2. An orbiting science, medical, materials, and new technologies laboratory.
3. A service and repair facility for payloads, spacecraft, and platforms.
4. An assembly facility where large structures or spacecraft components are manufactured and/or assembled and checked out.
5. A transportation node where payloads and vehicles are collected, stationed, processed, and launched and where fuel is manufactured.
6. A safe habitat for space crews.
7. A communications and/or relay station for manned or unmanned spacecraft.
8. An adaptation area (in variable "g") in preparation for long space flights.
9. A storage node for food, fuel, spare parts, etc.
10. A variable "g" research facility.
11. A commercial manufacturing facility (drugs, crystals, etc.)
12. An energy collection and relay station.
13. A diagnostic, medical, and convalescent facility.
14. A tourism attraction.
15. A horticultural research and food growth facility.
16. A technology demonstration facility.
17. A control center for manned and unmanned spacecraft.

problem. As an example, an HLLV to lift bigger and heavier payloads is easy to project, but the application of superconductivity to provide high energy magnetic rail launchers as a first stage launch facility may eventually prove to be a less costly and more reliable method of delivery of mass to LEO.

Many of the pacing technologies discussed in Section 9.1 identified the need for improvements of current capabilities. In fact, to base the ATSS on a design concept that had a criticality rating of 10 (cannot achieve the ATSS without this capability) and also require a major technology breakthrough to obtain the concept could be self-defeating. It is still interesting, however, to speculate on technology trends that might reshape or redefine the ATSS as now projected.

A few technology trends that could cause major ATSS changes are noted below.

- A. Medical advances might conceivably provide techniques to overcome the adverse effects of weightlessness on the human body and obviate the need for a large radius, rotating configuration. Discovery of medically beneficial effects of weightlessness for the cure of certain ailments might greatly increase the traffic to the station and increase the area devoted to hospital functions and medical research.
- B. Fusion power (as covered in Section 4) could physically reduce the area devoted to solar energy collection. High efficiency radiators such as liquid droplet radiators would further reduce the large surface areas needed. The availability of fusion power would also modify the propulsion system design and enhance the on-board manufacturing capability.

C. Practical high-temperature superconductivity would reflect throughout the station design, resulting in lower power requirements and readily available high intensity magnetic fields. In addition, energy storage might be achieved in high current inductances. Magnetic torquing might be one of the first superconducting applications as indicated in Table 9.1-2.

Finally, the fast moving trends in computer technology and artificial intelligence could impact crew requirements, implying an autonomous, self-tending, self-repairing station wherein the operational aspects and mechanical tasks are largely given over to computers, teleoperators, and robotics.

ORIGINAL PAGE IS
OF POOR QUALITY

REFERENCES

- 9-1 Queijo, M. J. et al.: An Advanced-Technology Space Station for the Year 2025, Study and Concepts, NASA CR-178208, March 1987.
- 9-2 Queijo, M. J. et al.: An Advanced-Technology Space Station for the Year 2025. Study and Concepts, NASA CR-178208, March 1987.
- 9-3 Queijo, M. J. et al.: Analysis of a Rotating Advanced-Technology Space Station for the Year 2025, NASA CR-178345, January 1988.
- 9-4 Queijo, M. J. et al.: Some Operational Aspects of a Rotating Advanced-Technology Space Station for the Year 2025, NASA CR 181617, June 1988.
- 9-5 Downer, James R. et al.: Application of Magnetic Bearings to High-Torque Satellite Attitude Control Wheels, In: IECEC '87; Proceedings of the Twenty-Second Intersociety Energy Conversion Engineering Conference, Philadelphia, PA, August 1987.

APPENDIX

ATSS ON-BOARD POWER GENERATION SYSTEM DESCRIPTIONS

The system descriptions extend the previous comparison study of solar dynamic and nuclear fission (Reference A-1) to include Pu^{238} radioisotope decay, fusion, and advanced photovoltaic sources for ATSS electrical power. The individual descriptions begin with an assessment of technology status or rationale for selection of the particular configuration and include an evaluation of potentially viable options within each of the alternatives. The descriptions contain the detail necessary to estimate masses, identify requirements for controls, and discuss any configuration-particular concerns associated with the use of that system for electrical power generation. The comparisons and rankings of the system are presented in the main body of this report as Section 4, and address the effects of mass, control requirements, and the particular concerns associated with the use of that configuration for generation of electrical power aboard the ATSS.

All of the descriptions continue to use the same set of thermodynamic parameters defined in the course of previous studies (References A-2 and A-3) and include:

1. Heat is converted into electrical energy with a 40-percent throughput efficiency.
2. The radiators for the converters operate at 320 K (576°R) and dissipate 0.59 kW/m^2 (0.055 kW/ft^2) using wastewater for the coolant.
3. The converters are closed cycle gas turbines with gaseous N_2 as the working fluid, and liquid NaK to provide the heat input.

4. The individual converters generate 450 kW and deliver 425 kW to the ATSS as 400 Hz 440 V, three-phase electrical power. (Table A-1 summarizes the thermodynamic cycle for conversion of heat energy to electrical power.)

A.1 RADIOISOTOPE DECAY HEAT SOURCE (Pu^{238})

A.1.1 Radioisotope Decay System Considerations

Radioisotope decay heat sources have an extensive history in spaceflight applications. The principal radioactive material and mode for application has been the plutonium isotope of mass number 238 as the hot junction for a thermoelectric generator (Reference A-4). The best known of these units has been the SNAP 19 configuration which powered the Viking lander and the SNAP 27 configuration which powered the ALSEP lunar instrumentation packages deployed as part of the Apollo program. The table of isotopes (Reference A-5) lists a number of potential candidates for heat source applications. However within that list, Pu^{238} becomes the isotope of choice for an ATSS. Pu^{238} shows a half life of 89 years which provides a near-constant power output, plus a generous decay energy in the form of 5.5 MeV alpha particles. The energy release occurs with only low energy gamma radiation, and the decay products have long half lives (U^{234} at more than 10^5 years and Th^{230} at 80,000 years). As PuO_2 the the heat released is about 5.3 W/cm^3 (87 W/in^3). Most system applications take advantage of the chemically inert oxide and carry the PuO_2 fuel as sintered pellets.

TABLE A-1 SUMMARY OF ENERGY CONVERSION PARAMETERS
FOR 2550 kW

A. Conversion of thermal energy to electrical energy by six closed cycle gas turbine driven alternators, 0.4 conversion efficiency. Parameters apply to each unit.

Mass Flow Gaseous N ₂	4.08 kg/sec	(9lb/sec)
Compression Ratio	2.666	
Compressor Inlet Pressure	2.07 MPa	(300 psia)
<u>Cycle Temperature</u>		
Compressor Inlet	350 K	(631 ^o R)
Compressor Outlet	471 K	(849 ^o R)
Regenerator Outlet	783 K	(1401 ^o R)
Turbine Inlet	1047 K	(1886 ^o R)
Turbine Outlet	815 K	(1468 ^o R)
Precooler Inlet	502 K	(906 ^o R)
Precooler Outlet	350 K	(631 ^o R)
<u>Energy Input, by NaK Liquid Metal Heat Exchanger</u>		
NaK Flow	39.4 kg/sec	(86.9 lb/sec)
NaK Inlet	1076 K	(1937 ^o R)
NaK Outlet	1048 K	(1887 ^o R)
Energy Exchanged	1124 kW	(1069 Btu/sec)
<u>Electrical Conversion, Energy to Three Phase 440 V 400 Hz</u>		
Turbine Output	472 kW	(450 Btu/sec)
Alternator Output	450 kW Total	
Delivered Energy to ATSS	425 kW	
<u>Energy Rejected to Radiators</u>		
Water Flow	5.58 kg/sec	12.3 lb/sec
Radiator Inlet	350 K	(631 ^o R)

TABLE A-1 SUMMARY OF ENERGY CONVERSION PARAMETERS
FOR 2550 kW (concluded)

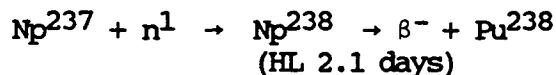
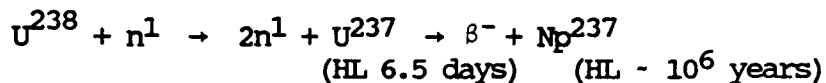
Energy Rejected to Radiators (cont'd)

Radiator Outlet	322 K	(581°R)
Radiation Surface Temperature	320 K	(576°R)
Energy Exchanged	652 kW	(618 Btu/sec)

B. Conversion of Solar Energy to Direct Current 0.2 Conversion Efficiency,
Deliver AC equivalent

Bus Voltage at ATSS	280 V
Continuous Current Required	9107 A

Pu^{238} is a reactor-generated isotope produced by double irradiation (Reference A-6). The reactions which generate Pu^{238} consist of:



The Pu^{238} for spaceflight applications is initially separated as the Np isotope and then resubjected to neutron radiation for conversion into the Pu^{238} . The presently used process is complex and costly, since the $\text{n} \rightarrow 2\text{n}$ reaction shows only a two percent occurrence in the irradiation of U^{238} . On the other hand, a large quantity of Pu^{238} resides within the present inventory of used power reactor fuel elements. A national energy policy to implement breeder-type reactors could provide a supply of Pu^{238} as a by-product to the fuel reprocessing cycle.

A heat source using Pu^{238} must have enough fuel to sustain 2550 kW over the ATSS mission life time of ten years. The system must have built-in redundancies such that the heat can always be extracted from the source. In addition, the system must have the shielding necessary to attenuate the low energy gamma radiation and stray neutrons associated with the radioactive decay. The concept therefore utilizes two independent cores as heat sources, each driving three converters. The converters must have a capability for cross feed which permits either core to drive any three converters. The concept also has the contingency capability for operating the converters at higher pressures to assure continuous extraction of heat from the cores. The concept includes a means for handling heat generation during core loadings, start up, and final shut down. Finally, the concept places the cores and heat transfer elements within a man-rated radiation shield. These features are

described below and lead to assessments of mass, description of controls, and a discussion of the operating conditions associated with a continuous heat source.

A.1.2 System Features for a Radioisotope Decay Power Source

The principal features for the Pu²³⁸ radioisotope decay power system are shown in Figure A-1; the system consists of the core, the heat transfer elements, and the accommodations for fueling and start up. Each feature interacts with the others to some degree; the interactions are addressed in descriptions which follow.

A.1.2.1 Core Concept, Power Level Definition

The 89-year half-life for Pu²³⁸ decay results in an eight-percent reduction in heat generation over a ten-year life span. For this application the initial fuel inventory will develop 2780 kW as 463 kW each from six converters and decay to 2550 kW from six converters after ten years of operation. This range of power output is within the control and operating capabilities of the baseline converters. The initial thermal output from each core is 3475 kW. The decay energy from Pu²³⁸ is 0.13 kW per gram mol, which equates to an initial inventory of 7217 kg (15913 lb) of PuO₂. This oxide has a density of 11460 kg/m³ (716 lb/ft³). Therefore, the volume of PuO₂ in each core is 0.63 m³ (22.2 ft³). To improve thermal conductivity and the extraction of heat, the PuO₂ is mixed with an equal volume of BeO resulting in a total fueled volume of 1.26 m³ (44.5 ft³) and fueled mass of 8980 kg (19800 lb). The accommodation of the fuel mix and details of the core configuration address both heat transfer and continuous heat release considerations;

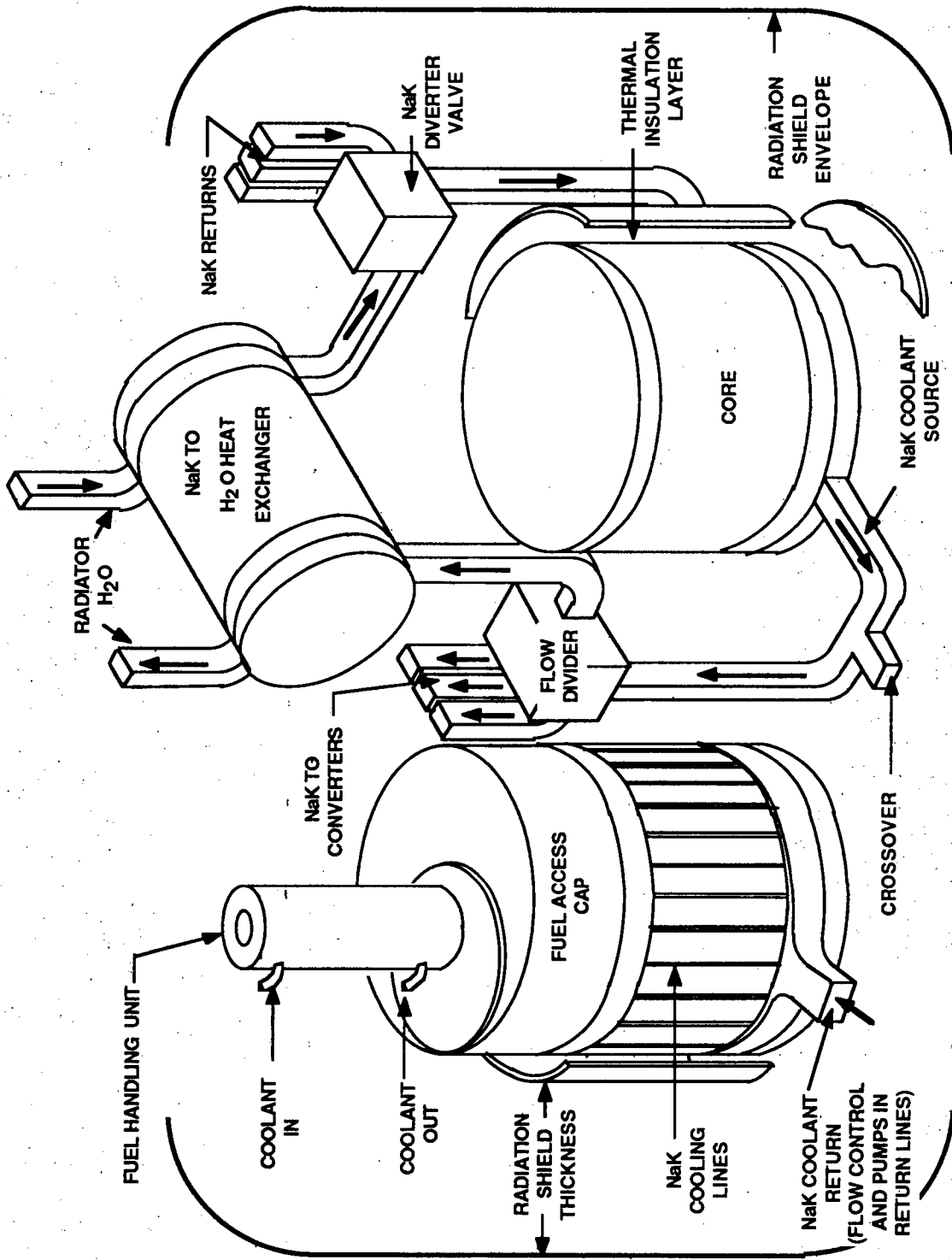


Figure A-1 Concept for a Pu^{238} Radioisotope Decay Heat Source

Figures A-2 and A-3 show the pertinent details of the core concept. The fuel mix is contained in hexagonal shaped segments 11.1 cm (4.4 in) long by 5 cm (2 in) across the flats. A fuel element consists of 12 segments, and the core contains 586 such fuel elements in the form of a right circular cylinder 1.34 m (4.4 ft) in diameter and 1.34 m (4.4 ft) long. The fuel elements are inserted and locked into a hexagonal cell structure with a tube-sheet and header at one end. All supporting structure and cladding utilizes a metal alloy compatible with liquid NaK. One candidate alloy is 79N-13Cr-7Fe, and this alloy has been used for estimates of mass.

A.1.2.2 Heat Transfer Considerations

The equal-volume mix of PuO_2 and BeO results in a power density of 2.65 W/cm^3 (43.4 W/in^3). Some spontaneous fissions occur within Pu^{238} . However, the rate is many orders of magnitude below the alpha particle emissions and would not cause unacceptable radioactivity within either the Na or K. Therefore, the core can be cooled directly by the NaK flow that powers the converters. The flow rate and temperature rise within the core match the flow rates for three converters and the temperature drop through the high temperature heat exchangers in the converters. A NaK flow rate of 118 kg/sec (260 lb/sec) through 586 tubes of 1.5 cm (0.6 in) diameter yields maximum wall temperatures of 1082 K (1947°R) and fuel temperatures of 1100 K (1980°R) which are 55 to 60 K (100 to 108°R) below the corresponding fuel and wall temperatures for a fission reactor (Reference A-1). The coolant flow passages for the Pu^{238} could utilize the same concept as for the fission reactors. In this case the inlet NaK provides a coolant passage between the ZrO_2 insulation (see Figure A-2),

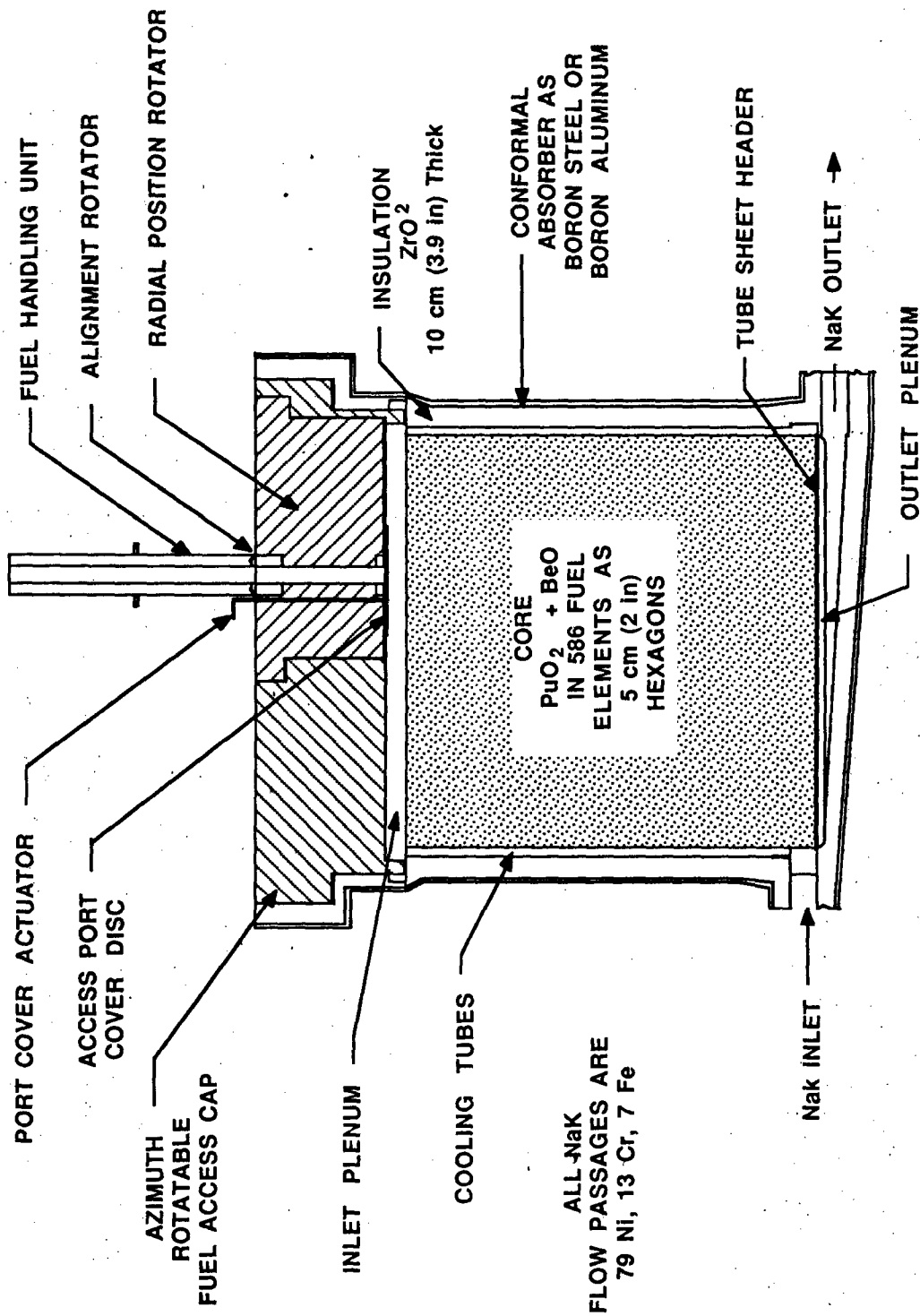
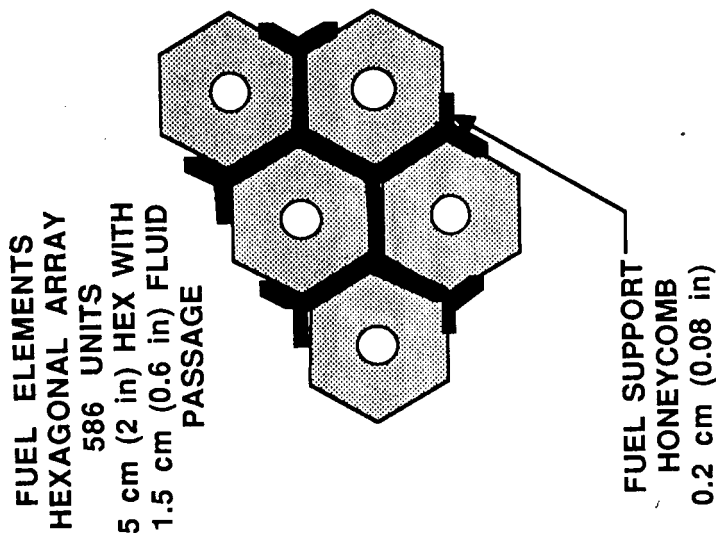
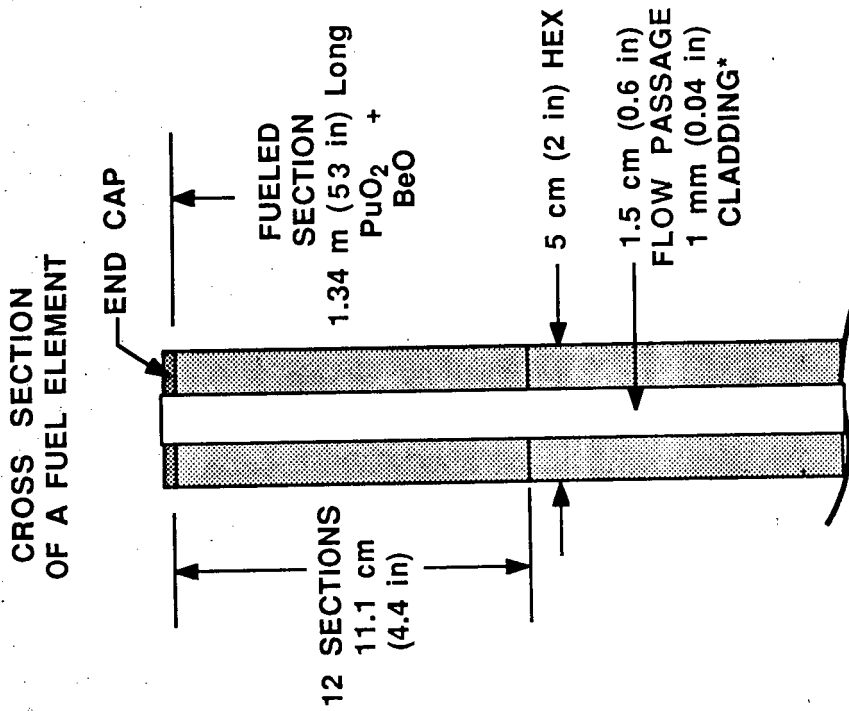


Figure A-2 Concept for a Pu238 Radioisotope Decay Heat Source



- CLADDING IS 79 Ni, 13 Cr, 7 Fe

Figure A-3 Pu238-BeO Core Component Details

and the core and flows into an inlet plenum. The NaK flows through the fuel element passages into an outlet plenum before distribution to the individual converters. Electromagnetic pumps (see Figure A-4) in the cold (NaK inlet) lines drive the flow.

A.1.2.3 Accommodations for Fueling and Start Up

The continuous heat released by radioactive decay requires an equally continuous heat extraction process. The concept for the core places the fuel mix in small (5 cm (2 in) hexagonal by 11.1 cm (4.4 in) long) sinterable segments which have manageable thermal requirements. A "new" fuel segment is a 494 W heat source. An assembled fuel element ready for insertion generates 5.93 kW. Therefore, the assembly and handling unit includes a coolant flow. This feature is included in the system concept shown in Figure A-1. The concept for insertion of fuel elements into the core is included in the fuel access cap details of Figure A-2. The inlet plenum, insulation, and shield become a rotatable assembly capable of any azimuth position relative to the core structure. Within the assembly, a second independent rotator provides radial positioning for a third "insertion rotator". A combination of angular positions for the azimuth and radial rotators will align the center line of the third rotator over any of the 586 fuel element locations. An angular position of the third rotator aligns a fuel element with the hexagonal cells in the core. A movement of a cover plate (a disk with an off-center hole) allows insertion or removal of a fuel element. The insertion involves latches, flow control elements, and adjustments in the liquid metal volume. One of the system thermodynamic considerations is the extraction of heat until enough fuel has been installed to power a converter. The NaK-to-

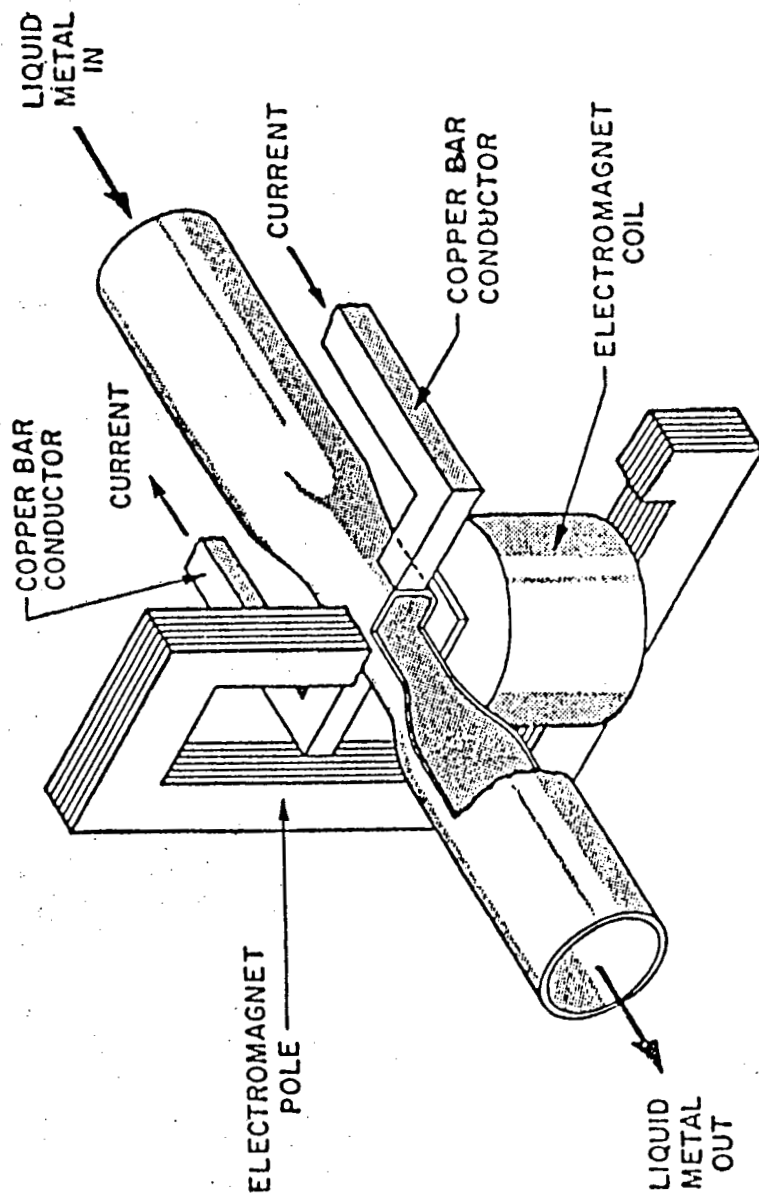


Figure A-4 Concept for a Liquid Metal Electromagnetic Pump
(from Reference A-7)

H₂O heat exchanger identified in Figure A-1 provides that interim capability.

The heat exchanger transfers 1150 kW through a 1 m (3.3 ft) long multi-tube counterflow unit. The NaK flows in 68 tubes 2.5 cm (1 in) in diameter, water flows in 56 tubes 1.2 cm (0.5 in) in diameter. The tubes are imbedded in silicon carbide to provide the thermal gradient buffer between NaK at 1076 K (1936°R) and water coolant.

The thermodynamic and physical parameters for a Pu²³⁸ based heat source are summarized in Table A-2.

A.1.3 Shielding Requirements

The table of isotopes (Reference A-5) lists six gamma rays for Pu²³⁸ all with energies below 1 MeV and relative intensities of 0.038 percent or less. A summing of the gamma activity for the core configuration yields the following energy source terms:

Gamma Energy within the Core	8.50 x 10 ⁷ MeV/cm ³ sec (1.4 x 10 ⁷ MeV/in ³ sec)
Core Surface Activity for λ = 4.25 cm, (λ = 1.67 in)	3.61 x 10 ⁸ MeV/cm ² sec (2.3 x 10 ⁹ MeV/in ² sec)
Gamma Energy into the Shield	1.46 x 10 ⁸ MeV/cm ² sec (9.5 x 10 ⁸ MeV/in ² sec)

If the allowable exposure to these gamma rays is established as less than 4000 MeV/cm²sec (2.5 x 10⁴ MeV/in²sec) then the required attenuation must exceed 3.65 x 10⁴ (Reference A-7). A shield thickness of 11 relaxation lengths will attenuate by a factor of 5.9874 x 10⁴ and thereby is an adequate thickness for the shield. The calculation of shield volumes and weights employs the model developed for the fission reactors with both cores in a common shield (Figure A-5). The shielding parameters and masses are summarized in Table A-3 for the options of a lead or steel shield. The requirements for fueling access limit the acceptable shield

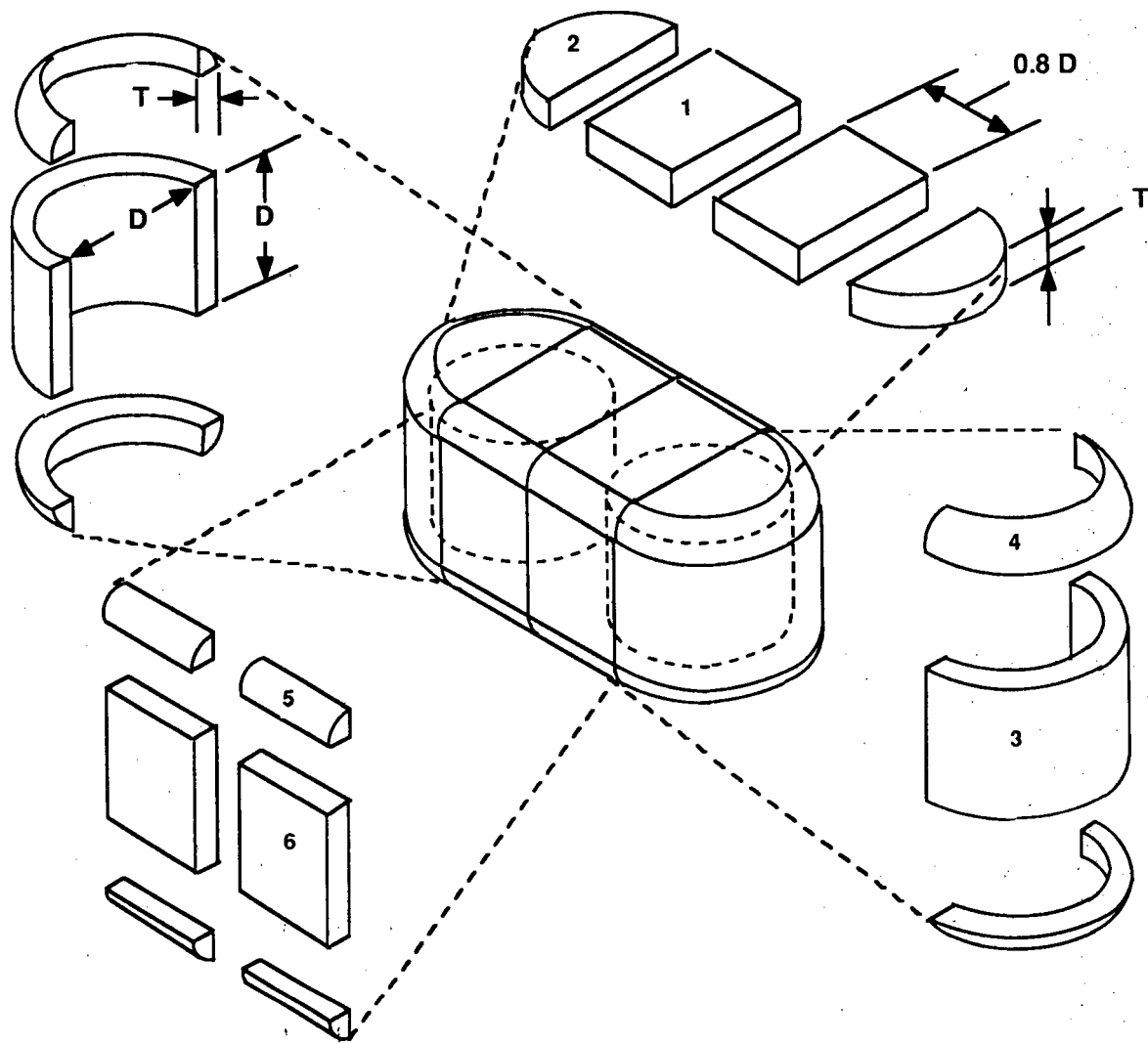
TABLE A-2 SUMMARY OF THERMODYNAMIC PERFORMANCE AND PHYSICAL PARAMETERS
FOR A Pu²³⁸ RADIOISOTOPE DECAY HEAT SOURCE

Thermal Performance Parameters:

Thermal Energy Required from Each Core (initial)	3475 kW
Heat Transfer Area, 586 Tubes 1.5 cm dia, 134 cm long (0.625 in) (52.75 in)	37 m ² (398 ft ²)
Average Heat Transfer Required	92 kW/m ² (8.54 kW/ft ²)
Maximum Wall Temperature	1082 K (1948 ^{OR})
Maximum Fuel Temperature	1102 K (1983 ^{OR})
Liquid Metal Flow Rate	118.2 kg/sec (260.6 lb/sec)
Liquid Metal Temperature In	1048 K (1886 ^{OR})
Out	1076 K (1936 ^{OR})

Fuel Element Handling Considerations:

Heat Generated by a Fuel Segment (storage)	0.495 kW
Heat Generated by a Fuel Element Assembly (insertion)	5.93 kW
Heat Generation for a Launch and Rendezvous (for half a converter)	580 kW
Heat Generation at Recovery (10-yr life for half a converter)	527 kW



1 Top (Rectangle)
2 Cap (Cylinder)

3 End (Cylinders)
4 Fairing (Toriod)

5 Filler (Cylinder)
6 Side (Rectangle)

Figure A-5 Shield Element Model

TABLE A-3 SUMMARY OF RADIATION SHIELDING PARAMETERS
FOR A Pu²³⁸ RADIOACTIVE DECAY POWER SOURCE

Surface activity energy input to the radiation shield 1.46×10^8 Mev/cm²-sec
(9.5×10^8 Mev/in²-sec)

PARAMETER	LEAD SHIELD	STEEL SHIELD
Relaxation Length	2.5 cm (1 in)	3.7 cm (1.45 in)
Number of Lengths Required	11	11
Shield Thickness	27.5 cm (10.8 in)	40.7 cm (16.02 in)
Core Diameter for Shield	1.55 m (5.08 ft)	1.55 m (5.08 ft)
Shield Volume	8.96 m ³ (316 ft ³)	14.50 m ³ (512 ft ³)
Material Density	11300 kg/m ³ (706 lb/ft ³)	7800 kg/m ³ (487 lb/ft ³)
Shield Mass kg	101305 kg (223377 lb)	113120 kg (249429 lb)

thickness such that concrete at 1.1 m (3.6 ft) thickness or water at a 3.3 m (10.8 ft) thickness would not be compatible with fueling operations. The lead and steel shields have significant masses. However, they represent a minimum mass condition for gamma energy released from any of the candidate isotopes for radioactive decay (Reference A-5). All the other candidates have a larger fraction of the decay energy appearing as gamma radiation. In modest quantities (up to 10 kg) Pu²³⁸ does not require a dedicated gamma shield. For example, the fuel rod for the ALSEP package was transported within the man-rated portion of the Apollo Lunar Excursion Module.

A.1.4 Summary of System Masses

The masses which comprise the Pu²³⁸ system are summarized in terms of the core elements, the shield, the converters, and the radiator. Each of these features is described briefly below, and Table A-4 summarizes the mass contributions for each element.

A.1.4.1 Core Elements

The fuel mixtures of PuO₂ at 11460 kg/m³ (712 lb/ft³) and BeO at 2800 kg/m³ (175 lb/ft³) combine to form the major single element. The cladding and support structure include all of the tubes, tube sheets, headers, and the elements of the rotators which contact liquid metal. The mass estimates are based upon a 79Ni-13Cr-7Fe alloy at 8400 kg/m² (525 lb/ft³) which represent present practice for containing liquid metal. The liquid metal ducts which interconnect the cores use 10 m (33 ft) of 0.1-m (4-in) diameter tubing with 6 mm (0.24 in) walls and three electromagnetic pumps (one in each converter return line) as the flow

TABLE A-4 SUMMARY OF MASS ESTIMATES FOR A Pu238 RADIOACTIVE HEAT SOURCE

A. Heat Generation and Heat Transfer Elements

	EACH CORE, kg (lb)	TOTAL FOR SYSTEM, kg (lb)
Fuel Mix (Equal volumes of PuO ₂ , BeO)	8980 (19800)	17966 (39600)
Cladding and Core Structure	3530 (7784)	7060 (15567)
Core Insulation Layer (ZrO ₂)	4670 (10297)	9340 (20594)
Liquid Metal (NaK) Ducting, Pumps	1400 (3087)	2800 (6174)
Liquid Metal (NaK)	450 (992)	900 (1984)
Heat Exchanger	2310 (5093)	4620 (10187)
TOTAL	21340 (47053)	42680 (94106)

B. System Elements

	LEAD SHIELD	STEEL SHIELD
Shielding Mass	101305 (223377)	113120 (249429)
Heat Generation and Transfer	42680 (94106)	42680 (94106)
Converters, six at 3836 kg (8458 lb) ea	23016 (50750)	23016 (50750)
Radiators, six at 27256 kg (60099 lb) ea	163536 (360596)	163536 (360596)
SYSTEM TOTAL	330537 (728829)	342352 (754881)

drivers. In operation, each core will have a flowing volume of about 0.6 m³ (21.2 ft³) of NaK at 730 kg/m³ (45.6 lb/ft³).

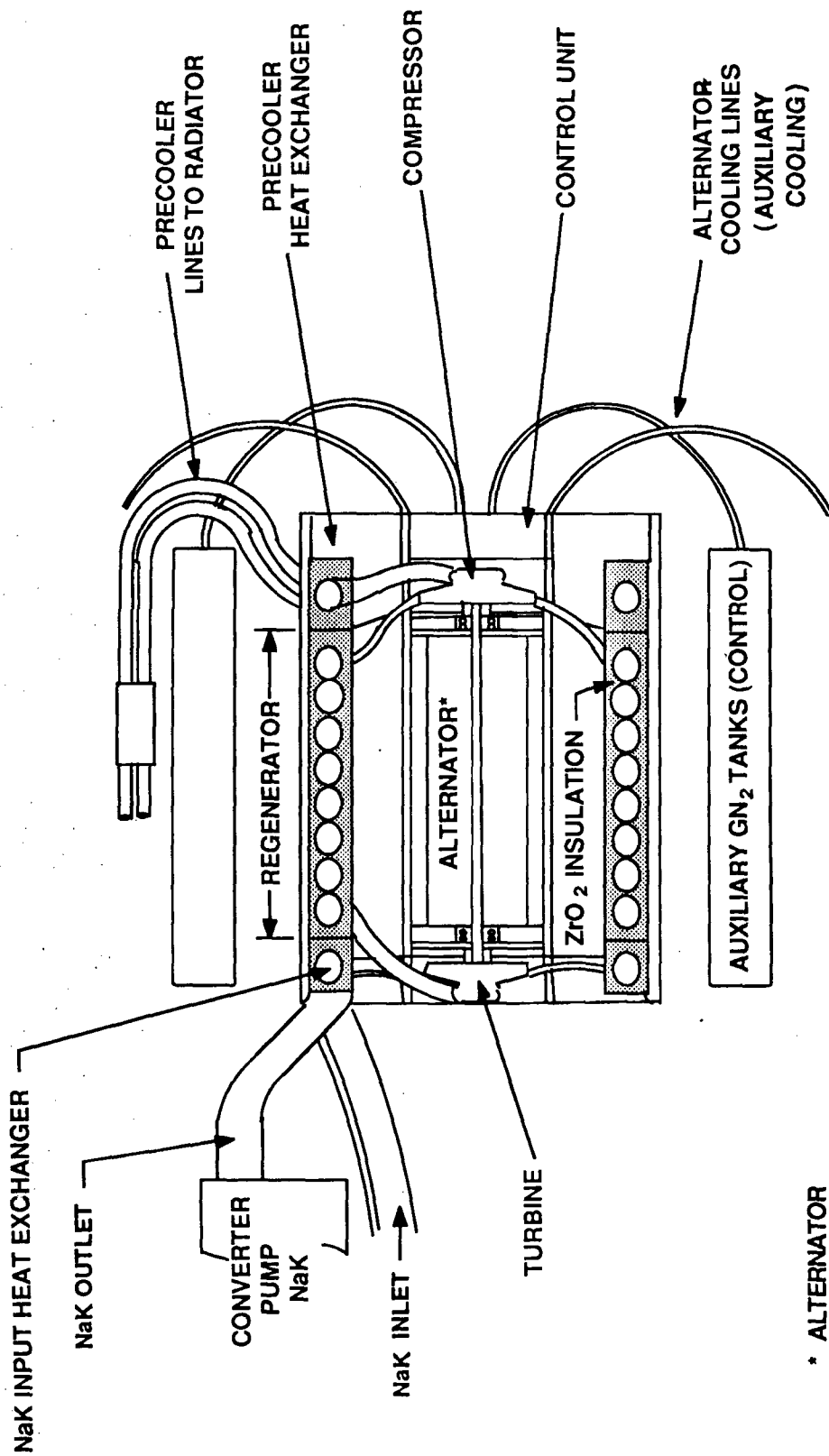
Thermal insulation consists of a 10 cm (4 in) thick layer of ZrO₂ at 50-percent density (3200 kg/m³, 200 lb/ft³) which surrounds the core plus an 8-cm (3.1-in) thick layer of ZrO₂ that encases all of the liquid metal lines, pumps, and valves. The transient (start up) heat exchanger consists of the diverter, the flow ducting, the silicon carbide buffer, headers, leads, insulation, and pumps for both the liquid metal and the radiator coolants. In the configuration shown, the heat generating fuel mix plus its necessary containment account for nearly 60 percent of the core mass, and the heat retaining insulation makes the second largest mass contribution.

A.1.4.2 Shields

The shields have mass estimates which are more than double the contribution from the heat generation and heat transfer components. These estimates of shield masses are conservative for the attenuation of gamma energy from a Pu²³⁸ source. For the ATSS application, man-rated shield mass accounts for more than 30 percent of the total system mass.

A.1.4.3 Converters

The converters are the same units as those defined for the solar dynamic systems; Figure A-6 shows the principal features (Reference A-1). The converters will experience a slow decrease in power output over the 10-year operating life, with outputs ranging from 463 kW at start up, to 425 kW at end of life. These changes are well within the range of power accommodation by adjustments in the operating ambient pressures. During



* ALTERNATOR
 4 POLE, 3 PHASE
 400 Hz, 440 V,
 12,000 RPM

Figure A-6 Converter Section Concept

the fueling and start up sequence, converters may need to operate above their rated power levels for a short period of time and thereby make use of the power margins available. The masses for the converters in the radioisotope application are the same as defined earlier for the baseline solar dynamic system, and represent less than 10 percent of the total mass for the system.

A.1.4.4. Radiators

The radiator assembly consists of the same number of radiating panels for each converter as employed for the baseline solar dynamic system; Figure A-7 shows the principal details for a panel. The principal differences are in the potential range of coolant temperatures and location. The radioactive decay system carries all 612 panels in three circumferential rows around the platform with cross flow interconnections to offset the effects of the Earth in the radiation field of view. For Pu^{238} radioisotope heat source, the radiators become the largest single element of mass and contribute almost half the total mass for the system.

The accommodation of fueling and start up presents the potential for operation at other than the nominal temperature range. The radiator installation that supports a converter dissipates 650 kW from a heat input of 1124 kW while operating with coolant temperatures that range from 350 K (630°R) inlet to 322 K (580°R) at the outlet. The radiator could dissipate 1124 kW if the coolant could operate between a 389 (700°R) inlet and 362 K (651°R) outlet, however the coolant could not be water at atmospheric pressure (boiling point is 373 K, 672°R). On the other hand, the converters could probably operate stably at 60 percent of

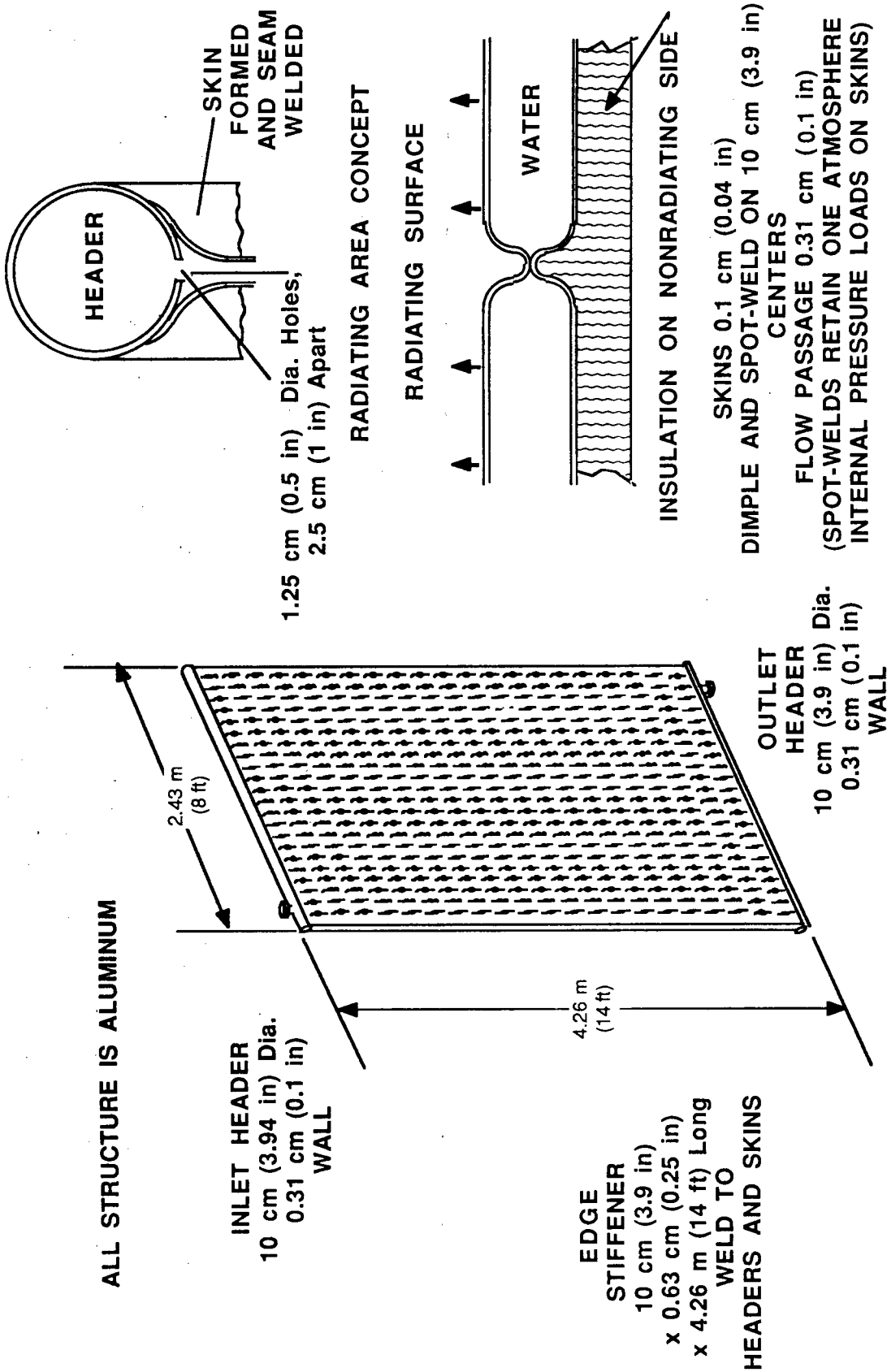


Figure A-7 Radiator Panel Concept (102 for Each Converter)

rated power such that the radiator coolant remained within nominal operating limits. The entire system could be brought to full power by balancing and sharing heat loads between radiators, therefore the masses for the radiator do not include an increment for an additional coolant.

A.1.5 Control Considerations

Controls for a Pu^{238} radioactive decay heat source which drive six converters must provide a steady, continuous exchange of heat and supply of electrical power. The redundancies within the system assure an interrupted flow of the core coolants. The control requirements are summarized in Table A-5 for the core heat transfer and in Table A-6 for the converters and radiator. The controls for the converters and radiators are the same as those for both the solar dynamic and nuclear fission systems described earlier. The installation places all six converters at a central location in an arrangement similar to that for a nuclear fission system (Reference A-1).

After fuel insertion has been completed, operations are continuous and essentially steady state throughout the ten-year lifetime. In the continuous operation, a slow cyclic variation could occur in the flow distribution within the radiator panels. Earth viewing panels would not have the same heat transfer as space viewing panels, and some cyclic adjustments in panel flow rates may be required to keep the compressor inlet conditions constant.

Start-up (and eventual shutdown) involve step-change transients in the thermal output of a core. The insertion of each fuel element generates a predictable change in the thermal balance of the system, and

TABLE A-5 SUMMARY OF Pu²³⁸ HEAT SOURCE CONTROL REQUIREMENTS

CONTROL ELEMENT OR FUNCTION	OUTPUT OR ACTION	RANGE	PRECISION	FREQUENCY
Core Thermal Control Algorithm				
Fuel mix temperature (multiple locations in fuel and cladding)	Input signals to NaK flow control, pumps, and valves	300 K to 1300 K (500°R to 2340°R)	2 K (3°R)	Steady
NaK temperatures (multiple locations core inlet, headers, outlet, and ducting)	Input signals to NaK flow control, pumps, and valves	300 K to 1200 K (500°R to 2160°R)	2 K (3°R)	Steady
NaK mass flow (multiple at inlet outlet and at valves locations)	Input signals to NaK flow control, pumps, and valves	0 to 150 kg/sec (0 to 300 lb/sec)	1 kg/sec (3 lb/sec)	Steady
NaK flow control valve positions (multiple)	Respond to temperature and flow demand	Any setting from closed to full open	1% position	Steady
NaK liquid metal pump operation (multiple electromagnetic)	Field current and drive current modulated in response to power generation	0 to 1100 A	2 A	Steady
Radiation Monitor and Safety Functions				
Structure and shield temperatures (multiple)	Input signals to auxiliary coolant flow control	300 K to 1200 K (540°R to 2160°R)	2 K (3°R)	Steady
Gamma radiation monitors (multiple)	Confirm shielding, leak detection	0 to 1.4×10^8 MeV/cm ² sec (0 to 8.6×10^8 MeV/in ² sec)	1%	Steady
Neutron population monitor (multiple)	Confirm shielding, leak detection	0 to 10^4 /cm ² sec (0 to 6.45×10^4 /in ² sec)	1%	Steady
Shield coolant temperature (multiple)	Input signal to pumps and valves	300 K to 360 K (540°R to 650°R)	2 K (3°R)	Steady

TABLE A-5 SUMMARY OF PU²³⁸ HEAT SOURCE CONTROL REQUIREMENTS (concluded)

CONTROL ELEMENT OR FUNCTION	OUTPUT OR ACTION	RANGE	PRECISION	FREQUENCY
Radiation Monitor and Safety Functions (cont'd.)				
Shield coolant flow valve position (multiple)	Response to demand	Close to open	1%	Steady
Coolant pump operation (water)	Response to demand	0 to 20 kg/sec (0 to 45 lb/sec)	0.1 kg/sec (0.25 lb/sec)	Steady
Core Fueling Operations				
NaK preheater operation (inductive or resistive coils in NaK return lines)	Response to power setting	0 to 440 V (0 to 1000 A)	10 V (10 A)	Steady
Rotator positioning (three rotators)	Response to locator command	0 to 360 deg	0.1 deg	Move to setpoint on command
Insertion sequence - port open, close - position, stroke and recover	Responds to commands	Open-close stroke 1.35 m (4.3 ft) plus shield thickness	1% position 0.1 cm, (0.04 in)	Sequence of operations
NaK to H ₂ O heat exchanger operation - NaK diverter valve position - water flow valve position - NaK pump operation - radiator pump operation	Responds to demand Responds to demand Responds to demand Responds to demand	Close to open Close to open 0 to 1100 A 0 to 440 V 0 to 100 A	1% position 1% position 2 A 1 V, 1 A	Transient with each insertion steady between insertions
Fuel element handling unit - coolant temperature - coolant flow	Responds to commands input to control algorithm Responds to demand	300 K to 400 K (520°R to 720°R) 0 to 10 kg/sec (0 to 22 lb/sec)	2 K (3°R) 0.1 kg (0.25 lb)	Steady at setpoint Steady at setpoint
- coolant pump operation	Responds to demand	0 to 440 V, (0 to 100 A)	1 V, 1 A	Steady at setpoint

TABLE A-6 SUMMARY OF CONTROL REQUIREMENTS FOR A 450 kW 400 HZ CONVERTER
(CLOSED CYCLE GAS TURBINE DRIVEN, LIQUID METAL HEAT TRANSFER ENERGY INPUT)

CONTROL ELEMENT OR FUNCTION	OUTPUT OR ACTION	RANGE	PRECISION	RATE/ FREQUENCY
Converter Operating Algorithm				
Rotation speed	Error signal to inlet valves and electric load balance	0-12200 rpm	0.1 rpm	Steady
Magnet current	Error signal to electric load	0-500 A	0.1 A	Steady
Electrical load and phase balance volts, amperes for each phase	Signal to valves switching signals to internal load leveling elements	0-500 A	0.1 A	Steady
Compressor inlet control and reservoir valves	Feed or bleed to maintain speed	Open-close profile	0.01 of profile	Steady
Regenerator temperature (multiple)	Signal to valves	320-1083 K (560-1950°R)	2 K (3°R)	Steady
Liquid metal heat exchanger temperatures (multiple)	Signal to valves	320-1083 K (560-1950°R)	2 K (3°R)	Steady
Precooler heat exchanger temperatures	Signal to valves	273 to 555 K (560 to 1000°R)	2 K (3°R)	Steady
Gas stream temperatures (compressor, regenerator turbine)	Signal to valves	320 to 1083 K (560 to 1950°R)	2 K (3°R)	Steady
Gas stream pressures (compressor regenerator turbine)	Signal to valves	0 to 6894 mPa (0 to 1000 psia)	34.5 kPa (5 psi)	Steady
Bearing, lube or gas supply (temperature pressure, flow)	Signal to control valves	Configuration-particular, each case	1 percent	Steady

TABLE A-6 SUMMARY OF CONTROL REQUIREMENTS FOR A 450 KW 400 HZ CONVERTER
(CLOSED CYCLE GAS TURBINE DRIVEN, LIQUID METAL HEAT TRANSFER ENERGY INPUT) (concluded)

CONTROL ELEMENT OR FUNCTION	OUTPUT OR ACTION	RANGE	PRECISION	RATE/ FREQUENCY
Radiator Heat Exchange Algorithm				
Radiator panel temperatures (multiple inlet, outlet)	Signal to flow control valves and pumps	260 K to 380 K (470°R to 700°R)	2 K (3°R)	Steady
Radiator coolant temperature (multiple) Inlet headers, and cross flow (multiple)	Signals to flow control valves and pumps	260 K to 380 K (470°R to 700°R)	2 K (3°R)	Steady
Coolant flow control valves, headers, and cross flow (multiple)	Modulation to maintain flow, pressure and temperature	0 to 50 kg/sec (0 to 115 lb/sec)	0.5 kg/sec (1.1 lb/sec)	Steady with low frequency cycling (1 per orbit)
Coolant flow pumps (multiple)	Modulation to maintain flow, pressure and temperature	0 to 50 kg/sec (0 to 115 lb/sec)	0.5 kg/sec (1.1 lb/sec)	Steady with low frequency cycling (1 per orbit)
Radiator system internal pressure	Modulate to prevent local boiling	0 to 12 KPa (0 to 17 psia)	50 Pa (0.1 psia)	Steady

the fueling sequence provides for the converter start-up transients. However, start-up and shutdown are one-time events.

A.1.6 Particular Considerations

The considerations particular to a Pu^{238} heat source relate to the helium released as the alpha particle decay product and the transport of fuel from Earth to the ATSS orbit.

A.1.6.1 Helium Released as Alpha Particles

The alpha particle decay results in the generation of helium at the rate of one He atom per decay event. For the fuel mix defined, the helium release amounts to 94 milligrams per hour (-0.5 standard liter). The fueled segments must accommodate this release as control of the sinter densities and provisions for a diffusion vent in the end caps. Extraction of helium from the NaK can be accomplished in a secondary loop containing a centrifugal separator. The alpha particle decay rate makes Pu^{238} a very toxic isotope if inhaled as dust or ingested as a food contaminant (Reference A-7). Preparation of the fuel segments on Earth must include the appropriate measures for protection. On the other hand, a sintered mix of PuO_2 and BeO is chemically inert to soil or life-related processes. As a clad fuel segment aboard the ATSS, the hazard to personnel reduces to just thermally hot metal.

A.1.6.2 Thermal Control During Fabrication and Transport

The Pu^{238} requires thermal control from the time of formation onward. The individual fuel segments have been sized to approximate the heat sources presently used for thermoelectric generators; therefore,

fabrication and on-Earth storage of the fuel segments does not present any new considerations. On the other hand, the transport of a workable fuel quantity presents a particular thermal consideration. A quantity of fuel segments equal to half-power for a converter has a thermal output of 580 kW that must be accommodated continuously from prelaunch preparation until orbital rendezvous. A four-hour flight time from lift-off to rendezvous with the ATSS would require a total heat dissipation equal to evaporating 5500 kg (12127 lb) of water at atmospheric pressure. Consequently, the fuel transport vehicle may require a minimum "live" payload of 7300 kg (16096 lb) as transported fuel and evaporated water coolant. In such a configuration, transport to orbit requires 12 launches of a dedicated spacecraft that has a nominal mass of 10000 kg (22050 lb) at lift-off. At rendezvous the fuel transporter needs access to the equivalent of a converter radiator while the fuel segments are assembled and loaded into the core.

A.2 FUSION POWER

A.2.1 Fusion as a Potential Heat Source

Fusion reactions involving the isotopes of hydrogen offer a mass efficient source of heat. Present research into fusion power works with the fusion reaction between deuterium (hydrogen of atomic mass number 2) and tritium (hydrogen of atomic mass number 3) which provides helium of mass number 4 and an extra neutron (Reference A-8). This reaction has the lowest energy threshold for ignition (4.4 KeV) and constitutes the principal thermonuclear reaction within the weapon known as the "H bomb". At the present time, thermonuclear weapons are the only systems which generate more energy from fusion than that required to initiate a

thermonuclear reaction; however, controlled fusion, in which the energy released matches the energy input, is anticipated within the next half decade. The prospects for controlled fusion as a heat source appear within reach by the year 2000; therefore, fusion power becomes a candidate for the ATSS.

The configuration of a fusion heat source for the ATSS is determined by the technique used for initiating the fusion reaction. Fusion occurs when an atom of deuterium and an atom of tritium can be brought to the point where the attracting nuclear forces exceed the electrostatic repulsion forces. Once the two nuclei are within the proximity range for the nuclear forces, the protons and neutrons rearrange into a "most stable" configuration and release the excess binding energy. For the deuterium-tritium reaction the most stable configuration becomes a helium atom containing two protons and two neutrons plus a free neutron. The reaction releases 17.6 MeV with helium recoil at 3.5 MeV and the neutron emitted with 14.1 MeV (velocity approximately one eighth the speed of light, Reference A-8). Present research has identified three potential approaches to controlled fusion power. These are described briefly below and thereby show the rationale for the selection of an inertially-confined laser-ignited system for the ATSS power source.

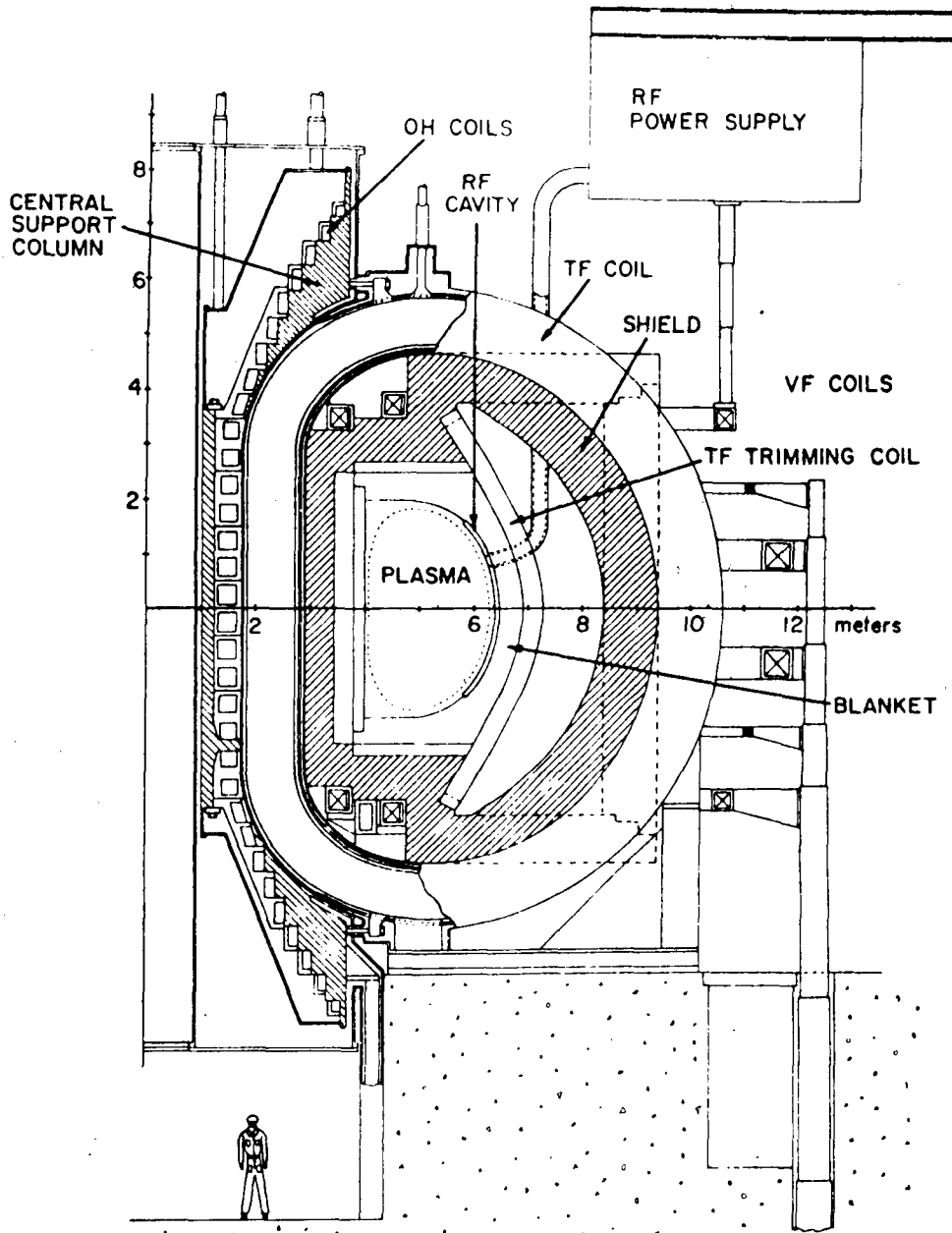
A.2.1.1 Magnetically Confined, Plasma Ignited Fusion

Fusion power systems that use magnetic fields interacting with gases in a plasma state (low density, single atoms, ionized) have received the major portion of fusion research. The systems have generated acronym based names such as "Stellarator", "Mars Tandem Mirror", "Elmo Bumpy Torus", etc. Systems which magnetically confine the plasma into a toroid

have been studied extensively by a number of nations, and these studies have coined the name "Tokamak" from the Russian acronym for a magnetically confined toroidal chamber (Reference A-8). Magnetically confined systems initiate fusion by heating a plasma mixture of deuterium and tritium gasses to the point where the thermal velocity energy can overcome the coulomb electrostatic repulsion. Magnetically confined plasmas have the potential for continuous controllable fusion and a number of experimental systems (principally Tokamak configurations) have ignited their plasmas and operated continuously. To date, however, no system has obtained more energy than that required for the combination of plasma control, fuel injection, and the extraction of combustion products. Break-even power generation is the next technical goal and is anticipated for a Tokamak configuration within the next half decade. The principal features are illustrated by Figure A-8. The considerations pertinent to a space power application include:

- a. Magnetic confinement involves toroidal fields in the range from 50,000 to 150,000 gauss supplemented by auxiliary vertical fields. Superconductivity is a requirement (present systems have cryogenic cooling by liquid helium).
- b. Plasma heating to ignition temperatures requires an auxiliary power input, (Present systems use AC supplemented by rf or particle beam heating.)
- c. The blanket, as the heat extracting member, operates in a harsh thermal and neutron radiation environment. Tritium fuel generation involves the irradiation of lithium by neutrons, therefore lithium in some form must be present within the blanket.

ORIGINAL PAGE IS
OF POOR QUALITY



OH OHMIC RESISTANCE HEATING COILS
TF TOROIDAL FIELD
VF VERTICAL FIELD
RF RADIO FREQUENCY HEATER

Figure A-8 Principal Features for a Magnetically Confined Toroid, "Tokamak", Fusion Heat Source (from Reference A-8)

- d. The fueling and extraction of combustion products (principally helium) require specialized injection techniques (cryopellets or gas) and an efficient vacuum system to maintain the operating pressure in the 10^{-4} to 10^{-8} Torr range.

A.2.1.2 Inertially Confined, Laser Ignited Systems

Thermonuclear weapons utilize an implosion for confinement and the heat of a fission reaction to achieve ignition conditions. The same principle can be applied on a minute scale with a small quantity (one milligram or less) of fuel imploded and heated by laser beams. Such concepts have been proposed, and preliminary experiments have been performed (Reference A-8). The limiting considerations appear to be the ability to deliver the laser energy into the fuel as a uniform illumination and maintain the energy penetration throughout the duration of the laser pulse. Ablation products from the pellet surface tend to absorb the last portion of the pulse. Consequently, energy penetration requires high frequency (short wavelength) lasers.

Recent developments in laser technology have produced the "excimer" type of laser which is based upon compounds which exist only in an excited state, and these lase in the ultraviolet portion of the spectrum. Typical wavelengths are argon fluoride at 193 nm, krypton fluoride at 248 nm, and xenon fluoride at 351 nm with average pulse durations of a few n sec (Reference A-9). These combinations of wavelengths and pulse durations appear compatible with the ignition requirement conditions. In addition, these lasers are pumped by electron beams, and electron beams provide the potential for operating with laser power efficiencies in the 10-to 20-percent range. A fusion power system will need this range of

efficiencies to achieve a useful net energy output. A fusion power system based upon inertial confinement and laser ignition becomes a repetition of small thermonuclear explosions that require the precise fabrication and delivery of a fuel pellet to a point where they can be uniformly irradiated by high-frequency (UV) short-duration laser pulses.

The principal features become:

- a. A fuel delivery system which can uniformly encapsulate a small quantity of a deuterium-tritium mix and inject the pellet with the precision necessary for uniform illumination by a laser beam. Cyclic rates for injection can range from 5 to 20 per second.
- b. A laser with the associated beam splitters and optics that will deliver the required ignition energy to the fuel pellet in a manner that accomplishes uniform illumination at cyclic rates from 5 to 20 per second.
- c. A containment and heat extraction system which will accept the photons, ions, and neutrons produced by the fusion reaction and transfer the thermal energy for electrical power conversion. Since lithium irradiation by neutrons provides the source for tritium, the containment has to include lithium in some form.
- d. A vacuum and gas separation system which can scavenge the combustion products from the containment system and separate the helium and the remains of the encapsulation material from unreacted deuterium and tritium.

A.2.1.3 Muon Catalyzed Fusion

Catalyzed fusion can be made to occur within a molecule of hydrogen gas that consists of a deuterium atom and a tritium atom. If a muon, a

negatively charged subatomic particle, replaces one of the electrons in the molecular configuration, the heavy muon will fall into a close orbit. The inertial reaction with the muon will then draw the two nuclei into the proximity range where fusion will occur. The fused nucleus then decays by ejection of a neutron and recoils with sufficient velocity to dislodge the muon which can then find another deuterium-tritium molecule to repeat the process. The reaction was first confirmed during the 1950's; however, the recent discovery of a resonance effect at a temperature of 1170 K (2106°R) has made the process a potential candidate for power system applications. Catalyzed fusion can occur at almost any temperature (it has been observed at 13 K, 23°R); however, at resonant temperature, a muon will repeat the reaction more than 100 times. With muons supplied from a particle accelerator, the operation can be sustained and produce useful amounts of energy (Reference A-10). Sustained muon-catalyzed fusion has been demonstrated at the laboratory experiment level. The principal features of a muon catalyzed system are:

- a. A muon supply consisting of an electromagnetic charged particle accelerator that places a beam of ions on a target material which reacts to form negatively-charged subatomic particles (muons).
- b. A gas supply that mixes deuterium and tritium in a manner which favors the formation of deuterium-tritium pairs within the population of hydrogen molecules.
- c. A reaction vessel that operates at the resonance temperature (-1170 K, 2106°R) and extracts the heat released. Lithium irradiation by the fusion neutrons produces the tritium fuel constituent; therefore, the vessel must have lithium present in some form.

d. A vacuum and scavenge system that maintains the operating atmosphere within the reaction chamber and separates the helium from unconsumed deuterium and tritium.

In summary, a power system based upon fusion appears inherently more complex than any other alternate. In ranking the fusion alternates toward an ATSS application, the following considerations dominate:

1. The magnetic confinement requirements will involve massive elements such as coils, heaters, and methods for handling the plasma.
2. The muon catalyzed system is just emerging from the "curiosity" stage, and eventually, may become an effective approach.
3. The inertially confined, laser-ignited system requires some major technical advances; however, advances are being made in high-energy, high-frequency, short-duration lasers.

The synergy with ongoing laser developments makes the inertially confined laser-ignited system the choice for ATSS application. The ATSS concept will draw upon features proposed for ground-based power systems and use a thermodynamic scale-down to ATSS levels.

A.2.2 Fusion System Considerations for the ATSS Application

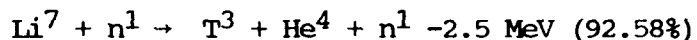
The fusion power system concept for the ATSS is based upon a thermodynamic scaling of a proposed configuration for a 1000 MW electrical generation station (Reference A-8); Table A-7 lists the pertinent parameters for the two systems. The electrical and thermal parameters are scaled at the nominal power ratio of 0.00255. In anticipation of future developments, the laser power efficiency is placed at 13 percent instead of 6.5 percent. The firing rate of 20 per second has redundancy by dividing the fuel supply and lasers into two systems

TABLE A-7 OPERATING PARAMETERS FOR AN ATSS FUSION HEAT SOURCE SCALED FROM A PROPOSED INERTIALLY CONFINED, LASER-IGNITED POWER STATION CONCEPT

PARAMETERS	POWER STATION	ATSS
Thermal Energy Released, MW	3440	8.52
Gross Electric Power, MW	1334	3.40
Delivered Electric Power, MW	1000	2.55
Laser Ignition Pulse, kW	1000	2.8
Laser Input Power, MW	300	0.425
Lasers and Pulse Rate Per Second	1 at 20	2 at 10
Fuel Burn Fraction	0.45	0.45
Fuel Mass Each Pulse, μg	1000	2.12
Heat Flux into Walls, kW/m^2 (kW/ft^2)	5000 (464)	565 (52.48)

each operating at 10 per second. The fuel burn fraction is the same for both systems but results in a slight reduction in total fuel for the ATSS requirement because of the 40-percent conversion efficiency for the ATSS compared to 30 percent for the proposed power plant. The principal difference is in the heat flux into the walls. The ATSS flux level is reduced by about an order of magnitude principally to accommodate liquid metal and tritium generation considerations.

The fueling usage listed assumes gas-filled silicon oxide spheres with the deuterium obtained from the electrolysis of water and the tritium generated by neutron irradiation of lithium. The tritium source reactions are:



Within these reactions, Li^6 has an affinity for thermal neutrons which decreases at higher neutron velocities. On the other hand, the Li^7 reaction has a threshold for neutrons absorption at 2.5 MeV which peaks in the 7 to 10 MeV range. For the ATSS application, tritium generation must equal tritium usage and, therefore, has to involve the secondary neutrons from the Li^7 reaction. Since the fusion neutrons are born with energies of 14.1 MeV, lithium must be among the first elements encountered by the products of fusion, and the wall of the reactor vessel needs to include a neutron moderator material. For this study, the moderator is carbon in the form of graphite. These considerations help define the features for the ATSS fusion power based electrical generation system.

A.2.3 ATSS Fusion System Features

The principal features for the ATSS fusion based electrical power generation system are listed in Table A-8. The system concept is shown in Figures A-9 and A-10. The pertinent elements and rationales are described below:

A.2.3.1 Reactor Vessel, Energy Containment

The reactor vessel must absorb the energy and contain the products from the fusion while providing a continuous flow of heat energy to the converters. The fusion containment concept is outlined in Figure A-9. The pertinent details of the confinement method appear in Figure A-11 which shows a cross section for the reactor vessel. The energy release from the fusion occurs at the center of the cylindrical cavity as a series of small explosions, one every 50 msec. The energy reaches the walls of the container in the form of photons, helium nuclei, and neutrons plus the residues from combustion which are atoms of deuterium, tritium, silicon, and oxygen. The first surface, a 5-cm (2-in) layer of flowing liquid lithium, absorbs all of the photons and atoms. The lithium also interacts with the neutrons and begins the tritium breeding process. Primary neutrons encounter lithium at energies above the threshold for the Li^7 reaction. The graphite layer behind the flowing lithium slows the primary neutrons and reflects both the primary and secondary neutrons back into the lithium layer. Leakage neutrons are slowed or absorbed by the ZrO_2 insulation. The boron steel of the pressure vessel absorbs the residual thermal neutrons. Some heat is generated in the graphite; therefore, the inlet flow of lithium first cools the graphite before entering the cavity area. The concept for the

TABLE A-8 PERTINENT FEATURES FOR THE ATSS INERTIALLY-CONFINED
LASER-IGNITED FUSION HEAT SOURCE

SYSTEM ELEMENT	PERTINENT FEATURES
Reactor:	Cavity: 2-m (6.5 ft) by 2-m (6.5 ft) cylinder with liquid lithium first surface.
	Walls: Flowing liquid lithium layer 5-cm (2 in) thick over clad graphite 34.3-cm (13.5 in) thick.
	Insulation: ZrO ₂ layer 20-cm (8 in) thick.
	Container: Boron steel vacuum shell 1-cm (0.4 in) walls.
Fuel:	Mix: Atmospheric density equal volume of deuterium and tritium.
	Capsule: Silicon oxide walls 0.05-mm (0.002 in) thick sphere 3-mm (0.12 in) dia. Usage rate is 246 grams/day (0.54 lb/day).
	Processing: Dual system for encapsulation, ready storage and injection. Centrifugal velocity injectors.
	Deuterium: Process 0.85 grams/day (0.03 oz/day) obtained by 25.5 kg/day (56 lb/day) of water electrolysis.
	Tritium: Process 1.27 grams/day (0.003 lb/day) obtained from lithium irradiation by neutrons. Li is consumed at 2.85 grams/day (0.0063 lb/day).
Ignition:	Lasers: Excimer type operating in the UV range.
	Beams: Deliver eight simultaneous pulses, 90 deg apart 4 in each hemisphere, 2.8 kW total in each pulse.
	Cooling: Laser cooling by a dedicated radiator.
Liquid Metal Li Heat Exchangers:	Lithium: Flowing wall temperature rise 27 K (50°R) in 12 sec. enters at 1103 K(1985°R), exits at 1130 K (2034°R), exit flow passes through separators.
	NaK: Heat transfer through counterflow exchangers, eight units supply, eight converters.
Reactor Pressure Control and Gas Recovery:	Pressure: Vacuum system maintains cavity at 10 ⁻⁴ torr or less.
	Gas Recovery: Unburned fuel and reaction products separated by membranes and electromagnetics into deuterium, tritium, and helium.

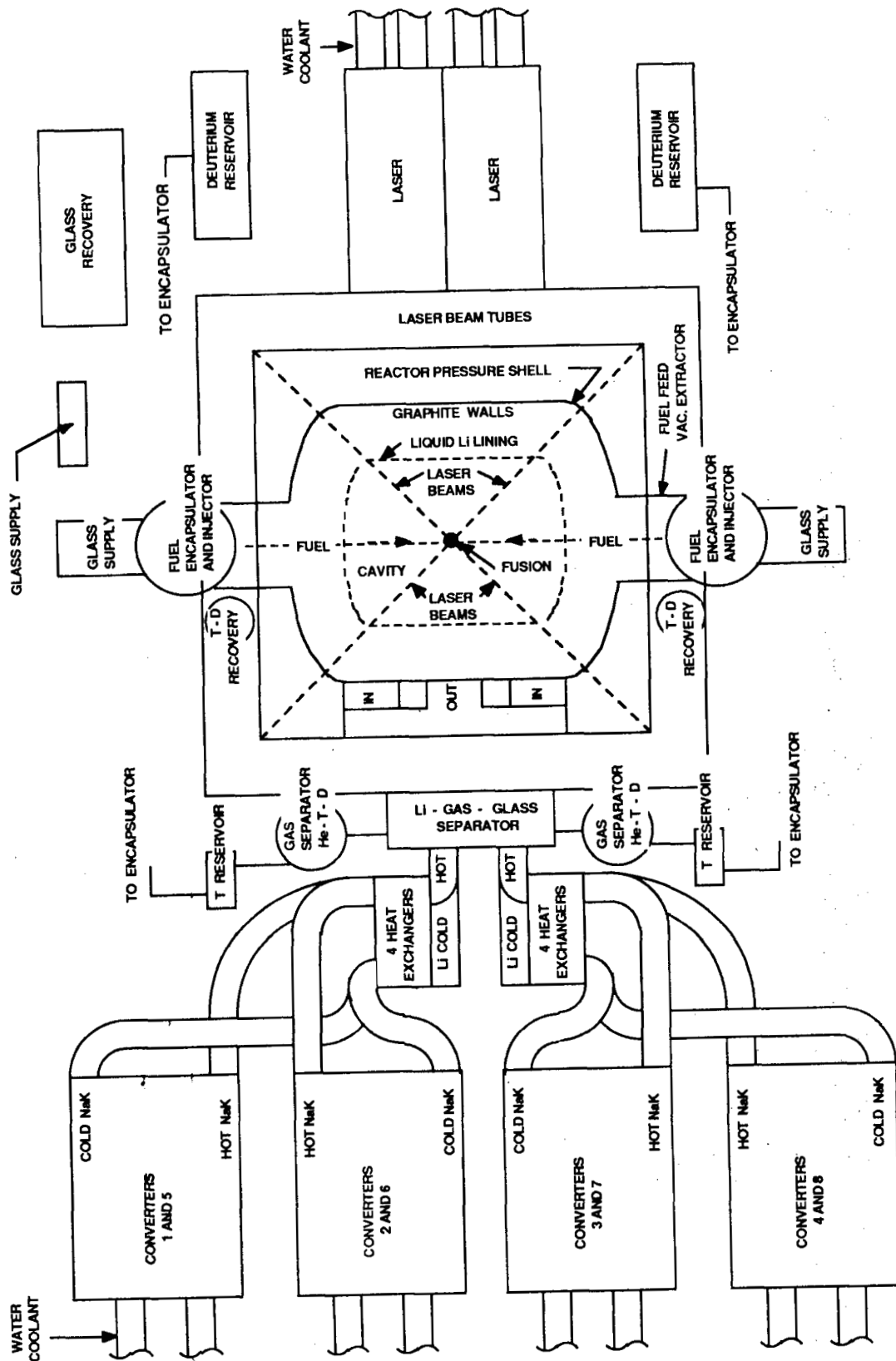


Figure A-9 Concept for the ATSS Fusion Power System, Plan View

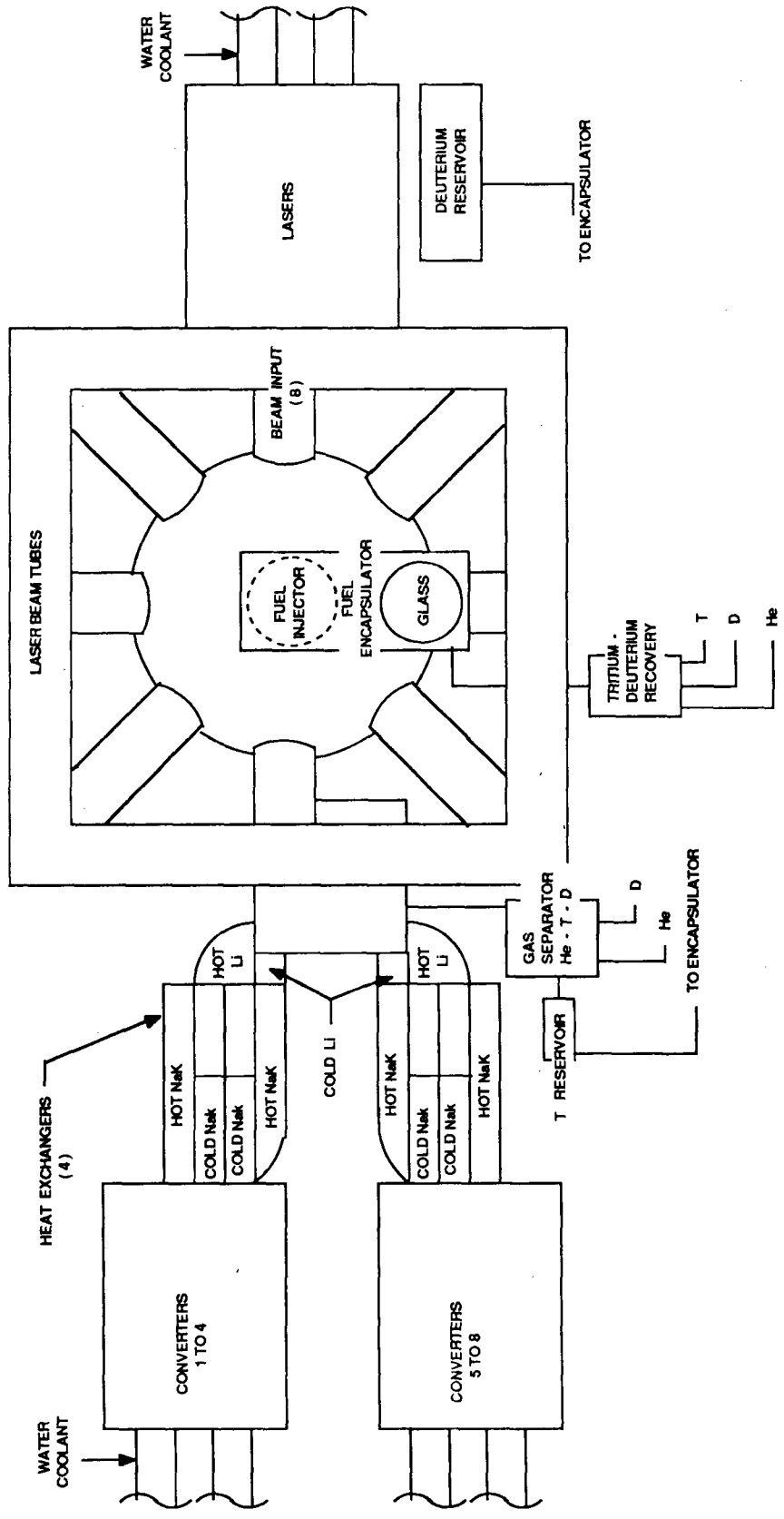


Figure A-10 Concept for the ATSS Fusion Power System, Side View

ORIGINAL PAGE IS
OF POOR QUALITY

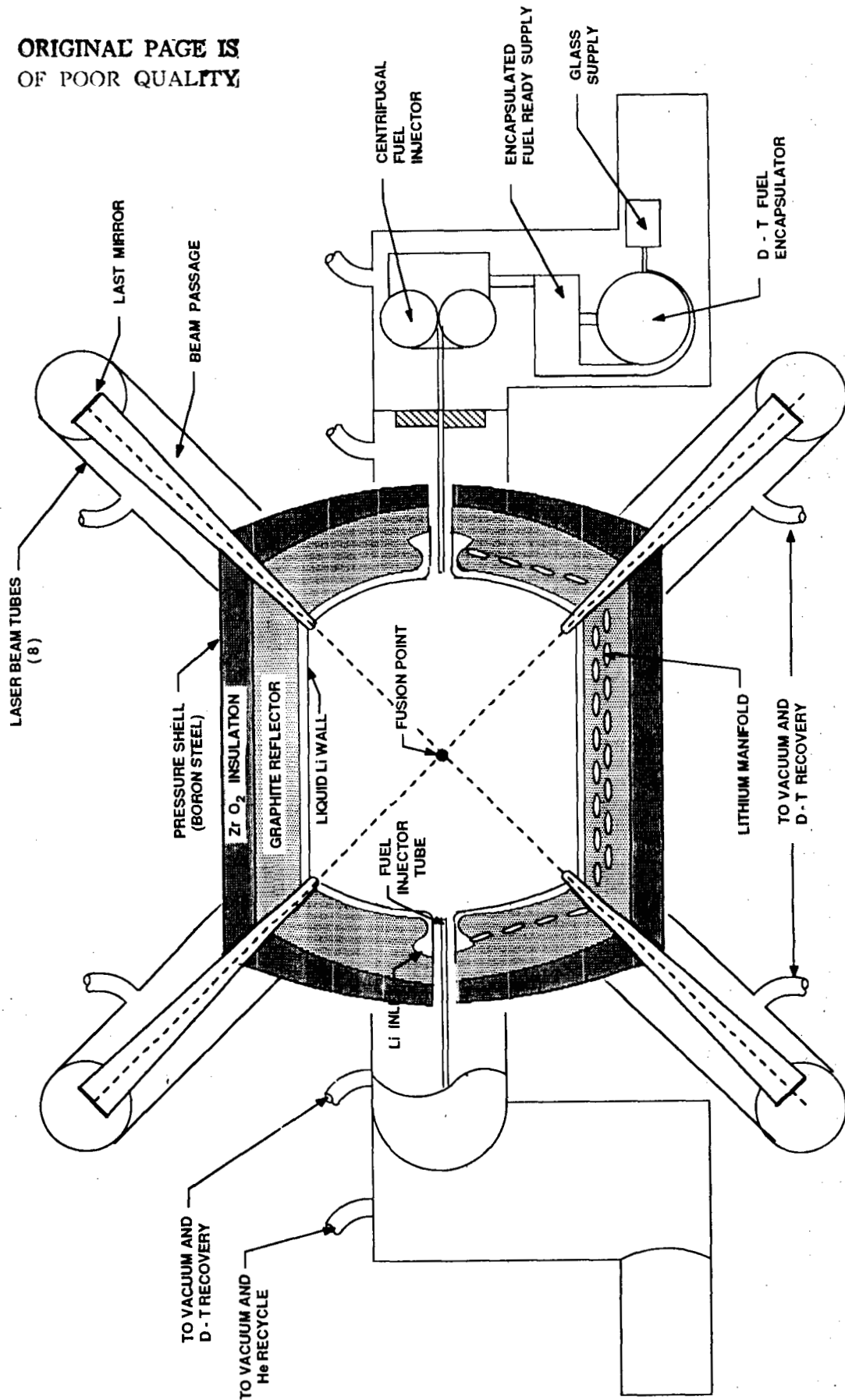


Figure A-11 Cross Section Through the Fusion Reactor Vessel

flowing lithium wall takes advantage of the microgravity environment available within the ATSS to create a continuously circulating layer as the receptor for the fusion energy.

The thickness of the layer, the velocities, and the flow rate have been balanced such that a 12-sec exposure increases the temperature of the lithium by 27 K (50°R) and absorbs 8520 kW in a mass flow of 73 kg/sec (161 lb/sec). The lithium flow enters the domed ends at the centerline and moves toward the cylindrical section in a combined radial and circumferential motion; auxiliary input jets maintain a uniform thickness. A divider at the dome-cylinder intersection recovers the flow for reinjection. The flow within the cylindrical section is shown in Figure A-12 and consists of circumferential channels that permit heat extraction from the graphite as the lithium flows to the injection port. Injection, extraction, and mixing occur at two diametrically opposed locations along the walls of the cylinders; Figure A-13 shows the concept for the injection-extraction and mixing segments of the wall. The flow balance for the system exposes the lithium for 3 sec in the ends (1.5 sec for each end) and 9 sec in the cylindrical section. The flow velocity around the cylindrical walls is 5.65 m/sec (18.5 ft/sec) to maintain a 5-cm (2-in) thickness of lithium. The inlet and outlet velocities within the feed and extraction lines are balanced accordingly. The entire flow balancing is achieved and controlled by electromagnetic pumps.

A.2.3.2 Fuel Encapsulation and Feed

A number of alternate configurations have been identified for fuel encapsulation; Figure A-14 illustrates some of the candidates. All of

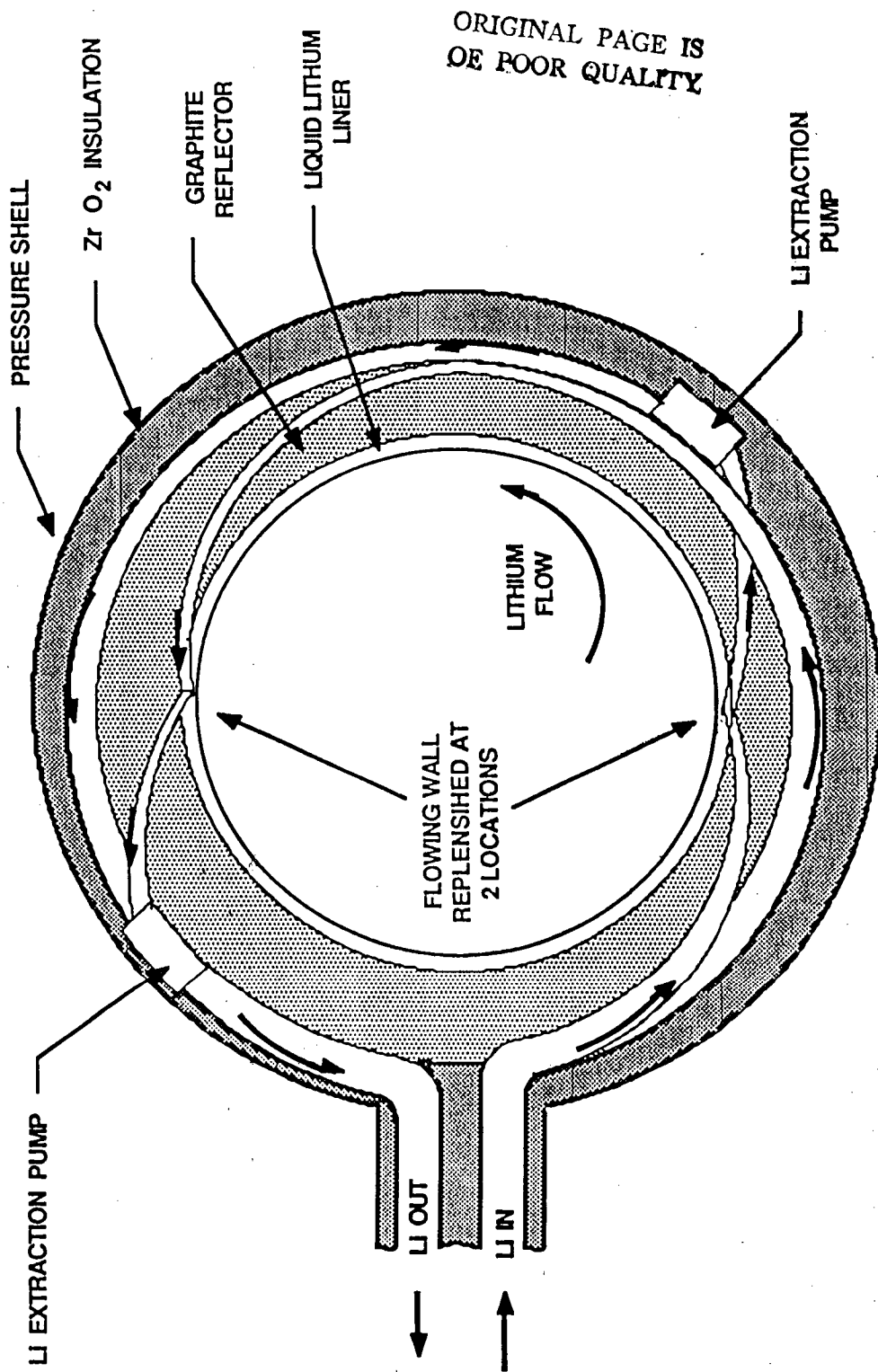


Figure A-12 Concept for Liquid Lithium Flow within the Reactor

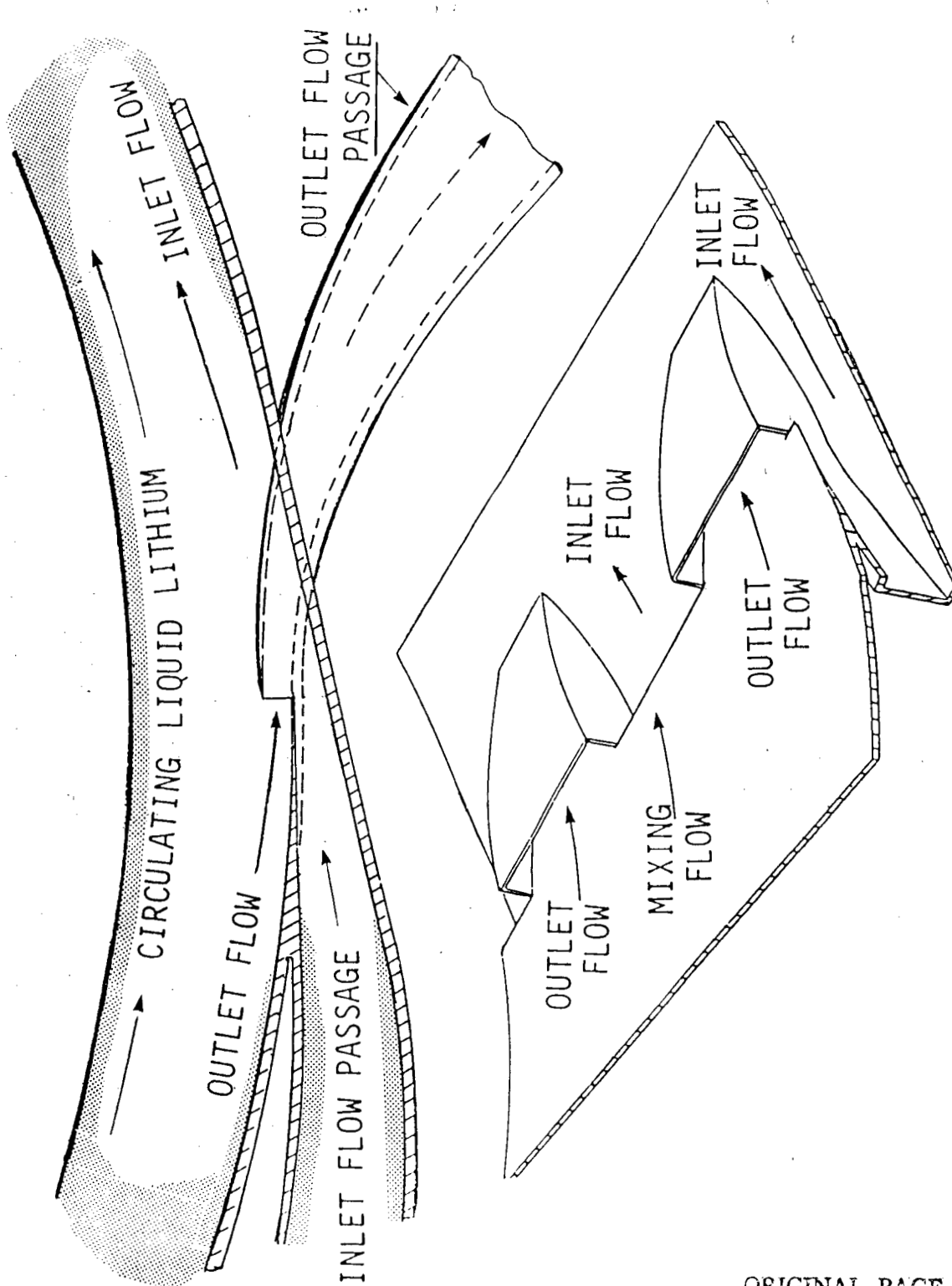


Figure A-13 Concept for Establishing a Flowing Liquid Lithium Wall within the Reactor Vessel

ORIGINAL PAGE IS
OF POOR QUALITY

ORIGINAL PAGE IS
OF POOR QUALITY.

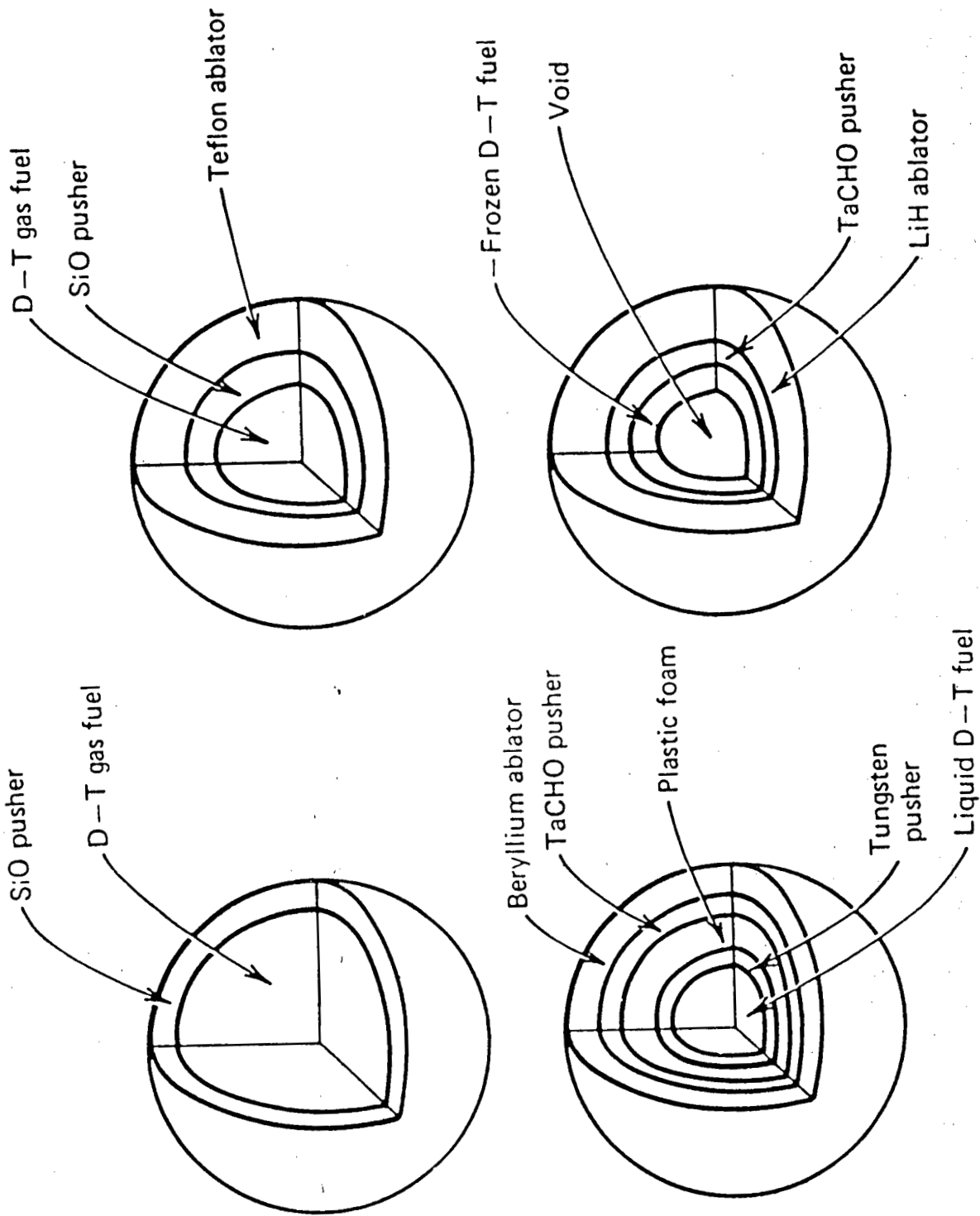


Figure A-14 Candidate Configurations for Encapsulated Fusion Fuel Pellets

the configurations utilize a pusher material that creates a compressing implosion when irradiated by a laser beam. This study uses the simplest of the fuel pellets and has a gas mixture at one atmosphere pressure enclosed in a silicon oxide sphere. The mass requirement for 2.67 μg in each pellet results in a 3-mm (0.12 in) diameter sphere with 0.05-mm (0.002 in) walls. These pellets will be injected along the centerline of the chamber at the rate of 10 per sec alternating from each end. The locations for the fuel feed are indicated in Figures A-9 and A-11, and conceptual injector elements are included in Figure A-11. The fuel pellets are formed by a glass blowing technique which provides a uniform sphere and a uniform gas content that will stabilize with one atmosphere internal pressure at ordinary temperatures. An inspection and storage magazine holds a one-hour supply (36000 pellets). Pellet injection at 100 m/sec (330 ft/sec) would involve about 20 msec of free flight and corresponds to a movement of 100 nm (1000 A) during the 1 nsec duration of the laser pulse. For a KrF laser operating at a wavelength of 220 nm (2200 A), the pellet moves only half a laser wavelength. Pellet delivery at 100 m/sec (330 ft/sec) utilizes the peripheral velocity for a wheel of 31-cm (12.2 in) diameter which runs at one-fourth of the converter frequency of 400 Hz. A pair of wheels driving a recirculating belt imparts a precise velocity and direction to a pellet when released at the point of tangency. Figure A-15 shows a schematic for such an injector configuration.

A.2.3.3 Laser Igniters

The ignition conditions for the deuterium-tritium reaction require temperatures in the order 10^8 K (1.8×10^8 °R) and concentration-time

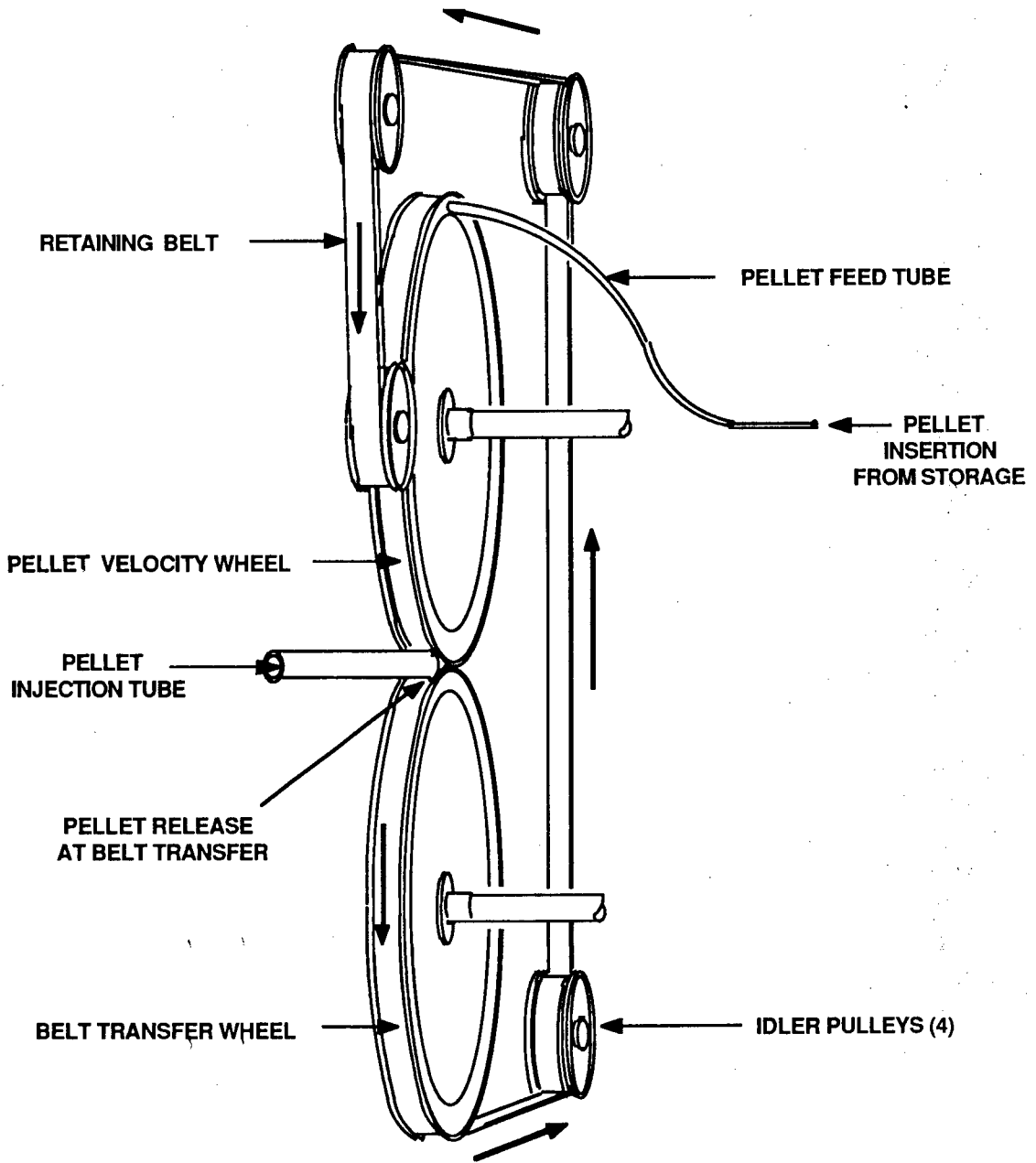
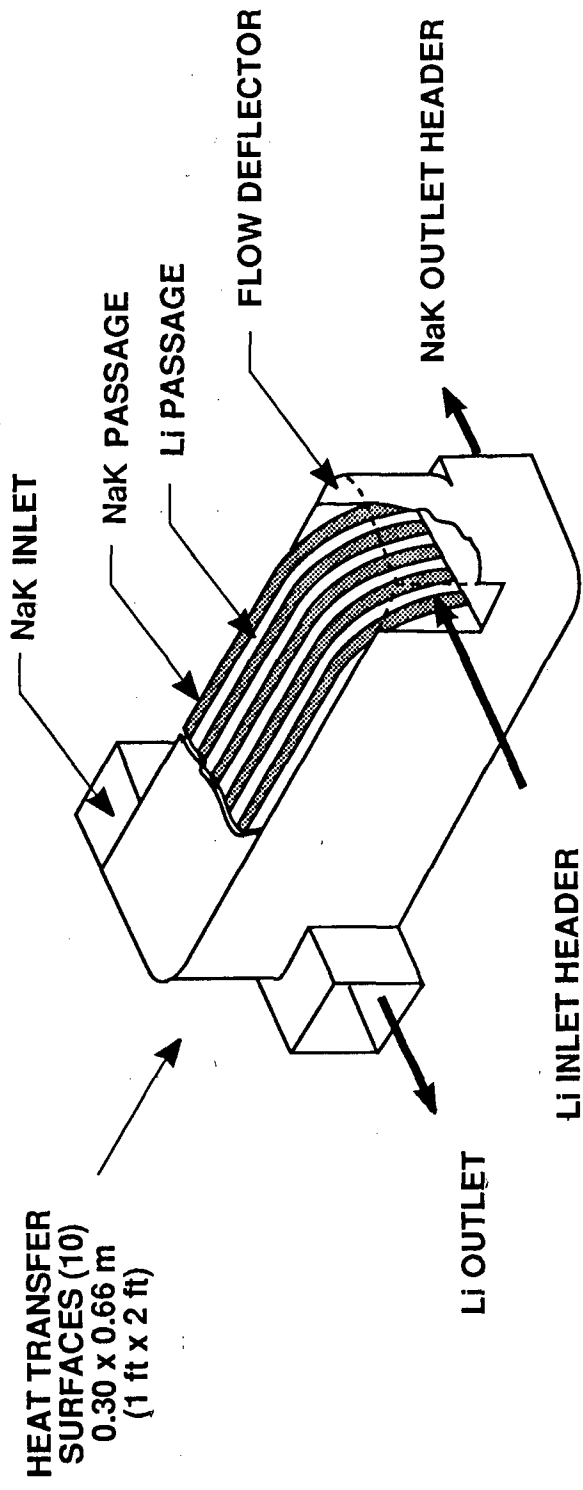


Figure A-15 Concept for a Rotating Wheel Fuel Pellet Injector

products of about 10^{20} nuclei sec/m^3 (2.8×10^{18} nuclei sec/ft^3) (Reference A-8). At standard conditions, gases contain 2.7×10^{25} molecules/ m^3 ($7.6 \times 10^{23}/\text{ft}^3$). The pusher portion of the encapsulant provides the auxiliary compression necessary to achieve ignition by a laser pulse lasting 10^{-9} sec. The system configuration summarized by Figures A-9, A-10, and A-11 includes an excimer laser beam as eight simultaneous pulses delivered four to each hemisphere 90 deg apart. Each laser operates in conjunction with one of the pellet injectors to provide dual injection and dual ignition. The laser installation involves the pulse generating elements as the pump, lasing section, and control. The lasers feed into the optical section which contains the beam splitters, formers, and final mirrors that deliver the energy to the pellet. The optical paths are complex. Each laser pulse must be divided into eight equal energy portions, and each portion of the beam has to reach the pellet through identical (equal transit time) optical paths.

A.2.3.4 Liquid Metal Heat Transfer

The liquid lithium absorbs the energy generated by the fusion reaction and delivers that energy to a series of heat exchangers which transfer the thermal energy into a NaK stream to power the electrical converters; Figure A-16 shows a concept for the heat exchanger. Fusion power systems utilize a significant amount of power internally. This fusion system has been configured with eight converters, operating at a nominal 425 kW each. Six converters provide the 2550 kW to the ATSS, and the other two provide the internal operating power. One converter unit is devoted to the laser system. The converter installations are at a central location within the ATSS as is the case for the Pu^{238} heat



HEAT TRANSFER SURFACES (10)
 0.30 x 0.66 m
 (1 ft x 2 ft)

WALLS ARE 3-mm
 (0.125 in) thick

STRUCTURE IS 79 Ni, 13 Cr, 7 Fe

Figure A-16 Features of a Liquid Lithium to NaK Heat Exchanger

source. Since this fusion system depends upon a microgravity environment to permit a flowing wall of liquid metal, the radiators for the converters are located around the periphery of the platform. The eight converters effectively double the platform-mounted radiator panel requirements as compared with four platform-mounted converters used in the solar dynamic system (Reference A-1). In addition, most of the energy that drives the laser transfers into coolant and establishes the need for an additional converter-equivalent radiator for a total of nine. Thus, the radiator panel inventory consists of 918 units (Figure A-7), mounted in four full rows and one partial row around the periphery of the platform.

When the liquid lithium leaves the reactor vessel, it has some entrained gasses and residuals from the encapsulant; an on-line separation process is included. At 1130 K (2034^oR), any residual silicon oxides are in a viscous molten state, whereas silicon itself is a solid. A centrifugal separator allows the gasses to escape and precipitates silicon and silicon oxides. The output legs of the liquid lithium lines include centrifugal separators.

A.2.3.5 Scavenge and Recovery, Vacuum Control, and Separation of Gasses

The atmosphere inside the reaction chamber uses 53.5 $\mu\text{g}/\text{sec}$ of deuterium-tritium gas which is released and partially converted to helium. The 53.5 μg equates to a pressure below 10^{-5} torr after the energy has been transferred into the lithium. A vacuum pumping system that maintains 10^{-5} torr is included and works from ports in the laser beam tubes and fuel injector sections. Separation of gaseous constituents has to consider D^2 , T^3 , He^3 , He^4 , Li^6 , Li^7 and O_2 as inputs.

The output must segregate and retain D^2 , T^3 , and He^4 . Separation of the helium from the deuterium and tritium may be accomplished by membrane diffusion. Separation of deuterium and tritium from other constituents may also be accomplished by membrane diffusion. In such an operation, the recovered deuterium-tritium mix can be brought to isotope balance with make-up deuterium and then cycled through the encapsulation process. Helium of mass number 3 appears as the radioactive decay product of tritium. The rate of buildup reflects the 12-year half life for tritium. Membrane diffusion during storage will keep the He^3 at an acceptable low level concentration in the deuterium-tritium mixture. Over a period of time, precipitations of silicon and silicon oxides build up in the separators. The operating system includes a number of parallel separator legs which can be individually shut down and refurbished. The recovered silicon oxides may be recycled.

A.2.4 Mass Assessments for the Fusion System

The assessment of masses for the principal elements which comprise the fusion power system are summarized in Table A-9. The assumptions and considerations for estimating the masses are described below.

A.2.4.1 Reactor and Containment Section

The mass for the reactor and containment elements include the lithium wall, the graphite reflector with cladding and ducting, an insulation layer, and the containment vessel itself. The liquid lithium provides a 5-cm (2.0-in) thick layer on the inside of a cylinder 1.93 m (6.33 ft) in diameter and 1.93 m (6.33 ft) long, and fills the cooling ducts that penetrates the reflector. At an operating temperature of 1130 K

TABLE A-9 SUMMARY MASS ESTIMATES FOR INERTIALLY CONFINED LASER-IGNITED FUSION HEAT SOURCE

SYSTEM ELEMENTS	MASS ESTIMATES, kg (lb)	PERCENT CONTRIBUTION
A. Reactor Section	41400 (91287)	10
• Container, Reflector, Lithium	23000 (50715)	
• Insulation (ZrO ₂)	18400 (40572)	
B. Fuel Feed and Encapsulation	7940 (17507)	2
• Mechanisms and Containment	3380 (7453)	
• Insulation (ZrO ₂)	4560 (10054)	
C. Laser-Ignition	35100 (77395)	8
• Two Lasers at 0.5 kg/W (1.1 lb/W) ea	28000 (61740)	
• Optical Path and Containers	7100 (15655)	
D. Reactor Pressure Control and Gas Separation	2440 (5380)	0.5
• Vacuum Pumps, Separators	1500 (3307)	
• Containment	940 (2073)	
E. External Heat Transfer	50030 (110316)	12
• Ducting and Liquid Metal Pumps	7665 (16900)	
• Heat Exchangers and Liquid Metal	2185 (4817)	
• Insulation Blanket (ZrO ₂)	40180 (88597)	
F. Converters, eight at 3836 kg (8458 lb) ea.	30690 (67671)	7.5
G. Radiators (nine units)	245300 (540886)	60
System Total	412900 (910442)	

(2034^{OR}), lithium has a density of 430 kg/m³ (26.9 lb/ft³) and the total contained lithium amounts to 551 kg (1215 lb). The graphite reflector has a nominal thickness of 0.343 m (13.5 in) and utilizes cladding and ducting based upon a 79Ni-13Cr-7Fe alloy. The pressure vessel has wall thicknesses of 1 cm (0.4 in) to provide boron for stray neutron absorption. The structural requirement for a vacuum shell could be achieved with a 2-mm (0.08 in) thickness. The insulation layer of 50-percent density ZrO₂ has a nominal thickness of 0.2 m (8 in) and provides the necessary thermal buffer between the graphite reflector and the walls of the chamber.

A.2.4.2 Fuel Feed Encapsulation

The fuel feed and encapsulation section consist of the glass blower encapsulator, the storage unit, and the injectors. Each segment is equivalent to a small electrically driven machine tool, and the six units total 860 kg (1896 lb). The mass for the encapsulating system includes the gas supply tanks. They would contain a 90-day supply stored at 10 atmospheres and contribute 440 kg (970 lb) of steel. The remainder of the mass consists of the 1 cm (0.4 in) thick boron steel vacuum container walls lined with 20 cm (7.9 in) of ZrO₂ insulation.

A.2.4.3 Laser Units

The present commercially available excimer lasers are pumped by an electron beam and have specific masses of 5 kg/W (11 lb/W) for power delivered to a target (pulse energy times repetition rate, Reference A-9). An order-of-magnitude reduction in specific mass for excimer lasers appears to be a reasonable extrapolation by the year 2025. Each

of the optical paths includes three beam splitters and turning mirrors (or prisms) and includes eight "last mirrors" which place the beam on the fuel pellet. The entire optical path and optical elements must be contained in a vacuum pressure enclosure fabricated from boron steel.

A.2.4.4 Scavenge and Separation

The scavenge and separation system consists of vacuum pumps which maintain the chamber pressure level and the separating mechanisms for recovering the individual gas constituents. The technique for separating gases will include semipermeable membranes and electromagnetic stages. The containment portion is the extraction manifold that connects to the vacuum pumps.

A.2.4.5 Heat Transfer Section

These ducts are external to the reactor vessel and use 15-cm (6 in) diameter tubes with 6-mm (0.24 in) walls of 79 Ni-13Cr-7Fe. The ducting includes the centrifugal separator stages in the output lines. The liquid metal pumps are all electromagnetic, 64 small units within the reactor vessel control local velocities, and these are fed from eight main lithium flow pumps to the heat exchangers. The converter flows utilize eight NaK pumps. The heat exchangers would have the same size and mass as used for the fission reactor (Reference A-1). The difference between sodium and lithium is accommodated by adjustments in the spacing of the flow passages. The volumes of the liquid metal account for the lengths of leads and contents of the heat exchangers and include about 0.75 m^3 (26.5 ft^3) of lithium and 1.25 m^3 (44.14 ft^3) of NaK external to the reactor vessel. Since the entire heat transfer section must operate

at "full red" to "orange" temperatures, a 15-cm (6 in) thick layer of ZrO_2 insulation encases the leads, pumps, and heat exchangers.

A.2.4.6 Converters and Radiators

The masses for the converters and the radiators are the same as estimated for the other systems. The principal difference is in the number of units with eight converters to supply the total electrical needs and nine radiator units required for heat rejection.

In summarizing the masses and their effects on the total system mass, the radiators make the largest contribution. Insulation that contains the high temperature components total about 72000 kg (1.58×10^5 lb) (each converter contains about 1000 kg (2205 lb) of ZrO_2) and makes the second largest contribution at 17 percent of the total. The materials which actively provide the fusion, transfer the heat, and generate the electricity contribute less than 25 percent of the total mass. If the mass required for thermal insulation and radiators can be reduced, then a fusion power system becomes a mass-effective alternate.

A.2.5 Fusion System Control Requirements

Fusion power system controls must maintain a continuous balance of flows and thermal inputs while precisely timing laser pulses to positions in the trajectory of a fuel pellet. The control requirements for the fusion power portion of the system are summarized in Table A-10. The converter control requirements are the same as those summarized in Table A-6 and are the same for each of the eight converters and nine radiators. An estimate of the relative complexity for fusion power system controls comes from comparison studies with ground power stations. A conventional

TABLE A-10 FUSION POWER SYSTEM CONTROL REQUIREMENTS

CONTROL ELEMENT OR FUNCTION	OUTPUT OR ACTION	RANGE	PRECISION	FREQUENCY
Fusion Operating Algorithm				
Pellet injection initiate timing	Fuel pellet enters injector timing and release	0 to 10 μ sec	0.1 μ sec	10 per sec each unit
Pellet velocity monitor and pellet trajectory error monitor	Laser system input to enable "laser fire"	90 to 110 m/sec (295 to 360 ft/sec) 0 to 0.5 cm (0 to 0.2 in)	0.01 cm/sec (0.004 in/sec) 0.005 cm (0.022 in)	10 per sec each unit
Pellet injected signal timing	Time references to laser fire	Time interval 0 to 1 ms	\pm 2 nsec	10 per sec each unit
Laser fire, timing	Laser energy release	0 to 1 μ sec	\pm 2 nsec	10 per sec each unit
Lithium layer thickness and velocity (multiple for each end and cylinder)	Lithium flow enable for "pellet inject" and "laser fire". Input to lithium pump control	0 to 6 cm (0 to 2.4 in) thickness 0 to 10 m/sec (0 to 33 ft/sec) velocity	\pm 0.2 cm (0.08 in) \pm 1 cm/sec (0.4 in/sec)	Steady Steady
Lithium temperatures (multiple) at inlet, outlets, and profiles	Inputs to lithium pump control	300 K to 1300 K (500 $^{\circ}$ R to 2340 $^{\circ}$ R)	2 K (3 $^{\circ}$ R)	Steady
Lithium pump control (multiple) as balance pumps and main flow pumps	Magnetic field current and drive current	0 to 1100 A	2 A	Steady

TABLE A-10 FUSION POWER SYSTEM CONTROL REQUIREMENTS (cont'd)

CONTROL ELEMENT OR FUNCTION	OUTPUT OR ACTION	RANGE	PRECISION	FREQUENCY
Fuel Preparation Sequence Algorithm				
Gas reservoirs pressures and temperatures (multiple for deuterium, tritium, helium, and deuterium-tritium mixtures)	Input signals to encapsulator gas metering valves. Input to environmental control	0.5 to 10 atm 300 to 700 K (500 to 1200°R)	± 0.01 atm 2 K (3°R)	Steady
Encapsulant supply reservoir status, and temperature	Input to control valves. Input to environmental control	0 to full 300 to 700 K (500 to 1260°R)	5 percent 2 K (3°R)	Steady
Encapsulation sequence timing as position, heat, fill, seal, cool	Valve operation Heater operation Mechanical motion	Open - close On - off Advances	2 percent position 0.01 cm (0.003 in)	10 per sec ea 10 per sec ea 10 per sec ea
	Pressure profile Temperature profile	0.2 to 5 atm 300 to 1000 K (500 to 1800°R)	0.01 atm 2 K (3°R)	10 per sec ea 10 per sec ea
	Time intervals	As needed in millisecc to sec	As needed microsec	10 per sec ea

TABLE A-10 FUSION POWER SYSTEM CONTROL REQUIREMENTS (cont'd)

CONTROL ELEMENT OR FUNCTION	OUTPUT OR ACTION	RANGE	PRECISION	FREQUENCY
Fuel Preparation Sequence Algorithm (cont'd)				
Pellet inspection parameters Pellet diameter, shape	Input to "accept reject" sequence	Diameter and concentricity 3 mm (0.12 in)	0.002 mm (0.0005 in)	10 per sec ea
Pellet leakage		Tritium decay product monitor	Electron leakage is rejection	10 per sec ea
Pellet storage status	Input to fusion control algorithm	0 to 4 x 10 ⁴	±10	Steady
Laser Operations				
Laser pumping power voltage, current	Input to "laser fire" enable	0 to 100 kV 0 to 10 A	±1 kV ±0.01 A	10 per sec ea
Lasing gas flow (Kr, F)	Input to "laser fire" enable	0 to 100 percent of required flow	1 percent of required flow	10 per sec ea
Laser coolant inlet flow rate and temperature	Input to "laser fire" enable	0 to 20 kg/sec (10 to 45 lb/sec) 270 to 370 K (450 to 572°R)	1 percent flow 2 K (3°R)	Steady

TABLE A-10 FUSION POWER SYSTEM CONTROL REQUIREMENTS (concl.)

CONTROL ELEMENT OR FUNCTION	OUTPUT OR ACTION	RANGE	PRECISION	FREQUENCY
Heat Transfer Control Algorithm				
Separator rotation speed	Input to fusion enable	0 to rated rpm	1 percent	Steady
Separator operating time	Input to change out sequence	0 to cycle limit	1 percent	Steady
Lithium flow valves position (NaK pumps and valves are part of converter controls)				
Separation-Recovery and Environmental Control				
Reactor pressure monitor	Input to fusion enable	10^{-5} to 10^{-3} torr	5 percent	Steady
Purge pump output pressure	Input to separator	10^{-5} torr to 1 atm	5 percent	Steady
Gas separator membrane stages; pressure, flow rate	Input to electromagnetic and pumps	0 to 1 atm 0 to 0.01 kg/sec (0 to 0.02 lb/sec)	5 percent 1 percent	Steady
Gas separator electromagnetic stages; current	Input to pumps	0 to 5 A	± 0.001 A	Steady
Gas storage, pumps, flow rate, pressure	Input to gas supply status	0 to 10 atm 0 to 0.01 kg/sec (0 to 0.02 lb/sec)	1 percent 1 percent	Steady
Stray neutron monitor (multiple)	Health monitor	0 to 10^5 /sec	1 percent	Steady
Tritium decay monitor (multiple)	Health monitor	0 to 10^5 /sec	1 percent	Steady
Container operating temperatures (multiple)	Input to fusion operation and coolant flow valves	270 to 500 K (400 to 900°R)	2 K (3°R)	Steady

1000 MW steam plant has a control system with about 5000 sensor inputs. In contrast, 50000 sensor inputs have been estimated for a 1000 MW power station using a magnetically confined plasma fusion technique (Reference A-8). The particular control complexities for an inertially confined laser ignited system are associated with the fusion ignition and the fuel preparations.

The extraction of heat energy from a fusion reaction begins with a near uniform irradiation of a 3-mm (0.12 in) diameter pellet by 8 laser beams. In the simplest of geometry, the laser beam diameter must be about 80 percent of the pellet diameter in order to have a full-sphere coverage with some overlap. On this basis, the tolerance on the trajectory appears as 10 percent of the pellet diameter or 0.03 cm (0.012 in). The generation of the laser pulse has to anticipate the arrival of the pellet at the point of fusion in a manner that allows all the energy to hit the pellet. The control requirements for fusion initiation need to assure that the pellet is moving along a trajectory path that allows uniform irradiation and that the laser pulse will hit the pellet when it reaches the fusion ignition point. These controls must operate with a firing decision for each pellet initiated precisely at the cyclic rate for the fusion pulses. The system can tolerate some lost pellets; however, the energy drain associated with a laser pulse requires a power return for each laser firing.

The energy release from the fusions has to be captured and transformed into a continuous flowing thermal stream. The establishment of a flowing wall of liquid metal implies a precise balancing of input flow velocities and exit flow velocities that accommodate the viscous forces, assure the proper mixing, and adjust for the temperature changes.

The internal lithium flow system involves the continuous balancing of field strengths and driver currents in 64 electromagnetic liquid metal pumps.

The preparation of the fuel pellets imposes both a technical and control challenge. Controls include the requirements for a high speed glass blower in which the internal and external pressures have to balance during the blow and cool operation such that the gas content of the sphere contains the proper mix at one atmosphere pressure and ordinary temperatures. An inspection process is needed to assure that each pellet is a uniform sphere and is not leaking. The storage requirement for a one-hour reserve is modest and allows a degree of change-out and replenishment.

The external heat transfer system has the added complexity of gas-and-solids separators in the high temperature lines. These require periodic change-out of elements to remove the precipitated encapsulant.

The environmental control has to maintain operation within a narrow range of temperatures and pressures. The unburned fuel has to be recovered and separated. Crew exposure to neutrons is a recognized health related concern. Tritium is radioactive by electron emission (beta particles), and the health concern is inhalation. The tritium must be totally contained.

A.2.6 Particular Considerations for a Fusion Power System

The particular considerations stem from the development requirements for the flow system, the constraints associated with continuous operation, and the accommodation of low level radiation from neutrons and tritium decay.

The concept of a flowing wall of liquid lithium was adapted from a ground fusion power station concept that used a falling wall of liquid lithium. The concept for the space power application takes advantage of operation in a microgravity environment to keep a flowing wall in contact with a neutron moderator and reflector. An effort to develop such a configuration requires access to a laboratory in a microgravity environment. For the ATSS, the application of a fusion power system appears as a growth condition in which the final stages of the flow development are performed on board. The concepts and conditions for flow balancing could be initially established using NaK at ordinary temperatures before switching to high temperature lithium. The incorporation of fusion power into the ATSS may culminate a development effort involving both ground and on-board activities such that the prototype unit becomes the power source which phases out an operating solar dynamic or photovoltaic system. A fusion system must have support from an on-board power system to liquify lithium, start the flow, and drive the laser.

A fusion power system operates continuously over a narrow range of output power. The details of the configuration must include the potential for change-out and repairs without interrupting power deliveries. A fusion power system has a complex start up sequence and a complex shut down sequence. Recovery of the encapsulant and separation of gases are done off line, and off line encapsulation capabilities are considered prudent to assure a fuel reserve. The incorporation of dual feeds and lasers provides redundancy. Near-full operation can be maintained with one injector-laser operating at a higher pulse rate. If the fusion power system is a growth version of the ATSS, then some

portion of the earlier power generating technique could be retained as a reserve or back up supply.

The radiation concerns appear modest. Ideally, the primary and secondary neutrons released are absorbed in the lithium to produce tritium. In reality, some neutrons will be lost and absorbed in graphite, zirconium, and the borated steel. The health-acceptable total neutron release from the reactor is approximately 1.5×10^6 per second (Reference A-7), and neutrons are born and used at the rate of 2.86×10^{15} per second. The reactor needs to operate with a very small excess of neutrons and have an effective absorber outside of the graphite reflector. Boron and cadmium provide the best readily available materials for neutron absorbing shields. Boron steel is proposed, with a cadmium compound added to the exterior if required. The metallic cladding elements within the reactor will absorb some of the excess neutrons and form radioactive nuclei with long half-lives. Nickel has an isotope of mass number 59, which has the longest half-life ($\sim 10^5$ years); therefore, at final shutdown, the system must be considered low level radioactive waste. The tritium produced on board is consumed on board. The decay product is an electron which can be contained within any tank or pipe. The system operates in a vacuum; therefore, tritium does not have any mechanism to enter the man-rated atmosphere.

A.3 ADVANCED PHOTOVOLTAIC ENERGY SOURCES

A.3.1 Photovoltaic System Considerations

Electrical energy produced by a photovoltaic effect has the advantage of conversion into direct current power at conditions compatible with ATSS on-board equipment. Both photovoltaic and solar

dynamic systems must store energy during the illuminated portion of the orbit. Energy storage for a photovoltaic system can use electrochemical means such as storage batteries or fuel cells, and flywheels offer an electromechanical option. The design of a photovoltaic system for a given power output must consider the conversion efficiency which is a property of the material, and the degradation of the conversion efficiency which occurs from long-term exposure to space radiation. The conversion efficiency of silicon-based photovoltaics has a limit at about 18 percent, gallium arsenide has a limit above 20 percent, and cells of the "multiple band-gap" type have the potential for a 30-percent conversion efficiency (Reference A-4). The development of photovoltaic cells has also included techniques for reducing radiation damage sensitivities and means for rejuvenating degraded cells in place (Reference A-4). Gallium arsenide or the "multiple band-gap" technology appears capable of providing the ATSS with photovoltaic cells which would sustain a 20-percent solar throughput energy conversion over a ten-year period. Therefore, a photovoltaic system based upon a 0.2 energy throughput efficiency is used as the basis for comparison with thermal dynamic heat source alternates operating with energy throughput efficiencies of 40 percent. For comparison purposes, a configuration is defined with a solar field which can provide 2550 kW continuous electrical power throughout a 90-min orbit. During the 60 min of illumination, the system will store enough energy to maintain the 2550 kW for the 30 min of darkness. Three energy storage methods are considered; batteries, advanced O₂-H₂ fuel cells, and flywheels. In addition, an evaluation is made of solar energy concentration as a means for reducing the requirements for photovoltaic cells.

A.3.2 Solar Array Areas and Solar Panel Requirements

The ATSS provides solar facing areas on the platform and on the torus that are considered appropriate for the installation of photovoltaic panels. Thermal equilibrium considerations make that determination. Within an array, some of the unconverted energy is reflected backward from the absorbing surface. The remainder must be removed by cooling coils, direct radiation, or both in combination. Photovoltaics, therefore, favor installations which enhance dark-side radiation. For the ATSS the prime areas for solar panels are those open to dark-side radiation and thereby avoiding any need for cooling coils. The solar facing areas of the ATSS available for photovoltaic arrays are indicated in Figure A-17 and summarized in Table A-11 with the prime areas and second choice areas identified. The requirement for 2550 kW continuous at a 20-percent conversion efficiency defines a minimum area for solar exposure, and the results summarized on Table A-11 show that the power requirements can be supplied using about half the available prime area. For comparison purposes, the advanced photovoltaic system utilizes the prime areas and operates in thermal equilibrium with a dark side temperature of 320 K (576°R). These thermal balance conditions assume 37 percent of the solar energy is radiated from the backside of the panel, 37 percent is re-radiated (or reflected) from the front surface, and 26 percent is converted to electricity, with 20 percent of the incident energy appearing as usable electrical power within the ATSS. The 0.5 h of darkness during each orbit requires an energy delivery from a storage system that totals 1275 kW-h. The energy losses associated with storing and retrieving add to the total storage requirement and increase the

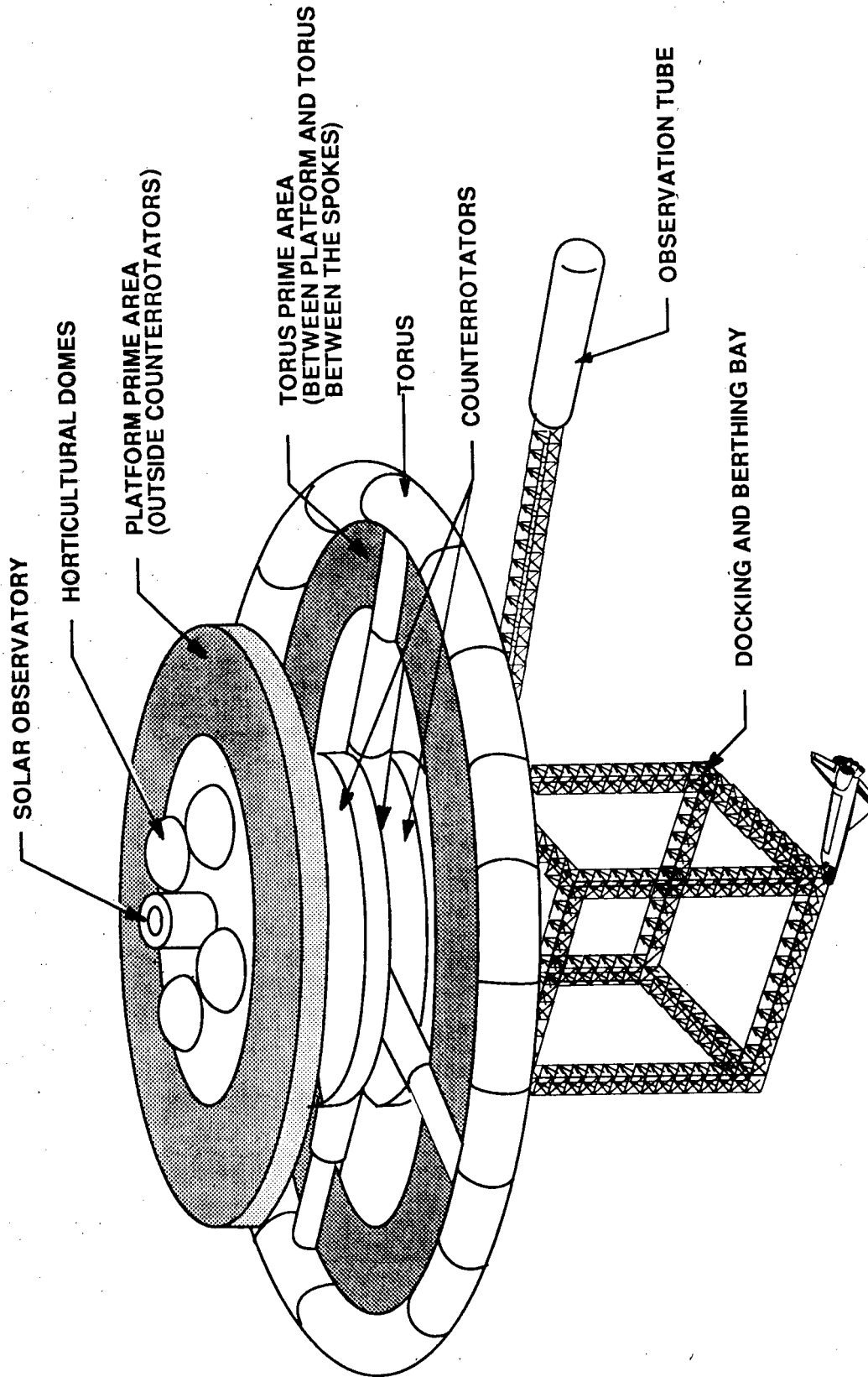


Figure A-17 ATSS Prime Areas for Locating Photovoltaic Panels

TABLE A-11 ATSS LOCATIONS AND AREAS AVAILABLE FOR PHOTOVOLTAIC PANEL INSTALLATIONS

	m ² (ft ²)
Platform: Total	17583 (189263)
Counterrotators to rim (prime)	13163 (141686)
Domes to counterrotator (second)	860 (9257)
Central tube to domes (second)	3560 (38320)
Torus: Total	26968 (290283)
Platform to rim torus inner diameter (prime)	15020 (161675)
On spokes open to solar (second)	1003 (10796)
On torus ring (second)	10945 (117812)
Total Prime	28183 (303362)
Total Second	16368 (176185)
Total Space Station	44551 (479546)
Area required for 2550 kW continuous at 0.2 Solar energy throughput	14310* (154032)

*Includes energy storage requirement for 1275 kW-h

total solar panel area. Therefore, configuring a photovoltaic power system requires the selection of an energy storage technique.

A.3.3 Energy Storage Considerations

The continuing development of energy storage techniques has produced a number of candidates for application to the ATSS. The electrochemical candidates are rechargeable (secondary) batteries or fuel cells. The electromechanical option is the flywheel.

The electrochemical options are three battery types and H_2-O_2 fuel cells. Comparison parameters and results are summarized in Table A-12. The battery types include the space-performance established Ni-Cd, the Space Station Freedom candidate Ni- H_2 , and an advanced Li-Na liquid sulphur system. None of these batteries have operated for ten years with an 80-percent discharge cycled at orbital frequencies. However, within each of their present development efforts, these appear to be one of the goals. The values listed as specific outputs are the near-maximum for applications that have good temperature control. The value cited for the Li-Na-S system is based upon projections from an extended development effort; however, some projections show only half this value (References A-2 and A-11). All the battery options are assumed to operate above 90-percent efficiency during the charge and discharge cycles. The on-board generation of H_2 and O_2 from the electrolysis of water limits fuel cells to a single candidate. The capability to use half the ATSS-delivered electrical power for fuel generation assures a ready fuel supply. The value cited for fuel cells assumes a continuing development to achieve the specific output and assigns an 85-percent efficiency for both the water electrolysis and cell operation (Reference A-12). The use of fuel

TABLE A-12 ATSS ELECTROCHEMICAL ENERGY STORAGE OPTIONS SUMMARY

CHEMICAL SYSTEM	Ni-Cd	Ni-H ₂	Li-Na LIQUID-SULPHUR	H ₂ -O ₂ FUEL CELLS
Specific output, W-h/kg (W-h/lb)	30 (13.6)	45 (20.4)	180 (81.6)	150 (W/kg) (68 W/lb)
Discharge depth (percent)	80	80	80	-
Efficiency	0.83	0.83	0.83	0.72
Energy required, kW-h	1536	1536	1536	1770.83
Required mass, kg (lb)	64006 (141433)	42670 (94087)	10667 (23520)	19600* (43218)
Energy loss kW-h	261	261	261	495.8
Extra area, m ² (ft ²)	967 (10408)	967 (10408)	967 (10408)	1836 (19762)
Radiator area, m ² (ft ²)	295 (3175)	295 (3175)	295 (3175)	559 (6017)
(number of panels)	(29)	(29)	(29)	(54)

* Includes four extra electrolytic cells to process 360 kg of water each orbit.

cells does expand the number of electrolysis units on board the ATSS to maintain the total deliverable H_2 and O_2 . In the comparisons, the specific mass of the batteries are modified by the discharge depth, and the energy storage requirement is increased to account for the efficiency. The increment of energy lost must be offset by an additional area of photovoltaics, and that lost energy must be dissipated by an array of radiator panels.

The electromechanical storage of energy compared flywheel configurations using high tensile strength steel, glass fiber reinforced composite, and an advanced graphite fiber reinforced composite. The materials parameters and the results of the evaluation are summarized in Table A-13. Figure A-18 shows the concept for a power storage unit that has a glass fiber reinforced composite flywheel. The steel evaluated is a 18Ni-400 precipitation hardened (maraging) alloy that shows the highest working stress for any present homogenous material. The flywheel is configured as a uniformly stressed disc (e.g., turbine discs) and at maximum energy storage, has all the metal at a uniform maximum stress which results in a specific energy shape factor of unity. The actual mass of material required depends upon the allowed change in rotation with a 50-percent speed reduction for a 75-percent energy extraction as the practical limit (Reference A-13). The total rotating mass must be configured in manageable elements; 10 units based upon wheels 3 m (10 ft) in diameter appeared practical. Since the electrical portion of all units are 255 kW motor-generators, the units are all configured within the same mounting and vacuum sphere. For this evaluation the electrical and internal support elements were assigned the same specific mass as used previously for the 440 V - 400 Hz alternators. The motor generator

TABLE A-13 ATSS FLYWHEEL ENERGY STORAGE, OPTIONS

(Deliver 1275 kW-hr at 0.9 energy throughput efficiency with rotation speed change of 50 percent)

PARAMETER	18 Ni-400 STEEL	S-1014 GLASS FIBER COMPOSITE	GRAPHITE FIBER COMPOSITE
Wheel Type, Shape Factor	Disc with uniform stress, 1.0	Rim of 0.8 mass with web, 0.4	Rim of 0.8 mass with web, 0.4
Density, kg/m ³ (lb/ft ²)	8000 (500)	1993 (124)	2000 (125)
Limit Stress MPa (psi)	1930 (280000)	600 (87000)	1930 (280000)
Specific Energy Storage, $\frac{N-m}{kg} \left(\frac{lb-ft}{lb} \right)$	241250 (348457)	133854 (217646)	386000 (598698)
Total Rotating Mass, kg (lb)	28186 (62150)	56513 (56515)	17640 (38896)
Configure as 10 Units With Rotors 3-m (9.84-ft) dia.	Hub thickness 15 cm (5.9 in)	Rim 026.4 cm (10.39 in) thick by 1 m (39.4 in) wide	Rim 16 cm (6.3 in) thick by 50 cm (19.7 in) wide
Maximum rpm	3008	3505	6255
Minimum rpm	1504	1753	3128
Mass Per Unit as Rotor, Motor/Generator and Vacuum Sphere, kg (lb)	4220 (9305)	7051 (15547)	3164 (7119)
Total Mass, kg (lb)	42200 (93051)	70510 (155474)	31640 (69766)
Extra Solar Panel Area, m ² (ft ²)	524 (5640)	524 (5640)	524 (5640)
Radiator Area, m ² (ft ²)	159 (1711)	159 (1711)	159 (1711)
Number of Radiator Panels	15	15	15

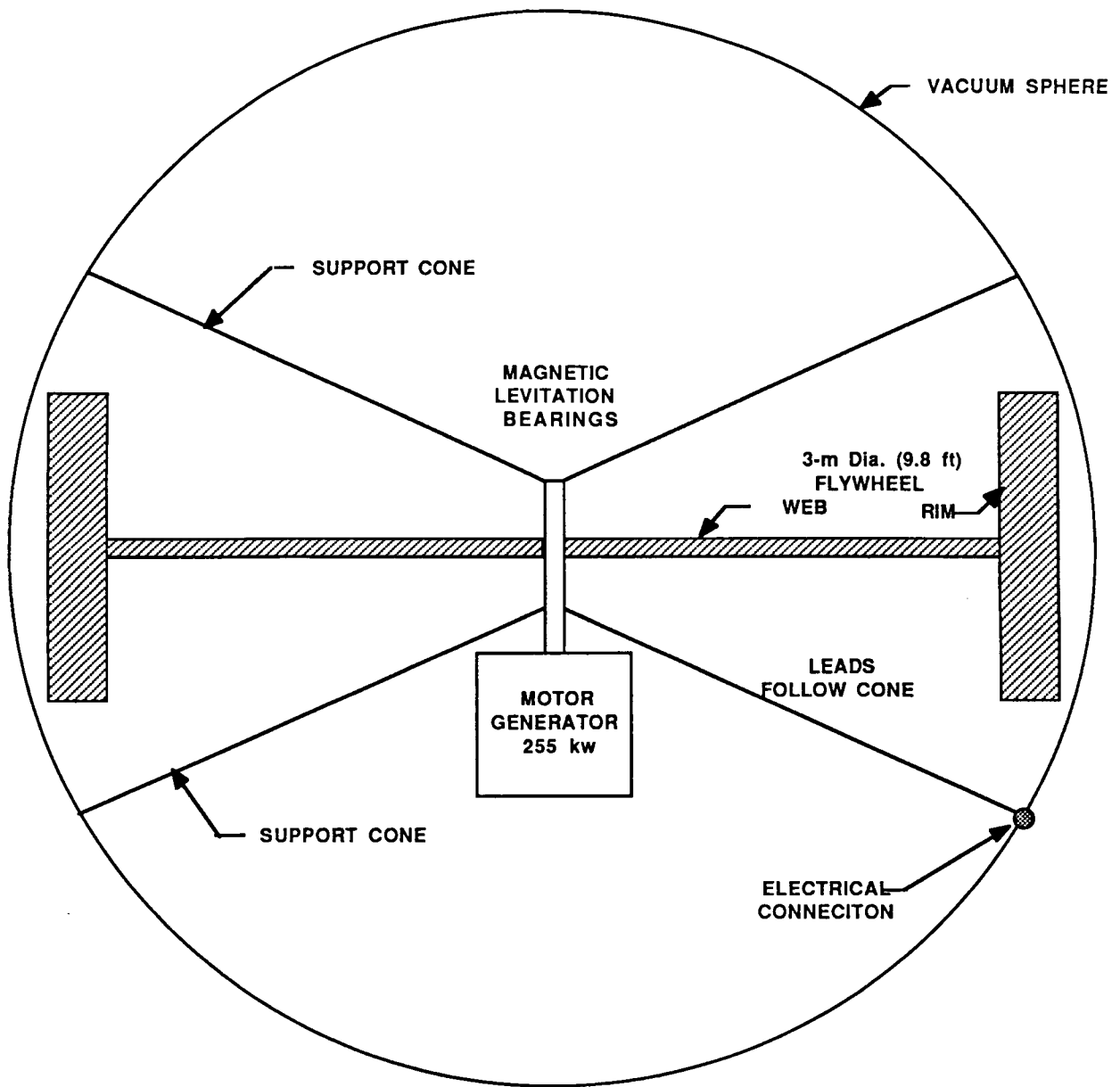


Figure A-18 Concept for an Energy Storage Unit Using a Glass Fiber Composite Flywheel

and support are mounted within a 3.2 m (12 ft) diameter aluminum sphere. The total mass amounts to 1400 kg (3090 lb) for each unit. The 0.9 electrical throughput efficiency assumes a minimum of frictional losses (rotation in vacuum) with magnetic levitation.

The two composite wheels utilize a practical configuration, as a rim with a web, that has $K_s = 0.4$ (Shape Factor, Figure 5.2-6). The glass fiber option represents present fabrication technology in which the maximum working stress for the composite is 0.4 of fiber yield stress. The advanced graphite fiber option uses graphite fibers with the same strength properties as the steel and an operating stress at 0.65 of fiber yield which is the same limit as steel.

A review of the tabulated results shows the limit of the present technology in Ni-Cd batteries and conservative-margin glass fiber composites. The options represented by steel flywheels and Ni-H₂ batteries show a general equality and could be considered near-term developments. The options for improved performance from longer term developments are Li-Na-S batteries, O₂-H₂ fuel cells, and advanced composite flywheels. These options show a near-equality for ATSS application. Graphite and aramid fibers have been developed with yield strengths above 2757 MPa (400,000 psi) (Reference A-14). Wheel shape factors can be improved toward the limit of 0.5 as a thin ring, and improved fabrication techniques will allow operation with less stress margin (0.8 yield instead of 0.65). Advances in fiber composite flywheels could result in a 50-percent reduction in required mass. For the Li-Na-S batteries, the projected specific output values have ranged from 90 to 200 W-h/kg and fuel cells in present use show specific outputs at or above 100 W/kg.

Of the three advanced technology options, none show a definitive mass advantage. Therefore, the ATSS will utilize the O₂-H₂ fuel cell option for synergy with the on-board generation of the fuel gasses and multiple usage of on-board water. The ATSS photovoltaic power system will consist of the following major elements.

1. Photovoltaic panels mounted in the prime location on the ATSS with area sufficient to produce 2550 kW continuous (14310 m², 154000 ft²) plus the extra area (1836 m², 19700 ft²) needed to compensate for storage losses.
2. O₂-H₂ fuel cells capable of delivering 2550 kW (17000 kg, 37485 lb) plus four electrolytic cells (2600 kg, 5733 lb).
3. Radiator for fuel and electrolyte cell cooling at 559 m² (6017 ft²) consisting of 54 panels.

A.3.4 Photovoltaic System Definition and Location

The principal feature for the photovoltaic system becomes the installation concept for the solar cells. The location for the fuel cells has no real restriction except that the electrolytic cells which generate the fuel and the storage reservoirs for the fuel are located in the torus. For convenience, therefore, radiator panels for the fuel cells are on the exterior of the torus, and the fuel cells are co-located with the electrolytic cells on the outer deck at spokes 2 and 4 (Reference A-3).

The installation for the solar cells assumes a mounting arrangement in the form of a 3-m by 4-m (9.8-ft by 13.1-ft) rectangle. The total installation requires a minimum of 1347 such panels. The inventory will consist of 1347 panels with 795 located on the prime area of the

platform and 552 mounted in the prime area between spokes on the insides of the torus. Electrically, the panels operate in groups of three. The resulting layout is shown for the platform in Figure A-19 and for the torus in Figure A-20. The panel arrangement on the platform is a regular array consisting of seven rows arranged as concentric rings. The rings all fit within the prime area defined by the perimeter of the platform and the outside diameter of the counterrotators (Figure A-17). The installation as groups of three makes the necessary electrical interconnection along the inner edge of the panels. Space between the groups provides the access for installation or replacement and will be accomplished by manipulators on an EVA support vehicle. The panel arrangement on the torus takes advantage of the rotating field to hang groups of three panels from a beam; Figure A-21 illustrates the concept for the support and shows some of the construction features. The hanger beam spans the distance between spokes and carries the electrical bus attached to the web. A stanchion tube that reaches from the hanger beam to the torus provides stabilization between each set of six panels. The installation of the panels and the electrical interconnections are performed from a teleoperated crane on the torus.

A.3.5. Summary of Mass Estimates

The system mass estimates include contributions from the panels, the panel support structure, the radiators, and the energy storage components; Table A-14 summarizes the mass contribution for each of the alternates.

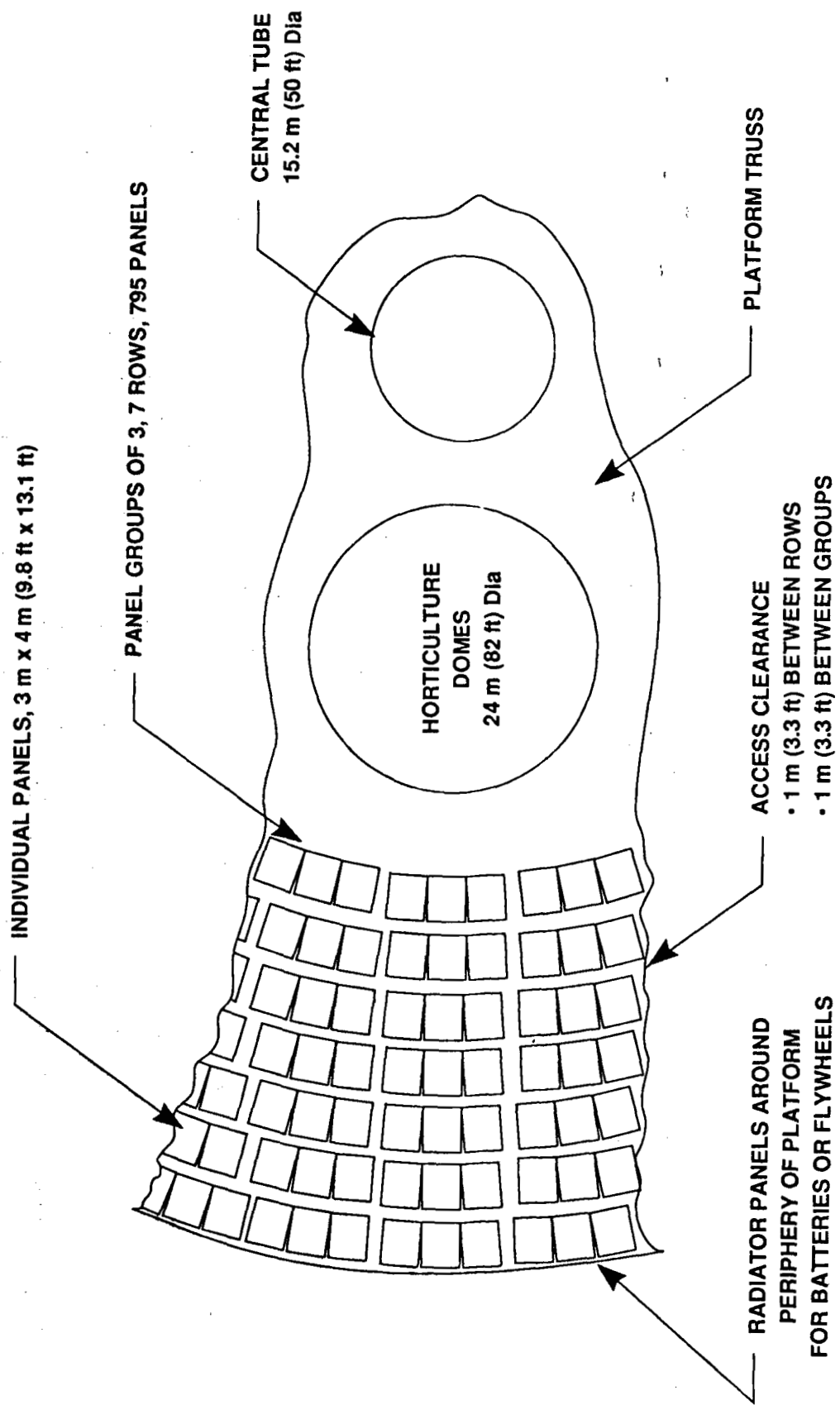


Figure A-19 Photovoltaic Panel Locations on the Platform

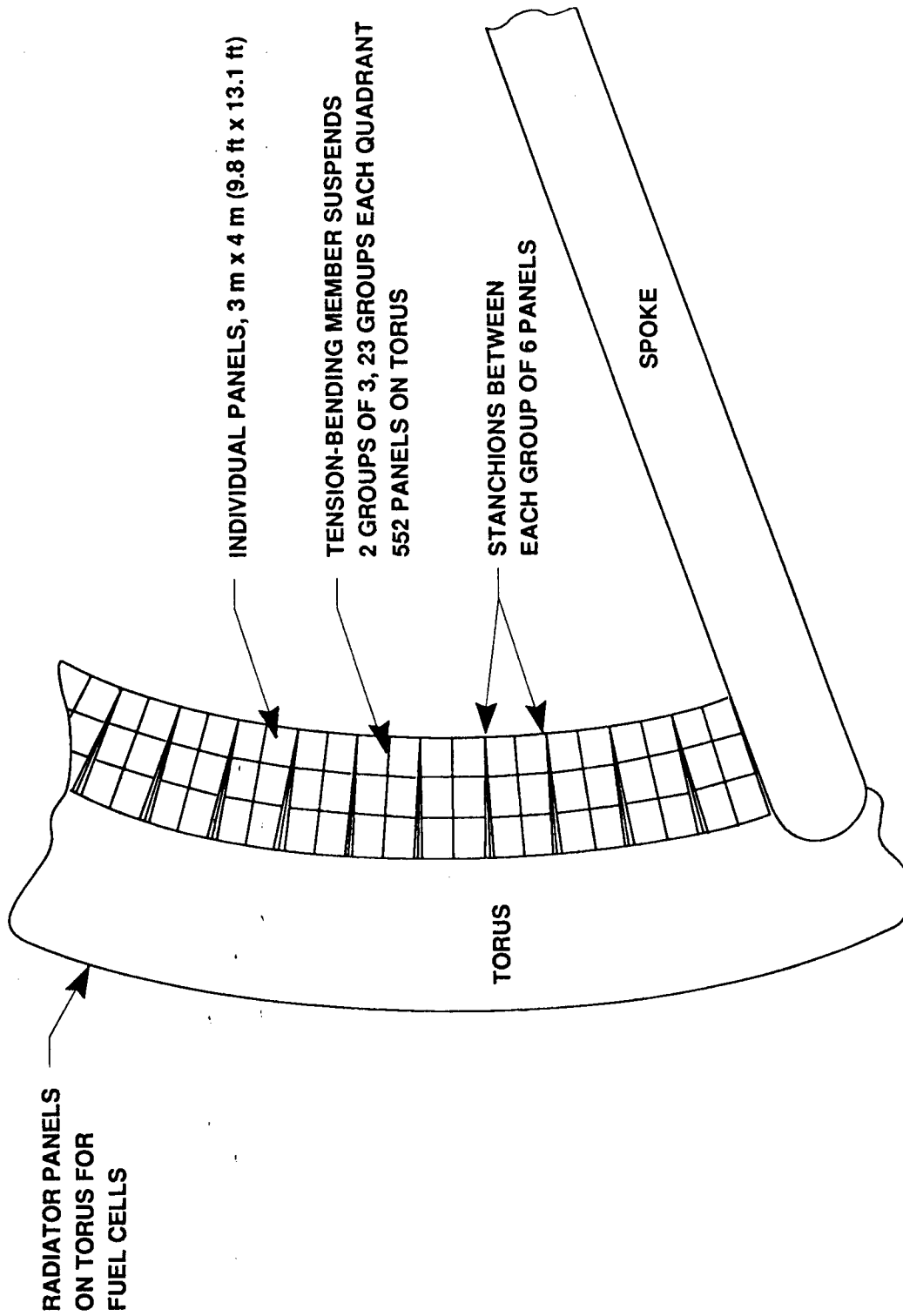


Figure A-20 Concept for Mounting Photovoltaic Panels on the Torus

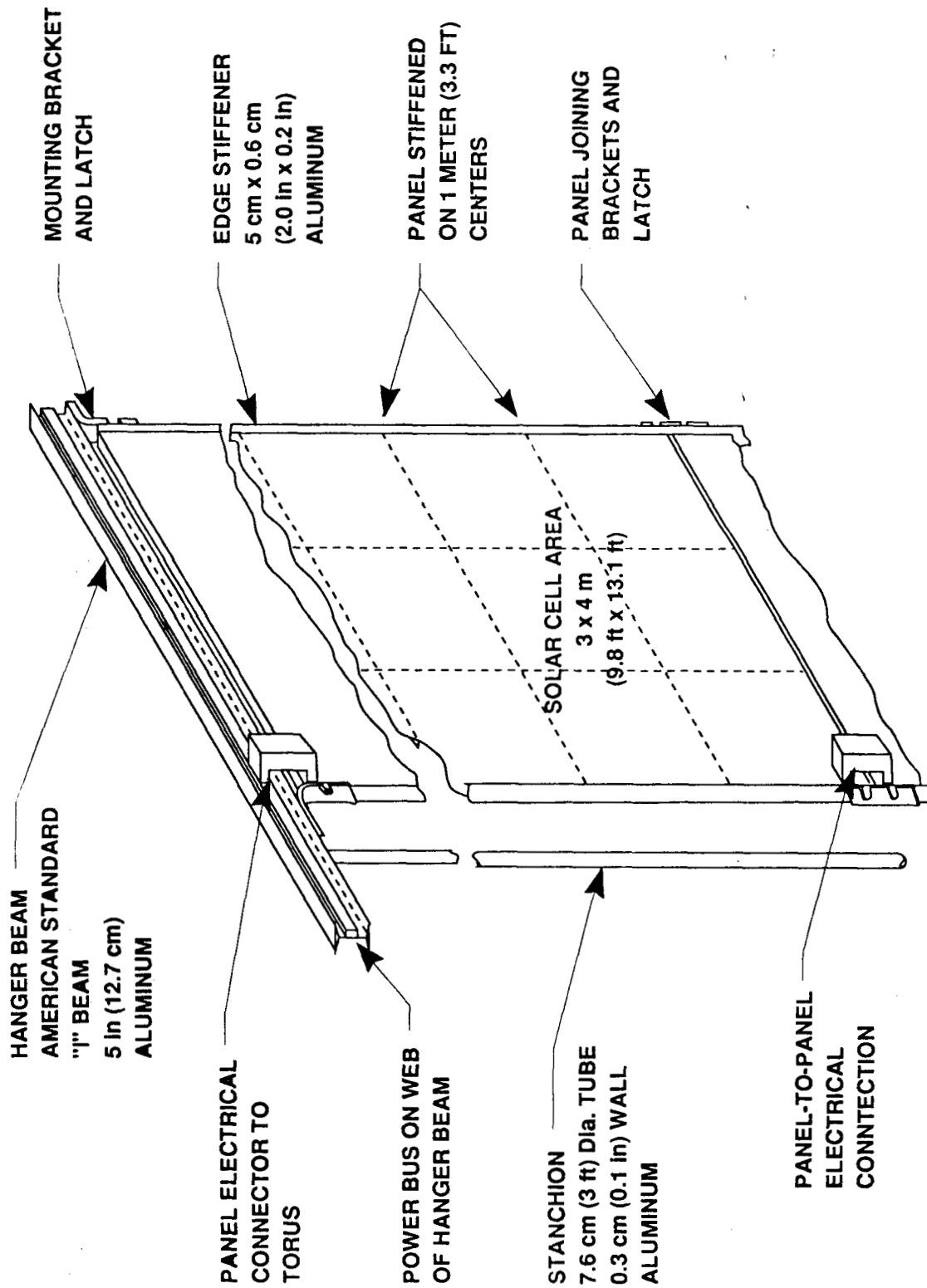


Figure A-21 Torus-mounted Panel Concept and Features

TABLE A-14 SUMMARY OF MASS ESTIMATES FOR ATSS PHOTOVOLTAIC SYSTEM OPTIONS

Storage Method	Fuel Cells O ₂ -H ₂	Li-Na-S Battery	Ni-H ₂ Battery	Ni-Od Battery	Graphite Fiber Wheels	18Ni-400 Steel Wheels	Glass Fiber Wheels
Number Solar Panels	1347	1275	1275	1275	1236	1236	1236
Panel Total Mass, kg (lb)	53880 (118805)	51000 (112455)	51000 (112455)	51000 (112455)	49440 (109015)	49440 (109015)	49440 (109015)
Platform Support, kg (lb)	13250 (29217)	12050 (26571)	12050 (26571)	12050 (26571)	11400 (25138)	11400 (25138)	11400 (25138)
Torus Support, kg (lb)	4775 (10528)	4775 (10528)	4775 (10528)	4775 (10528)	4775 (10528)	4775 (10528)	4775 (10528)
Storage Unit Mass, kg (lb)	19600 (43218)	10677 (23543)	42670 (94088)	64006 (141134)	31640 (69767)	42200 (93051)	70510 (155475)
Radiator Panels	54	29	29	29	15	15	15
Radiator Panels Mass, kg (lb)	14429 (31815)	7749 (17086)	7749 (17086)	7749 (17086)	4008 (8837)	4008 (8837)	4008 (8837)
Total System Mass, kg (lb)	105934 (233584)	86251 (190183)	118244 (260728)	139580 (307774)	101263 (223285)	111823 (246569)	140133 (308993)

A.3.5.1. Panel Mass Estimates

The photovoltaic cells require a mounting plane which accounts for much of the total mass, photovoltaics, and their mountings have been assigned 2 kg/m^2 (0.4 lb/ft^2). The panel stiffeners and edge supports are aluminum strap and angle that contribute 14 kg (31 lb); electrical conductors and connectors add 2 kg (4.4 lb) to total 40 kg (88 lb) for each panel. The mass totals for panels are shown in the Table A-14. In each of the options, the number of panels on the torus remains the same. The differences are in the number of panels on the innermost ring of the platform. The flywheel configurations require only six rings of panels with the innermost not completely filled.

A.3.5.2. Panel Support Structure Estimates

The support structure for the platform installations consist of aluminum frames that secure the panels in groups of three and provide the electrical connections to the bus bars. The aluminum perimeter material contributes 42 kg (92 lb), and the electrical leads contribute 8 kg (17.6 lb) for a total of 50 kg (110 lb) assigned to each set of three panels on the platform. The torus support consists of the hanger beam and stanchions. The bending loads imposed by a 1-g rotation field are within the capabilities for an American standard "5 inch" aluminum I-beam. The mass estimates include the beam, the stanchion as aluminum tubing 7.62 cm (3 in) in diameter with 3 mm (0.125 in) walls plus the bus bars along the web of the beam to total 4775 kg (10530 lb) for the torus support structure.

A.3.5.3. Radiator Estimates

The radiator requirements are extracted from the mass defined for a converter installation on a "per panel" ratio basis. A complete converter radiator using 102 of the panels described in Figure A-7, has total mass of 27256 kg (60100 lb) for structure, fill, and connecting lines.

In summary, the total mass estimates for each of the options show a general agreement. The extreme values represented by Li-Na-S batteries and Ni-Cd batteries differ by less than a factor of two, whereas the masses for the storage elements range over a factor of five. The higher electrical efficiencies that require less radiator area offset the mass differences within the energy storage options.

A.3.6 Effects of Concentration

The output of a photovoltaic system responds to the intensity of incident radiation such that a concentration of the solar flux permits a corresponding reduction in the required area of photovoltaics. The effects of concentration are discussed below.

Concentrators for an ATSS application take the form of linear parabolic reflectors; Figure A-22 shows a concept for a reflecting concentrator that would have the same footprint as the 3 m (9.8 ft) by 4 m (13.1 ft) flat panels. The concept shown uses two reflecting linear parabolic surfaces to concentrate the solar flux on two linear parabolic surfaces covered with photovoltaic cells. The configuration can provide concentration ratios ranging from two to four using essentially the same structure. The concentrators can operate in the same locations as defined for the flat panels. Concentration increases the reject heat

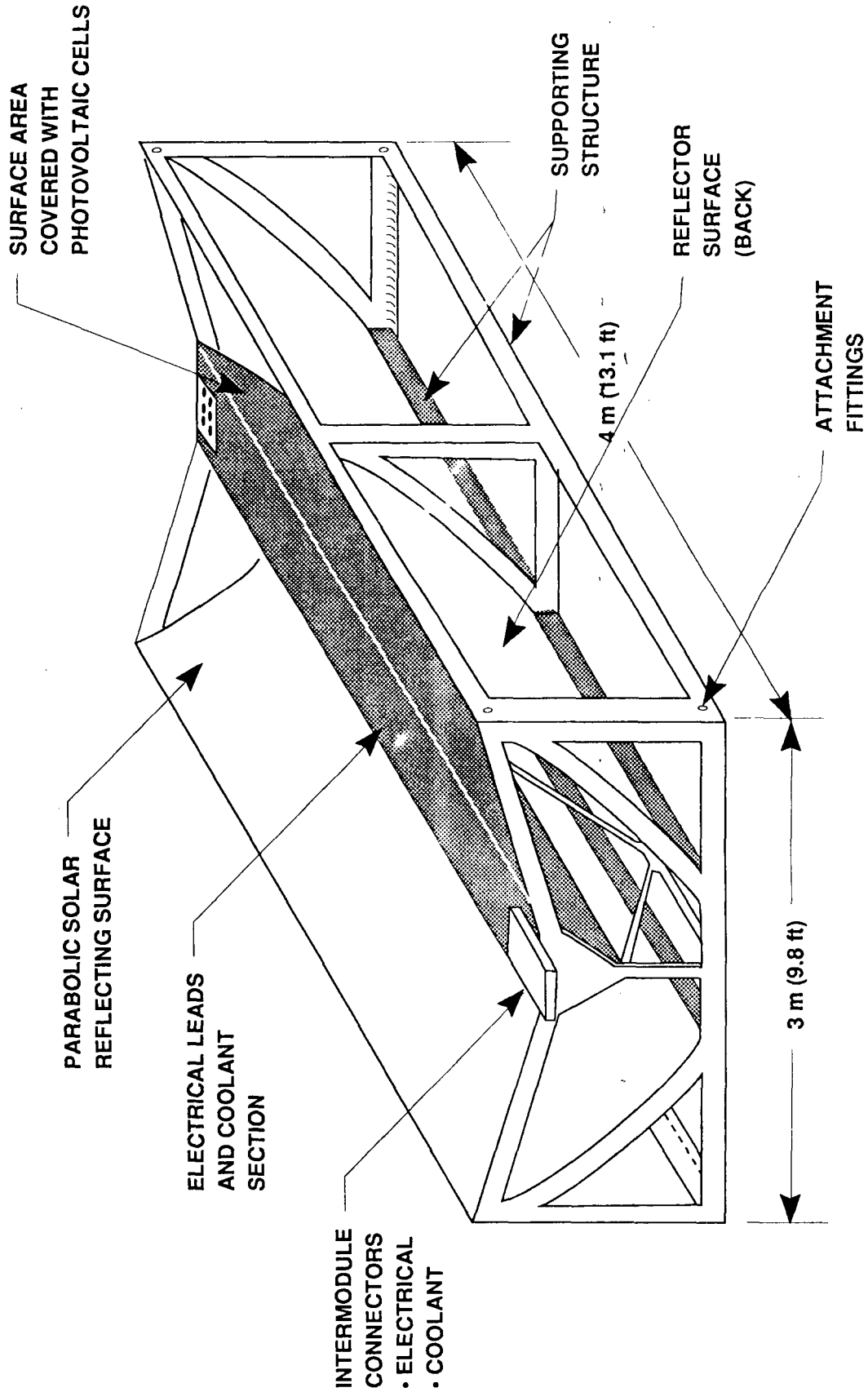


Figure A-22 Concept for a Concentrating Solar Photovoltaic Power Module

flux from the solar cells such that some form of active cooling will be necessary. With active cooling, concentrator units could be placed in any convenient location on the ATSS.

The mounting of the photovoltaics cells in the reflecting configuration shown decreases the total area available for the solar energy intercept. The portion obscured is a function of the concentration ratio. Figure A-23 illustrates the effect for a concentration ratio of two. The obscuration and the related system effects are summarized in Table A-15, which compares the open panels with concentration ratios of two, three, and four. The reduction in collection area must be offset by an increase in the number of units. The values are shown relative to a baseline need for 1347 units. The total area for photovoltaic cells is defined as the product of the solar intercept area per unit divided by the concentration ratio and multiplied by the number of units required. The reduction ratio relative to open panels is somewhat less than the concentration ratio by about 10 percent.

The cooling requirements for the photovoltaic cells are defined by their thermal balance in a radiation field. If the 37 percent of the input energy has to be removed from the back side of the solar cells, then the coolant absorbs 8072 kW-h, which must be dissipated over the period of an orbit. The average heat rejection rate is 5328 kW and requires 9032 m² (97220 ft²) of radiator area for operation at 320 K (576°R). The cyclic operation associated with orbits plus the contributions from the storage elements during the dark period will not result in the near uniform conditions associated with rotating converters. Therefore, for this comparison, the radiator temperature will increase and assume an average operating temperature at 348 K

CONCENTRATION FACTOR OF 2 AS SHOWN

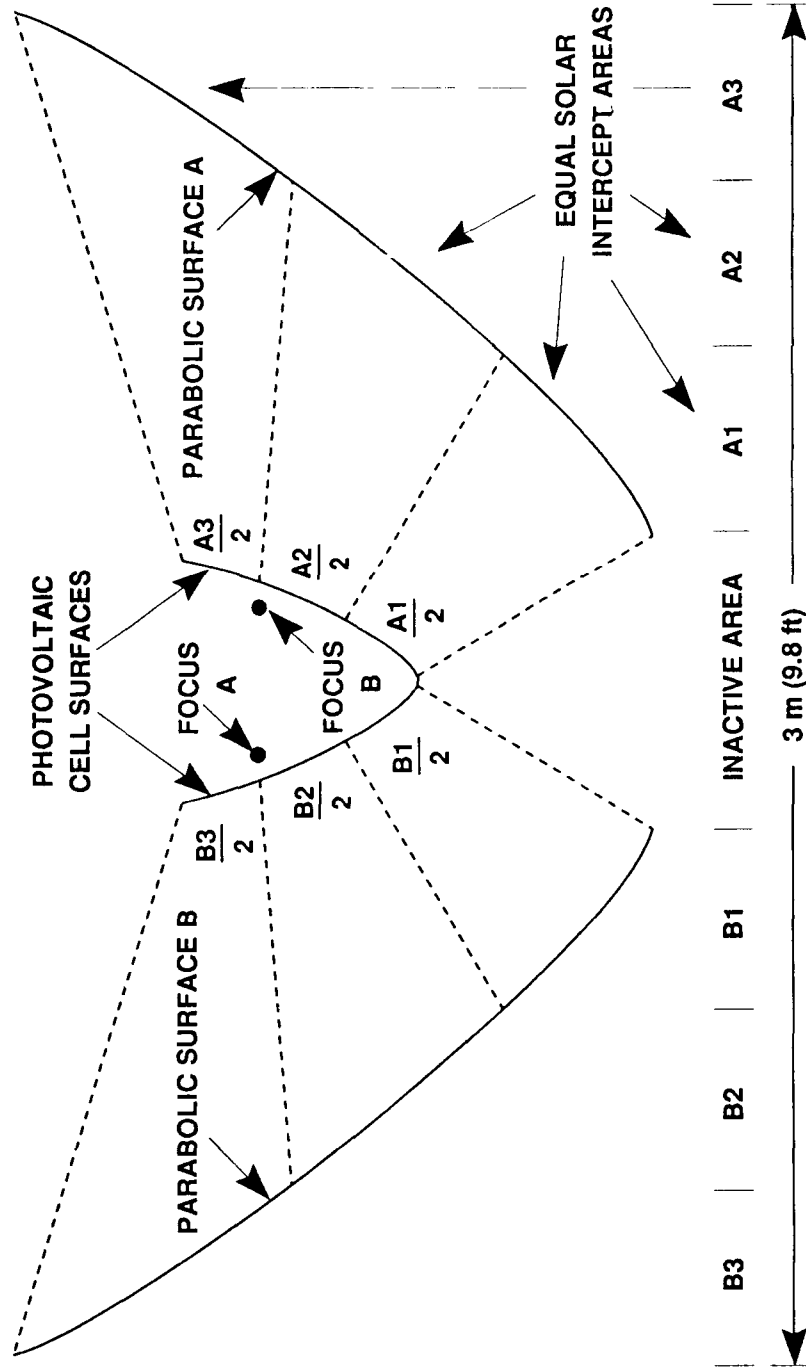


Figure A-23 Geometric Considerations for Linear Parabolic Reflecting Concentrators

TABLE A-15 EFFECTS OF SOLAR CONCENTRATION

Concentration Ratio	1 (OPEN)	2	3	4
Panel Effective Area m^2 (ft^2)	12 (129)	9.2 (99)	8.84 (95)	8.67 (93)
Panels Required	1347	1953	2029	2069
Photovoltaic Cell Area m^2 (ft^2)	16164 (173989)	8983 (966693)	5978 (64347)	4543 (48901)
Photovoltaic Area Reduction Ratio	1	0.55	0.37	0.28
Average Thermal Energy to Radiator kW	-	6400	6400	6400
Radiator Panels (365 K) (657°R)	-	612	612	612

(626°R), with an average heat flux of 0.82 kW/m^2 (0.076 kW/ft^2), such that the concentrated photovoltaic system operates with the same total radiator requirement as the solar dynamic system (Reference A-1).

The system masses can be compared in terms of the radiator, the storage elements, and the concentrator units. Table A-16 summarizes the mass contributions. The concentrator units are essentially welded aluminum structures fabricated from angles and sheets. The units have been assigned a mass of 125 kg (275 lb) each which includes an increment for support elements and electrical interconnections. Energy storage utilizes fuel cells, and the radiator requirement for the fuel cells is included in the total for the concentrator units. The effects of concentration indicate a factor of four increase in the total system mass. The structure for the concentrating reflectors adds a factor of three to the collection elements, and the need for a radiator introduces an additional mass increment.

A.3.7 Photovoltaic System Controls

A photovoltaic system must control the electrical output from the panels, sequence the storage elements, and maintain the thermal balance. Each portion of the system responds to its own particular requirements; the overall system controls are summarized in Table A-17 for the baseline option of energy storage using $\text{O}_2\text{-H}_2$ fuel cells.

The photovoltaics produce a constant voltage during the illuminated portion of the orbit. The voltage decays to zero in about seven minutes during sunset and recovers 30 minutes later during the sunrise. The control system algorithm, therefore, has to accommodate phased power transients two times in each orbit. In full Sun, the control must direct

TABLE A-16 SUMMARY OF SYSTEM MASSES FOR SOLAR CONCENTRATION SYSTEM

Concentration Ratio	1 (open)	2	3	4
No panels or concentrator units	1347	1953	2029	2069
Panel system mass, kg (lb)	71905 (158551)	244125 (538296)	253625 (559244)	258625 (570269)
Fuel cell storage, kg (lb)	19600 (43218)	19600 (43218)	19600 (43218)	19600 (43218)
Radiator, kg (lb)	14429 (31815)	163536 (360596)	162536 (360596)	163536 (360596)
Total system, kg (lb)	105934 (233584)	427261 (942110)	436761 (963058)	441761 (974083)

TABLE A-17 SUMMARY OF PHOTOVOLTAIC POWER SYSTEM CONTROL REQUIREMENTS

CONTROL ELEMENT OR FUNCTION	OUTPUT OR ACTION	RANGE	PRECISION	FREQUENCY
Photovoltaic Field Operation Algorithm				
Panel output voltages monitor (multiple)	Input to power profile	0 to 300 V	0.1 V	Orbital cycle
Panel output current (multiples in ranges)	Input to power profile	0 to 10 A (panel) 0 to 100 A (Section) 0 to 1000 A (System)	0.1 A 1.0 A 10. A	Orbital cycle
Panel temperature monitor	Input to power profile	165 to 415 K (297 to 747 °R)	2 K (3 °R)	Orbital cycle
Power Profile Control Algorithm				
Orbit timing sequence	Power switching between solar panels and storage	0 to 90 min as increments	0.1 sec	Orbital cycle
Power share to storage (excess above 2550 kW)	Switching signals and regulation to energy storage	Switch and regulate 0 to 10 kW (unit) 0 to 500 kW (section) 0 to 2500 kW (system)	0.1 W 1.0 W 10 W	Orbital cycle
Power balance (First 2550 kW)	Switch and regulate power to the station	Switch and regulate 0 to 10 kW (unit) 0 to 500 kW (section) 0 to 2500 kW (system)	0.1 W 1.0 W 10 W	Orbital cycle
Power extraction from storage (2550 kW)	Switch and regulate power from storage unit	0 to 10 kW (unit) 0 to 500 kW (section) 0 to 2500 kW (system)	0.1 W 1.0 W 10 W	Orbital cycle

TABLE A-17 SUMMARY OF PHOTOVOLTAIC POWER SYSTEM CONTROL REQUIREMENTS (cont'd)

CONTROL ELEMENT OR FUNCTION	OUTPUT OR ACTION	RANGE	PRECISION	FREQUENCY
Energy Storage Operating and Regulating Algorithm				
Electrolytic cell voltage monitor	Feedback to regulator	0 to 300 V	0.1 V	Orbital cycle
Electrolytic cell current	Feedback to regulator	0 to 1000 A	1.0 A	Orbital cycle
Fuel water pump and regulator	Switch and modulate	0 to 1 kg/min (0 to 2.5 lb/min) combined total	0.1 kg/min	Demand cyclic partial orbit
H ₂ transfer pump and regulator	Switch and modulate	0 to 1 kg/min (0 to 2.5 lb/min) combined total	0.1 kg/min (0.2 lb/min)	Demand cyclic partial orbit
O ₂ transfer pump regulator	Switch and modulate	0 to 1 kg/min (0 to 2.5 lb/min) combined total	0.1 kg/min (0.2 lb/min)	Demand cyclic partial orbit
Cell, pump, and reservoir temperatures	Feedback to regulator	250 to 415 K (450 to 750 °R)	2 K (3 °R)	Steady
Fuel cell operating temperature	Feedback to regulator	250 to 415 K (450 to 750 °R)	2 K (3 °R)	Cyclic with orbit and demand
Fuel cell H ₂ supply	Switch and modulate in response to command	0 to 1 kg/min (0 to 2.5 lb/min) combined total	0.1 kg/min (0.02 kg/min)	Demand cyclic partial orbit
Fuel cell O ₂ supply				
Fuel cell water extraction (duplicate for 10 units)				
Energy storage regulation, timing, and modulation	Converter power profile commands to regulator inputs	Logic signals timing 0 to 90 min	- 0.1 sec	Orbital cycle

TABLE A-17 SUMMARY OF PHOTOVOLTAIC POWER SYSTEM CONTROL REQUIREMENTS (concl'd)

CONTROL ELEMENT OR FUNCTION	OUTPUT OR ACTION	RANGE	PRECISION	FREQUENCY
Radiator Control Algorithm				
Radiator temperature	Inputs for flow control	270 to 370 K (460 to 700 °R)	2 K (3°R)	Orbital cycle about 320 K (576°R)
Coolant pump operation	Respond to command	0 to 20 kg/sec (0 to 60 lb/sec)	0.1 kg/sec (0.2 lb/sec)	Orbital cyclic about a nominal flow valve
Coolant valve position	Respond to command	Open to close	1% position	Cyclic with orbit
Coolant inlet temperature	Input to flow control	270 to 370 K (460 to 780°R)	2 K (3°R)	Cyclic about nominal
Coolant outlet temperature	Input to flow control	270 to 370 K (460 to 780°R)	2 K (3°R)	Cyclic about nominal

the required excess energy into the storage elements while maintaining a constant 2550 kW input to the ATSS. Photovoltaics benefit when operated at constant current; energy not extracted as electricity has to be dissipated thermally. Photovoltaics converting 25 to 27 percent of the solar energy into electrical power will need to operate with near maximum current to preserve thermal equilibrium. The on-board generation of O₂ and H₂ again provides the necessary load leveling capacity for the system. The energy storage system does have some inherent flexibility when configured as fuel cells. In nominal operations the fuel cells operate to balance the orbital power profile. However, under special conditions, the cells can operate to augment the photovoltaics such that the power delivered could approach 5100 kW for a portion of an orbit. The other storage alternatives would not offer that capability unless some extra capacity were included. Batteries or flywheels need to cycle in sequence with the orbit to avoid compromise of the photovoltaics by thermal effects, or the ATSS will be forced to operate power-short during the dark portion of an orbit. The controls for the energy storage are conventional. The system operates the electrolytic cells and stores fuel during the illuminated portion of the orbit, then powers-up the fuel cells during the dark portion of the orbit. In orbital operation neither section is completely inactive. Instead, the currents and voltage modulate between a standby, or idle, mode and full power.

The requirements for heat extraction and radiator cooling are cyclic. For the fuel cells, the maximum cooling demand occurs when the radiators have an unobscured field of view; consequently, the radiator temperature and coolant flow will vary with orbit position.

A.3.8. Particular Considerations

The particular considerations relate to the installation of the system and the on-orbit maintenance of the system.

The phasing of the photovoltaic panels into the on-orbit assembly of the ATSS requires some attention. The photovoltaic panels cannot be put in place and exposed without any electrical connections. The installation of the panel field involves a continuing activity for on-orbit assembly. There may be a need for reflecting covers if the capability to store energy is limited while assembly is in progress. The internal configuration for the ATSS places all of the O_2-H_2 generating capability in the torus. Fuel cell auxiliary power may not be available during the build-up sequence, and battery cells may be needed on a temporary basis.

The area devoted to photovoltaic panels is both extensive and exposed. Debris damage can be anticipated. In operation, damage to a panel would only compromise that unit (or at most, that group). The on-board mobile crane and air locks are configured to handle units the size of a panel, and the on-board spares would be stocked to accomplish such a repair.

The utilization of flywheel energy storage requires the management of the rotating inertias. Bearing requirements are eased if the flywheel units are mounted in the nonrotating portion of the station; a location in the plane of the platform adjacent to the central tube appears convenient. Unless the rotational inertias can contribute to the operation of the station, the units may need pairing such that a pair always rotates at the same speed while turning in opposite directions (inverted relative to each other). Such a configuration transmits some

local gyroscopic forces to the structure, but at the ATSS system level,
all such forces would cancel.

REFERENCES

- A-1 Queijo, M. J. et al.: Some Operational Aspects of a Rotating Advanced Technology Space Station for the Year 2025, NASA CR 181617, June 1988.
- A-2 Queijo, M. J. et al.: An Advanced-Technology Space Station for the Year 2025, Study and Concepts, NASA CR 178208 March 1987.
- A-3 Queijo, M. J. et al.: Analyses of a Rotating Advanced-Technology Space Station for the Year 2025, NASA CR 178345, January, 1988.
- A-4 Hord, R. M.: Handbook of Space Technology Status and Projections, CRC Press, 1985.
- A-5 Weast, R. C.: Handbook of Chemistry and Physics, 49th Edition, Chemical Rubber Co., 1968.
- A-6 Zinn, W. W. et al.: Nuclear Power USA, McGrawHill Book Co., 1964.
- A-7 Glasstone, Samuel: Principles of Nuclear Reactor Engineering, D. Van Nostrand, 1955.
- A-8 Gross, R. A.: Fusion Energy, John Wiley and Sons, 1984.
- A-9 1988 Laser Focus, Electric Optical Buyers Guide, Volume 23, Specification Table, pp. 45-143, January 1988.
- A-10 Rafeski, J. and Jones, S.E.: Cold Nuclear Fusion, Scientific American, July 1987.
- A-11 Ambrus, J.: Overview of NASA Battery Technology Programs, The 1980 Goddard Space Flight Center Battery Workshop.
- A-12 NASA Space Systems Technology Model, volume 2, Data Base Technology Analyses, NASA-TM-88126, Sixth Edition.
- A-13 Lawson, Louis J.: Design and Testing of High Energy Density Flywheels for Application to Flywheel/Heat Engine Hybrid Vehicle Drive, 1971 Intersociety Energy Conversion Engineering Conference, Boston, Massachusetts, August 3-5, 1971.
- A-14 Lubin, G. et al.: Handbook of Composites, Van Nostrand Reinhold Co., 1982.



Report Documentation Page

1. Report No. NASA CR-181668	2. Government Accession No.	3. Recipient's Catalog No.	
4. Title and Subtitle System Design Analyses of a Rotating Advanced-Technology Space Station for the Year 2025		5. Report Date December 1988	6. Performing Organization Code
		8. Performing Organization Report No.	
7. Author(s) M. J. Queijo, A. J. Butterfield, W. F. Cuddihy, R. W. Stone, J. R. Wrobel, and P. A. Garn		10. Work Unit No. 506-49-31-01	11. Contract or Grant No. NAS1-18267
		13. Type of Report and Period Covered Interim 11/87-5/88	
9. Performing Organization Name and Address The Bionetics Corporation 20 Research Drive Hampton, VA 23666		14. Sponsoring Agency Code	
		12. Sponsoring Agency Name and Address National Aeronautics and Space Administration Langley Research Center Hampton, VA 23665-5225	
15. Supplementary Notes Langley Technical Monitor, Melvin J. Ferebee Jr.			
16. Abstract <p>This is the fourth in a series of reports which document studies of an advanced-technology space station configured to implement subsystem technologies projected for availability in the time period 2000 to 2025. These studies have examined the practical synergies in operational performance available through subsystem technology selection and identified the needs for technology development. In this study further analyses are performed on power system alternates, momentum management and stabilization, electrothermal propulsion, composite materials and structures, launch vehicle alternates, and lunar and planetary missions. Concluding remarks are made regarding the advanced-technology space station concept, its intersubsystem synergies, and its system operational subsystem advanced technology development needs.</p>			
17. Key Words (Suggested by Author(s)) Space Station Artificial Gravity Advanced Systems		18. Distribution Statement Unclassified Unlimited Subject Categories 18 and 54	
19. Security Classif. (of this report) Unclassified	20. Security Classif. (of this page) Unclassified	21. No. of pages 248	22. Price A11